NUREG/CR-6580
SAND97-2632

Performance Testing of Passive Autocatalytic Recombiners

Prepared by
T. K. Blanchat/SNL
A. Malliakos/NRC

Sandia National Laboratories

Prepared for
U.S. Nuclear Regulatory Commission

D602

AVAILABILITY NOTICE

Availability of Reference Materials Cited in NRC Publications

Most documents cited in NRC publications will be available from one of the following sources:

1. The NRC Public Document Room, 2120 L Street, NW., Lower Level, Washington, DC 20555-0001

2. The Superintendent of Documents, U.S. Government Printing Office, P. O. Box 37082, Washington, DC 20402-9328

3. The National Technical Information Service, Springfield, VA 22161-0002

Although the listing that follows represents the majority of documents cited in NRC publications, it is not intended to be exhaustive.

Referenced documents available for inspection and copying for a fee from the NRC Public Document Room include NRC correspondence and internal NRC memoranda; NRC bulletins, circulars, information notices, inspection and investigation notices; licensee event reports; vendor reports and correspondence; Commission papers; and applicant and licensee documents and correspondence.

The following documents in the NUREG series are available for purchase from the Government Printing Office: formal NRC staff and contractor reports, NRC-sponsored conference proceedings, international agreement reports, grantee reports, and NRC booklets and brochures. Also available are regulatory guides, NRC regulations in the *Code of Federal Regulations*, and *Nuclear Regulatory Commission Issuances*.

Documents available from the National Technical Information Service include NUREG-series reports and technical reports prepared by other Federal agencies and reports prepared by the Atomic Energy Commission, forerunner agency to the Nuclear Regulatory Commission.

Documents available from public and special technical libraries include all open literature items, such as books, journal articles, and transactions. *Federal Register* notices, Federal and State legislation, and congressional reports can usually be obtained from these libraries.

Documents such as theses, dissertations, foreign reports and translations, and non-NRC conference proceedings are available for purchase from the organization sponsoring the publication cited.

Single copies of NRC draft reports are available free, to the extent of supply, upon written request to the Office of Administration, Distribution and Mail Services Section, U.S. Nuclear Regulatory Commission, Washington, DC 20555-0001.

Copies of industry codes and standards used in a substantive manner in the NRC regulatory process are maintained at the NRC Library, Two White Flint North, 11545 Rockville Pike, Rockville, MD 20852-2738, for use by the public. Codes and standards are usually copyrighted and may be purchased from the originating organization or, if they are American National Standards, from the American National Standards Institute, 1430 Broadway, New York, NY 10018-3308.

DISCLAIMER NOTICE

NUREG/CR-6580
SAND97-2632

Performance Testing of Passive Autocatalytic Recombiners

Prepared by
T. K. Blanchat/SNL
A. Malliakos/NRC

Sandia National Laboratories

Prepared for
U.S. Nuclear Regulatory Commission

D602

AVAILABILITY NOTICE

Availability of Reference Materials Cited in NRC Publications

Most documents cited in NRC publications will be available from one of the following sources:

1. The NRC Public Document Room, 2120 L Street, NW., Lower Level, Washington, DC 20555-0001

2. The Superintendent of Documents, U.S. Government Printing Office, P. O. Box 37082, Washington, DC 20402-9328

3. The National Technical Information Service, Springfield, VA 22161-0002

Although the listing that follows represents the majority of documents cited in NRC publications, it is not intended to be exhaustive.

Referenced documents available for inspection and copying for a fee from the NRC Public Document Room include NRC correspondence and internal NRC memoranda; NRC bulletins, circulars, information notices, inspection and investigation notices; licensee event reports; vendor reports and correspondence; Commission papers; and applicant and licensee documents and correspondence.

The following documents in the NUREG series are available for purchase from the Government Printing Office: formal NRC staff and contractor reports, NRC-sponsored conference proceedings, international agreement reports, grantee reports, and NRC booklets and brochures. Also available are regulatory guides, NRC regulations in the *Code of Federal Regulations*, and *Nuclear Regulatory Commission Issuances*.

Documents available from the National Technical Information Service include NUREG-series reports and technical reports prepared by other Federal agencies and reports prepared by the Atomic Energy Commission, forerunner agency to the Nuclear Regulatory Commission.

Documents available from public and special technical libraries include all open literature items, such as books, journal articles, and transactions. *Federal Register* notices, Federal and State legislation, and [illegible]ssional reports can usually be obtained from these libraries.

Documents such as theses, dissertations, foreign reports and translations, and non-NRC conference proceedings are available for purchase from the organization sponsoring the publication cited.

Single copies of NRC draft reports are available free, to the extent of supply, upon written request to the Office of Administration, Distribution and Mail Services Section, U.S. Nuclear Regulatory Commission, Washington, DC 20555-0001.

Copies of industry codes and standards used in a substantive manner in the NRC regulatory process are maintained at the NRC Library, Two White Flint North, 11545 Rockville Pike, Rockville, MD 20852-2738, for use by the public. Codes and standards are usually copyrighted and may be purchased from the originating organization or, if they are American National Standards, from the American National Standards Institute, 1430 Broadway, New York, NY 10018-3308.

DISCLAIMER NOTICE

This report was prepared as an account of work sponsored by an agency of the United States Government. [illegible]ther the United States Government nor any agency thereof, nor any of their employees, makes any warranty, [illegible]ssed or implied, or assumes any legal liability or responsibility for any third party's use, or the results of [illegible]use, of any information, apparatus, product, or process disclosed in this report, or represents that its use by such third party would not infringe privately owned rights.

NUREG/CR-6580
SAND97-2632

Performance Testing of Passive Autocatalytic Recombiners

Manuscript Completed: June 1998
Date Published: June 1998

Prepared by
T. K. Blanchat/SNL
A. Malliakos/NRC

Sandia National Laboratories
Albuquerque, NM 87185

A. Malliakos, NRC Project Manager

Prepared for
Division of Systems Technology
Office of Nuclear Regulatory Research
U.S. Nuclear Regulatory Commission
Washington, DC 20555-0001
NRC Job Code L2443

For sale by the U.S. Government Printing Office
Superintendent of Documents, Mail Stop: SSOP, Washington, DC 20402-9328
ISBN 0-16-049654-3

Abstract

Performance tests of a scaled passive autocatalytic recombiner (PAR) were performed in the Surtsey test vessel at Sandia National Laboratories. The test program included experiments to: 1) define the startup characteristics of PARs, 2) confirm a hydrogen depletion rate curve of PARs, 3) define the PAR performance in the presence of steam, 4) evaluate the effect of scale (number of cartridges) on the PAR performance at both low and high hydrogen concentrations, 5) define the PAR performance with and without the hydrophobic coat, 6) determine if the PAR could ignite hydrogen mixtures, 7) define the PAR performance in well-mixed conditions, and 8) define the PAR performance in a low oxygen environment. The tests determined that the PAR startup delay times decrease with increasing hydrogen concentrations in steamy environments. Measured depletion rate data were obtained and compared with previous work. Depletion rate appears to be proportional to scale. PAR performance in steamy environments and the lack of hydrophobic coating was investigated. Placement of the PAR near a wall (as opposed to a center location) appeared to have an effect on depletion rates. The PAR ignited hydrogen at relatively high concentrations (5-10 mole %). Low oxygen concentrations appeared to have an effect on the hydrogen/oxygen recombination rate. The effect of well-mixed conditions during depletion rate measurements were inconclusive.

Contents

Contents (continued)

Figures

Figures

Figures

Figures

Figures

Figures

Figures

Tables

Acknowledgments

The authors would like to thank K. O. Reil for his oversight and guidance of the experimental program. The authors express their gratitude to M. S. Oliver and C. Hanks, who were the electronics and instrumentation technicians for these experiments, and to T. T. Covert and D. Trump, who were the mechanical technicians. All operations at the Surtsey Test Site were performed under the capable management of the site supervisor and mechanical engineer, R. T. Nichols. The gas mass spectrometry technical assistance and analyses were provided by S. M. Thornberg and S. L. Metzger. J. H. Bentz and D. W. Stamps (University of Evansville) reviewed the report, providing numerous helpful comments. M. L. Garcia typed, compiled, and edited the manuscript.

This work was supported by the Accident Evaluation Branch, Office of Nuclear Regulatory Research, of the U.S. Nuclear Regulatory Commission and was performed at Sandia National Laboratories, which is operated for the U.S. Department of Energy under Contract No. DE-AC04-94AL85000.

Nomenclature

PAR	passive autocatalytic recombiner
ALWR	advanced light water reactor
U.S.	United States
SNL	Sandia National Laboratories
USNRC	U. S. Nuclear Regulatory Commission
I&C	instrumentation and control
PC	personal computer
DAS	data acquisition system
GMS	gas mass spectrometer
CCD	charge coupled device
IR	infrared
RH	relative humidity
X_{steam}	steam concentration
P_{sat}	saturation pressure of steam
f_{NC}^{o}	initial noncondensible fraction
N_{total}^{o}	total pretest moles of gas including steam and noncondensible gases
X_{i}^{o}	initial pretest mole fraction of species i at time = 0
N_{i}^{o}	initial pretest gas moles for species i
X_{i}^{t}	mole fraction of species i at time t
N_{i}^{t}	gas moles of species i at time t
SMPS	Standard Meters Per Second
V_s	standard velocity
V	actual velocity
ρ	actual density
ρ_s	standard air density
ΔP	differential pressure across the velocity probe
C	calibration constant for the velocity probe
P_s	standard pressure in absolute units

Nomenclature (continued)

P_a	actual pressure in absolute units
T_s	standard temperature in absolute units
T_a	actual temperature in absolute units
F_s	standard volumetric flow
F_a	actual volumetric flow
Q	steady-state volumetric flow
C_H	hydrogen volume fraction in containment
R	hydrogen removal rate
ε	efficiency factor for hydrogen removal
ρ_H	mass density of hydrogen in the PAR
X_H	hydrogen molar fraction at the PAR inlet
P	vessel pressure
R_H	hydrogen gas constant
T	temperature of the PAR inlet

Performance Testing of Passive Autocatalytic Recombiners

1.0 Introduction

Passive autocatalytic recombiners (PARs) have been under consideration in the United States (U.S.) as a combustible gas control system in operating plants and advanced light water reactor (ALWR) containments for design basis accidents. PARs do not require a source of power; instead, they use a catalyst to recombine hydrogen and oxygen gases into water vapor upon contact with the catalyst. The heat produced from the recombination of hydrogen with oxygen creates buoyancy effects which promote the influx of the surrounding gases into the recombiner. The recombination rate of the PAR system needs to be great enough to keep the concentration of hydrogen below acceptable limits.

There are several catalytic recombiner concepts under development worldwide. The PAR design tested at Sandia National Laboratories (SNL) has been developed by the NIS Company, Hanau, Germany. Detailed tests and analyses were made in cooperation with the Battelle Institute, Frankfurt, and the Technical University, Munich. Its development has been sponsored by the German utility, RWE Energie.

The NIS/RWE PAR device contains flat rectangular cartridges filled with porous spherical ceramic pellets, which are coated with palladium. The large surface area of the palladium layer of the pellets acts on diffused gas molecules to recombine hydrogen with oxygen. Between the cartridges, the PAR device has open flow channels to allow heavier particles or aerosols in the atmosphere to flow through with little plugging of the pellet surface.

Sandia National Laboratories, under the sponsorship and direction of the U.S. Nuclear Regulatory Commission (USNRC), has conducted an experimental program to evaluate the performance of PARs. A PAR was tested at the Surtsey experimental test facility (domed cylinder with a volume of 99 cubic meters (m^3)) at SNL. The test program included the following experiments:

- Experiments to define the startup characteristics of PARs (i.e., to define what is the lowest hydrogen concentration where the PAR starts recombining the hydrogen with oxygen).

- Experiments to confirm the hydrogen depletion rate curve of PARs which was provided to the USNRC (EPRI, 1993).

- Experiments to define the PAR performance in the presence of steam.

- Experiments to evaluate the effect of scale (number of cartridges) on the PAR performance at both low and high hydrogen concentrations.

- Experiments to define the PAR performance with and without the hydrophobic coating.

- Experiments to determine if the PAR could ignite hydrogen mixtures.
- Experiments to define the PAR performance in well-mixed conditions.
- Experiments to define the PAR performance in low oxygen environments.

The following describes the configuration of the PAR, the test facility, the instrumentation, the control and data acquisition system, the test conditions, and the test results and analyses.

2.0 Experiment Description

2.1 PAR Description

Figure 1 shows the 1/4 scale PAR test module steel housing and chimney section. The PAR test module was a scaled version of the prototype PAR [EPRI, 1993] that was developed and fabricated by NIS INGENIEURGESELLSCHAFT MBH (Hanau, Germany). The prototype PAR contains two rows of standard catalytic cartridges (44 cartridges per row) and has dimensions of 1 m by 1 m. The PAR test module (also manufactured by NIS) contains only one row of standard catalytic cartridges and could be assembled as either a 1/2 scale, 1/4 scale, or 1/8 scale PAR by removing cartridges and using smaller (length) front and back panels. Note that the 1/2 scale PAR test module configuration has dimensions of ~0.5 m by ~1.0 m. Figure 2 shows a top view comparing the PAR test module at the three scales.

Figure 3 shows that the PAR test module housing holds the catalyst cartridges in a vertical direction and guides the air flow. A vertical flow channel with a spacing of about 1 centimeter (cm) is formed between the cartridges. These flow channels (along with the PAR body or housing) define the flow area for convection of the heat generated by the heat of reaction. The PAR exit has a chimney with a free cross-sectional area equal to the cross-sectional area through the cartridges. This eliminates downward flow in the PAR and improves the volume flow through the PAR.

Figure 4 shows that the catalyst material is inserted into rectangular cartridges (0.45 m length, 0.01 m wide, 0.20 m tall). The cartridges are filled with the catalyst pellets. The steel sides of the cartridges are perforated with many slotted-like openings that allow hydrogen to enter into the cartridge. The catalyst is a palladium-coated (0.5 weight %) aluminum oxide pellet with a diameter of about 4-6 millimeter (mm) and a bulk density of ~0.5 kilogram/liter (kg/L). The porous oxide pellet provides a large inside surface area (~100 m^2/g) of palladium.

A hydrophobic coating is placed on each pellet to minimize startup delays due to surface water, either from steam condensation or activation of the containment spray system. NIS states that the hydrophobic coating is probably destroyed when the PAR catalyst exceeds temperatures of about 473 K. The PAR catalyst would reach these temperatures at about 2 mole % hydrogen gas (H_2) in cold dry air and about 1 mole % H_2 in the hot air/steam environment.

2.2 Test Facility Description

Figure 5 shows the location of the PAR test module in the Surtsey vessel. The PAR was located at the Surtsey vessel centerline, ~1 m above the midline elevation (except in PAR-9, where the PAR was moved to within 0.3 m of the vessel wall). Horizontal and vertical I-beams exist in the lower half of the Surtsey vessel but there are no I-beams located directly below the PAR. Figure 6 shows the layout of the PAR and the horizontal I-beams (top view). The flow area through the beam openings is 47 % of the total Surtsey cross-sectional area.

The Surtsey vessel (Figure 7) is an ASME-approved steel pressure vessel. It has a cylindrical shape with removable, dished heads attached to both ends, and is 3.6 m in diameter by 10.3 m high. The Surtsey vessel has a maximum allowable working pressure of 1 megapascal (MPa) at 533 K, but has a burst diaphragm installed to limit the pressure in the vessel to less than 0.9 MPa. It is supported approximately 2 m off the ground by a structural steel framework with its longitudinal axis oriented vertically. A total of twenty 30.5-cm (12-inch) and 61-cm (24-inch) instrument penetration ports exist at six different levels around the perimeter of the vessel. The vessel walls and heads are 3/8-inch thick and covered with at least 4 inches of fiberglass insulation, or equivalent material. A false floor currently installed between the lower head and the cylindrical wall section reduces the freeboard volume of the Surtsey vessel to 99 m^3.

Numerous flanges on the vessel were modified to allow steam, noncondensible gas, water, electrical, and video service into and out of the vessel. Figure 8 shows the ports that have been modified for these purposes.

2.3 Instrumentation, Control, and Data Acquisition

The most significant variables measured in the PAR experiments were: (1) the pressure and temperature in the Surtsey vessel, (2) the gas constituents and steam concentrations, (3) the PAR pellet and channel gap temperatures, (4) the flow velocity through the PAR, and (5) the amounts of hydrogen and oxygen injected into the vessel. Figure 9 shows the major instrumentation and equipment installed in the Surtsey vessel for the PAR experiments.

Due to the novelty of the PAR test module and the complexity of the planned tests, the instrumentation and control (I&C) equipment and the data acquisition system were designed to be very flexible. This allowed changing the test conditions (during the course of a test) based on real-time test results. A personal computer (PC)-based data acquisition system (DAS) was designed to control and monitor the course of the test in real-time. The control panel is shown in Figure 10. The PC-based DAS gave instantaneous readouts of the cartridge pellets and corresponding cartridge air gap temperature; Surtsey vessel pressure, temperature, and gas concentrations; and valve positions for steam, hydrogen, and oxygen additions. In addition, the DAS controlled the hydrogen target concentration and the duration of the gas addition interval.

Table 1 is a listing of the instrumentation used in the PAR experiments. The boxed numbers in Figures 10 and 12 correspond to the channel numbers in the data acquisition system listed in Table 1. Instrumentation changed slightly as the PAR experiments progressed. The analysis and techniques used to describe key data from the test instrumentation are described in the section below.

Four pressure transducers were used to measure the pressure in the Surtsey vessel. Two transducers have ranges of 0-1.38 MPa; the other two have ranges of 0-2.07 MPa. The four transducers were mounted in level 6 penetrations on the Surtsey vessel. All of the transducers were metal diaphragm strain gauge-type pressure transducers (Precise Sensor, Inc., Monrovia, CA). The specified accuracy from the manufacturer for the pressure transducers is better than

± 0.50 percent at full-scale output. The transducer's frequency response is greater than 22 kilohertz (kHz) (16 millisecond (ms) rise time). These instruments are routinely recalibrated at SNL against instruments traceable to the National Institute of Standards and Technology, and accuracies are always within the manufacturer's specifications.

The gas temperature in the Surtsey vessel was measured with twenty thermocouples installed in two rakes. Figure 11 shows thermocouple locations. The two thermocouple rakes were installed vertically in the vessel; one rake at the vessel centerline (array A) and one rake (array B) located about 0.32 m from the vessel wall. Ten equally-spaced type-K thermocouples (1.0 m spacing) were located on each rake. All type-K thermocouples were made of 0.254-mm wire with a 1.6-mm sheath. The temperature range of the type-K thermocouples is 273 K to 1523 K. The maximum error using the manufacturer's calibration is ± 9.4 K at 1523 K.

Six type-K thermocouples were installed in the Surtsey vessel steel walls. Five thermocouples measured wall temperature and one thermocouple measured floor temperature. In addition, thermocouples measured the injected oxygen and hydrogen temperatures, both at the respective manifolds and also at each steam/gas diffuser. In order to minimize steam condensation, steam was mixed with the oxygen and/or hydrogen during each gas injection. The temperature of the inlet steam was also recorded.

A real-time gas mass spectroscopy (GMS) system was used to determine the concentrations of nitrogen, oxygen, and hydrogen in the vessel at four sample points. The four sample points were at the PAR inlet, the PAR outlet, high in the vessel near the dome, and low in the vessel near the floor. To ensure representative samples and to minimize the delay time due to purging sample lines, each line was purged for ~1 minute prior to sampling. This necessitated a continuous purge of gas out of the vessel. The sample lines and purge rates were sized to allow no more than a 1.0 % loss (by volume) of gas out of the vessel over the course of a 12 hour test. Since the PAR inlet was the sample point of greatest interest, this point was selected for every other sample (i.e., PAR inlet, PAR outlet, PAR inlet, Surtsey dome, PAR inlet, Surtsey floor, PAR inlet, PAR outlet, ...).

Ten to twenty pre-evacuated 500-cm^3 gas grab sample bottles were used to collect samples from the vessel. Most of the gas grab samples were taken at the PAR inlet; however, any of the four gas sample points could have been selected. These gas grab samples were used as an independent verification of the gas composition. The sample times were chosen based on the expected PAR performance and the estimated test duration time. All sample lines were purged prior to filling the gas grab bottles to ensure representative samples. All of the gas samples were analyzed posttest using gas mass spectroscopy by the Gas Analysis Laboratory at SNL.

A high resolution 1/2-inch charge-coupled device (CCD) color camera was mounted on a level 5 port, and viewed the PAR through a tempered glass window. In addition to the digital camera, an infrared (IR) camera also viewed the PAR through a different level 5 port. The camera view could see the PAR exit (top of the chimney) and provide visual evidence in the event of a deflagration event.

The hydrogen and oxygen gas was supplied to the vessel from separate manifolds. Standard 44 liter compressed gas cylinders were installed on the manifolds. In the tests that involved a prototypic air/steam atmosphere, the cold gas entering the vessel was mixed with an appropriate amount of steam to heat the cold gas to near the desired test temperature. Mixing was done in a diffuser/mixer pipe that was located near the floor of the vessel. This was necessary to prevent condensation of the steam. The amount of hydrogen added was usually based on the difference between the actual hydrogen concentration at the PAR inlet (from the gas mass spectroscopy instrument) and the target hydrogen concentration. For every mole of hydrogen that was added, typically, one-half mole of oxygen was also added in those tests at high hydrogen concentrations. Mass flow controllers were used to provide precise metering of the hydrogen and oxygen into the vessel. Two mixing fans were installed in the vessel (see Figures 6 and 9). They were located on opposite sides of the PAR at the openings of the false floor support I-beams; one pointed upward and one pointed downward. The fans were usually operated when hydrogen was injected and prior to taking gas grab samples.

Other instrumentation included a hygrometer to measure relative humidity; and pitot-tube differential pressure transducers and a hot-wire anemometer to measure the velocity of the gas at the PAR inlet and outlet.

Figure 12 shows the location of the thermocouples that monitored PAR temperature. Twelve thermocouples monitored the catalyst temperature at three cartridge locations; PAR middle (and a PAR middle backup), PAR edge, and PAR corner. Three vertical positions for temperature measurement were monitored at each location (2 cm from the bottom, middle, and 2 cm from the top). These thermocouples were inserted into the cartridges and surrounded by the catalyst pellets. Twelve thermocouples monitored the temperature of the gas in the gap between the cartridges and were located opposite of the catalyst thermocouples. Four thermocouples monitored the PAR inlet temperature. Two thermocouples were located at the centerline middle and two were located at the centerline edge (within 2 cm of the PAR bottom). Four thermocouples monitored the PAR outlet temperature. Two thermocouples were located at the centerline middle and two were located at the centerline edge (within 2 cm of the chimney exit).

Real-time plots of the pertinent parameters provided indications of the PAR heat up and hydrogen depletion during the course of the test. The plots included the vessel hydrogen, oxygen, and steam, concentrations, oxygen and hydrogen total flow and flow rates, PAR temperatures, gas temperatures from the two vertical arrays, vessel pressure, and the velocity of the gas at the PAR inlet and outlet.

3.0 Gas Composition Measurements and Analyses

The GMS system cannot measure steam concentrations, a dry sample must be presented to the GMS system. In order to achieve this, a condenser and condensate trap (and heated gas inlet lines) were installed on each gas measurement line. This yielded dry-basis gas concentrations; however, to determine wet-basis gas concentrations, the steam fraction must be known. A hygrometer was used to determine the relative humidity (RH). Then, the steam concentration (X_{steam}) was calculated by,

$$X_{steam} = RH \frac{P_{sat}}{P_{total}} \quad (1)$$

where the saturation pressure of steam (P_{sat}) is determined from the saturated steam tables using the vessel average gas temperature. The thermocouples on array B were used to determine the vessel average temperature.

The nitrogen-ratio method was used to determine wet-basis gas concentrations as a second independent method (Blanchat, 1994). The nitrogen-ratio method does not require an estimate of the posttest noncondensible fraction. It does, however, require the pretest noncondensible fraction. The data and assumptions required for the nitrogen-ratio method are listed below:

1. The initial noncondensible fraction, f^0_{NC}, must be known.
2. The total pretest moles of gas, N^0_{total}, including steam and noncondensible gases, must be known.
3. The measured ratios of the pretest and posttest noncondensible gases must be known.
4. It must be assumed that nitrogen is neither produced nor consumed by chemical reactions.
5. It must be assumed that leakage between the time for which the pretest numbers apply and the time of the posttest samples does not change the ratios of the noncondensible gases.

Let X^0_i be the initial (pretest) mole fraction of species i at time t = 0 in the Surtsey vessel and let N^0_{total} be the initial number of steam and noncondensible gas moles in the vessel. The initial number of gas moles for all species is

$$N^0_i = X^0_i \; N^0_{total} \; . \quad (2)$$

Let X^t_i be the mole fraction of species i at time t. For the various posttest times, the number of moles of nitrogen is assumed to be unchanged, and the numbers of moles of the other gases are therefore given by,

$$N^t_i = N^0_{N_2} \frac{X^t_i}{X^t_{N_2}} . \quad (3)$$

It is not necessary to know the posttest noncondensible fraction; only the ratio of the posttest gas species mole fractions are needed. Furthermore, provided all noncondensible gases leak in the same proportion, a correction for posttest leakage is not needed.

The nitrogen-ratio method calculated the total number of noncondensible moles. Total moles in the vessel is calculated using ideal gas law relationships. Therefore, the number of steam moles is simply the difference between the total vessel moles and the total noncondensible moles. The steam fraction is found from the ratio of steam moles to total vessel moles.

4.0 Test Matrix

Twenty PAR tests were conducted. The test matrix is summarized in Table 2. The PAR was located at the Surtsey vessel centerline in all tests except PAR-9.

The goal of the first three tests was to determine the minimum hydrogen concentration at which the PAR begins to recombine, both in cold air (PAR-1 and PAR-2) and in steam atmospheres (PAR-3). These startup tests were all performed at 1/2 scale.

PAR performance at low hydrogen concentrations was determined in the PAR-4 (at 1/2 scale), the PAR-5 (at 1/4 scale), and the PAR-6 (at 1/8 scale) experiments. NIS states that the hydrophobic coating is probably destroyed when the PAR catalyst exceeds temperatures of about 473 K. The PAR catalyst reached these temperatures at about 2% H_2 in cold dry air and about 1% H_2 in the hot air/steam environment. Tests PAR-4, PAR-5, and PAR-6 were performed at hydrogen concentrations that would not destroy the hydrophobic coating.

The effect of the hydrophobic coating was determined in two counterpart tests, PAR-7 and PAR-8. Both tests were performed at 1/8 scale and at relatively high hydrogen concentrations. The hydrophobic coating was intentionally destroyed during the PAR-7 experiment. A repeat test, PAR-8R, yielded performance data at 1/8 scale and high hydrogen concentrations.

The PAR-9 experiment was performed at 1/8 scale to determine the effect on performance when the PAR is located near a wall. New cartridges were used and the depletion rate data from PAR-9 was compared to the counterpart test, PAR-6 (also at 1/8 scale but at the vessel center location).

Hydrogen ignition by the PAR was intentionally tested in the PAR-10 experiment. The PAR-11 test (a planned counterpart high concentration hydrogen ignition test) was not performed. The PAR-12 experiment (at 1/4 scale) and the PAR-13 and PAR-13R experiments (at 1/2 scale) yielded the scaled counterpart high hydrogen concentration performance data and completed the test series.

Obtaining hydrogen depletion rate at steady-state **well-mixed** conditions was the goal of the PAR-demo1, PAR-demo2, and PAR-demo3 experiments. The mixing fans were operated continuously (at slow speed) throughout most of each test. These experiments were performed with old cartridges that had been last configured for the PAR-8R experiment. Steady-state well-mixed depletion rate data was also obtained in the PAR-14 and PAR-15 experiments. New cartridges were installed in the 1/8 scale housing prior to starting the PAR-14 experiment.

The PAR-16 experiment was designed to investigate oxygen limits. The PAR was configured as a 1/8 scale device and was located at the centerline of the Surtsey vessel and about one meter above the false floor support I-beams.

5.0 Experimental Results

Some general pretest and posttest observations from the twenty tests are described in the following paragraphs. The specific experimental results and test observations are then presented in the respective test sections.

The atmosphere for the first two tests was air, at a pressure of about 0.21 MPa. The next twelve tests used a mixture of 0.107 MPa of air and 0.107 MPa of steam, for a total pressure of about 0.21 MPa. To achieve these conditions, the vessel was sealed with about 0.083 MPa of cold air inside (one Albuquerque atmosphere at about 293 K). To achieve a steam atmosphere, the Surtsey vessel was heated internally with steam to obtain a gas temperature of about 375 K. A portable steam boiler provided a low-pressure, saturated steam heat source (227 kg/hr) into Surtsey. Initially, the steam that entered Surtsey condensed and yielded latent heat to the vessel walls and atmosphere. A steam trap installed in the Surtsey floor removed the condensate without removing gases. As the vessel heated, the vessel pressurized with steam. The vessel bulk gas and wall heat up was accomplished in about 12 hours. At a temperature of 375 K, the air and steam pressures become equal. Note that the air pressure increased from 0.083 MPa to 0.107 MPa because of the increase in air temperature from 293 K to 375 K.

Five **well-mixed** tests were performed in air-only atmospheres and at pressures of about 0.21 MPa (PAR-demo1, PAR-demo2, PAR-demo3, PAR-14, and PAR-15). The purpose of the experiments was to obtain depletion rate data from a hydrogen concentration of about 5 mole % (dry-basis) in an air atmosphere (no steam). In all five tests, the PAR was first operated at a steady-state well-mixed condition by continuously injecting hydrogen. The PAR was configured as a 1/8 scale device and was located at the centerline of the Surtsey vessel and about one meter above the false floor support I-beams. The mixing fans were operated continuously at a slow speed throughout most of each test. The "demo" tests used old cartridges. A set of new cartridges was obtained prior to performing the PAR-14, PAR-15, and PAR-16 experiments.

Depletion rate data were not obtained in the PAR-demo1 and PAR-demo2 tests due to premature burns. The following points can be made in regards to the "demo" tests: 1) Hydrogen burns occurred in all three tests. The source of the burns has not been determined. Further investigation will be needed to identify the ignition source. 2) The PAR startup delay time increased with each successive test, from ten minutes in PAR-demo1 to forty-five minutes in PAR-demo3, 3) Well-mixed conditions were obtained by operating the mixing fans at slow speed, and 4) A depletion rate comparison between PAR-8R (a non-mixed 1/8 scale test with hydrogen/air/steam mixtures at 2 bar pressure and without mixing fans) and PAR-demo3 (a well-mixed test) shows that the depletion rate was smaller in PAR-demo3. One possible explanation is that a more accurate depletion rate was obtained with the mixing fans running continuously in PAR-demo3 since the PAR was now depleting the entire volume uniformly. The depletion rate calculation assumes that the entire Surtsey volume is being depleted and that the hydrogen concentration in the vessel is uniformly the same concentration as that measured by the GMS at the PAR inlet sample point. However, there may be another explanation. The cartridges in the

1/8 scale PAR have been operated at high temperatures for many hours and the catalyst may have degraded.

Low oxygen concentrations were suspected to have yielded a poor depletion rate performance in the PAR-7 experiment. The PAR-16 experiment was designed to investigate this effect.

A series of about twelve figures is presented for each of the twenty experiments described below. The first two figures show the temperatures recorded by the two vertical vessel gas thermocouple arrays. A linear-average is given on each respective temperature plot. Also, the time of the mixing fan operation is given on the array B plot. The next two figures show the cartridge catalyst and gap temperatures, respectively. The six *middle* thermocouples in the catalyst and also the gap were used to provide average temperatures. A figure shows the PAR inlet and outlet temperatures from the middle thermocouples along with the gas addition flow rates as measured from the hydrogen and oxygen flow controllers. A figure compares vessel pressure and saturation pressure (using the array B average temperature) to the steam fraction (as determined from Equation 1) and the relative humidity fraction. A figure shows the velocity of the gas (in meters per second) at the PAR inlet and the chimney exit using the pitot-tube differential pressure transducers and the hot-wire anemometer. The last five figures focus on gas concentration measurements. The dry-basis gas concentration at the PAR inlet sample point as determined from the real-time gas mass spectrometer is shown and compared to the gas grab sample (GGS) post-test measurements. Next, the wet-basis concentrations of hydrogen, oxygen, nitrogen, and steam (also at the PAR inlet sample point) are given. The next figure focuses on the wet-basis hydrogen concentrations at the vessel floor, PAR inlet, PAR outlet, and vessel dome locations. This figure also shows the integrated hydrogen (and oxygen, if used) addition. The last two figures compare hydrogen and oxygen wet-basis concentrations (at the PAR inlet) and integrated additions to either the average catalyst temperature or the PAR ΔT. The PAR ΔT (differential temperature) was calculated from the difference of the PAR outlet and inlet average temperatures.

Steam fractions, as determined from the ratio of saturation steam pressure to total pressure in the Surtsey vessel, and also from the nitrogen ratio method, were very similar during the course of the majority of the tests. A few deviations were seen in the later tests and the steam fraction determined by the method of pressure ratio may not be accurate; these deviations were attributed to problems with the hygrometer, especially after it was damaged by the deflagration event in the PAR-8 experiment and subsequently repaired.

Two observations can be made regarding most of the PAR tests. The first is that the PAR started within 10 minutes in tests with both cold air atmospheres and with hot air/steam mixtures when hydrogen concentrations were quickly increased to > 1.0 mole %. In cold air tests, similar startups were also seen even with hydrogen additions to only 0.2 mole %. However, startup delays were seen in tests with steam atmospheres with low hydrogen concentrations. These startup delays decreased in time when the hydrogen concentrations were increased.

The second observation is that at steady-state operation the PAR appeared to generate a convective flow loop in the Surtsey vessel from the PAR outlet to the dome, down the Surtsey wall (until reaching the height of the PAR inlet), and then returning to the PAR inlet; as indicated by both the hydrogen concentration and the vessel gas temperature measurements. Since the convection flow pattern did not extend to the Surtsey floor, the vessel was not completely well-mixed by the PAR during steady-state operation. The hydrogen concentration from the sample point located near the floor always showed a higher concentration when measurements were taken after the last addition, as compared to the other sample points. This indicated that the depletion below the PAR near the floor was lower than that in the upper half of the Surtsey vessel. Also, the convective loop appeared to be driven further downward into the lower half of the Surtsey vessel in those tests with the higher hydrogen concentrations.

5.1 The PAR-1 Experiment

The PAR-1 experiment was designed to measure the minimum startup hydrogen concentration (refer to Figures 13-24). The PAR was configured for 1/2 scale. The Surtsey vessel was sealed and pressurized with bottled air to about 0.21 MPa. The initial vessel average gas temperature was about 290 K.

In most of the PAR tests, the gas concentrations measured by the mass spectrometer could be identified and separated by sample location (see Figure 32, gas concentrations in PAR-2); however, in PAR-1 (and also in PAR-3), the location identifier was not recorded. Therefore, separate color traces of hydrogen concentration of the individual locations are not available for PAR-1 and PAR-3. Gas concentrations at specific locations *were displayed on the monitors* during the course of the test (and therefore indicated on Figures 21 and 22) and are consistent with the measurements recorded in the other tests.

The PAR started recombining after the first hydrogen addition to about 0.3 mole %. There was essentially no delay in startup. This was shown by the vessel gas and the catalyst temperature increase, the flow increase at the PAR outlet, and the decreasing hydrogen concentration.

The PAR appeared to generate a convective flow loop in the Surtsey vessel from the PAR outlet to the dome, down the Surtsey wall (until reaching the height of the PAR inlet), and then returning to the PAR inlet. This was shown by the relatively flat temperatures and small temperature gradient for the thermocouples located below the PAR on the thermocouple array B. Also, the hydrogen concentration from the sample point located near the floor showed small decreases, as compared to the other sample points. At t = 4.2 hours, just prior to turning on the mixing fans, the hydrogen concentration in the dome and near the floor was 0.2 mole % and 1.6 mole %, respectively. A simple mole-average of the dome and floor values yield a concentration of 0.9 mole %. The true vessel average, determined after mixing the vessel, was 0.6 mole %. This indicated that little depletion occurred in the lower half of the Surtsey vessel.

5.2 The PAR-2 Experiment

The PAR-2 experiment, essentially a repeat of the PAR-1 experiment, was designed to measure the minimum startup hydrogen concentration (refer to Figures 25-34). The PAR was configured for 1/2 scale. The Surtsey vessel was sealed and pressurized with bottled air to about 0.21 MPa. The initial gas temperature was about 297 K. The PAR started recombining after the first hydrogen addition to about 0.15 mole %. There was essentially no delay in startup. As in PAR-1, the PAR appeared to generate a convective flow loop in the Surtsey vessel from the PAR outlet to the dome, down the Surtsey wall (until reaching the height of the PAR inlet), and then returning to the PAR inlet. The hydrogen concentration from the sample point located near the floor showed small decreases as time progressed, compared to the other sample points. This indicated that little depletion occurred in the lower half of the Surtsey vessel.

5.3 The PAR-3 Experiment

The PAR-3 experiment was designed to measure the minimum startup hydrogen concentration in a hot air/steam environment (refer to Figures 35-46). The hydrogen gas injections were very similar to the PAR-1 and the PAR-2 experiments. The PAR was configured for 1/2 scale. The Surtsey vessel was sealed and contained air at about 0.083 MPa. Steam was then added to heat the vessel and the air until a pressure of about 0.21 MPa was achieved. The gas temperature was about 375 K. The steam concentration at the beginning of the test was about 52 mole %.

The PAR did not give a strong response after the first two hydrogen additions. Note that there was a 1 hour wait period after each addition. A close inspection of the data showed that near the end of the second addition: 1) the temperature of the catalyst increased, 2) there was an increase in flow at the PAR outlet, and 3) decreased hydrogen concentration at the PAR outlet was accompanied by a slight decrease in the hydrogen concentration at the PAR inlet.

The startup response of the hot, wet PAR was delayed as compared to the cold, dry tests (PAR-1 and PAR-2). The PAR started immediately at a level of 0.15 mole % hydrogen in PAR-2. The PAR started within 2 hours at a concentration of 0.4 mole % in PAR-3. Again, the PAR appeared to generate a convective flow loop in the Surtsey vessel.

5.4 The PAR-4 Experiment

The PAR-4 experiment was designed to operate the 1/2 scale PAR at a steady-state condition while maintaining the temperature of the catalyst below 473 K to prevent destruction of the hydrophobic coating (refer to Figures 47-58). The Surtsey vessel was sealed with air at about 0.083 MPa. Steam was then added to heat the vessel and the air until a pressure of about 0.21 MPa was achieved at a gas temperature of about 377 K. The steam concentration at the beginning of the test was about 46 mole %.

Hydrogen was added to achieve a steady-state concentration. Hydrogen concentration was slowly increased using a series of hydrogen additions. The PAR started about 5 minutes after the hydrogen concentration reached about 0.4 mole %. Note that the mixing fans were turned on

during each addition (and remained on for 30 s after the addition was stopped). The PAR started about 1 hour after the hydrogen additions were commenced, with the average hydrogen concentration at about 0.7 mole %. A steady-state condition of the PAR was achieved at about 3.8 hours. The steady-state hydrogen concentration was about 0.8 mole %. At steady-state, the ΔT across the PAR was about 30 K and the average catalyst temperature was about 455 K.

After the last hydrogen addition at 3.8 hours, the hydrogen concentration at the PAR inlet decreased from about 0.85 mole % to about 0.2 mole % in about 0.8 hours. This decrease in hydrogen concentration yields depletion rate information, which is discussed in detail in Section 6.

The DAQ computer inadvertently stopped at about t = 5 hours. In order to extend the wet-basis gas concentration measurements to about t = 8 hours, regression fits of pressure and temperature data (from about t = 4 hours to t = 5 hours) were calculated.

As in the previous startup experiments, the PAR appeared to generate a convective flow loop in the Surtsey vessel during steady-state operation. The hydrogen concentration from the sample point located near the floor always showed a higher concentration after the last addition, as compared to the other sample points. This indicated that the vessel was not completely well-mixed by the PAR during steady-state operation.

5.5 The PAR-5 Experiment

The PAR-5 experiment was designed to operate the 1/4 scale PAR at a steady-state condition while maintaining the temperature of the catalyst below 473 K to prevent destruction of the hydrophobic coating (refer to Figures 59-70). The Surtsey vessel was sealed and contained air at about 0.083 MPa. Steam was then added to heat the vessel and the air until a pressure of about 0.21 MPa was achieved. The gas temperature was about 376 K. The steam concentration at the beginning of the test was about 54 mole %.

The PAR started immediately after the first addition of hydrogen as the hydrogen concentration approached 0.6 mole %. A steady-state condition of the PAR was achieved at about 1.82 hours. The steady-state hydrogen concentration was about 0.5 mole %. At steady-state, the ΔT across the PAR was about 34 K and the average catalyst temperature was about 455 K.

To prevent any disturbance of the convective flow recirculation pattern started by the PAR, the mixing fans were turned on only twice during the test, at 0.3 hrs prior to the first gas grab sample and near the end of the test at 3.3 hrs, just before the last gas grab sample. The vessel remained well-mixed during the hydrogen adds as indicated by identical hydrogen concentrations at the PAR inlet and at the vessel floor. This was attributed to the mode of addition (hot buoyant hydrogen added with steam through the diffuser mounted near the vessel floor) along with the convective mixing set up by the PAR in the upper half of the Surtsey vessel. Note that this helps mix the gases during hydrogen adds, but not during the depletion test. This can be observed by

the divergence of the hydrogen concentration at the PAR inlet and vessel floor after 1.8 hours in Figure 68.

At steady-state operation, the convective flow loop in the Surtsey vessel was very similar to that seen in the PAR-4 experiment.

5.6 The PAR-6 Experiment

The PAR-6 experiment was designed to operate the 1/8 scale PAR at a steady-state condition while maintaining the temperature of the catalyst below 473 K to prevent destruction of the hydrophobic coating (refer to Figures 71-82). The Surtsey vessel was sealed and contained air at about 0.083 MPa. Steam was then added to heat the vessel and the air until a pressure of about 0.21 MPa was achieved. The gas temperature was about 375 K. The steam concentration at the beginning of the test was about 52 mole %.

The PAR started within twenty minutes after the first addition of hydrogen as the hydrogen concentration approached 0.9 mole %. A steady-state condition of the PAR was achieved at about 1.92 hours. The steady-state hydrogen concentration was about 0.6 mole %. At steady-state, the ΔT across the PAR was about 27 K and the average catalyst temperature was about 460 K.

To prevent disturbing the convective flow recirculation pattern started by the PAR, the mixing fans were turned on only at the beginning of the test, prior to some gas grab samples (at 0.27 hrs, 0.39 hrs, and 3.28 hrs), and near the end of the test just before the last gas grab sample (at 5.45 hrs). The vessel remained fairly well-mixed during the hydrogen adds.

At steady-state operation, the convective flow loop in the Surtsey vessel was very similar to that seen in the PAR-4 and PAR-5 experiments.

5.7 The PAR-7 Experiment

The PAR-7 experiment was designed to operate the 1/8 scale PAR at a steady-state condition by continuously injecting hydrogen to maintain a hydrogen concentration of about 7 mole % (wet-basis). NIS states that operating at high hydrogen concentrations will cause the temperature of the catalyst to exceed 473 K and should destroy the hydrophobic coating (refer to Figures 83-94). The Surtsey vessel was sealed and contained air at about 0.083 MPa. Steam was then added to heat the vessel and the air until a pressure of about 0.21 MPa was achieved. The gas temperature was about 375 K. The steam concentrati[illegible] the beginning of the test was about 54 mole %.

The PAR started about seven minutes after the first hydrogen addition commenced. The PAR temperatures peaked and then started to decline while the hydrogen was being added (t = 0 to t = 1.5 hours). During this time, when the hydrogen concentration increased from 0% to 8%, oxygen levels decreased from 12% to about 5%. Because it was suspected that the reduced PAR temperatures were due to reduced oxygen levels, oxygen was added from t = 1.1 hours to

t = 2.5 hours in an attempt to understand this effect. As the oxygen was added and the oxygen concentration increased from 5% to 8% the PAR appeared to "restart", as indicated by increasing catalyst temperatures.

The steady-state hydrogen concentration was about 3.5 mole %. At steady-state, the ΔT across the PAR was about 130 K and the average catalyst temperature was about 760 K.

5.8 The PAR-8 Experiment

The PAR-8 experiment was designed to replicate the conditions of PAR-7 and to determine if the lack of the hydrophobic coating would delay the startup in a steam environment (refer to Figures 95-106). The PAR was configured as a 1/8 scale device (with the same cartridges used in PAR-7) and located in the middle of the Surtsey vessel. In PAR-7, the hydrogen concentration reached about 8 mole % and the catalyst temperature reached 1000 K, which destroyed the hydrophobic coating. In addition, a steady-state depletion curve from about 7 mole % hydrogen was to be attempted.

The Surtsey vessel was sealed and contained air at about 0.083 MPa. Steam was then added to heat the vessel and the air until a pressure of about 0.21 MPa was achieved. The gas temperature was about 375 K. The steam concentration at the beginning of the test was about 51 mole %.

The first hydrogen addition replicated the first hydrogen addition in PAR-7. The PAR started about eighteen minutes after the first hydrogen addition (as compared to seven minutes in PAR-7). Based on these results, it appeared that the lack of the hydrophobic coating had little effect in delaying the PAR startup. The conditions after the first hydrogen addition were: 1) the maximum hydrogen concentration reached about 10.0 mole %, 2) the maximum ΔT across the PAR was about 260 K, and 3) the average catalyst temperature reached about 1000 K.

A second hydrogen addition (along with a concurrent oxygen addition) was performed to obtain a steady-state depletion curve from a hydrogen concentration of about 7 mole % (due to a drift in the mass spectrometer calibration, hydrogen concentration was believed to be only about 6 mole % at the time of the addition). About four minutes after the completion of the hydrogen addition (the oxygen addition was still being performed and the mixing fans were operating), a deflagration occurred in the Surtsey vessel. Immediately before the burn, the hydrogen and oxygen concentrations were about 11 mole % and 9 mole %, respectively. The catalyst temperatures were rising at the time of the burn and had reached about 1140 K, the ΔT across the PAR was about 280 K.

The Surtsey vessel pressure peaked to about 0.56 MPa and the average gas temperature reached about 800 K during the burn. Due to the ongoing oxygen addition, about 2 mole % of oxygen was added immediately after the burn. After the burn, the hydrogen concentration was about 0 mole % and the oxygen concentration was about 5.5 mole %. A steady-state depletion curve was not obtained due to the deflagration event.

5.9 The PAR-8R Experiment

The PAR-8R experiment was designed to operate the PAR at a steady-state condition by continuously injecting hydrogen to maintain a hydrogen concentration of about 5 mole % (wet-basis) (refer to Figures 107-118). Note that this condition was not met in PAR-8 because a deflagration consumed all of the hydrogen in the vessel prior to achieving a steady-state condition. The PAR was configured as a 1/8 scale device and was located at the centerline of the Surtsey vessel and about one meter above the false floor support I-beams.

The Surtsey vessel was sealed and contained air at about 0.083 MPa. Steam was then added to heat the vessel and the air until a pressure of about 0.21 MPa was achieved. The gas temperature was about 378 K. The steam concentration at the beginning of the test was about 55 mole %.

The PAR started about fifteen minutes after the start of first hydrogen injections. A steady-state condition was reached at t = 1 hour. At steady-state: 1) the hydrogen and oxygen concentrations were about 5.5 mole % and 9.5 mole %, respectively, 2) the ΔT across the PAR was about 190 K, and 3) the average catalyst temperature was about 860 K. Note that the vessel pressure and average temperature at steady-state were about 0.24 MPa and 392 K, respectively, and the steam concentration was about 52 mole %. The small increase in vessel pressure and temperature was caused by the gas (and steam) additions in conjunction with PAR heating of the vessel gases while setting the steady-state operating condition.

No hydrogen burns occurred and no small particles were seen floating inside the Surtsey vessel (as was seen in PAR-13 and PAR-13R).

5.10 The PAR-9 Experiment

The PAR-9 experiment was designed to operate the PAR at a steady-state condition by continuously injecting hydrogen to maintain a hydrogen concentration of about 1 mole % (wet-basis) (refer to Figures 119-130) and compare the results with PAR-6. In PAR-6, the PAR was *located at the vessel centerline*. In PAR-9, the PAR was configured as a 1/8 scale device (**using new cartridges**) and was *located about 0.3 m from the wall* of the Surtsey vessel. As in all of the tests, the PAR was located about one meter above the false floor support I-beams.

The Surtsey vessel was sealed and contained air at about 0.083 MPa. Steam was then added to heat the vessel and the air until a pressure of about 0.20 MPa was achieved. The gas temperature was about 372 K. The steam concentration at the beginning of the test was about 48 mole %.

The PAR started about six minutes after the first hydrogen injection. The PAR reached a steady-state condition at t = 1.2 hours. At steady-state: 1) the hydrogen and oxygen concentrations were about 1.0 mole % and about 11.5 mole %, respectively, 2) the ΔT across the PAR was about 95 K, and 3) the average catalyst temperature was about 490 K.

Some of the PAR temperatures from the thermocouples embedded in the catalyst spiked upward at about t = 0.5 hours during the incremental gas additions (2-min. intervals) and quickly returned to earlier values. It is not known why this occurred. Refer to Section 6.2 for comparisons between PAR-9 and PAR-6 results.

5.11 The PAR-10 Experiment

The PAR-10 experiment was designed to determine if a PAR could ignite an air/steam/hydrogen mixture with an initial hydrogen concentration of about 10 mole % (refer to Figures 131-142). The PAR was configured as a 1/8 scale device (with the same cartridges used in PAR-8) and located in the middle of the Surtsey vessel.

The Surtsey vessel was sealed and contained air at about 0.083 MPa. Steam was then added to heat the vessel and the air until a pressure of about 0.22 MPa was achieved. The gas temperature was about 375 K. The steam concentration at the beginning of the test was about 48 mole %.

The PAR started about eight minutes after the hydrogen injection was commenced. Because it was necessary to add a large amount of hydrogen in a small time frame; the flow controller was partially bypassed and hydrogen was directly added from the hydrogen manifold. Steam was added and mixed with the hydrogen using the hydrogen diffuser nozzle located near the floor of the Surtsey vessel. The mixing fans were operating during the hydrogen addition. A deflagration event occurred in the Surtsey vessel about 12 minutes after the completion of the hydrogen addition. The conditions just prior to the hydrogen burn were: 1) the maximum indicated hydrogen concentration was about 10.5 mole %, 2) the maximum ΔT across the PAR was about 70 K, and 3) the average catalyst temperature reached about 740 K. Note that the peak catalyst temperature reached 950 K just before the burn.

Assuming no hydrogen was consumed prior to the burn, the wet-basis hydrogen concentration should have reached about 13 mole %. It is believed that the sampling system did not have enough time to adequately purge sample lines and capture the actual concentration inside the Surtsey vessel at the time of the burn. Unfortunately, the gas grab sample taken after the hydrogen addition and just before the burn was bad, and could not verify the dry-basis gas mass spectrometer results.

The oxygen concentration was about 13 mole % immediately before the burn. The Surtsey vessel pressure peaked to about 0.64 MPa during the burn and the average gas temperature reached about 880 K. After the burn, the hydrogen concentration was about 0 mole % and the oxygen concentration was about 8 mole %. A steady-state depletion curve was not obtained due to the deflagration event.

5.12 The PAR-12 Experiment

The PAR-12 experiment was designed to operate the PAR at a steady-state condition by continuously injecting hydrogen to maintain a hydrogen concentration of about 5 mole % (refer

to Figures 143-154). The PAR was configured as a 1/4 scale and located at the centerline of the Surtsey vessel about one meter above the false floor support I-beams.

The Surtsey vessel was sealed and contained air at about 0.083 MPa. Steam was then added to heat the vessel and the air until a pressure of about 0.21 MPa was achieved. The gas temperature was about 375 K. The steam concentration at the beginning of the test was about 48 mole %.

The PAR started about ten minutes after the first hydrogen injection was commenced. A steady-state condition was reached at 1.6 hours. At steady-state: 1) the hydrogen and oxygen concentrations were both about 6 mole %, 2) the ΔT across the PAR was about 230 K, and 3) the average catalyst temperature was about 880 K. Note that the vessel pressure and average temperature at steady-state were about 0.33 MPa and 440 K, respectively, and the steam concentration was about 62 mole %. This was caused by the gas (and steam) additions in conjunction with PAR heating of the vessel gases while setting the steady-state operating conditions. Steady-state hydrogen depletion data was taken until t = 5.2 hours and then the mixing fans were turned on.

5.13 The PAR-13 Experiment

The PAR-13 experiment was designed to operate the PAR at a steady-state condition by continuously injecting hydrogen to maintain a hydrogen concentration of about 5 mole % (refer to Figures 155-166). The PAR was configured as a 1/2 scale and located at the centerline of the Surtsey vessel about one meter above the false floor support I-beams.

The Surtsey vessel was sealed and contained air at about 0.083 MPa. Steam was then added to heat the vessel and the air until a pressure of about 0.21 MPa was achieved. The gas temperature was about 375 K. The steam concentration at the beginning of the test was about 52 mole %.

The PAR started about ten minutes after the first hydrogen injection. A steady-state condition was reached at t = 1.4 hours. At steady-state: 1) the hydrogen and oxygen concentrations were about 4 mole % and 11 mole %, respectively, 2) the ΔT across the PAR was about 120 K, and 3) the average catalyst temperature was about 650 K. Note that the vessel pressure and average temperature at steady-state were about 0.32 MPa and 420 K, respectively, and the steam concentration was about 58 mole %. This was caused by the gas (and steam) additions in conjunction with PAR heating of the vessel gases while setting the steady-state operating conditions.

As hydrogen was being added to the vessel; a series of three small hydrogen burns occurred. The first burn occurred at about t = 0.6 hours; the maximum PAR temperature at that time was about 600 K. The IR video showed many small (possibly glowing) particles floating inside the vessel. It is believed that the particles were composed of the catalyst hydrophobic coating (a polymer). These whitish particles have been seen in other tests when the catalyst temperature has exceeded 500 K. The burn at about t = 0.8 hrs was particularly interesting because the video showed that a large burst of white particles ejected from the chimney seconds before the deflagration.

One of the mixing fans failed during the test which prevented obtaining a well-mixed condition in the vessel. Therefore, depletion rate data was not obtained from an initial well-mixed condition.

5.14 The PAR-13R Experiment

The PAR-13R experiment was designed to operate the PAR at a steady-state condition by continuously injecting hydrogen to maintain a hydrogen concentration of about 5 mole % (refer to Figures 167-178). The PAR was configured as a 1/2 scale and located at the centerline of the Surtsey vessel about one meter above the false floor support I-beams. This test was intended as a repeat of PAR-13; most of the hydrophobic coating should have been removed in PAR-13 and it was anticipated that no burns would occur during the repeat test.

The Surtsey vessel was sealed and contained air at about 0.083 MPa. Steam was then added to heat the vessel and the air until a pressure of about 0.21 MPa was achieved. The gas temperature was about 375 K. The steam concentration at the beginning of the test was about 48 mole %.

The PAR started about ten minutes after the first hydrogen injection. A steady-state condition was reached at t = 1.1 hours At steady-state: 1) the hydrogen and oxygen concentrations were about 6.5 mole % and 12.0 mole %, respectively, 2) the ΔT across the PAR was about 110 K, and 3) the average catalyst temperature was about 900 K. Note that the vessel pressure and average temperature at steady-state were about 0.29 MPa and 420 K, respectively, and the steam concentration was about 50 mole %. This was caused by the gas (and steam) additions in conjunction with PAR heating of the vessel gases while setting the steady-state operating condition.

The corner and the edge catalyst cartridge temperatures were much colder than the middle cartridge temperatures (Figure 169). This large variation in temperature had not been seen in earlier tests. This probably caused a lower than expected PAR performance during the depletion interval, as shown in the PAR performance analyses section.

Two small hydrogen burns occurred during the hydrogen injection interval. The first burn occurred at about t = 0.7 hours. The maximum PAR catalyst temperature at that time was about 700 K. These burns were very similar to those seen in PAR-13. The IR video showed a few small (possibly glowing) particles floating inside the vessel (noticeably less particles than that seen in PAR-13). No more particles were seen after the second burn at t = 0.8 hours and hydrogen was added uneventfully until the desired well-mixed, steady-state condition was achieved.

Note that saturation pressure (P_{sat}) does not have any meaning when a burn occurs as shown in Figure 172. The steam is superheated from the burn, temperatures are very high, and therefore, so is P_{sat}. Since the hygrometer reads 100% RH this yields $X_{steam} > 1$, which is nonphysical.

5.15 The PAR-demo1 Experiment

The PAR-demo1 experiment was designed to operate the PAR at a steady-state well-mixed condition by continuously injecting hydrogen and then obtain depletion rate data from a hydrogen concentration of about 5 mole % (dry-basis) in an air atmosphere (no steam) (refer to Figures 179-190). The PAR was configured as a 1/8 scale device and was located at the centerline of the Surtsey vessel and about one meter above the false floor support I-beams. The mixing fans were operated continuously (at slow speed) throughout most of the test.

The Surtsey vessel was sealed and contained air at about 0.21 MPa. The gas temperature was about 300 K. The PAR started about ten minutes after the first hydrogen addition. As hydrogen was being added to the vessel; a series of three hydrogen burns occurred. The first burn occurred at about t = 0.77 hours; hydrogen concentration was about 7 mole % and the maximum PAR temperature at that time was about 840 K. The infrared camera showed a flame front (coming into the view from above the PAR) that burned downward past the PAR. The hot-wire anemometer was turned off after that burn (since it presented a possible ignition source). Some of the temperature data was expanded over the burn intervals in an attempt to isolate flame front information, however, the results were inconclusive. The second burn occurred at about t = 1.32 hours; hydrogen concentration was about 7 mole % and the maximum PAR temperature at that time was about 820 K. Again, the infrared camera showed a flame that burned downward past the PAR. Since the quartz lamps (mounted near the vessel dome) were now suspected as the ignition source, they were deenergized after the second burn. A third burn occurred at about t = 1.74 hours; hydrogen concentration was about 8 mole % and the maximum PAR temperature at that time was about 1000 K. The IR camera now showed flames initiating at the PAR chimney exit. Since the hot-wire anemometer and the quartz lamps were turned off, they were not the ignition source. The PAR definitely appeared to be the ignition source.

The catalyst hydrophobic coating can probably be discounted as the ignition source for all of the burns in the PAR-demo1 test since the IR video showed no small particles floating inside the vessel prior to the burns.

The hydrogen addition was not stopped after the first and third burns. The hydrogen concentration in the Surtsey facility did not increase with the continued additions since the burns ignited the hydrogen jets at the diffuser outlet. The flames attached to the diffuser outlet were extinguished only when the hydrogen additions were stopped.

The mixing fans appeared to be effective in maintaining a well-mixed condition inside the Surtsey vessel. The hydrogen concentration from the sample point located near the floor closely tracked the PAR inlet sample point.

5.16 The PAR-demo2 Experiment

The PAR-demo2 experiment was designed to operate the PAR at a steady-state well-mixed condition by continuously injecting hydrogen and then obtain depletion rate data from a hydrogen concentration of about 5 mole % (dry-basis) in an air atmosphere (no steam)) (refer to

Figures 191-202). Note that this test was essentially a repeat of the PAR-demo1 attempt. The PAR was configured as a 1/8 scale device and was located at the centerline of the Surtsey vessel and about one meter above the false floor support I-beams. The mixing fans were operated continuously (at slow speed) throughout the test.

The Surtsey vessel was sealed and contained air at about 0.21 MPa. The gas temperature was about 300 K. The PAR started later than in the PAR-demo1 test, about twenty minutes after beginning the hydrogen addition as compared to ten minutes in PAR-demo1. Due to incorrect mass spectrometer calibration settings, the actual hydrogen concentration in the Surtsey vessel was greater than indicated during the performance of the test. As hydrogen was being added a large burn occurred that consumed all of the hydrogen in the vessel. The burn occurred at about t = 0.685 hours with the hydrogen concentration at about 11 mole % and the maximum PAR temperature at about 680 K. The PAR catalyst was not hot enough to be a hot-surface ignition source. The infrared camera showed an upward propagating flame front coming into the view from **below** the false floor support I-beams. The flames eventually engulfed the PAR and rose toward the dome.

The hot-wire anemometer and the quartz lamps had been turned off about ten minutes prior to the burn, they were not the ignition source. The catalyst hydrophobic coating can probably be discounted as the ignition source since the IR video showed no small particles floating inside the vessel prior to the burn

Some of the temperature data was expanded over the burn interval in an attempt to isolate flame front information. Both thermocouple arrays show temperatures first increasing at low levels in the Surtsey vessel (i.e., within two meters above the floor). It was determined that the burn commenced immediately after the hydrogen addition was turned off.

The mixing fans maintained a well-mixed condition inside the Surtsey vessel. The gas sample point located near the floor indicated hydrogen concentrations very similar to those indicated by the gas sample point at the inlet of the PAR.

5.17 The PAR-demo3 Experiment

The PAR-demo3 experiment was designed to operate the PAR at a steady-state well-mixed condition by continuously injecting hydrogen and then obtain depletion rate data from a hydrogen concentration of about 5 mole % (dry-basis) in an air atmosphere (no steam)) (refer to Figures 203-214). Note that this test was essentially a repeat of the PAR-demo1 and PAR-demo2 attempts. The PAR was configured as a 1/8 scale device and was located at the centerline of the Surtsey vessel and about one meter above the false floor support I-beams. The mixing fans were operated continuously (at slow speed) throughout the test.

The Surtsey vessel was sealed and contained air at about 0.21 MPa. The gas temperature was about 300 K. The PAR started later than in the earlier tests, about forty-five minutes after

beginning the hydrogen addition as compared to ten minutes in PAR-demo1 and twenty minutes in PAR-demo2.

After the hydrogen was added a small burn occurred that consumed a small amount of the hydrogen in the vessel. The burn occurred at about t = 1.3 hours with the hydrogen concentration at about 6.5 mole % and the maximum measured PAR temperature at about 840 K. The PAR catalyst may have been hot enough to cause hot-surface ignition. Helical igniters have ignited 6 % hydrogen/air mixtures at temperatures near 850 K. The infrared camera showed a downward moving flame front coming into the view from the dome region **above** the PAR. The flames eventually engulfed the PAR and then appeared to die out as they approached the false floor support I-beams. The camera showed that a hot particle was ejected out of the chimney immediately prior to the burn. Since, the hot-wire anemometer and the quartz lamps had been turned off about one hour prior to the burn, they were not the ignition source.

Some of the temperature data was expanded over the burn interval in an attempt to isolate flame front information. Both thermocouple arrays show temperatures first increasing at high levels near the dome in the Surtsey vessel, followed by increasing temperatures in the lower levels of the vessel.

The mixing fans maintained a well-mixed condition inside the Surtsey vessel.

5.18 The PAR-14 Experiment

The PAR-14 experiment was designed to operate the PAR at a steady-state well-mixed condition by continuously injecting hydrogen and then obtain depletion rate data from a hydrogen concentration of about 2 mole % (dry-basis) in an air atmosphere (no steam) (refer to Figures 215-226). Note that this test was essentially a repeat of the PAR-1 and PAR-2 experiments with the exception that the mixing fans were operated continuously (at slow speed) throughout the test. The PAR was configured as a 1/8 scale device and was located at the centerline of the Surtsey vessel and about one meter above the false floor support I-beams. The 1/8 scale PAR housed eleven **new** cartridges that contained catalyst material with undamaged hydrophobic coating. This test was performed at a low hydrogen concentration in order to keep the PAR temperature below 473 K (200°C) to avoid burning the hydrophobic coating.

The Surtsey vessel was sealed and contained air at about 0.21 MPa. The gas temperature was about 280 K. After the mixing fans were started, the hydrogen addition commenced at t = 0.46 hours. The hydrogen flow rate was based on calculations showing that the addition rate (about 100 liter/minute (lpm)) was about twice the scaled depletion rate. The PAR started about thirteen minutes later with the hydrogen concentration at about 0.5 mole % in the Surtsey vessel. The mixing fans maintained a well-mixed condition inside the Surtsey vessel.

At t = 1.87 hours, the hydrogen flow rate was reduced to 50 lpm in order to reach a steady-state condition. About two minutes later, catalyst temperatures spiked. The catalyst temperature ranged from 600 K to 850 K during the spike. Just before the sharp rise in catalyst temperatures:

1) the hydrogen and oxygen concentrations were about 2.0 and 20.5 mole %, respectively 2) the ΔT across the PAR was about 75 K, and 3) the maximum catalyst temperature was about 453 K (180°C). The catalyst temperatures returned to values observed before the spike within about ten minutes. A similar event occurred in the PAR-9 experiment (which also used new catalyst). A hydrogen deflagration event was not observed during the temperature spike.

The second unusual event occurred about 1.5 hours after the hydrogen additions were stopped, during the depletion rate portion of the test. It appeared that the PAR stopped depleting hydrogen. This was indicated by the decrease in catalyst temperatures to ambient temperature, little ΔT and gas flow across the PAR, and constant hydrogen concentrations (about 0.9 mole %) in the vessel. Mixing fans were turned off at t = 5.4 hours to determine if they were causing the shutdown. No effect was noted after the fans were turned off. Note that a similar shutdown may have occurred at the end of the PAR-demo3 experiment (the catalyst temperature data shows sharp decreases near the end of the test). The causes for the spike in catalyst temperature and the shutdown of the PAR are not clearly understood.

5.19 The PAR-15 Experiment

The PAR-15 experiment was designed to operate the PAR at a steady-state well-mixed condition by continuously injecting hydrogen and then obtain depletion rate data from a hydrogen concentration of about 2 mole % (dry-basis) in an air atmosphere (no steam) (refer to Figures 227-238). The PAR was configured as a 1/8 scale device (eleven cartridges) and was located at the centerline of the Surtsey vessel and about one meter above the false floor support I-beams. Note that this test was essentially a repeat of the PAR-14 experiment, and similar to the PAR-1 and PAR-2 experiments with the exception that the mixing fans were operated continuously (at slow speed) throughout the test. Note also that the hydrophobic coating on the catalytic material was damaged in the previous experiment (PAR-14).

The Surtsey vessel was sealed and contained air at about 0.21 MPa. The gas temperature was about 285 K. After the mixing fans were started, the hydrogen addition commenced at t = 0.1 hours. The PAR started about fifteen minutes later with the hydrogen concentration at about 0.5 mole % in the Surtsey vessel. The mixing fans maintained a well-mixed condition inside the Surtsey vessel.

At t = 1.50 hours, the hydrogen additions were stopped in order to obtain depletion rate data. Just prior to stopping the hydrogen additions: 1) the hydrogen and oxygen concentrations were about 2.0 and 20.5 mole %, respectively, 2) the ΔT across the PAR was about 90 K, and 3) the maximum catalyst temperature was about 473 K (200°C).

The spike in catalyst temperatures seen in the PAR-14 experiment did not occur in PAR-15. Also, the PAR did not shutdown at 1.0 mole % hydrogen concentration, as was seen in PAR-14. The PAR continued to deplete hydrogen to a level of about 0.3 mole % hydrogen. The only visual difference between the two tests was that the atmosphere was foggy in PAR-14 and clear in PAR-15.

5.20 The PAR-16 Experiment

The PAR-16 experiment was designed to determine the PAR oxygen limits (refer to Figures 239-251). The PAR was configured as a 1/8 scale device (eleven cartridges) and was located at the centerline of the Surtsey vessel and about one meter above the false floor support I-beams.

The Surtsey vessel was sealed and inerted with nitrogen. The inerting process consisted of adding nitrogen (~ 95 psia) to the Surtsey vessel to reduce the oxygen concentration to about 0.2 mole %, and then venting the vessel to the target test pressure. At the beginning of the test, the nitrogen and oxygen concentrations were 99.7 and 0.3 mole %, respectively, as determined by the on-line gas mass spectrometer. The vessel pressure was about 0.22 MPa. The gas temperature was about 274 K. The mixing fans were operated continuously (at slow speed) throughout most of the test.

After the mixing fans were started, a hydrogen addition to about 1.8 mole % commenced at t = 0.1 hours. Slight increases in PAR temperature indicated that the PAR started recombining with oxygen concentration at 0.2 mole %. Additional increases in temperature occurred with incremental oxygen additions at t = 1.3 hours and t = 2.5 hours. Catalyst temperature did not increase after a hydrogen addition at t = 3.3 hours. The mixing fans maintained a well-mixed condition inside the Surtsey vessel.

This experiment determined that reduced oxygen concentrations resulted in degraded PAR performance. Figure 250 shows two points in time (t = 4.7 hrs and t = 6.2 hrs) that have the same hydrogen concentration (3.0 mole %) but different oxygen concentrations (1.5 mole % and 4.0 mole %). Note that catalyst temperature is a direct measurement of PAR performance. The catalyst temperature was 380 K at 1.5 mole % oxygen and 520 K at 4.0 mole % oxygen.

At t = 6.2 hours, the hydrogen additions were stopped in order to obtain depletion rate data. Just prior to stopping the hydrogen additions: 1) the hydrogen and oxygen concentrations were about 3.0 and 4.0 mole %, respectively, 2) the ΔT across the PAR was about 130 K, and 3) the maximum catalyst temperature was about 520 K. The mixing fans were turned off at t = 7.2 hours. The depletion rate will be calculated by two methods, using the change in hydrogen concentration and the PAR velocity.

6.0 PAR Performance Analyses

Hydrogen depletion rates are used to measure the performance of a PAR. The hydrogen depletion rate is usually determined as a function of the hydrogen concentration in the vessel. Depletion rate analyses can also be used to show the effect of various factors, such as PAR location, oxygen concentration, catalyst poison, etc., on PAR performance.

The following procedure was used to determine the depletion rate. First, the time-dependent amount of hydrogen in the Surtsey vessel (in moles) was determined by multiplying the average hydrogen concentration by the total number of moles in the Surtsey vessel. The average hydrogen concentration was assumed to be that measured by the gas mass spectrometer at the PAR inlet sample point. The total number of moles in the vessel was calculated using the ideal gas law with an average temperature determined from the array B thermocouples.

As shown earlier in the results section, the hydrogen concentrations measured at the four sample locations diverged from some initially equal value over the course of a test (unmixed tests). This was because the mixing fans were off while depletion rate data were taken and the PAR flow was not sufficient to maintain a mixed condition in the vessel. The methodology used to determine the depletion rate assumed that the vessel was well-mixed at all times; this introduced some error since the average hydrogen concentration was not actually measured and cannot be calculated since the local steam concentrations were not known. The measured depletion rates generally overpredicted hydrogen consumption at the stated hydrogen level since the hydrogen concentration at the PAR inlet sample point, just before the fans were turned on, was lower than the average value (for example, see Figure 176 at t = 2.5 hours.).

The depletion rate was then determined by calculating the difference in hydrogen moles at each successive time interval, using the fitted data from the steady-state depletion interval, after the hydrogen additions were stopped. The calculated depletion rate was then plotted against the measured hydrogen concentration.

6.1 Scale Effect

PAR performance and the effects of scale were determined with tests at both low and high hydrogen concentrations. Note that the initial conditions for all tests started with a vessel pressure of about 2 bar, with approximately 50/50 mixtures of air and steam.

Figures 252 and 253 show the PAR performance with low hydrogen concentrations (< 0.7 mole %) at three scales: 1/2 scale (PAR-4), 1/4 scale (PAR-5), and 1/8 scale (PAR-6). A regression fit of the number of moles in the vessel during the steady-state depletion interval is shown in Figure 252 for each test. These fits were then used to calculate the fitted depletion rates shown in Figure 253 (along with the 95 % confidence intervals). Note that the 1/2 scale depletion rate is ~4 times the 1/8 scale depletion rate.

Figures 254 and 255 show the PAR performance with high hydrogen concentrations (3-6 mole %) and at three scales: 1/2 scale (PAR-13 and PAR-13R), 1/4 scale (PAR-12), and 1/8 scale (PAR-8R). Simple scaling does not appear to apply to depletion rates at high hydrogen concentrations. Also, a higher removal rate occurred in PAR-13 than in the repeat test, PAR-13R. This may be due to the fact that a well-mixed initial condition was not totally achieved in PAR-13 due to a failed mixing fan (shown by the different measured hydrogen concentrations at the floor and PAR inlet sample points in Figure 164). However, note that the PAR-13R ΔT was far below normal (see Section 6.3); therefore, the PAR-13R depletion rate is suspect.

A better comparison of the scaled depletion rate data can be made by normalizing the data. Figure 256 gives hydrogen depletion rate predictions for both the Fischer and the Sher depletion rate models (Fischer 1995; Sher et al. 1995). Both models show that the depletion rate is directly proportional to the PAR scale (i.e., number of cartridges in the PAR). These models assume that the hydrogen depletion rate is simply a function of the hydrogen concentration, pressure, and temperature at the PAR inlet. Therefore, a simple scale factor can be used to normalize the data. There are no corrections for scaled heat losses. Neither model can predict the mixing behavior inside the facility; therefore, the models were used under the assumption that the Surtsey vessel was well mixed at all times.

However, if the PAR only consumes hydrogen in a small portion of the total vessel volume, the depletion rate calculation can overpredict consumption if the vessel is not well-mixed at all times. Note that most of the Surtsey tests were not well-mixed. The depletion rate measurements then become scale-dependent since tests with larger scale and/or higher concentrations appear to deplete larger pockets of hydrogen within the total vessel volume. This is indicated in Figure 257, which gives the temperature difference measured between successive array B thermocouples (see Figure 11) at and below the PAR location. The temperature differences shown in Figure 257 indicate that the convective loop ends at different heights below the PAR for different test conditions; possibly revealing that larger pockets of hydrogen are depleted at larger scale and at higher hydrogen concentrations.

Figures 258 and 259 show the scaled depletion rate data normalized to full-scale by applying the scale factor (x2 for 1/2 scale, x4 for 1/4 scale, and x8 for 1/8 scale). Figure 258 shows that the calculated depletion rates for these tests at low hydrogen concentrations are indeed directly proportional to scale. However, at high hydrogen concentrations, Figure 259 shows the calculated depletion rates in the tests using the large scale PAR are lower than depletion rates in tests with the small scale PAR. The depletion rate calculation does not take into account hydrogen stagnation in the lower part of the Surtsey vessel and that the large scale PAR provides better mixing than the small scale PAR.

Figures 258 and 259 are used to compare SNL test results with published depletion rate data (EPRI 1993: Fischer 1995; Sher et al. 1995) at pressures of 2 bar and 1 bar. Data at 1 bar is only presented to highlight the physics; depletion of hydrogen by the PAR is a mass diffusion process driven by density gradients. The comparison shows that the SNL data correlates reasonably well with the Fischer model at 2 bar pressure when hydrogen concentrations were below 4-5 mole %.

The steady-state conditions of PAR-12, -13, and -13R were ~3 bar. This means that the those test data should really be compared to theoretical depletion rate curves at 3 bar pressure. In these comparisons it must be noted that different PAR designs may have different performance curves. Both the Fischer model and the Sher model are based on the Battelle experiments applicable to the NIS prototype PAR design (EPRI 1993; Fischer 1995; Sher et al. 1995); note that the NIS prototype PAR described in the EPRI (1993) report did not have the taller chimney that was used in the SNL PAR tests.

Because the PAR takes a while to heat up (thermal inertia), it will also be hotter than its equilibrium value (due to the same thermal inertia) as the hydrogen is depleted. This effect should be less pronounced for the 1/8 scale versus the 1/2 scale. This is corroborated by the data. As hydrogen concentration decreased from 2 mole % to 0.5 mole %, the average catalyst temperature decreased about 150 K in PAR-8R and only about 100 K in PAR-13R. The only time the PAR will not affect performance is when hydrogen concentration varies slowly relative to temperature change in the PAR.

6.2 Depletion Rates Under Well-Mixed Conditions

Figures 260 and 261 show depletion rate comparisons between PAR-8R (a non-mixed 1/8 scale test with hydrogen/air/steam mixtures at 2 bar pressure and without mixing fans) and PAR-demo3, PAR-14, PAR-15, and PAR-16 (well-mixed 1/8 scale tests with hydrogen/air mixtures at 2 bar pressure).

The depletion rate for PAR-demo3 was smaller than for PAR-8R. One possible explanation is that a more accurate depletion rate was obtained with the mixing fans running continuously in PAR-demo3 since the PAR was now depleting the entire volume uniformly. The depletion rate calculation assumes that the entire Surtsey volume is being depleted and that the hydrogen concentration in the vessel is uniformly the same concentration as that measured by the GMS at the PAR inlet sample point. However, there may be another explanation. The cartridges in the 1/8 scale PAR have been operated at high temperatures for many hours and the catalyst may have degraded. Tables 3 and 4 show which cartridges were used for each PAR test and give its location in the housing.

The PAR-15 experimental data supports the explanation that a well-mixed vessel will yield a lower depletion rate curve. However, the PAR-14 and the PAR-16 depletion rate data were similar to that seen in PAR-8 (possibly caused by the test anomalies that occurred in PAR-14 and the nature of the PAR-16 test). Therefore, tests performed under well-mixed conditions did not yield definitive evidence that well-mixed conditions reduce the depletion rate.

6.3 Catalyst Temperature and PAR ΔT as Functions of Hydrogen Concentration

The catalyst temperature and the difference in temperature between the PAR inlet and the PAR outlet both provide evidence of PAR performance. Figures 262 and 263 show PAR catalyst temperatures and PAR ΔT as a function of hydrogen concentration during the steady-state

depletion intervals, respectively. The catalyst temperature increased about 96 K for each 1% of hydrogen concentration, regardless of the starting temperature. The PAR ΔT increased about 34 K for each 1% of hydrogen concentration. This is much less than the EPRI PAR results (80 K for each 1 mole % of hydrogen concentration). Note that the SNL PAR tests were performed with an additional 0.5 m tall chimney section. This chimney section probably increased flow through the PAR which reduced the ΔT.

Note that the PAR-13R ΔT data shown in Figure 263 lies well below the norm. Remember that the corner and the edge catalyst cartridge temperatures in PAR-13R were much colder than the middle cartridge temperatures (Figure 169). This anomaly does not show on Figure 262 because it plots the average of the *middle* catalyst thermocouples. This probably caused a lower than expected PAR performance during the depletion interval.

Figures 264 and 265 plot PAR-16 catalyst temperature and PAR-16 ΔT as a function of hydrogen concentration during seven steady-state depletion intervals, respectively. Temperatures are definitely reduced in those intervals with low oxygen concentrations, when compared to other PAR tests (with 10-20 mole % oxygen) and also the last steady-state interval for PAR-16 (starting at 3.7 mole % oxygen).

6.4 Wall Effect

Two counterpart experiments were performed to determine if the placement of a PAR near a wall would affect performance, as compared to placement of a PAR in an open volume. Both tests were performed at 1/8 scale and at 2 bar pressure, with a 50/50 mixture of air and steam. Figures 266 and 267 show the hydrogen moles in Surtsey and the depletion rates, respectively, for PAR-6 (center location) and PAR-9 (wall location). The wall clearly appeared to have an effect at low hydrogen concentrations, yielding a smaller depletion rate as compared to the open volume test. This was probably because the wall impedes natural convective flows.

6.5 Oxygen Limit Effect

The PAR appeared to "slowdown" in the PAR-7 experiment with hydrogen concentration increasing and oxygen concentration decreasing. The PAR "restarted" when oxygen was added. The PAR-8R test was performed at similar conditions; however, oxygen was maintained near 12 mole % throughout the test.

Figures 268 and 269 show the hydrogen moles in Surtsey and the depletion rates, respectively, for PAR-7 (low oxygen) and PAR-8R (excess oxygen). Above 4 mole % hydrogen concentrations, the hydrogen depletion rate in PAR-7 was substantially smaller than in PAR-8R. Reduced oxygen levels did not impact the PAR-7 depletion rate data below 3 mole % hydrogen concentration because oxygen was added in PAR-7 as the hydrogen concentration was about 4 mole % and decreasing.

PAR performance at limited oxygen concentrations was intentionally tested in PAR-16. Figure 270 gives the hydrogen and oxygen concentration history for PAR-16. Figure 271 shows the depletion rate at various times during the PAR-16 experiment. Note that the PAR depleted hydrogen at very low oxygen concentrations; however, oxygen starvation certainly yielded reduced depletion rates (i.e., low oxygen concentrations do limit the amount of hydrogen that can recombine to something less than stoichiometric levels).

6.6 Hydrogen Ignition by the PAR

Deflagrations of hydrogen were seen in the air/steam tests (PAR-8, PAR-10, PAR-13, and PAR-13R experiments) and also in the air-only tests (PAR-demo1, PAR-demo2, and PAR-demo3). There appeared to be two separate ignition sources.

The first ignition source was probably the PAR catalyst hot surface. Surface temperatures greater than 1000 K are in the range for hot surface ignition in 50 mole % steam environments. A large deflagration was seen in PAR-8 after hydrogen was increased from ~9 mole % to ~11 mole %. The peak catalyst temperature was about 1100 K. A large deflagration also was seen in PAR-10 immediately after hydrogen was quickly increased to about ~12-13 mole % (the measured peak hydrogen concentration was only ~11 mole %, probably because the sample system did not have adequate time to purge the sample line and capture the true concentration). The peak catalyst temperature was about 950 K.

Ignition also occurred at much lower hydrogen concentrations (4-5 mole %) and with peak catalyst temperatures in the range of 600-800 K. These surface temperatures are too low to ignite hydrogen. In PAR-13 and PAR-13R, a combination of new and old catalyst cartridges were used. Videos of these and other tests showed small, whitish-looking particles floating in the vessel whenever new cartridges (with undamaged coating on the catalyst pellets) were heated to temperatures above 500 K. In the PAR-13 video, a burn started in the PAR immediately after a burst of these small whitish-looking particles ejected out of the chimney. It is important to note that the cartridges used in the PAR-8 and the PAR-10 experiments were previously subjected to high concentrations of hydrogen and that the hydrophobic coating was mostly destroyed prior to performing these tests.

In the PAR-demo tests, flame fronts were seen descending from above the PAR, ascending from below the PAR, and also exiting the PAR outlet chimney. Some of the ignitions may have been caused by extraneous sources, such as the quartz lamps or friction-induced static discharges. However, since ignition still occurred in later tests when these extraneous sources were eliminated, the actual ignition source still remains unknown. Table 5 summarizes the conditions in the vessel and in the PAR immediately prior to the hydrogen burns.

7.0 Depletion Rate Calculations Using Velocity Measurements

The KURZ thermal anemometer was calibrated at the manufacturers using *air* at 25°C and at 1 atmosphere pressure. The specified range and accuracy of the Series 450 insertion mass flow element is approximately 0-6 m/s and ± 2% reading, respectively. Note that the thermal anemometer measures a mass rate normalized to a standard density and therefore yields a standard velocity in units of Standard Meters Per Second (SMPS).

Standard velocity =

$$V_s = \rho V / \rho_s \qquad (4)$$

where

ρ = actual density (kg/m^3)
V = actual velocity (m/s)
ρ_s = standard air density (1.186 kg/m^3).

The bi-directional velocity probe (or pitot-tube probe) (Kent and Schneider, 1987) provides gas velocity using the following equation.

$$V = \sqrt{\frac{\Delta P}{1/2\rho C^2}} \qquad (5)$$

where

ΔP = differential pressure across the probe (Pa)
C = calibration constant for the probe (1.5).

Since the gas at the chimney outlet was essentially air in PAR-2, conversion of standard velocity to actual velocity requires only scaling the result for the gas density according to the ideal gas law.

Actual velocity =

$$V = V_s(P_s / P_a)(T_a / T_s) \qquad (6)$$

where

V = actual velocity (m/s)
P_s = standard pressure in absolute units (0.101 MPa)
P_a = actual pressure in absolute units
T_s = standard temperature in absolute units (298 K)
T_a = actual temperature in absolute units.

Measurements from the vessel pressure transducers and the thermocouples at the chimney exit were used with Equation 6 to convert the hot-wire signals to actual velocity.

The pitot-tube pressure transducer data (in voltage units) at the PAR inlet and the chimney outlet was converted to differential pressure (Pa) using the following conversions along with Equation 5.

ΔP (inlet) = inlet volts x 7.5658 Pa/volt
ΔP (outlet) = outlet volts x 7.6220 Pa/volt.

The pitot-tube probes were calibrated; a calibration constant of 1.5 was determined. This was slightly different than the 1.07 calibration constant used by Kent and Schneider (1987). The difference can be attributed to a modified probe design that utilized a slotted cutout on the static side (to drain steam condensate). The density in Equation 5 was calculated using thermocouple data at the PAR inlet and chimney outlet and assuming that the gas composition was 100% air. The pitot-tube at the PAR inlet did not yield good results, probably because the differential pressure was too small (tenths of inches of water). Better data was provided by the outlet pitot-tube probe because the flow is focused by the chimney (note that the outlet pitot-tube velocity is within a factor of 2 calculated from the thermal anemometer data).

A volumetric flow rate must be calculated in order to use the velocity measurement for depletion rate calculations. The thermal anemometer measures standard volumetric flow by the following equation:

$$Standard\ Volumetric\ Flow = F_s = Area\ x\ V_s \qquad (7)$$

where the Area is equal to the cross-sectional area of the chimney (0.25 m^2 for the 1/2 scale PAR).

The actual volumetric flow is determined by scaling the result for the gas density according to the ideal gas law:

$$Actual\ Volumetric\ Flow = F_a = F_s (P_s / P_a) (T_a / T_s) \qquad (8)$$

Figure 272 shows the time-dependent volumetric flow rate at the PAR inlet using the thermal anemometer measurements. A correction factor of 0.8 was applied to the flow in order to convert the local peak velocity measurement to an average velocity (Bird et al., 1960). This was based upon assuming average flow velocity in turbulent tube flow (for ease of calculation) and using a hydraulic diameter of 0.25 m. Note that volumetric flow rate at the PAR inlet can be obtained by scaling the PAR chimney outlet results by the PAR inlet temperature (i.e., x T_{inlet}/T_{outlet}).

A check on the volumetric flow rate calculation can be performed. Fischer (1995) found that the experiment results obtained at Battelle were best fit by assuming flow rate is an exponential function of the volume fraction of hydrogen:

$$Q = 0.67\, C_H^{0.307} \qquad \textbf{(9)}$$

where

Q	=	steady-state volumetric flow (m^3/s)
C_H	=	hydrogen volume fraction in the containment.

This equation was based on the prototype full-scale PAR. In order to use Equation 9, the hydrogen concentration must be determined. Figure 273 shows the hydrogen concentration in PAR-2 as measured at the PAR inlet. Figure 274 then compares the PAR-2 volumetric flow rate data to the Fischer equation, scaled by a factor of 2 to match the 1/2 scale PAR used in the PAR-2 experiment. The flow rate in PAR-2 exceeds the flow rate predicted by the Fischer model. This higher flow rate is expected since the PAR-2 test was performed with the additional 0.5 m chimney.

A depletion rate can be determined using the volumetric flow rate measurements. The hydrogen removal rate (in kg/hr) for the PAR can be calculated using:

$$R = \varepsilon\, Q\, \rho_H \qquad \textbf{(10)}$$

where

ε	=	efficiency factor for hydrogen removal
Q	=	volumetric flow rate of containment gas through the PAR (m^3/hr)
ρ_H	=	mass density of hydrogen in the PAR (kg/m^3).

The density of the hydrogen gas at the PAR inlet was calculated using:

$$\rho_H = X_H \frac{P}{R_H T} \qquad \textbf{(11)}$$

where

X_H	=	hydrogen molar fraction at the PAR inlet (from Figure 273)
P	=	vessel pressure (Pa)
R_H	=	hydrogen gas constant (4124)
T	=	temperature at the PAR inlet (K).

Figure 275 compares the hydrogen depletion rate calculated by two methods. The first method is based on the measured rate of change of hydrogen concentration (dM/dt method) described in Section 6.0 Figure 275 shows the curve giving the fit of the data from the PAR-4 (1/2 scale) test. Figure 275 also shows the depletion rate for the PAR-2 experiment using Equation 10 (velocity

method). An efficiency factor of 0.85 was used to be consistent with that recommended by Fischer (1995).

The two depletion rate methods yielded almost identical results for the PAR-2 experiment. This exercise can be repeated for other tests; however, the conversion of the standard velocity to actual velocity cannot be performed with confidence on the hot-wire anemometer data for the majority of the tests due to the lack of *air/steam* gas mixture calibration data.

8.0 Summary

Performance tests of a scaled passive autocatalytic recombiner (PAR) were performed in the Surtsey test vessel at Sandia National Laboratories. The test program included experiments to: 1) define the startup characteristics of PARs, 2) confirm a hydrogen depletion rate curve of PARs, 3) define the PAR performance in the presence of steam, 4) evaluate the effect of scale (number of cartridges) on the PAR performance at both low and high hydrogen concentrations, 5) define the PAR performance with and without the hydrophobic coat, 6) determine if the PAR could ignite hydrogen mixtures, 7) define the PAR performance in well-mixed conditions, and 8) define the PAR performance in the presence of low oxygen concentrations.

The following conclusions can be made. The PAR started immediately with low concentrations of hydrogen (0.2 mole %) in cold air atmospheres. The PAR startup was delayed about 2 hours in a test with a low concentration of hydrogen (0.4 mole %) in a hot, steamy atmosphere. The PAR started in about 10 minutes in hot, steamy atmospheres when exposed to hydrogen concentrations in the range of 3-5 mole %.

The SNL test results were compared to published depletion rate data based on the Battelle experiments that used the NIS prototype PAR design (EPRI 1993; Fischer 1995; Sher et al. 1995). The comparison shows that the SNL test data correlates reasonably well to the published Battelle depletion rate data. Differences in the depletion rates are probably due to differences in PAR designs and test methodology and analysis.

The PAR appeared to generate a convective flow loop in the Surtsey vessel from the PAR outlet to the dome, down the Surtsey wall until reaching a height near the PAR inlet, and then returned to the PAR inlet. This was shown by the relatively flat and equal temperatures from the thermocouples located at elevations below the PAR. The loop appeared to drive further downward below the PAR with higher hydrogen concentrations and also with larger PAR scale. Also, the hydrogen concentrations from the sample point located near the floor showed small decreases over time, as compared to the other sample points.

Assuming a well-mixed condition in the vessel, the hydrogen depletion rate is most likely proportional to scale. Assuming well-mixed conditions, the Fischer correlation (Fischer, 1995) is well within the range of the Surtsey PAR test depletion rate data. The parameter that affects scale proportionality is the well-mixed assumption in the methodology used to determine the depletion rate. Since the PAR only consumes hydrogen in a portion of the total vessel volume, the depletion rate calculation can overpredict consumption. The depletion rate measurements then become scale-dependent since tests with larger scale and/or higher concentrations appear to deplete larger pockets of hydrogen within the total vessel volume.

Two counterpart experiments were performed to determine if the lack of the hydrophobic coating would cause a startup delay in tests with hot, steamy environments and hydrogen concentrations > 5 mole %. A startup delay of about 18 minutes occurred in the test with no coating, as compared to the test with the hydrophobic coating, which had a startup delay of 7 minutes.

Ignition of hydrogen by PARs is possible. The ignition source is suspected to be the high surface temperature of the catalyst at high hydrogen concentrations. Additional experiments will be necessary to determine and verify the source of ignition.

The oxygen limit effect was intentionally tested. The PAR depleted hydrogen at very low oxygen concentrations; however, oxygen starvation certainly yielded reduced depletion rates and PAR temperatures (i.e., low oxygen concentrations do limit the amount of hydrogen that can recombine at rates less than those observed at stoichiometric levels).

Counterpart experiments determined that the placement of a PAR near a wall yielded depletion rates smaller than those obtained with the PAR placed in the middle of the facility.

9.0 References

1. Bird, R., W. Stewart, and E. Lightfoot, 1960, "Transport Phenomena," John Wiley & Sons, New York, 1960.

2. Blanchat, T. K., M. D. Allen, M. Pilch, and R. T. Nichols, 1994, "Experiments to Investigate Direct Containment Heating Phenomena with Scaled Models of the Surry Nuclear Power Plant," NUREG/CR-6152, SAND93-2519, Sandia National Laboratories, Albuquerque, NM, June 1994.

3. Electric Power Research Institute (EPRI), 1993, "Qualification of Passive Autocatalytic Recombiners for Combustion Gas Control in ALWR Containments," Electric Power Research Institute, Advanced Light Water Reactor Program, Palo Alto, CA, April 8, 1993.

4. Fischer, K., 1995, "Qualification of a Passive Catalytic for Hydrogen Mitigation," *Nuclear Technology*, Vol. 112, October 1995.

5. Kent, L. and M. Schneider, 1987, "The Design and Application of Bi-directional Velocity Probes for Measurements in Large Pool Fires," ISA Transactions, Vol. 26, No. 4, 1987.

6. Sher. R., J. Li, and D.E. Leaver, 1995, "Models for Evaluating the Performance of Passive Autocatalytic Recombiners (PARs)," 1995 National Heat Transfer Conference, *ANS Proceedings HTC, Vol. 8*, Portland, OR, August 5-9, 1995.

Table 1. PAR instrumentation (continued)

Channel Number	Description*	Units
21	Vessel Pressure Kulite BM-1100	psia
22	Vessel Pressure Kulite BM-1100	psia
23	Vessel Pressure Kulite BM-1100	psia
24	Vessel Pressure Precise Sensor 555	psia
25	H_2 Manifold Pressure	psig
26	O_2 Manifold Pressure	psig
27	Boiler Pressure	psig
20	Hygrometer Temperature	°C
19	Hygrometer Dew Point	°C
17	Mass Flow Meter	SMPS
16	Pitot Tube Inlet	Volts
15	Pitot Tube Outlet	Volts
12	Mass Spec Pressure	Volts
31	Pressure H_2 Vessel side of MFC	psia
32	Pressure H_2 Regulator side of MFC	psia
33	Pressure O_2 Vessel side of MFC	psia
34	Pressure O_2 Regulator side of MFC	psia
35	H_2 Manifold Temp	°C
36	O_2 Manifold Temp	°C
37	H_2 MFC Inlet Temp	°C
38	O_2 MFC Inlet Temp	°C
41	TC Array A1	°C
42	TC Array A2	°C
43	TC Array A3	°C
44	TC Array A4	°C
45	TC Array A5	°C
46	Mass Spec	°C
47	TC Array A7	°C
48	TC Array A8	°C
49	TC Array A9	°C
50	TC Array A10	°C
51	TC Array B1	°C
52	TC Array B2	°C
53	TC Array B3	°C
54	TC Array B4	°C
55	TC Array B5	°C
56	TC Array B6	°C
57	TC Array B7	°C

Table 1. PAR instrumentation (continued)

Channel Number	Description*	Units
58	TC Array B8	°C
59	TC Array B9	°C
60	TC Array B10	°C
61	Surtsey Shell 1	°C
62	Surtsey Shell 2	°C
63	Surtsey Shell 3	°C
64	Surtsey Shell 4	°C
65	Surtsey Shell 5	°C
66	Surtsey Shell 6	°C
67	Mass Spec Cabinet	°C
68	H_2 Diffuser	°C
90	O_2 Diffuser	°C
91	Hygrometer Temp	°C
92	Atmosphere Temp	°C
93	Corner Gap 3	°C
68	PAR in Middle	°C
69	PAR in Middle	°C
70	PAR in Edge	°C
71	PAR in Edge	°C
84	PAR out Middle	°C
85	PAR out Middle	°C
86	PAR out Edge	°C
87	PAR out Edge	°C
72	Middle Cartridge 1	°C
73	Middle Cartridge 2	°C
74	Middle Cartridge 3	°C
75	Middle Gap 1	°C
76	Middle Gap 2	°C
77	Middle Gap 3	°C
78	Edge Cartridge 1	°C
79	Edge Cartridge 2	°C
94	Edge Cartridge 3	°C
81	Edge Gap 1	°C
82	Edge Gap 2	°C
83	Edge Gap 3	°C
95	Middle Cartridge backup 1	°C
[illegible]	Middle Cartridge backup 2	°C
97	Middle Cartridge backup 3	°C
99	Middle Gap backup 1	°C
100	Middle Gap backup 2	°C

Table 1. PAR instrumentation (continued)

Channel Number	Description*	Units
101	Middle Gap backup 3	°C
102	Corner Cartridge 1	°C
103	Corner Cartridge 2	°C
104	Corner Cartridge 3	°C
105	Corner Gap 1	°C
106	Corner Gap 2	°C

*All temperature measurements used Type-K thermocouples.

Table 2. PA[illegible] test matrix

Test	Purpose	Scale	Atmosphere
1	Startup in Air Find $X_{H2, air\ start}$	1/2	2 bar air, no steam, 0.2%, 0.4%, 0.6% H_2...$X_{H2, air\ start}$
2	Performance at Startup	1/2	2 bar air, no steam, inject $X_{H2, start}$ (single injection)
3	Startup in Air/Steam Find $X_{H2, air/steam\ start}$	1/2	1 bar air, 1 bar steam, 0.2%, 0.4%, 0.6% H_2...$X_{H2, air/steam\ start}$
4	Scale/depletion rate without startup transient	1/2	1 bar air, 1 bar steam, continuous injection to maintain 1.4% H_2 until PAR reaches steady-state (SS)
5	Scale/depletion rate wit[illegible] startup transient	1/4	1 bar air, 1 bar steam, continuous injection to maintain 1.4% H_2 until PAR reaches SS (same as PAR-4)
6	Scale/depletion rate without startup transient	1/8	1 bar air, 1 bar steam, continuous injection to maintain 1.4% H_2 until PAR reaches SS (same as PAR-4)
7	Performance (this test will destroy the hydrophobic coating)	1/8	1 bar air, 1 bar steam, continuous injection to maintain 7.0% H_2 until PAR reaches SS
8 8R	Performance (without the hydrophobic coating)	1/8	1 bar air, 1 bar steam, continuous injection to maintain 7.0% H_2 until PAR reaches SS (same as PAR-7)
9	PAR at wall to measure short circuit effects (use new catalyst with intact hydrophobic coating)	1/8	1 bar air, 1 bar steam, continuous injection to maintain 1.4% H_2 until PAR reaches SS (same as PAR-6)
10	Hydrogen ignition by PAR PAR back to vessel centerline	1/8	1 bar air, 1 bar steam, quick injection of 10% H_2
12	Performance/scale/depletion rate without startup transient	1/4	1 bar air, 1 bar steam, continuous injection to maintain 7.0% H_2 until PAR reaches SS (same as PAR-7)
13 13R	Performance/scale/depletion rate without startup transient	1/2	1 bar air, 1 bar steam, continuous injection to maintain 7.0% H_2 until PAR reaches SS (same as PAR-7)

Table 2. PAR test matrix (continued)

Test	Purpose	Scale	Atmosphere
demo1 demo2 demo3	Performance/depletion rate in a well-mixed environment	1/8	2 bar air, no steam, continuous mixing, 6.0-10.0% H_2
14	Performance/depletion rate in a well-mixed environment (new catalyst)	1/8	2 bar air, no steam, continuous mixing, 2.0% H_2
15	Performance/depletion rate in a well-mixed environment (same catalyst as PAR-14)	1/8	2 bar air, no steam, continuous mixing, 2.0% H_2
16	Performance in low oxygen environment (same catalyst as PAR-14)	1/8	2 bar nitrogen, no steam, continuous mixing, 2.0-4.0% H_2, 0.0-4.0% O_2

Table 3. Cartridge location in the PAR tests (left to right)

Cartridge	PAR 1 PAR-2 PAR-3 PAR-4	PAR 5 *	PAR 6 PAR-7 PAR-8 PAR-10	PAR 9	PAR 12	PAR 13 PAR-13R	PAR 8R	PAR demo1 PAR demo2 PAR demo3
Scale	1/2	1/4	1/8	1/8	1/4	1/2	1/8	1/8
4167/CA/1	2	2			2	2		
4167/CA/2	1	1			3	3		
4167/CA/3	3	3			4	4		
4167/CA/4	4	4			5	5		
4167/CA/5	5	5			6	6		
4167/CA/6	6	6			7	7		
4167/CA/7	7	7		1	1	1	11	11
4167/CA/8	8	8		8	8	8		
4167/CA/9	9	9			9	9		
4167/CA/10	10	10			10	10		
4167/CA/11	11	13		6	13	11		
4167/CA/12	12	14		4	14	12		
4167/CA/13	13	15		10	15	13		
4167/CA/14	14	16		9	16	14		
4167/CA/16	15	17		5	11	22	7	7
4167/CA/17	16	18		11	22	44	1	1
4167/CA/18	17	19		7	12	23	5	5
4167/CA/19	18	20		2	17	15		
4167/CA/20	19				18	16		
4167/CA/21	20				19	17		
4167/CA/22	21	11				33	6	6
4167/CA/23	22	21		3	20	18		
4167/CA/24	23	12			21	19		
4167/CA/25	24		2			42		
4167/CA/26	25		3			40		
4167/CA/27	26		4			25		
4167/CA/28	27		6			24		
4167/CA/29	28					26		
4167/CA/30	29					32	10	10
4167/CA/31	30					31	9	9
4167/CA/32	31					30		
4167/CA/33	32					29		
4167/CA/34	33					21	3	3
4167/CA/35	34					20	2	2
4167/CA/36	35					27		
4167/CA/37	36					28	8	8
4167/CA/38	37		8			43		
4167/CA/39	38		10			41		
4167/CA/40	39		11			35		
4167/CA/41	40		9			39		
4167/CA/42	41		5			37		
4167/CA/43	42		1			38		
4167/CA/44	45	22				34	4	4
4167/CA/45	44		7			36		
4167/CA/46								

* Computer locked up while testing auto add controls after the PAR-5 test, about 900 psi (from 1 bottle) was added to Surtsey (this raised H_2 to about 1.6%, catalyst temperatures reached ~280°C for about 1000 s).

Table 4. Cartridge location in the PAR-14, -15, and -16 tests (left to right)

Cartridge	PAR 14 PAR-15 PAR-16
Scale	1/8
4542/CA/1	8
4542/CA/2	9
4542/CA/3	10
4542/CA/4	5
4542/CA/5	3
4542/CA/6	2
4542/CA/7	7
4542/CA/8	1
4542/CA/9	11
4542/CA/10	6
4542/CA/11	4

Table 5. Initial conditions prior to the hydrogen burn

PAR	H_2 (%)	O_2 (%)	Steam (%)	P_{vessel} (MPa)	T_{vessel} (K)	$T_{catalyst}$ (K)	ΔT (K)	Scale	ΔP (MPa)	Notes
8	11.0	9	48	0.26	392	1140	280	1/8	0.30	1
10	13.0	13	48	0.25	380	950	70	1/8	0.39	
13	4.4	12	50	0.24	378	880	20	1/2	0.02	1,2,3
13	5.5	12	50	0.26	380	780	10	1/2	0.06	1,2,3,5
13	4.0	11.5	55	0.30	415	800	160	1/2	0.04	1,2,3
13R	6.0	15	46	0.25	380	740	90	1/2	0.05	1,2,3
13R	6.0	14	46	0.27	410	880	140	1/2	0.03	1,2,3
demo1	7.0	20	6	0.24	320	840	170	1/8	0.15	2,6
demo1	6.8	15	1	0.24	330	820	160	1/8	0.07	2,6,7
demo1	8.5	13	2	0.25	340	1020	220	1/8	0.30	2,5,7,8
demo2	11.0	19	0	0.22	310	680	35	1/8	0.47	2,4,7,8
demo3	6.0	19	1	0.23	320	850	160	1/8	0.04	6,7,8

Notes:

1) during O_2 add
2) during H_2 add
3) white particles floating in vessel
4) flame front from floor
5) flame front from PAR outlet
6) flame front from ceiling
7) no hot-wire anemometer
8) no quartz lamps

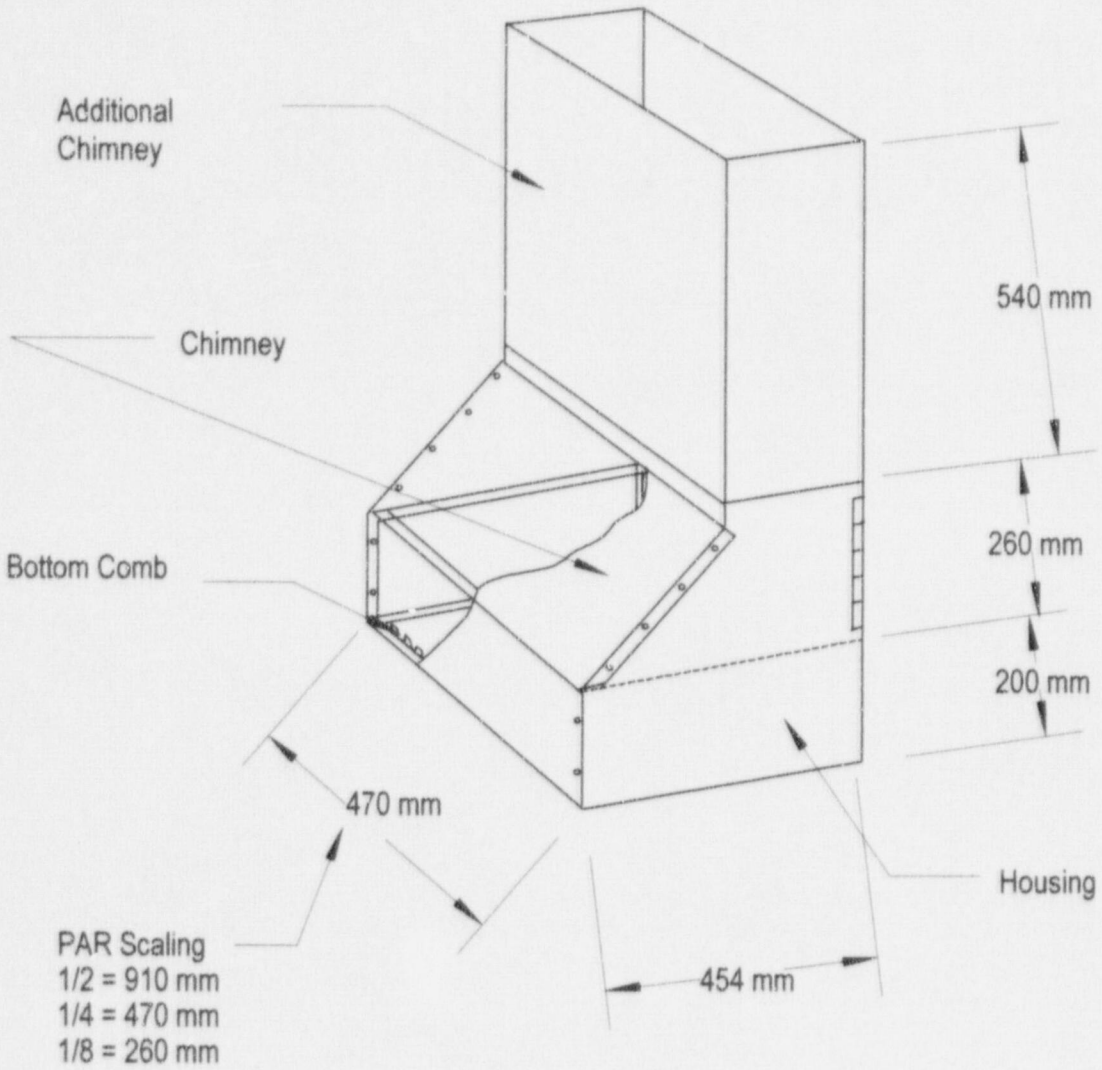

Figure 1. 1/4 scale PAR test module housing.

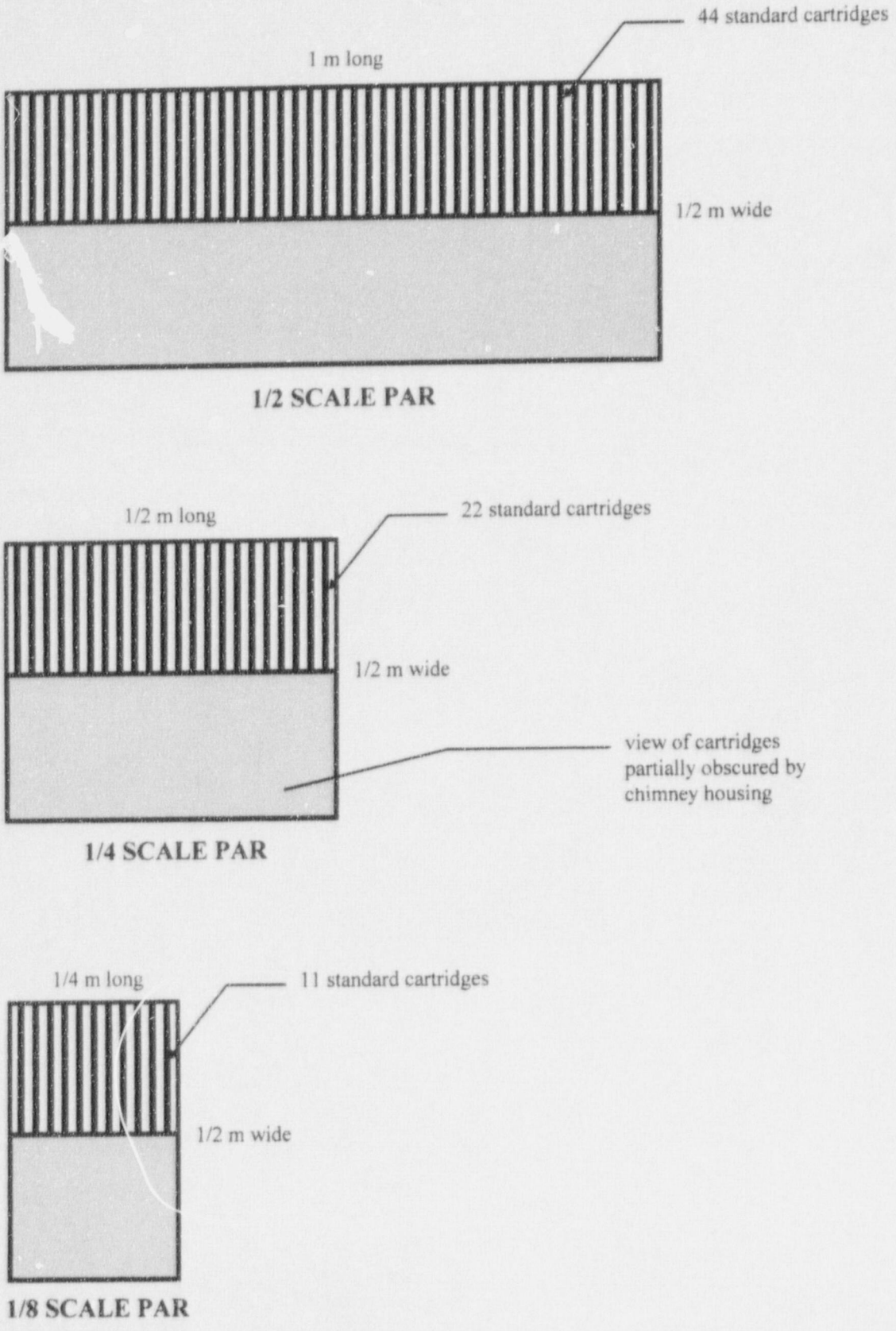

Figure 2 Top View of the RWE/NIS PAR Module (assembled for 1/2, 1/4, and 1/8 scale tests).

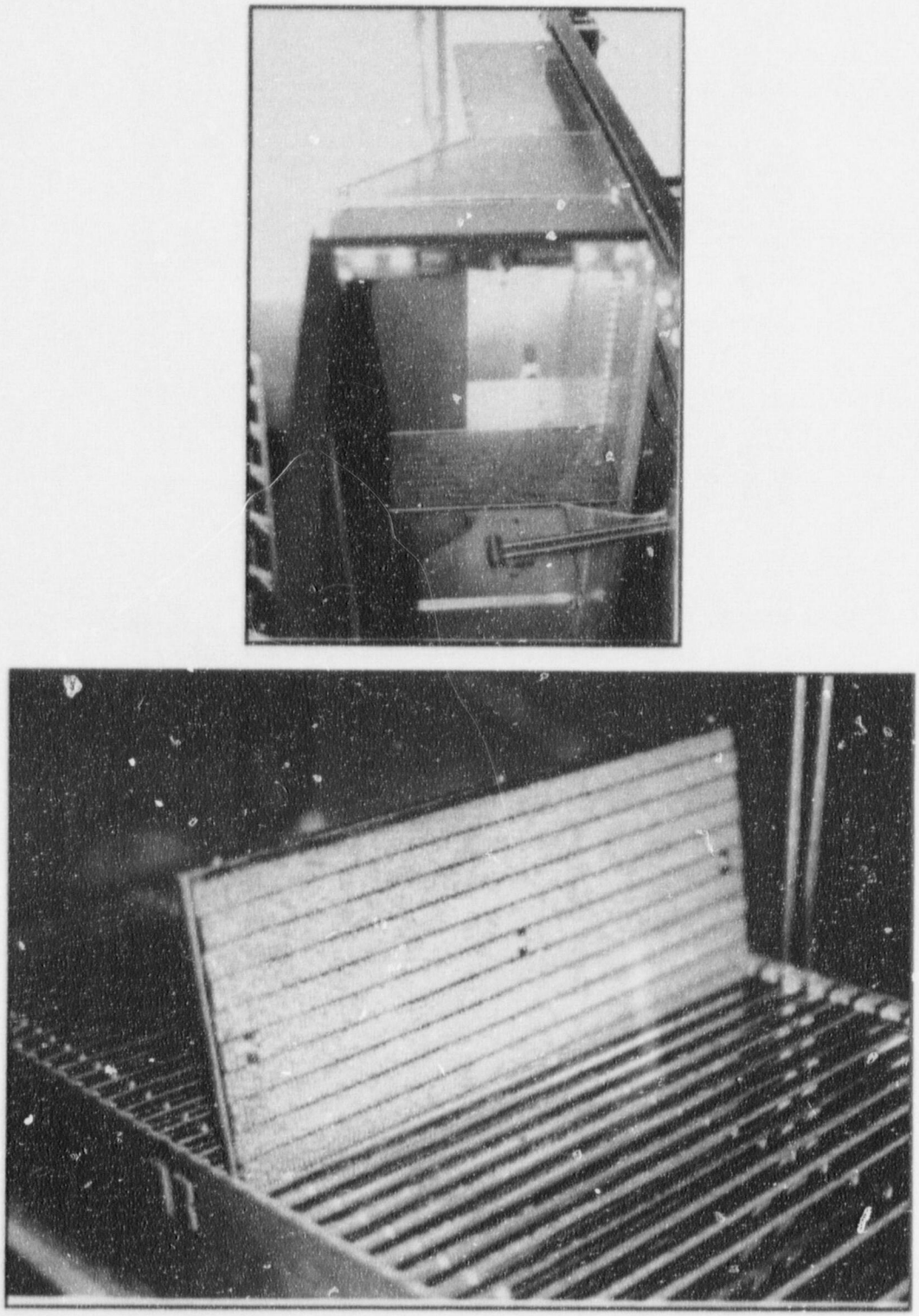

Figure 3. Cartridges held in a vertical configuration by the PAR housing.

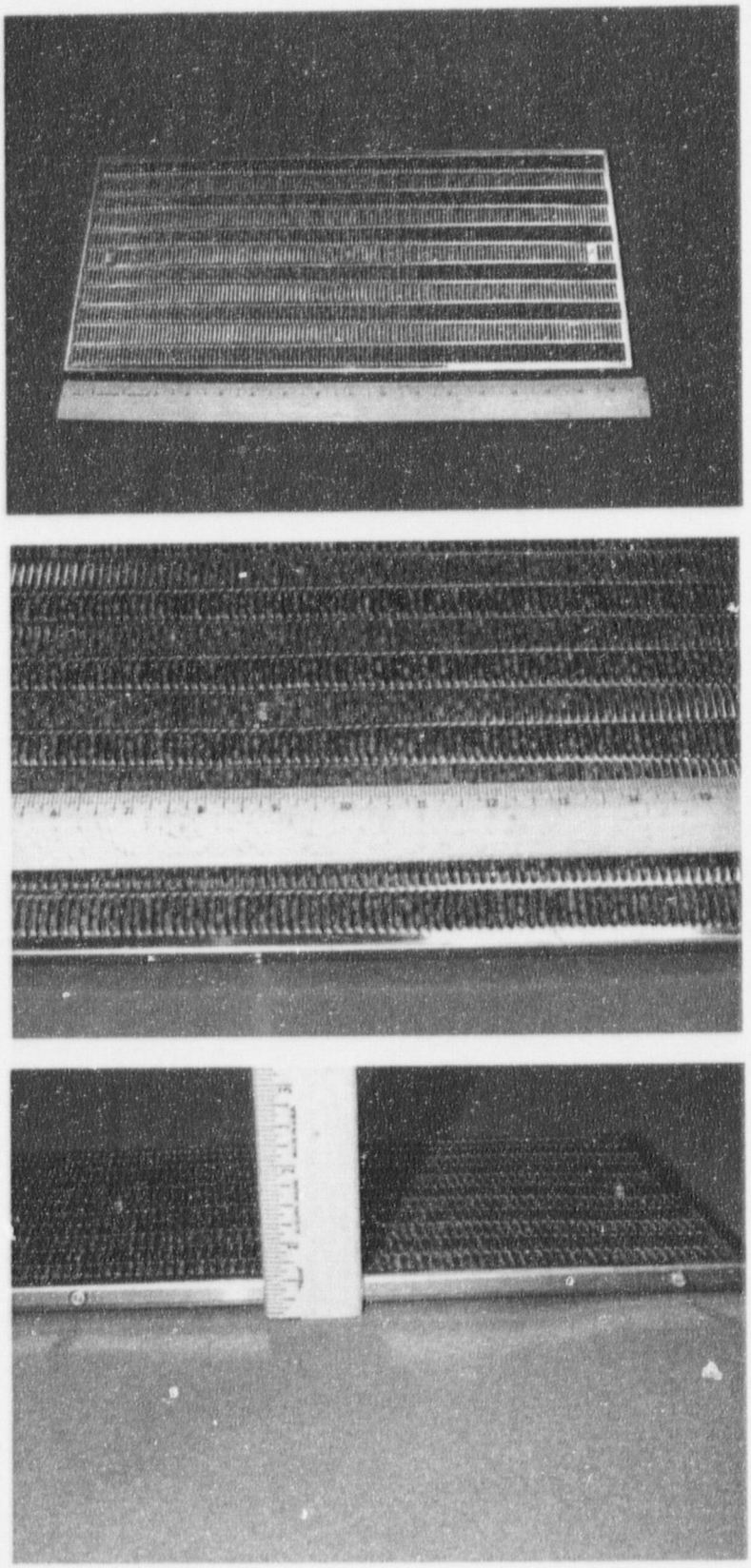

Figure 4. PAR cartridge and catalyst pellets.

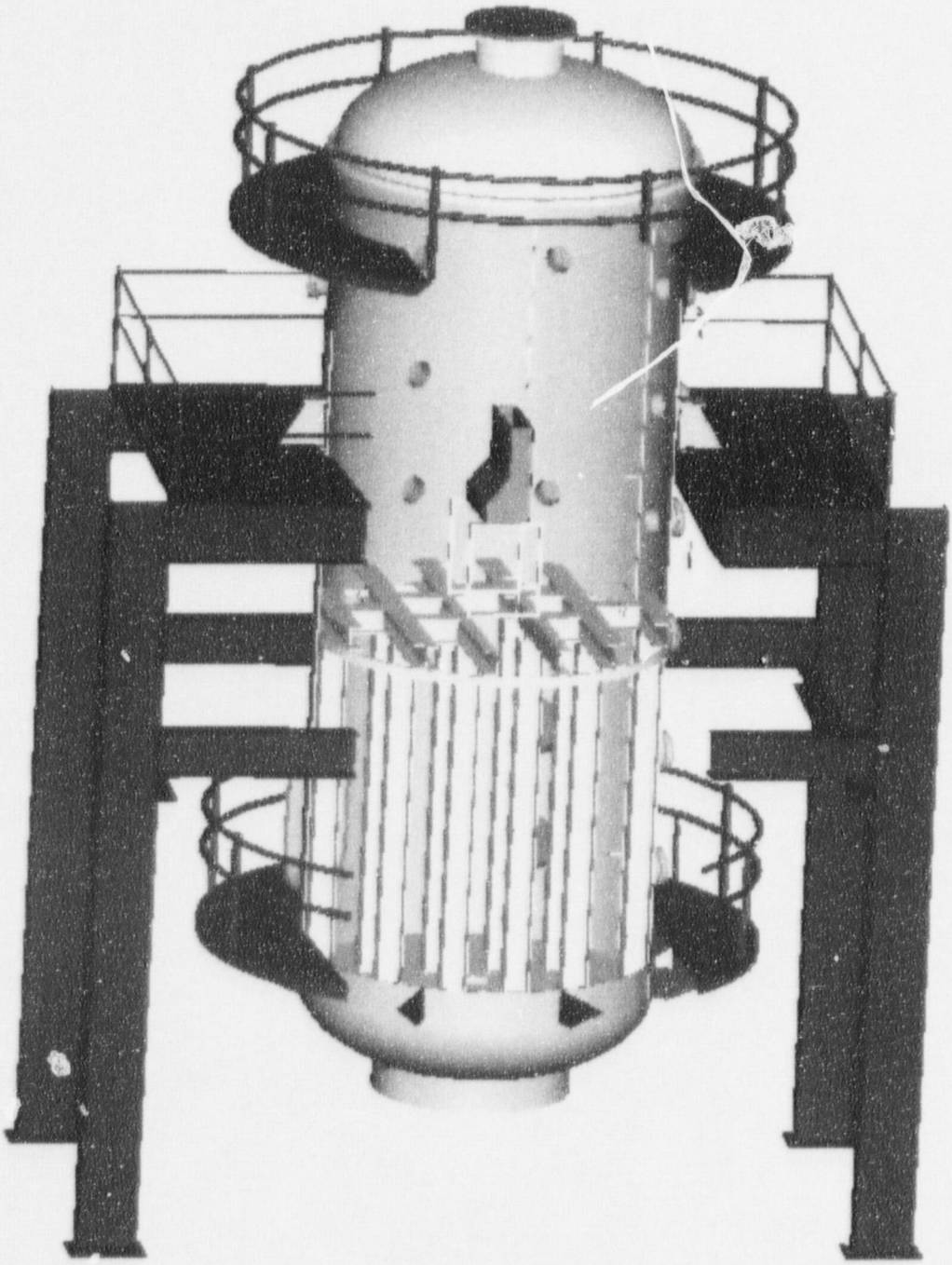

Figure 5. PAR location in the Surtsey vessel.

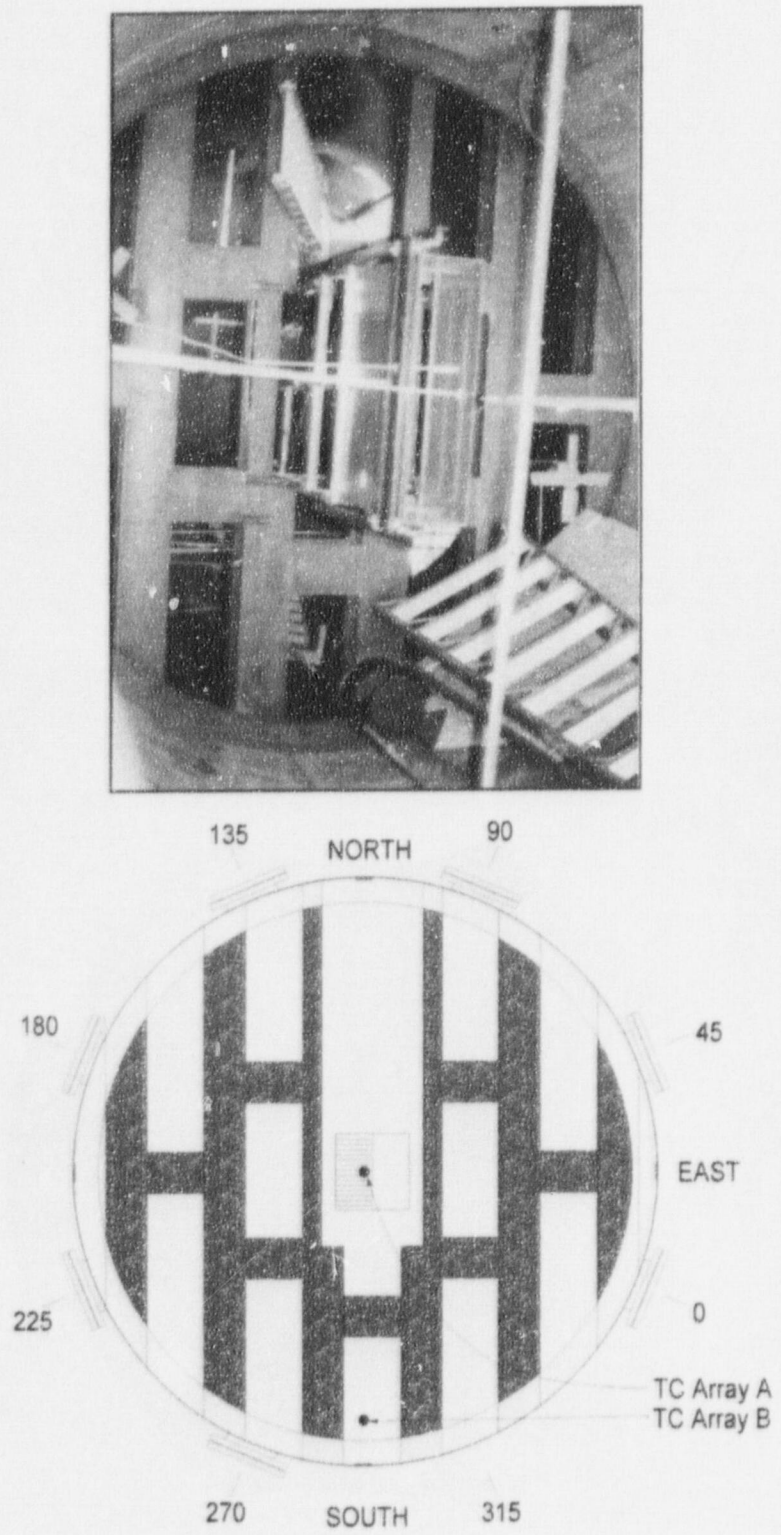

Figure 6. Top view of the PAR housing and location above the support beams.

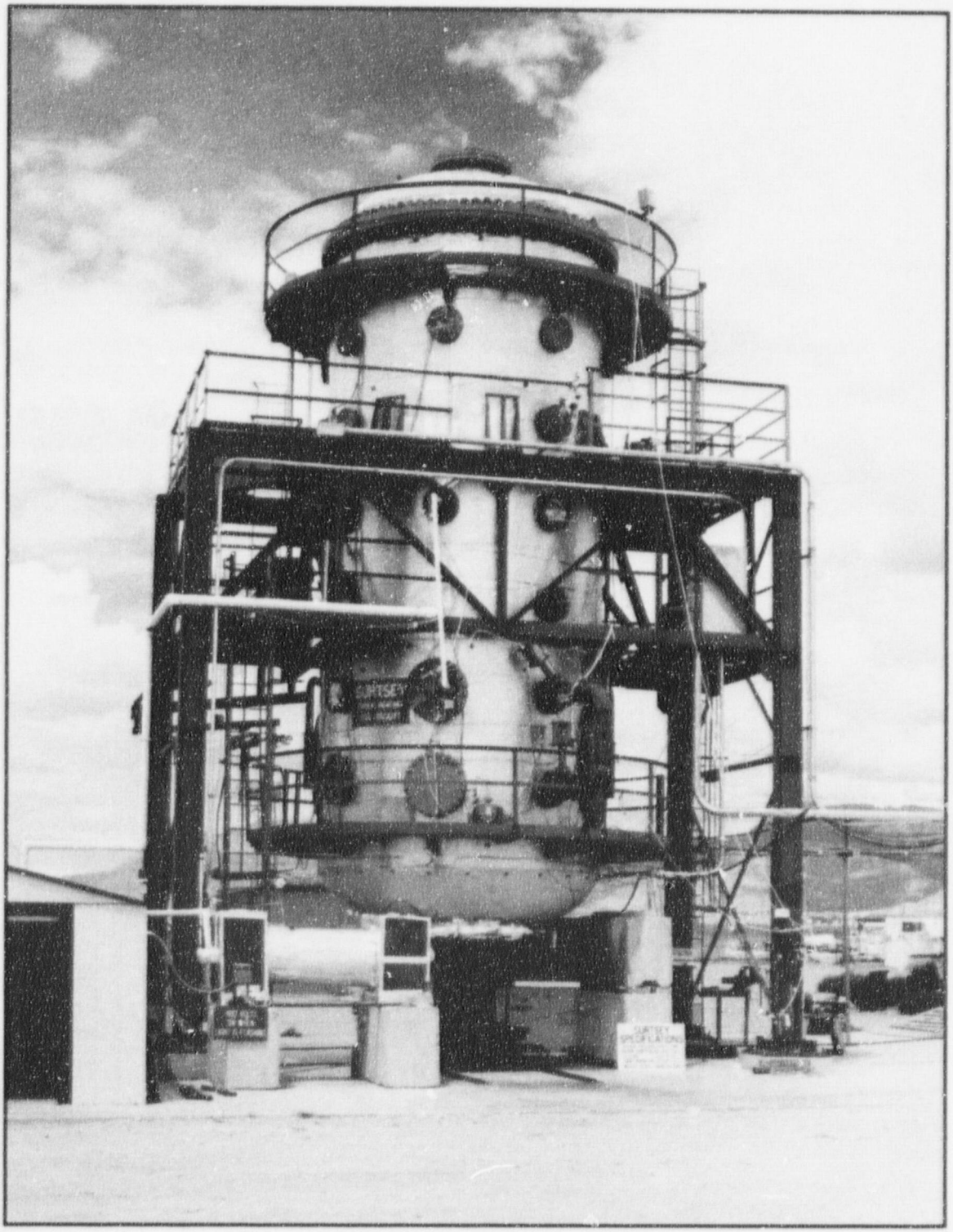

Figure 7. The Surtsey vessel.

Figure 8. Surtsey vessel ports used for steam, gas, instrumentation, and video services.

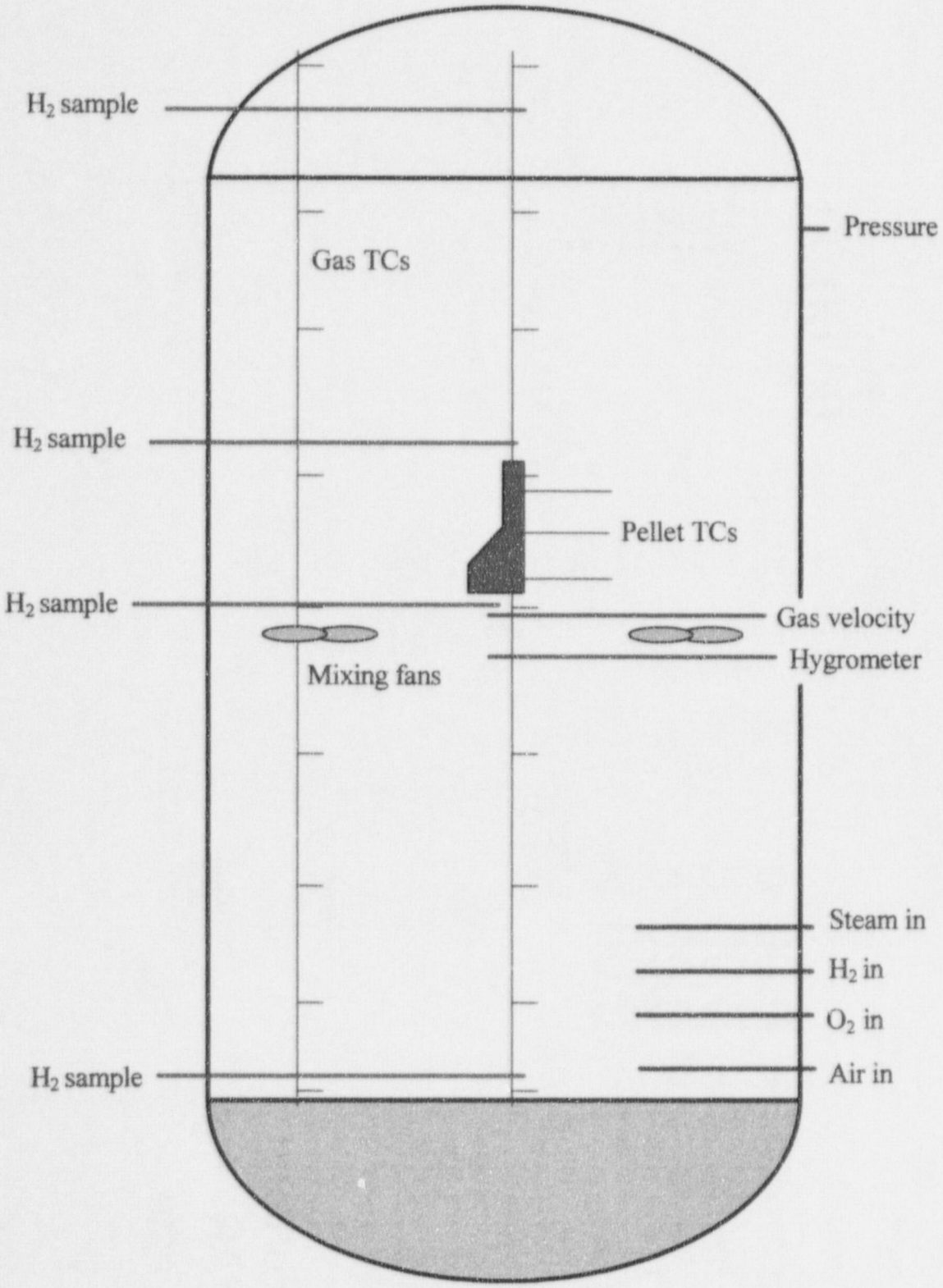

Figure 9. PAR instrumentation and systems.

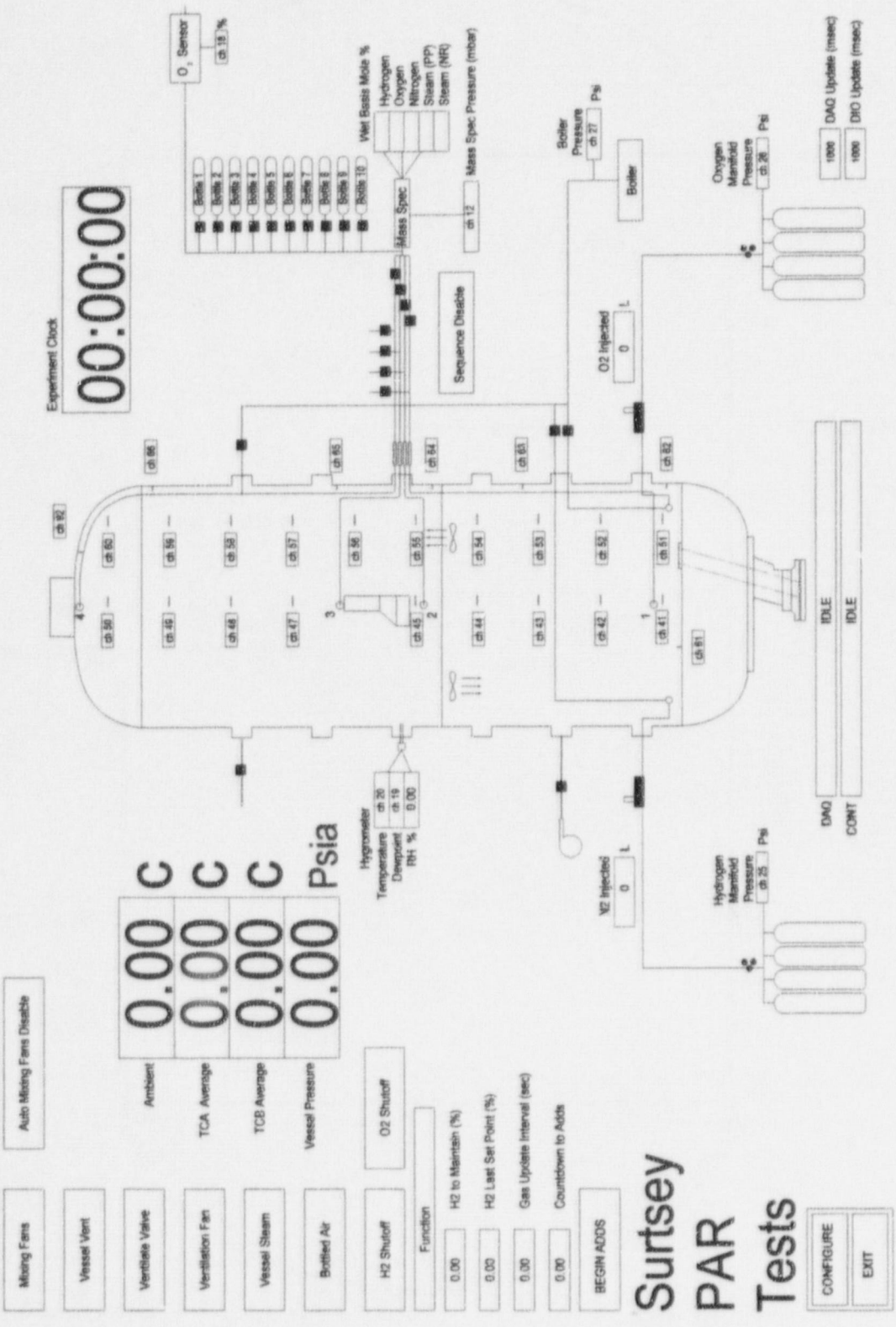

Figure 10. The PC-based control panel for the PAR experiments.

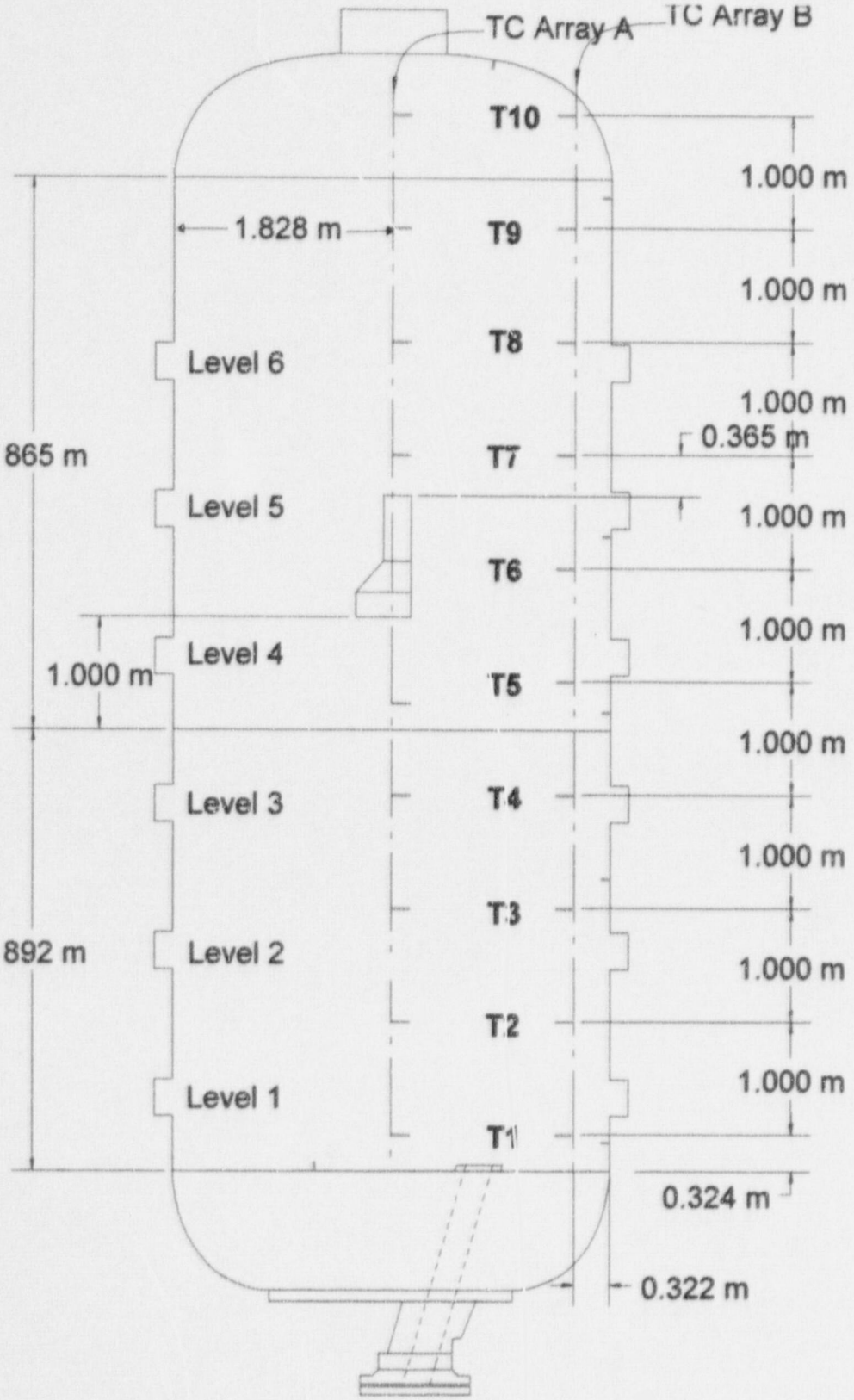

Figure 11. Locations of the vertical thermocouple arrays in the Surtsey vessel.

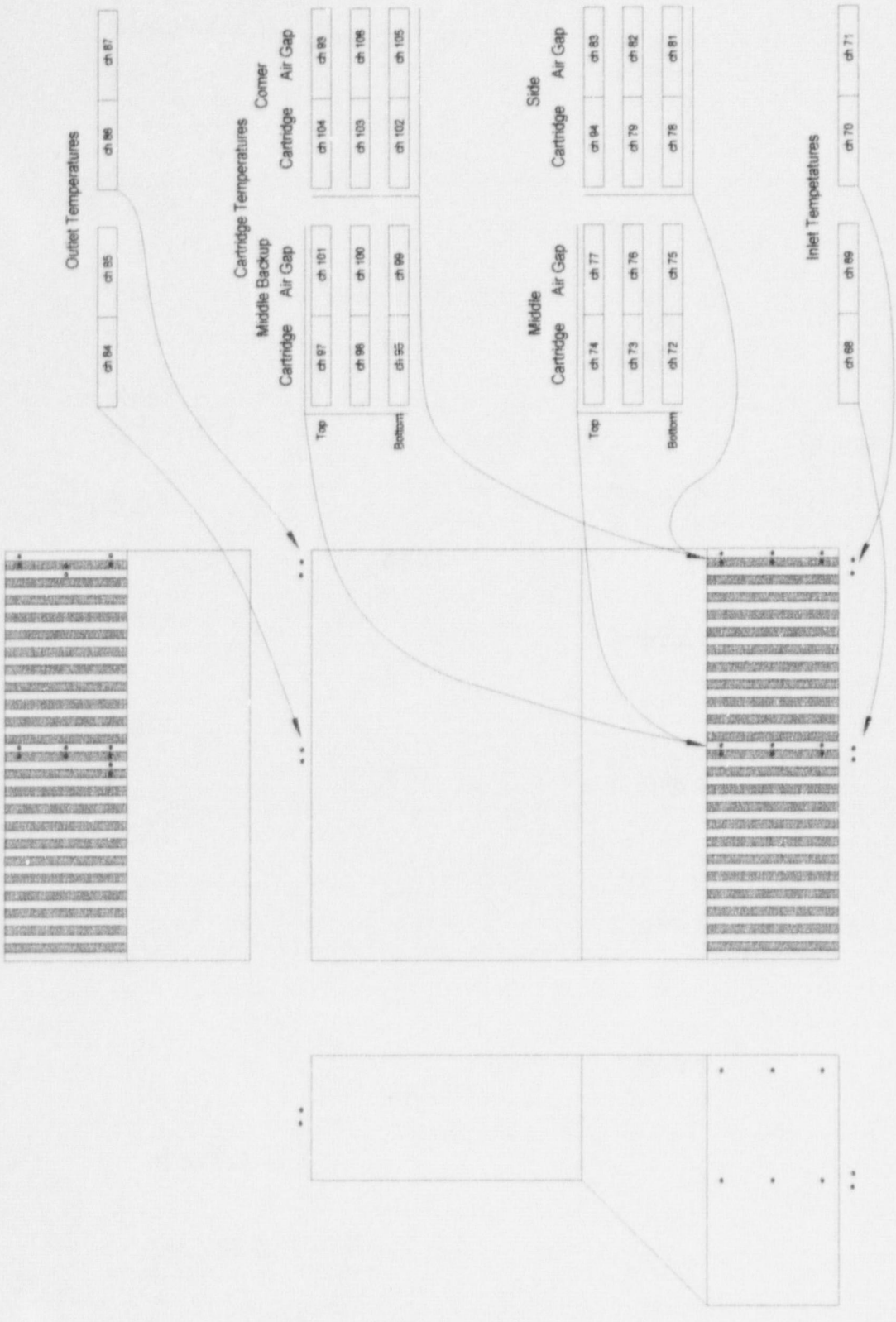

Figure 12. PAR catalyst and gap thermocouple locations.

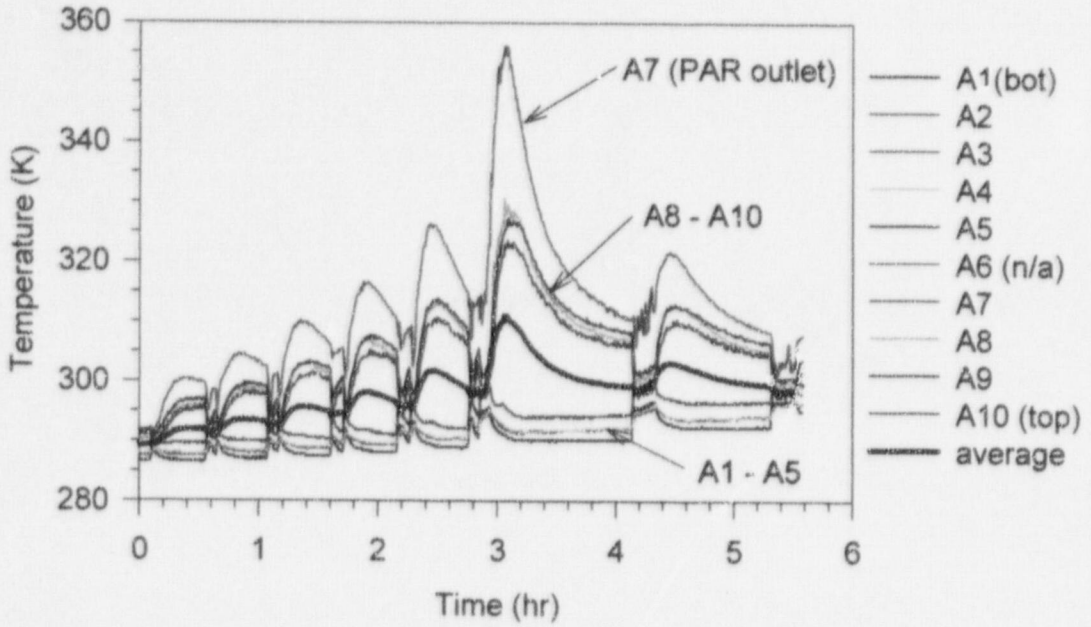

Figure 13. Surtsey vessel centerline gas temperatures from TC array A in PAR-1.

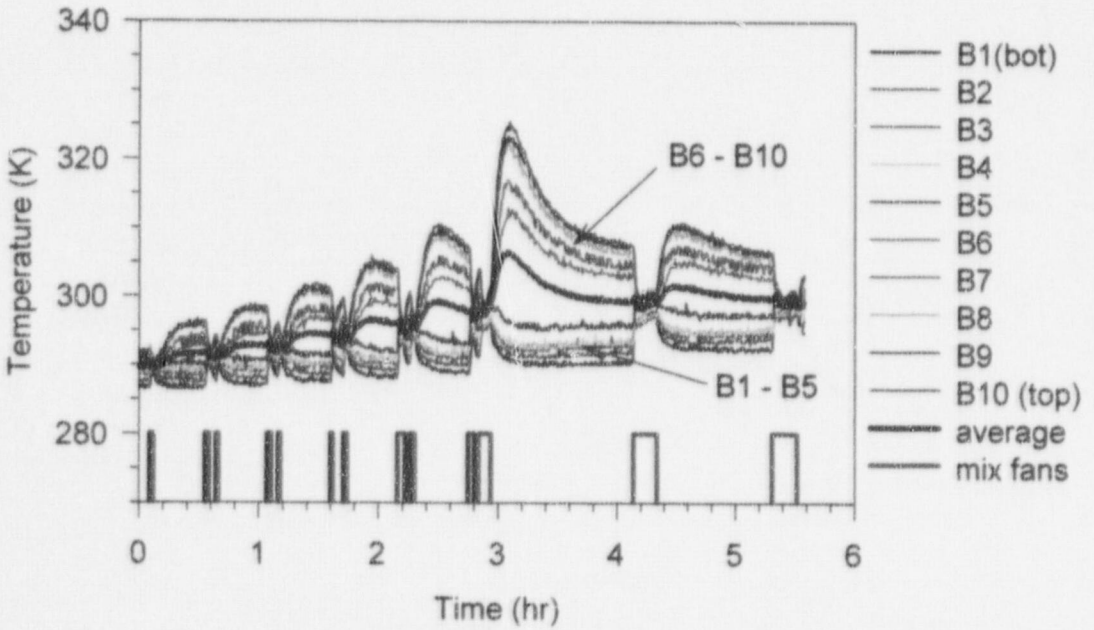

Figure 14. Surtsey vessel wall gas temperatures from TC array B in PAR-1.

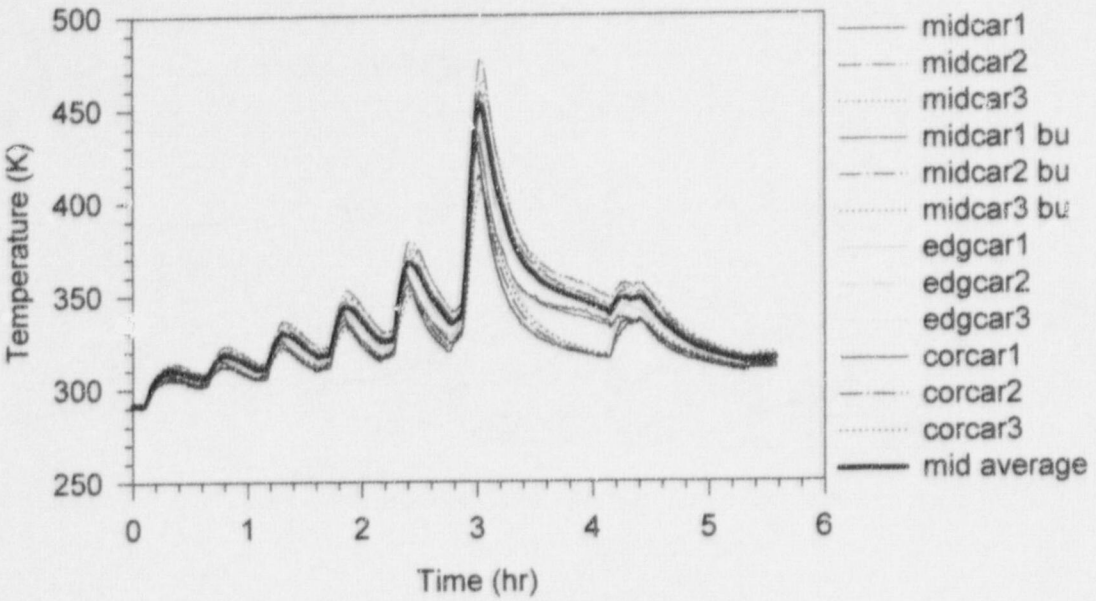

Figure 15. Catalyst cartridge temperatures in PAR-1.

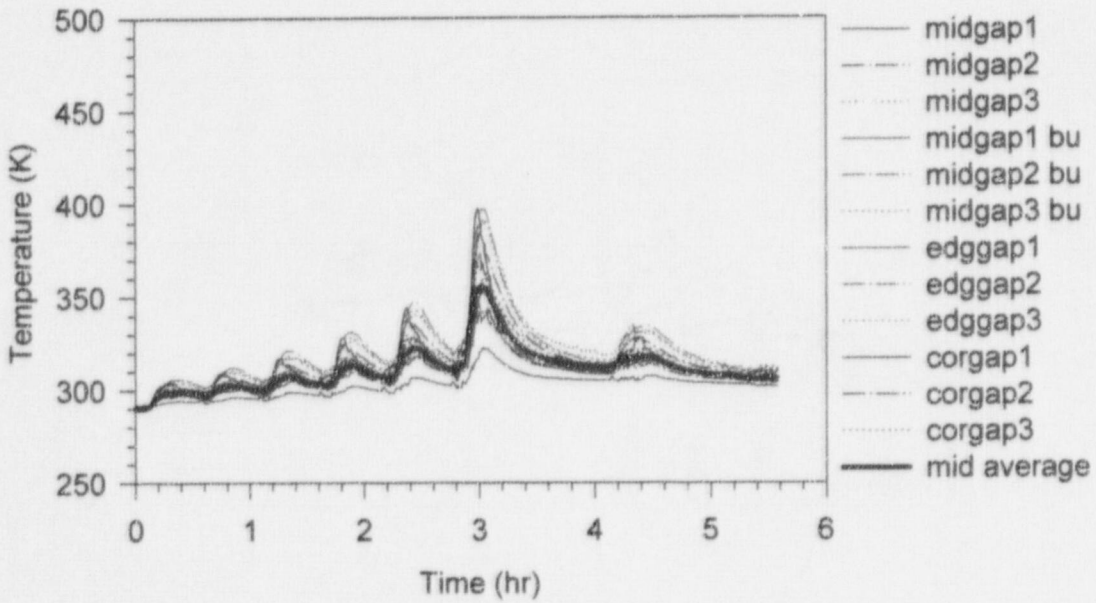

Figure 16. Catalyst gap temperatures in PAR-1.

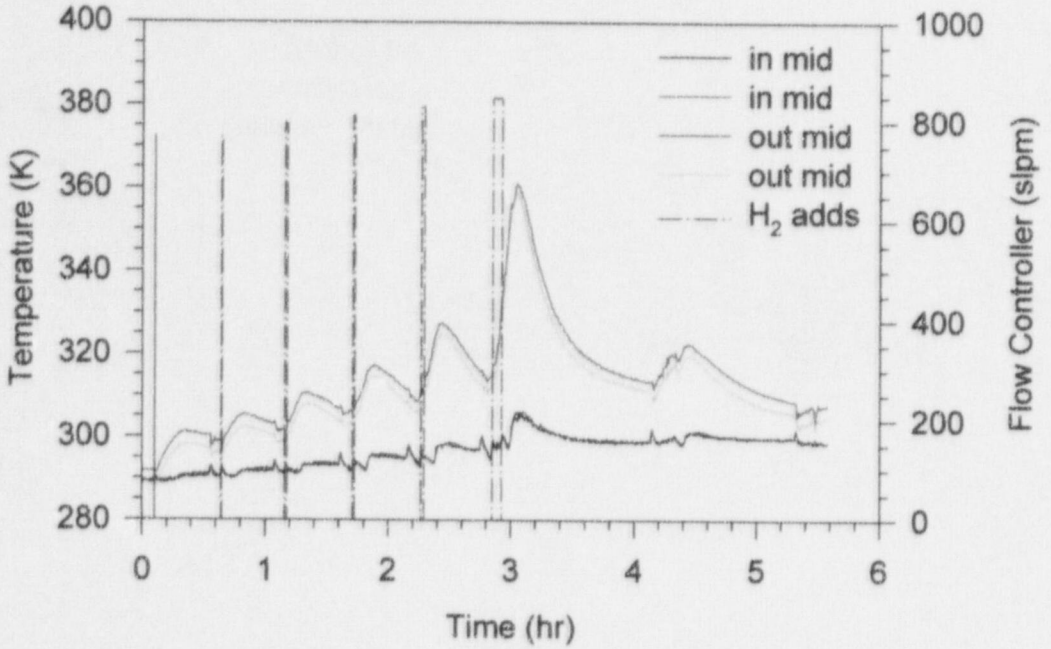

Figure 17. Inlet and outlet temperatures in PAR-1.

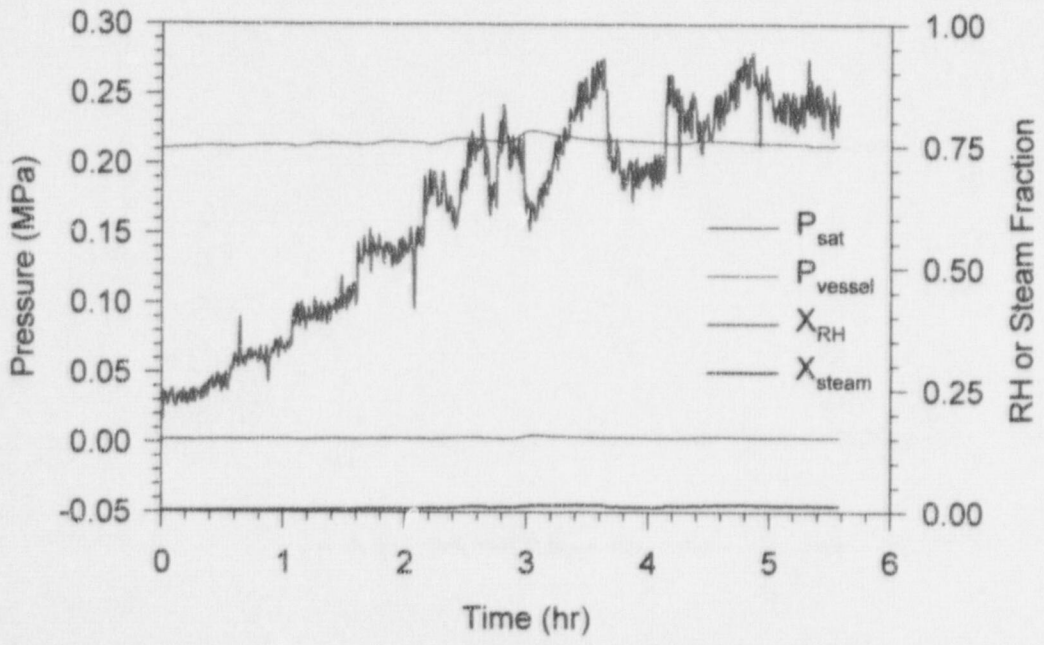

Figure 18. Saturation pressure, vessel pressure, relative humidity, and steam fraction in PAR-1.

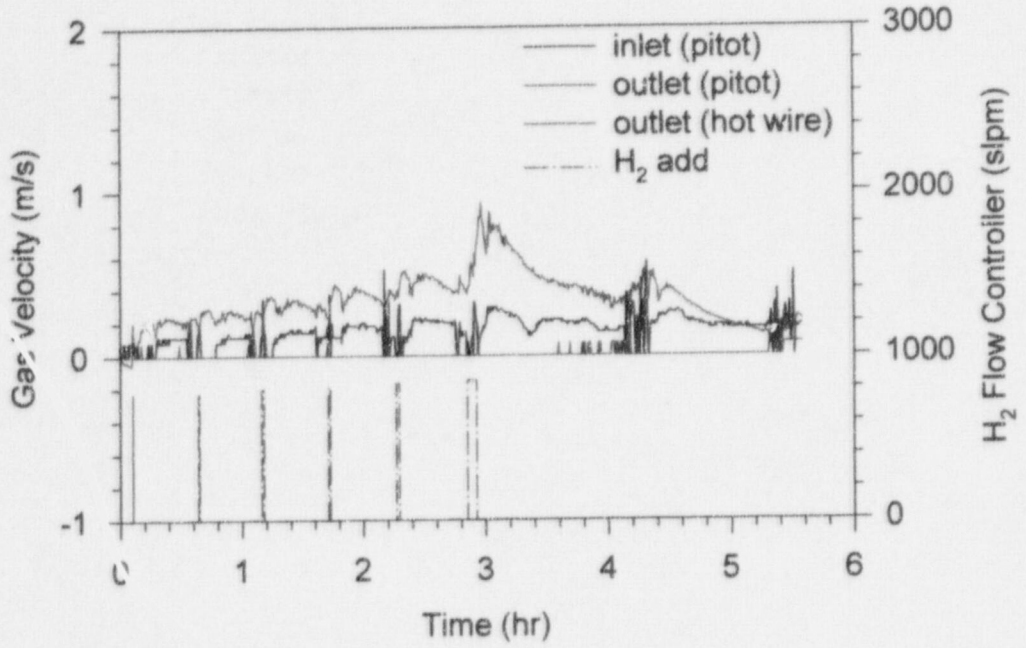

Figure 19. PAR gas velocity in PAR-1.

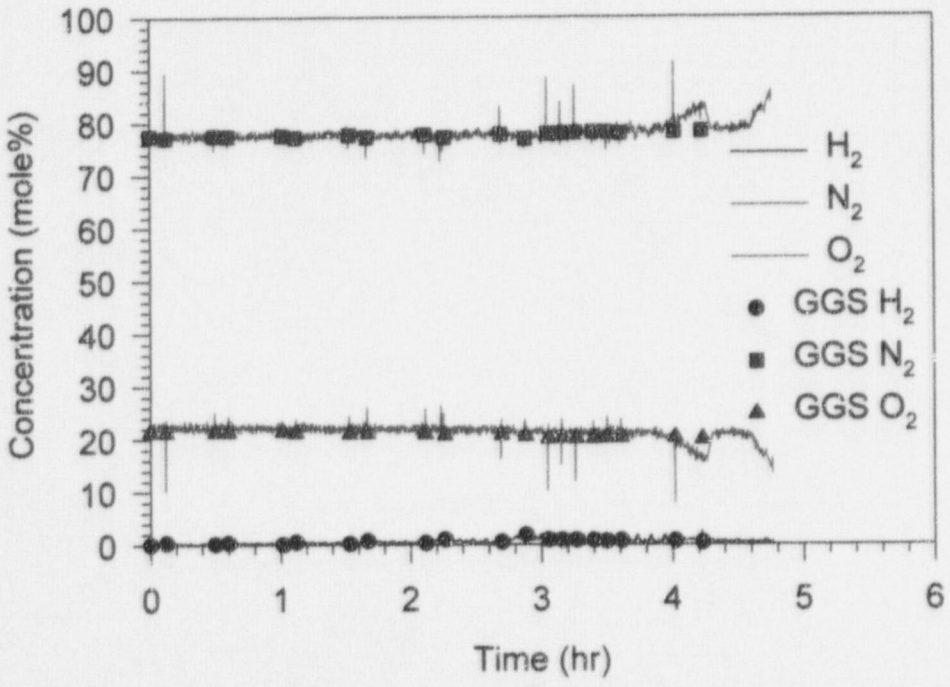

Figure 20. Gas concentrations (dry-basis) in PAR-1.

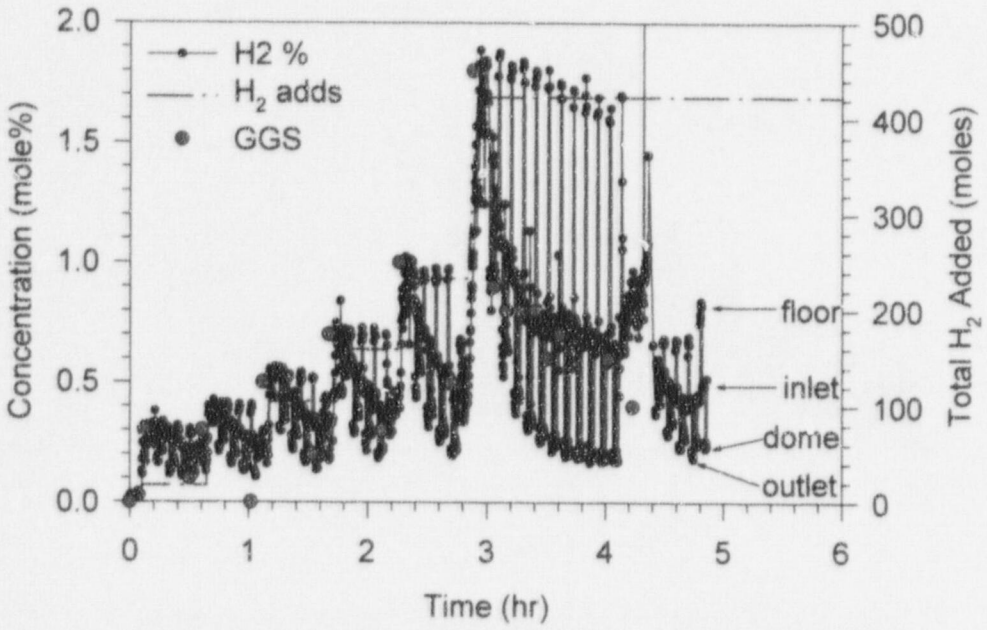

Figure 21. H_2 concentrations (dry-basis) in PAR-1.

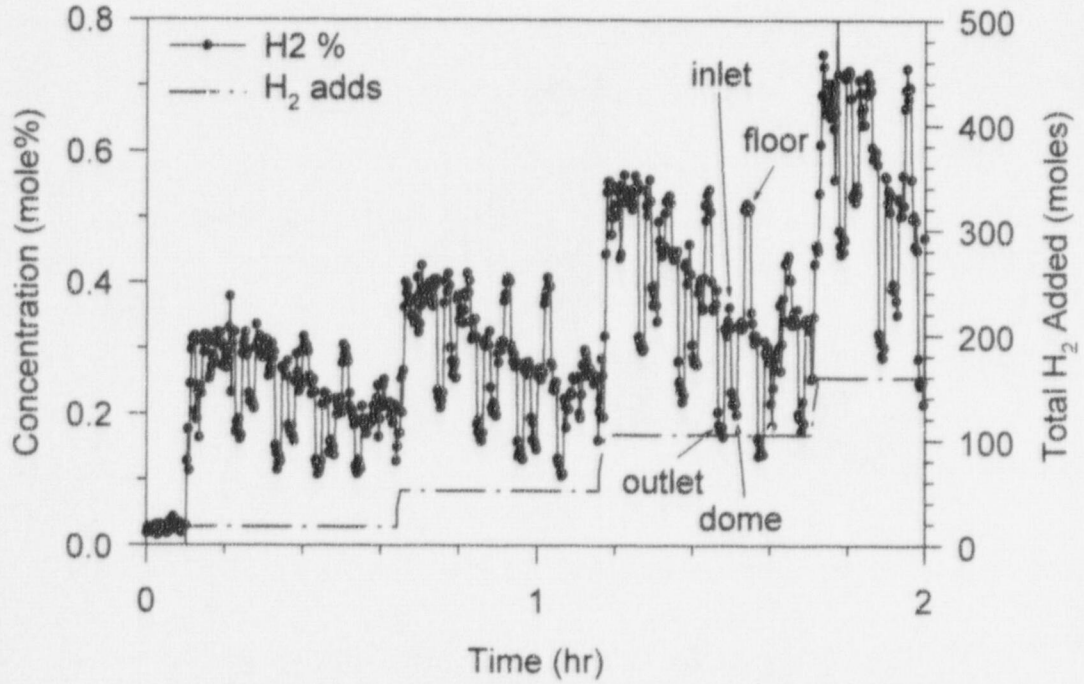

Figure 22. H_2 concentrations (dry-basis) in PAR-1 from 0 to 2 hrs.

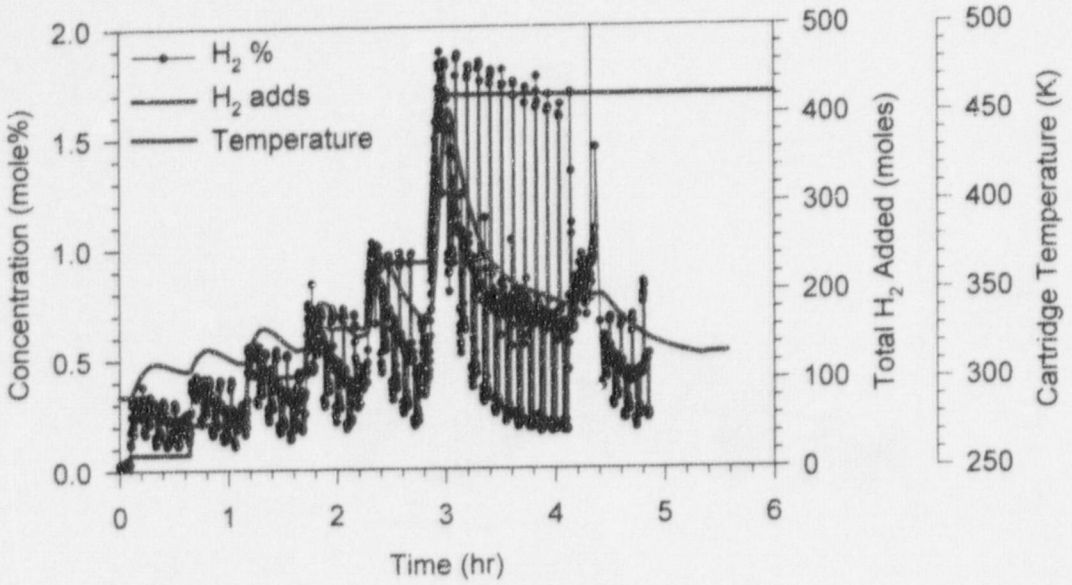

Figure 23. Catalyst temperature compared to H_2 additions and concentrations in PAR-1.

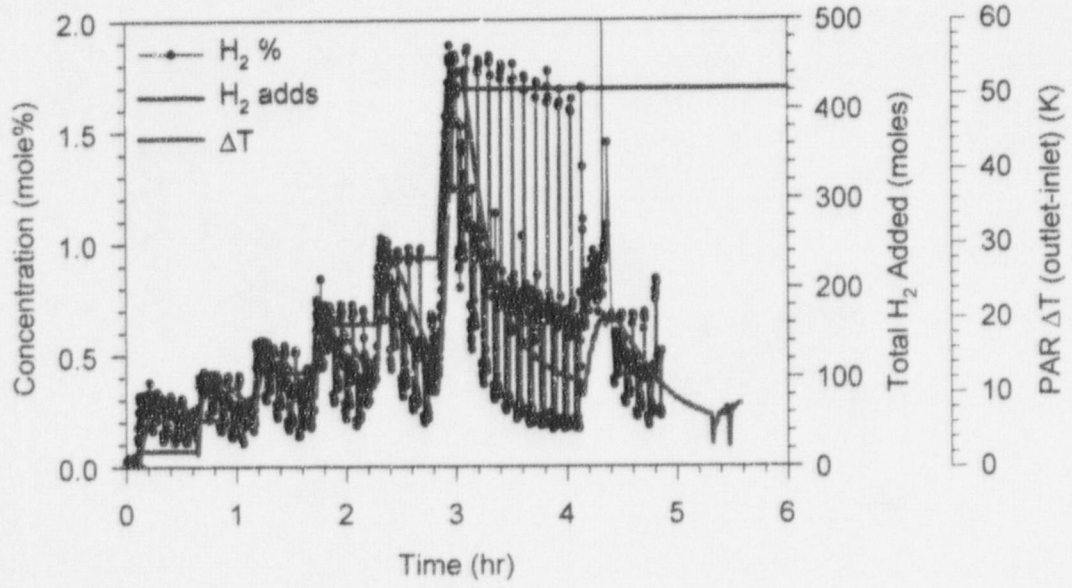

Figure 24. PAR ΔT compared to H_2 additions and concentrations in PAR-1.

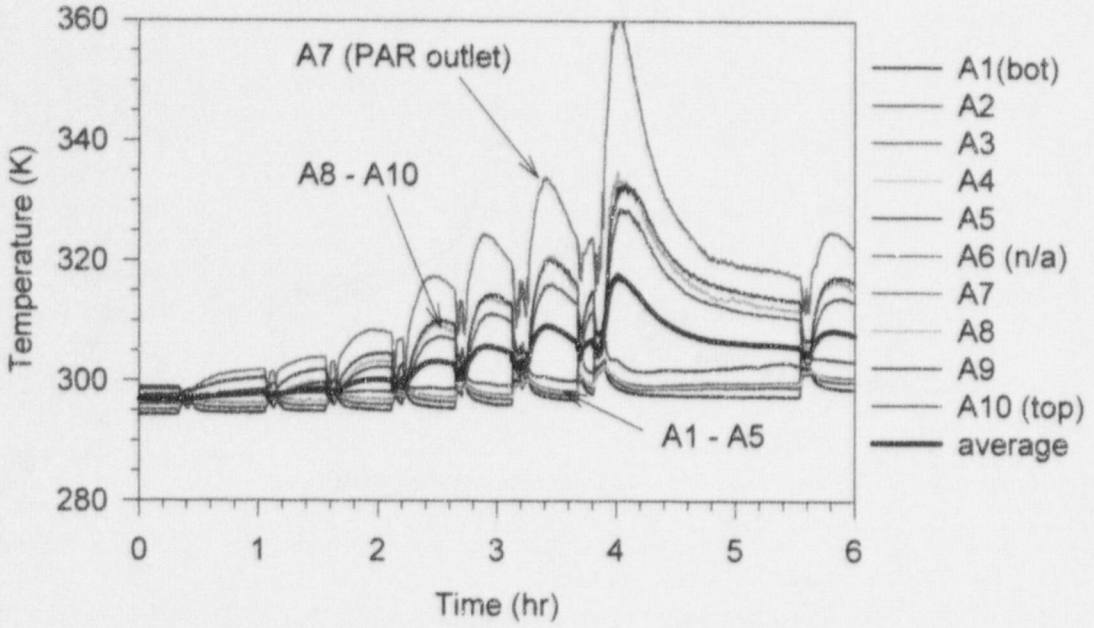

Figure 25. Surtsey vessel centerline gas temperatures from TC array A in PAR-2.

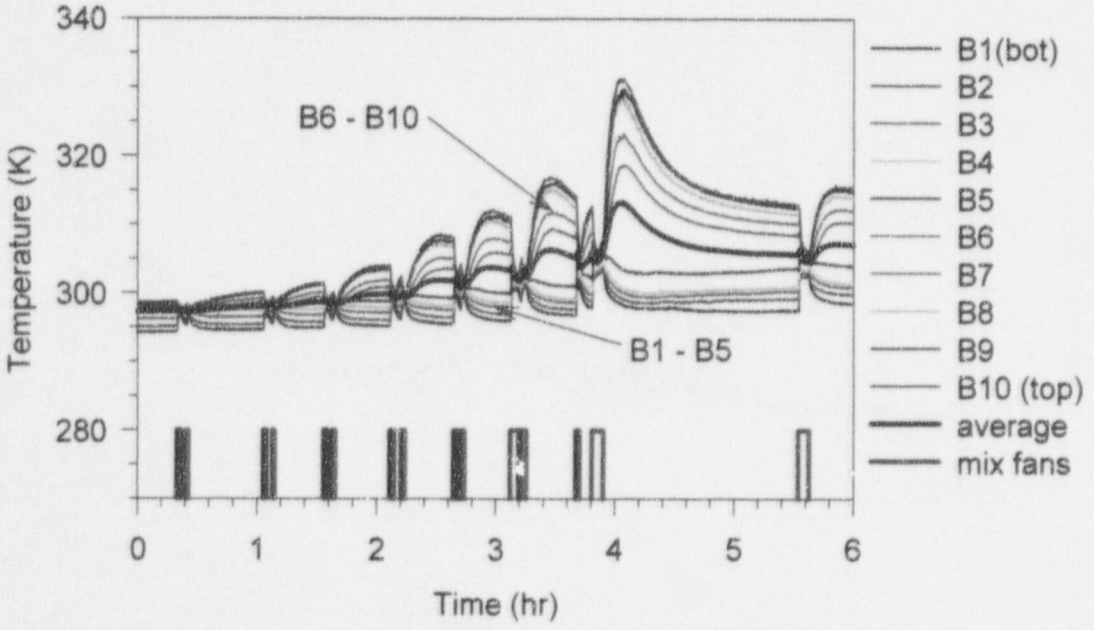

Figure 26. Surtsey vessel wall gas temperatures from TC array B in PAR-2.

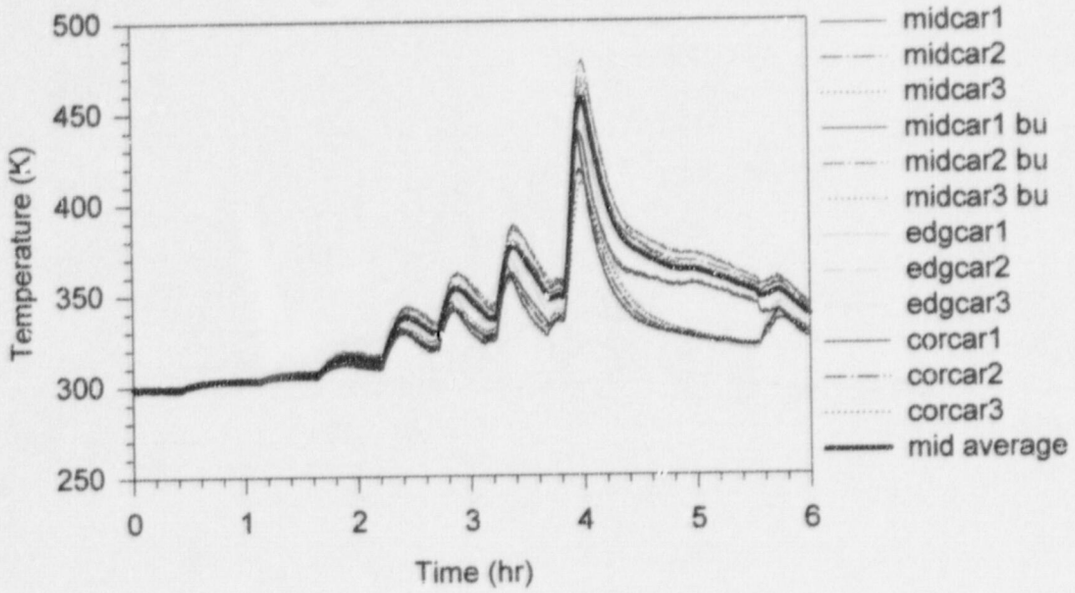

Figure 27. Catalyst cartridge temperatures in PAR-2.

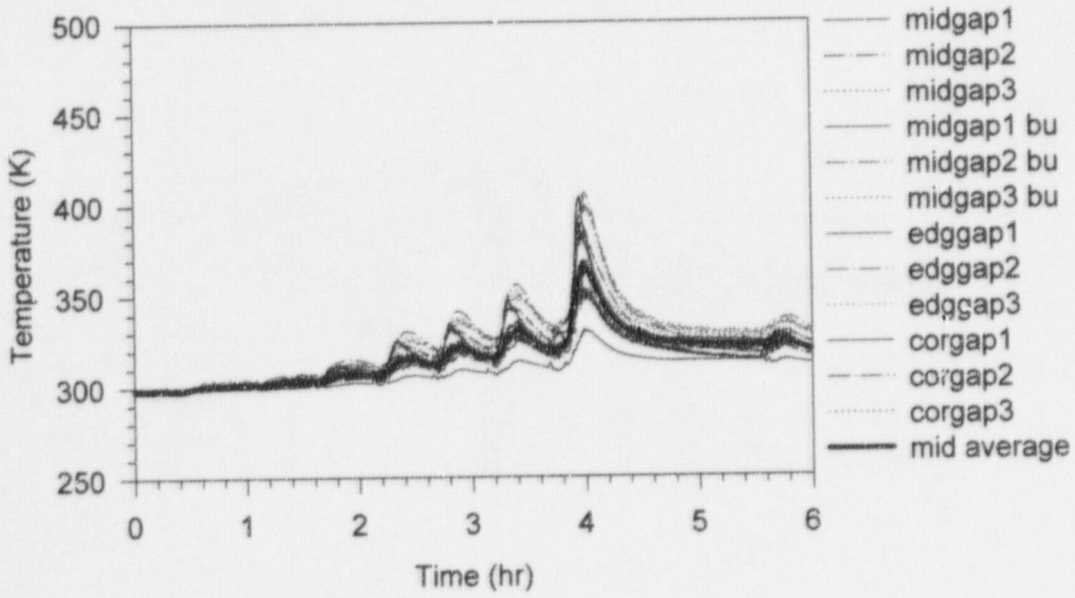

Figure 28. Catalyst gap temperatures in PAR-2.

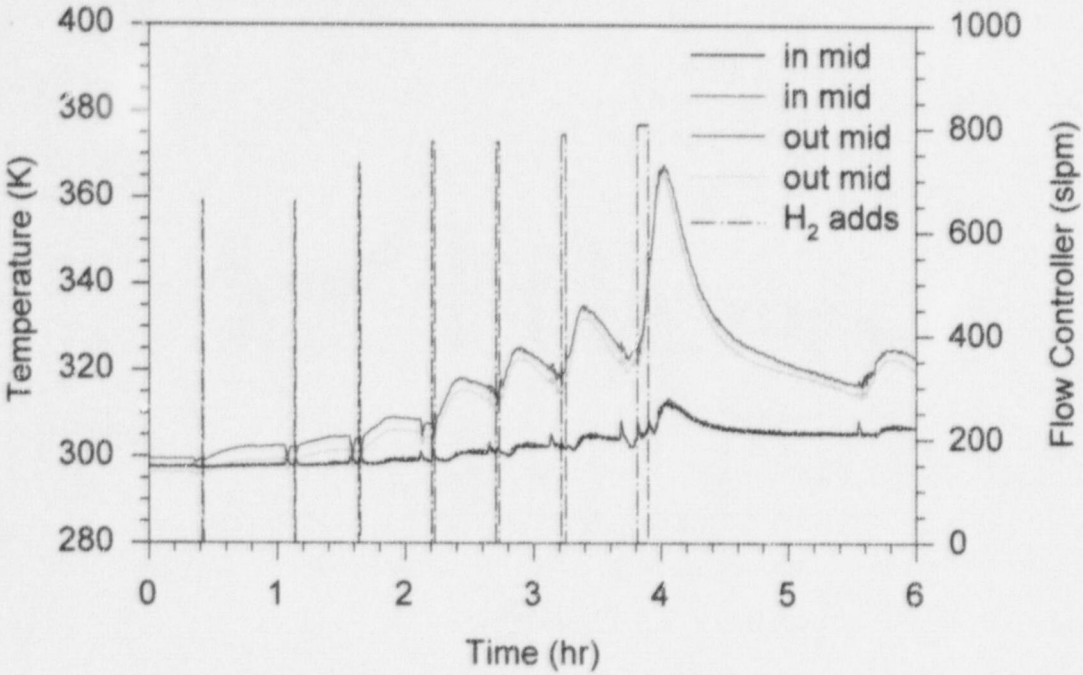

Figure 29. Inlet and outlet temperatures in PAR-2.

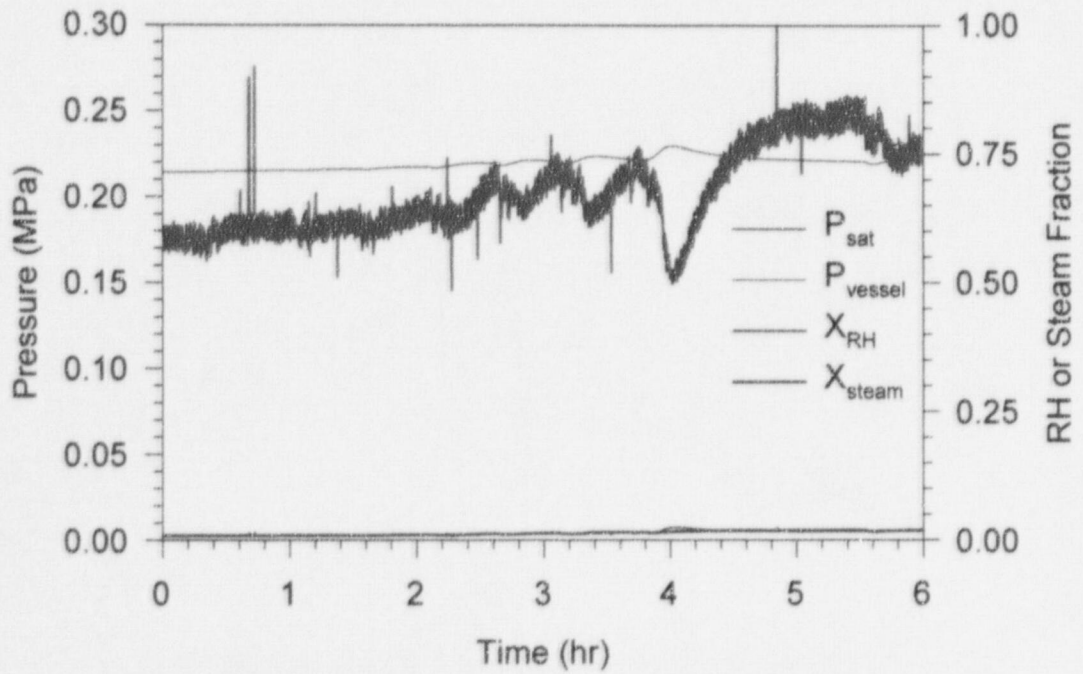

Figure 30. Saturation pressure, vessel pressure, relative humidity, and steam fraction in PAR-2.

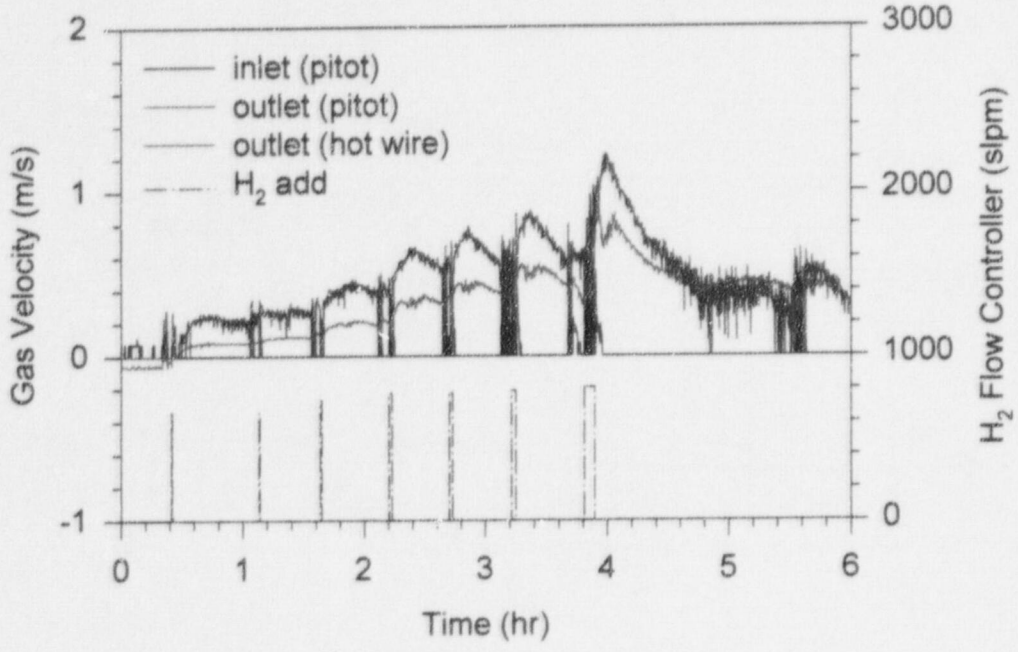

Figure 31. PAR gas velocity in PAR-2.

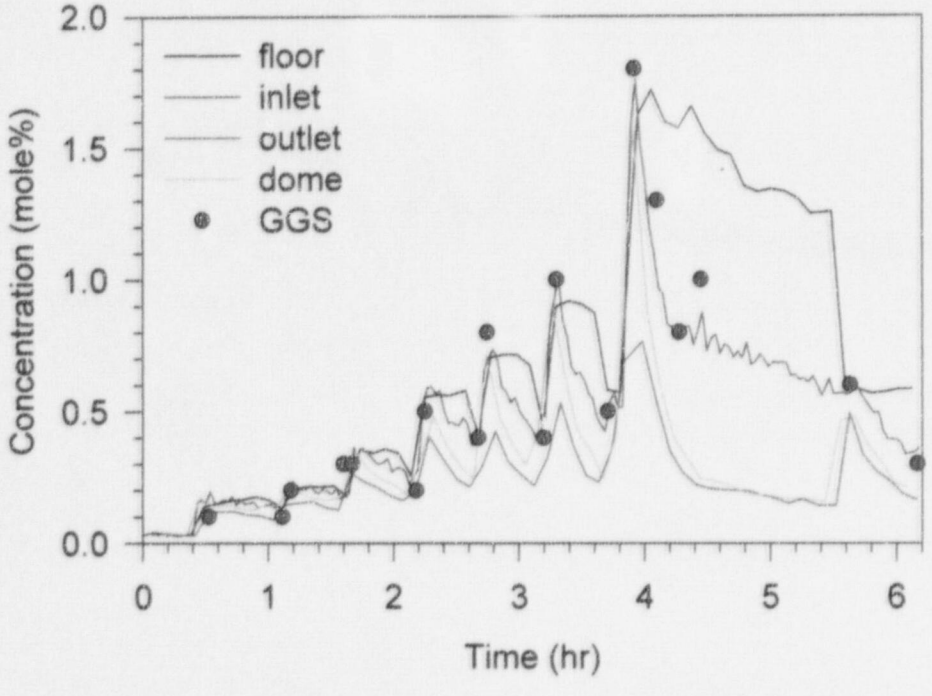

Figure 32. Gas concentrations (dry-basis) in PAR-2.

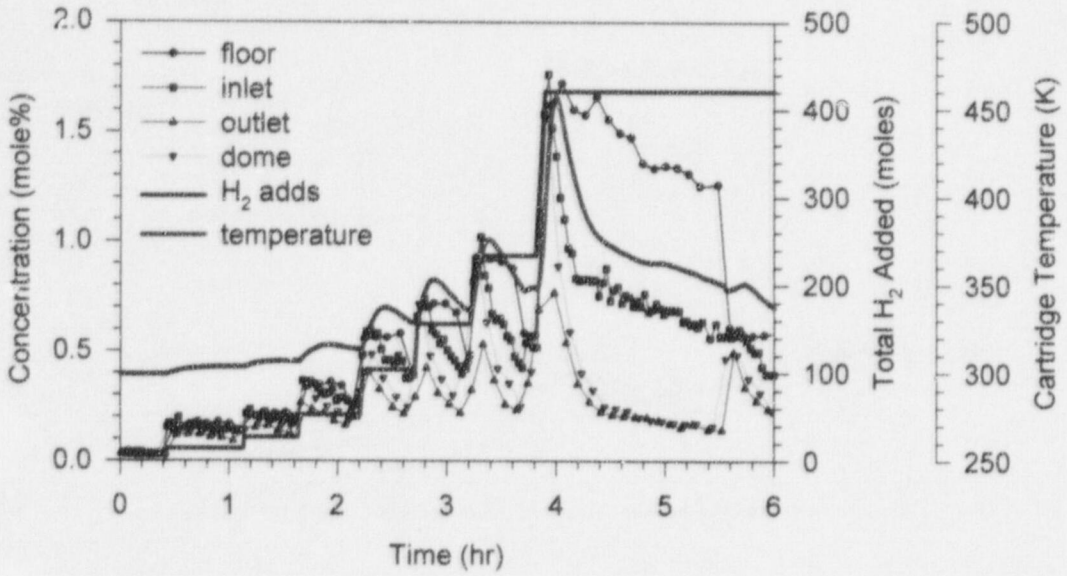

Figure 33. Catalyst temperature compared to H_2 additions and concentrations in PAR-2.

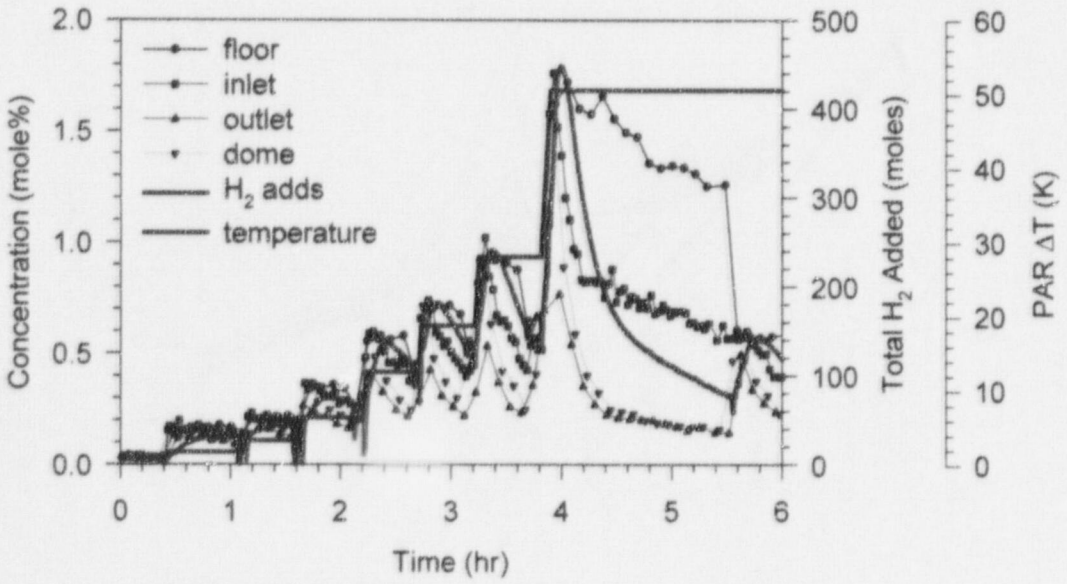

Figure 34. PAR ΔT compared to H_2 additions and concentrations in PAR-2.

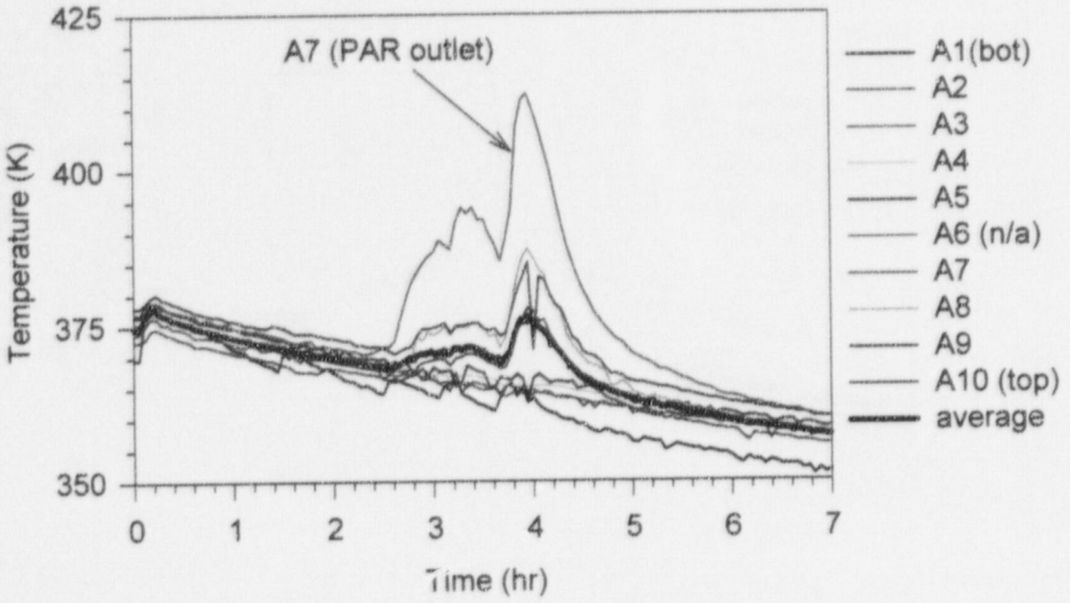

Figure 35. Surtsey vessel centerline gas temperatures from TC array A in PAR-3.

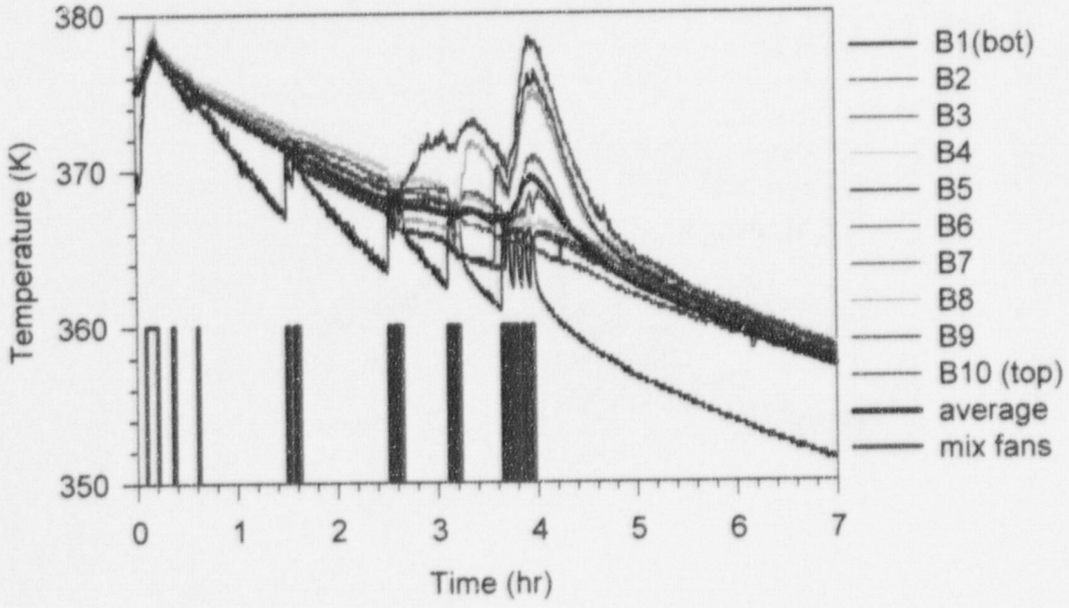

Figure 36. Surtsey vessel wall gas temperatures from TC array B in PAR-3.

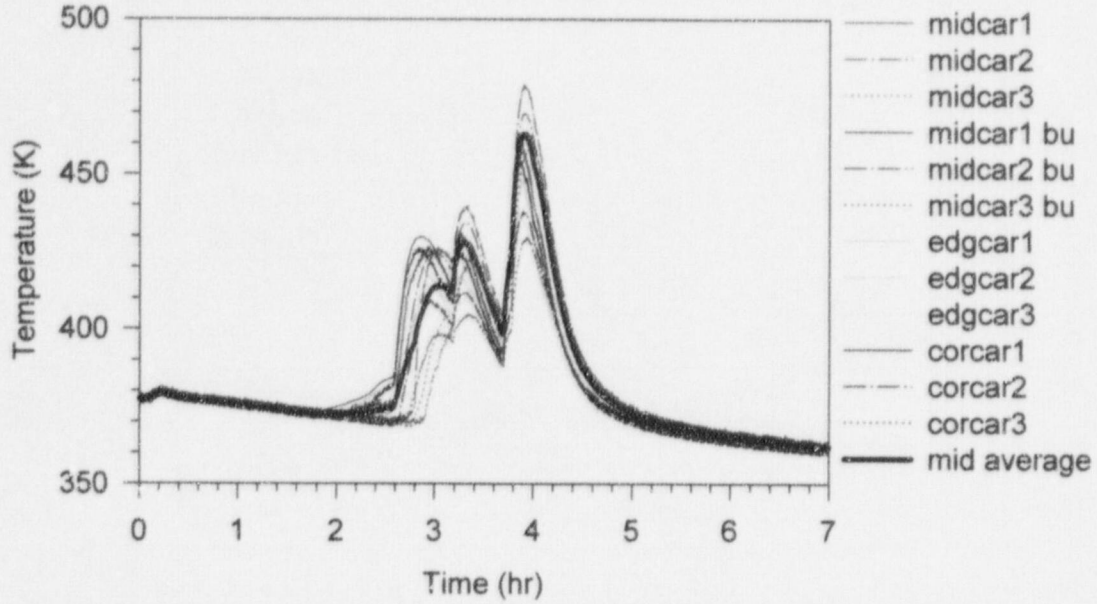

Figure 37. Catalyst cartridge temperatures in PAR-3.

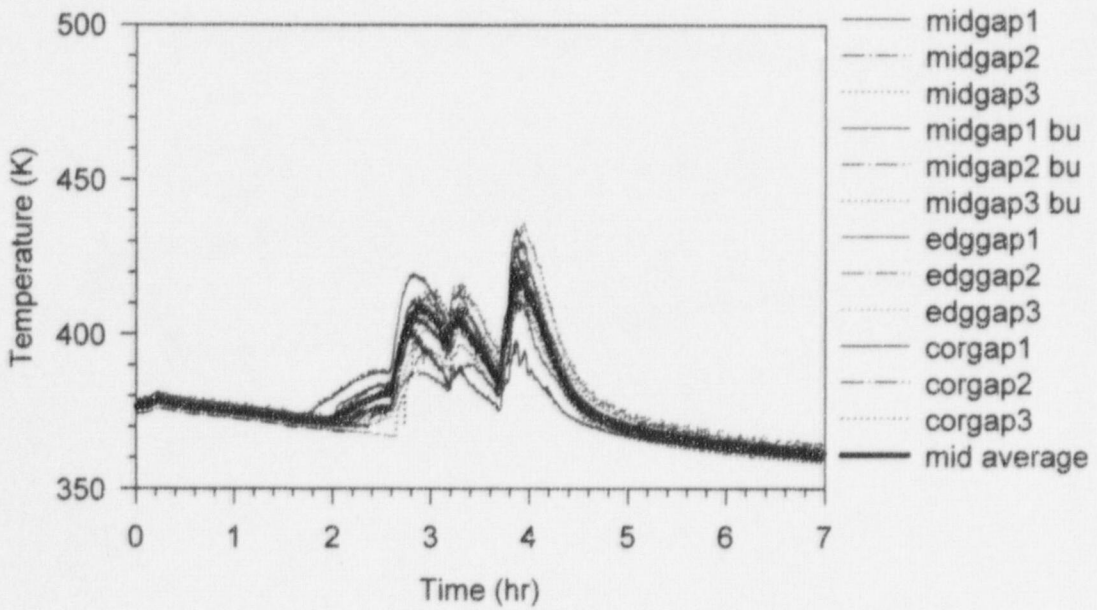

Figure 38. Catalyst gap temperatures in PAR-3.

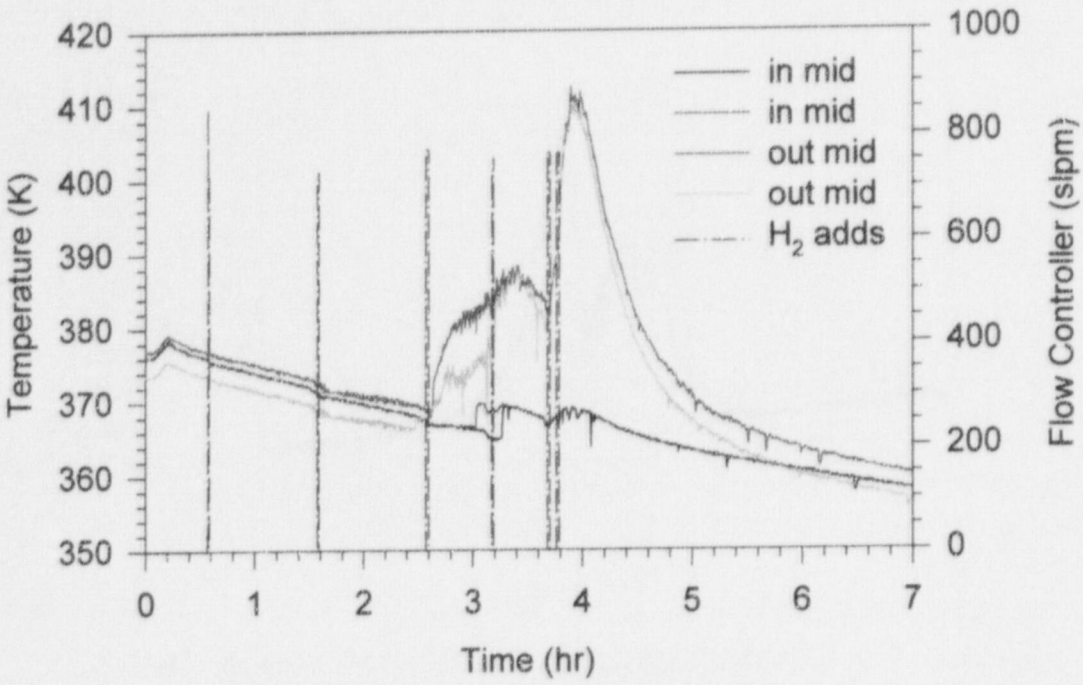

Figure 39. Inlet and outlet temperatures in PAR-3.

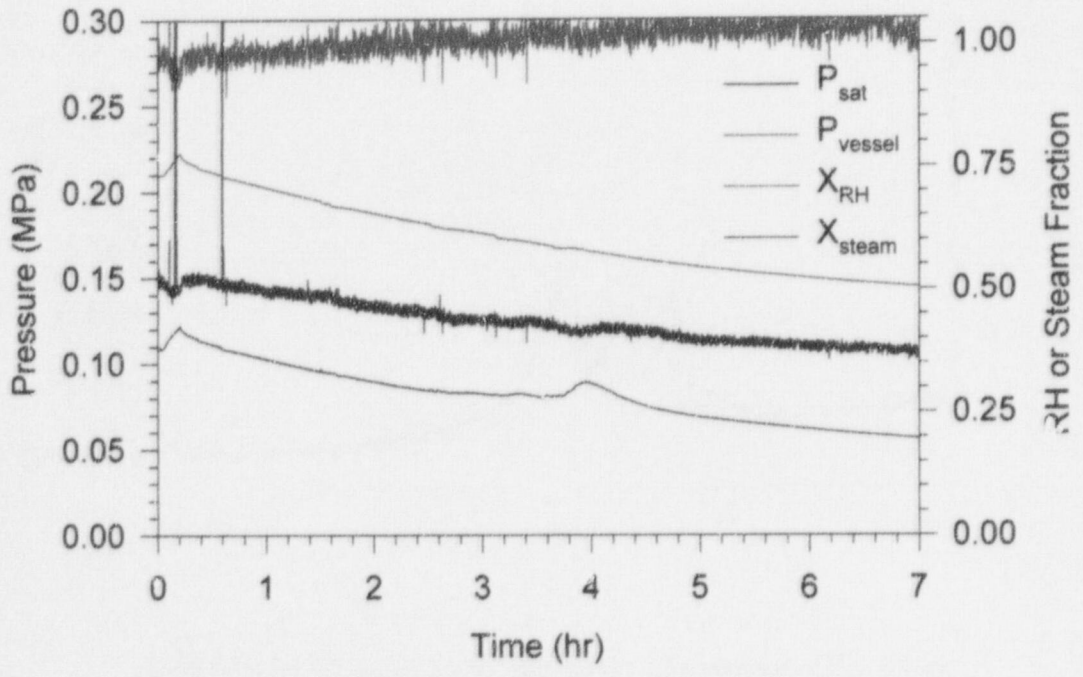

Figure 40. Saturation pressure, vessel pressure, relative humidity, and steam fraction in PAR-3.

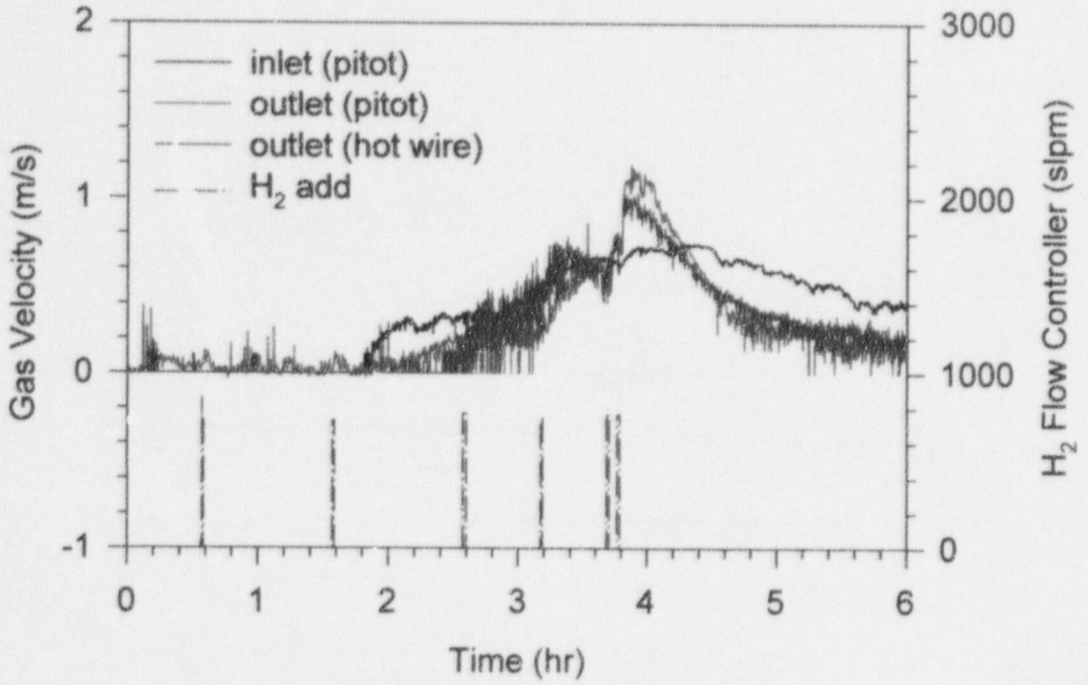

Figure 41. PAR gas velocity in PAR-3.

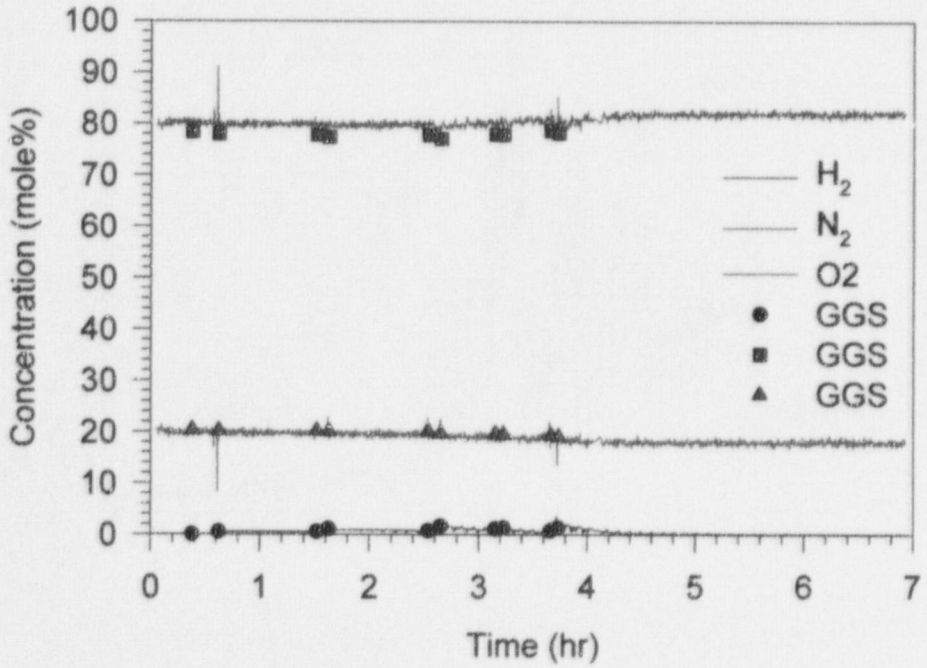

Figure 42. Gas concentrations (dry-basis) in PAR-3.

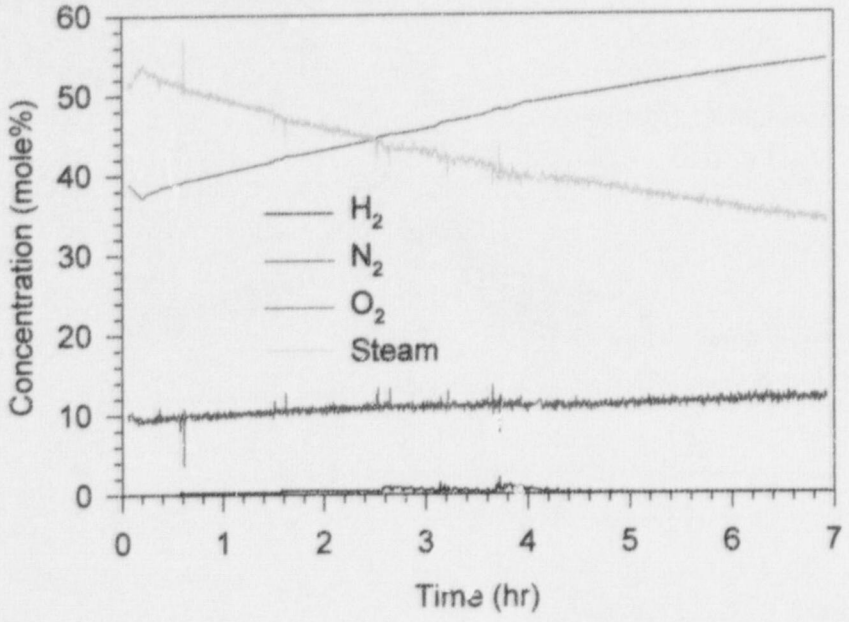

Figure 43. Gas concentrations (wet-basis) in PAR-3.

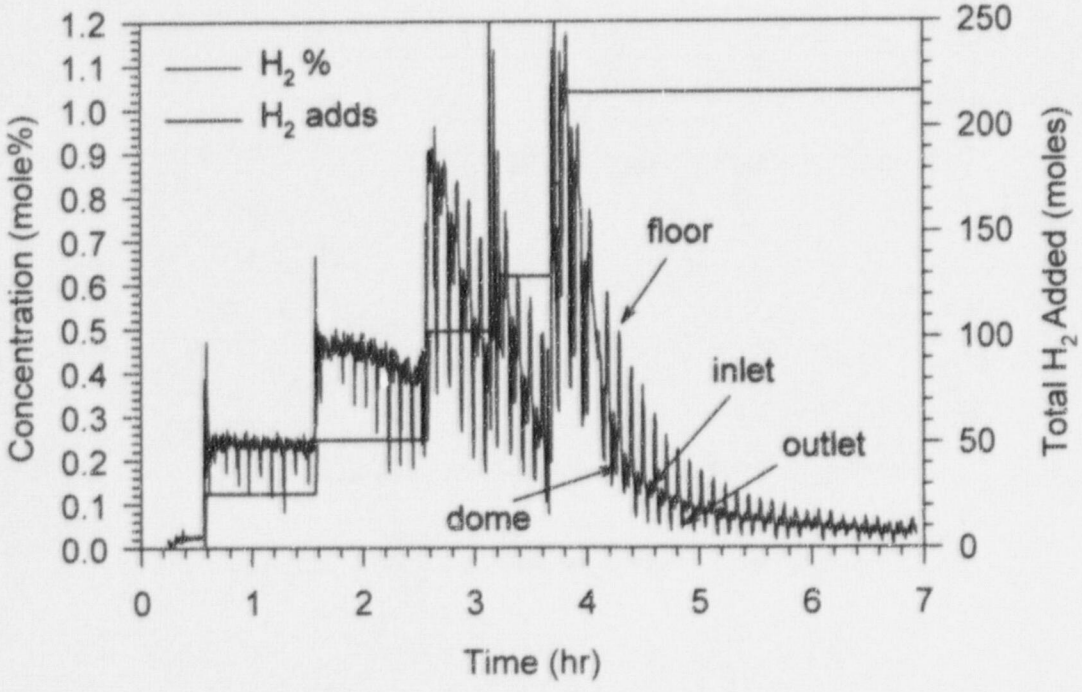

Figure 44. H_2 concentrations (wet-basis) in PAR-3.

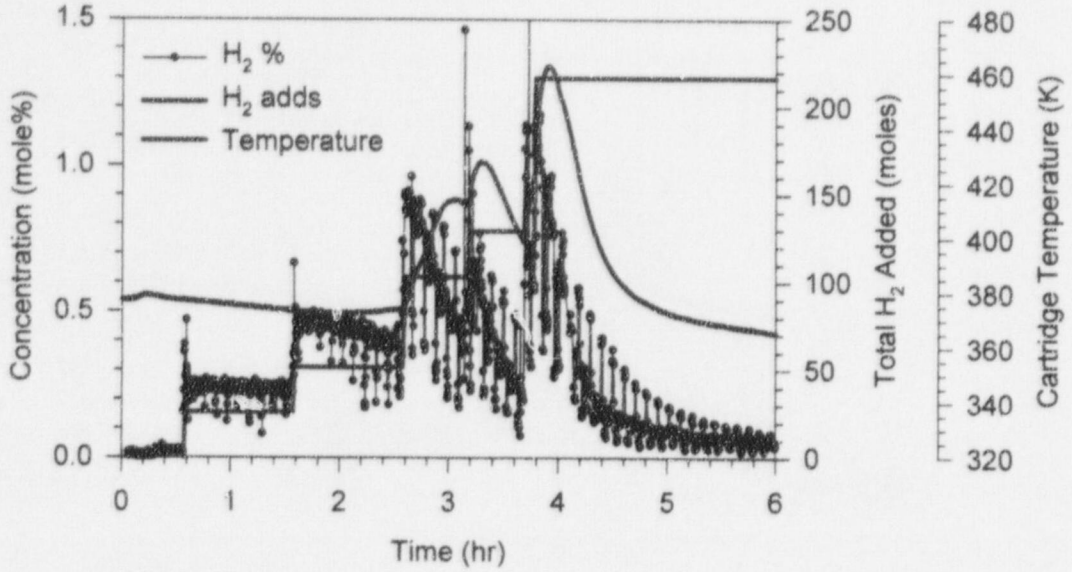

Figure 45. Catalyst temperature compared to H_2 additions and concentrations in PAR-3.

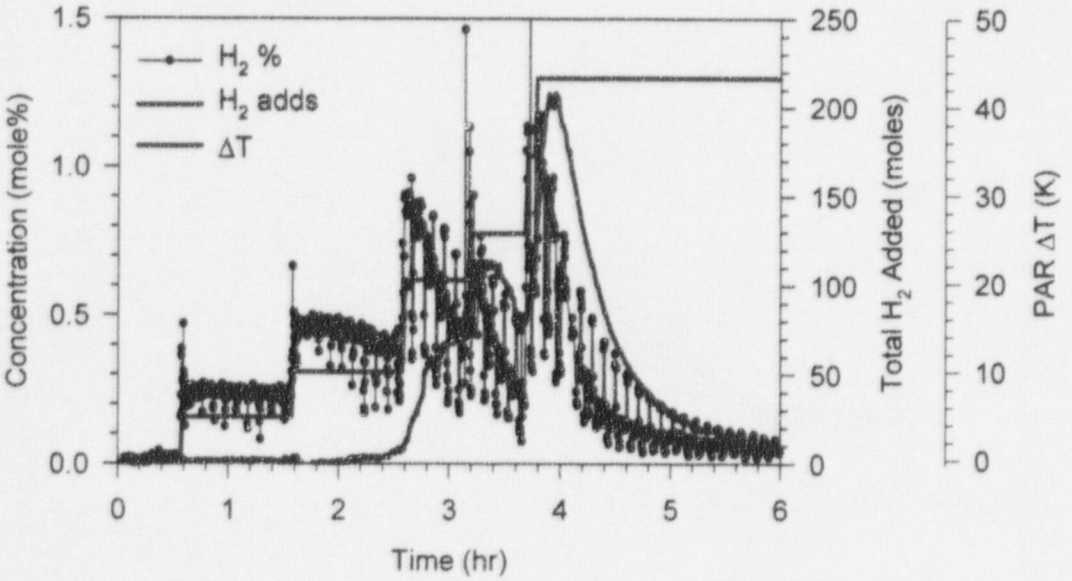

Figure 46. PAR ΔT compared to H_2 additions and concentrations in PAR-3.

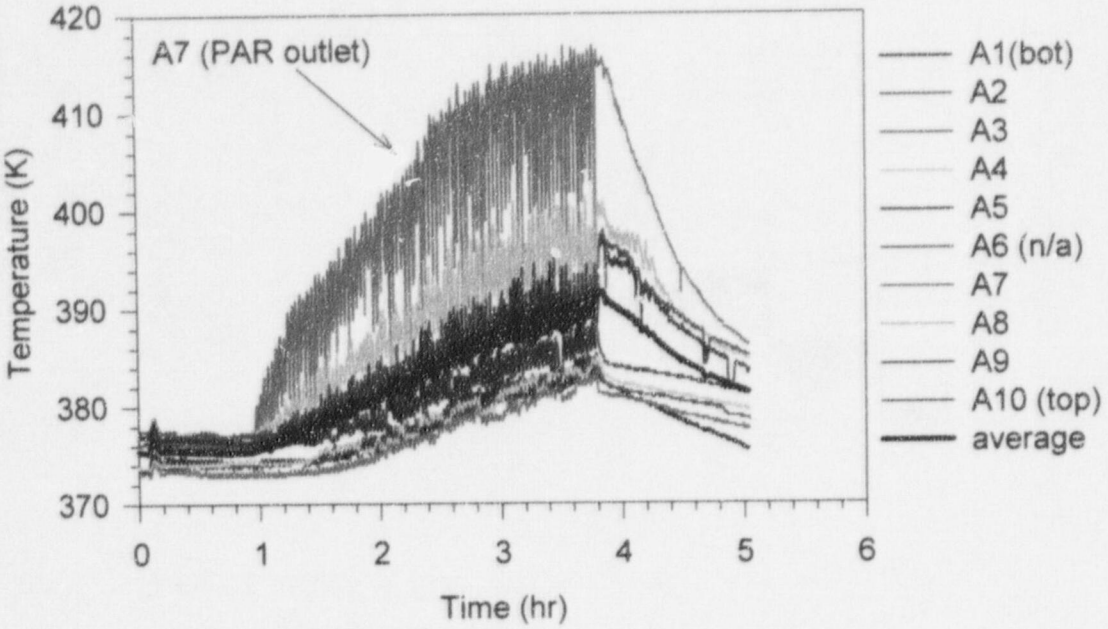

Figure 47. Surtsey vessel centerline gas temperatures from TC array A in PAR-4.

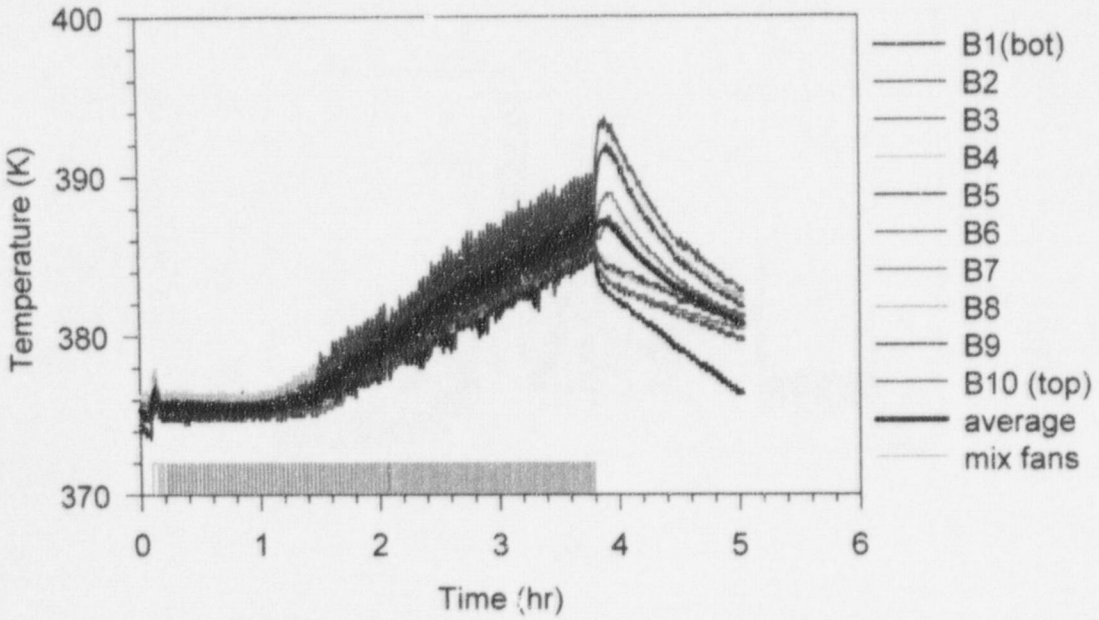

Figure 48. Surtsey vessel wall gas temperatures from TC array B in PAR-4.

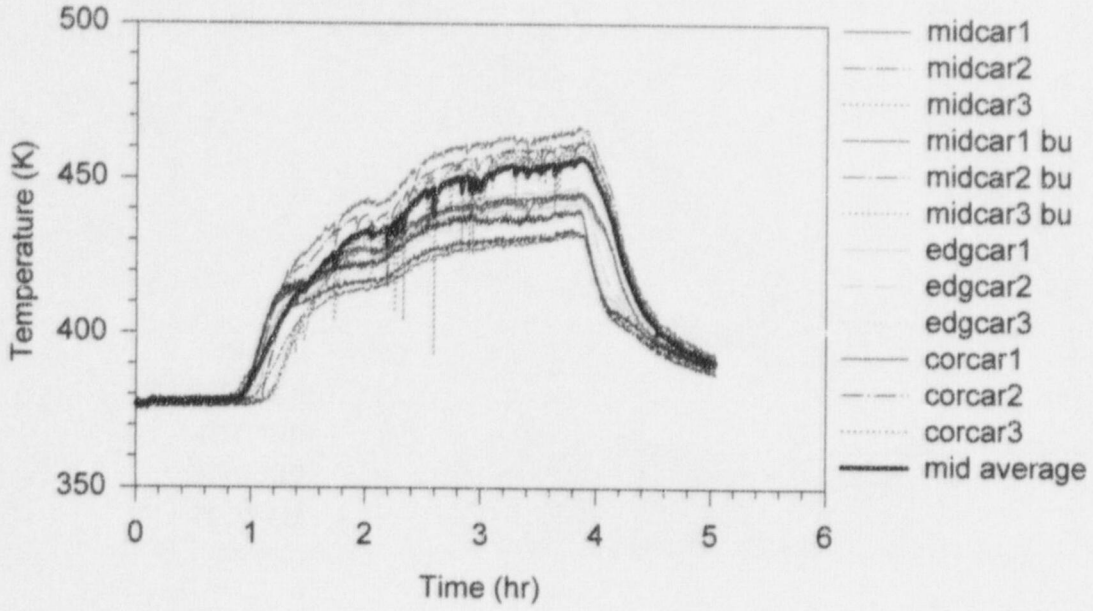

Figure 49. Catalyst cartridge temperatures in PAR-4.

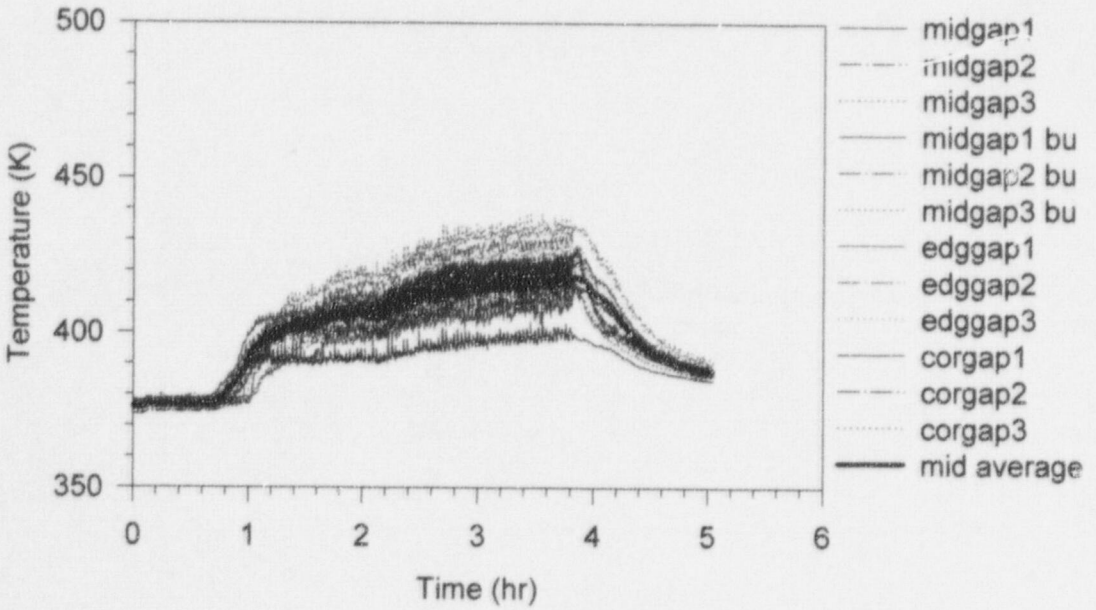

Figure 50. Catalyst gap temperatures in PAR-4.

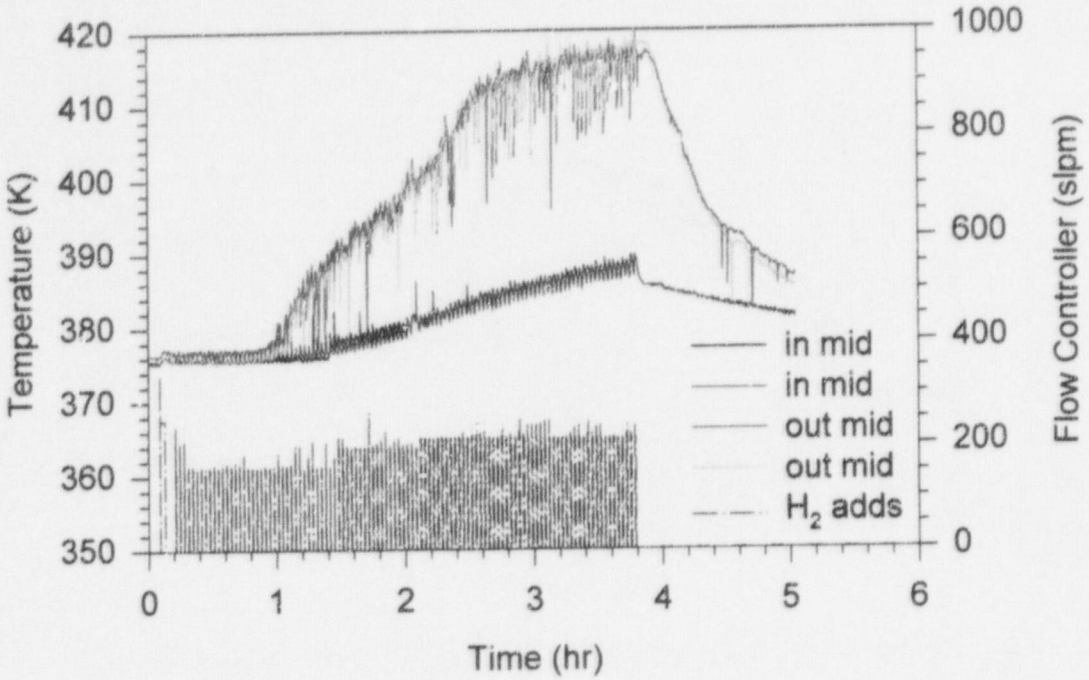

Figure 51. Inlet and outlet temperatures in PAR-4.

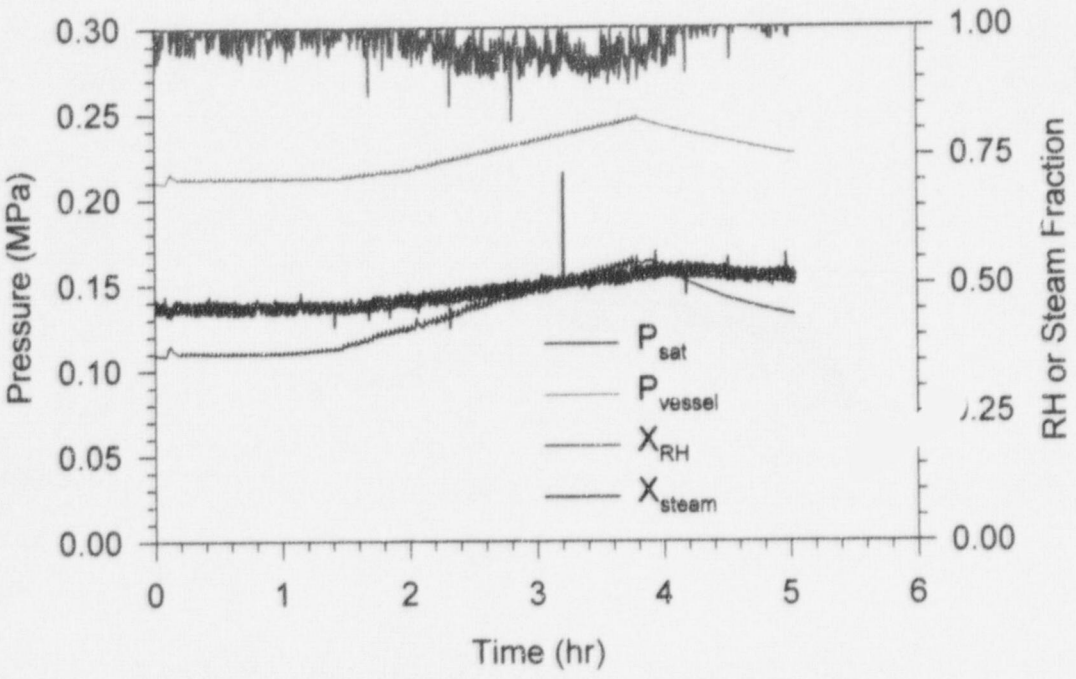

Figure 52. Saturation pressure, vessel pressure, relative humidity, and steam fraction in PAR-4.

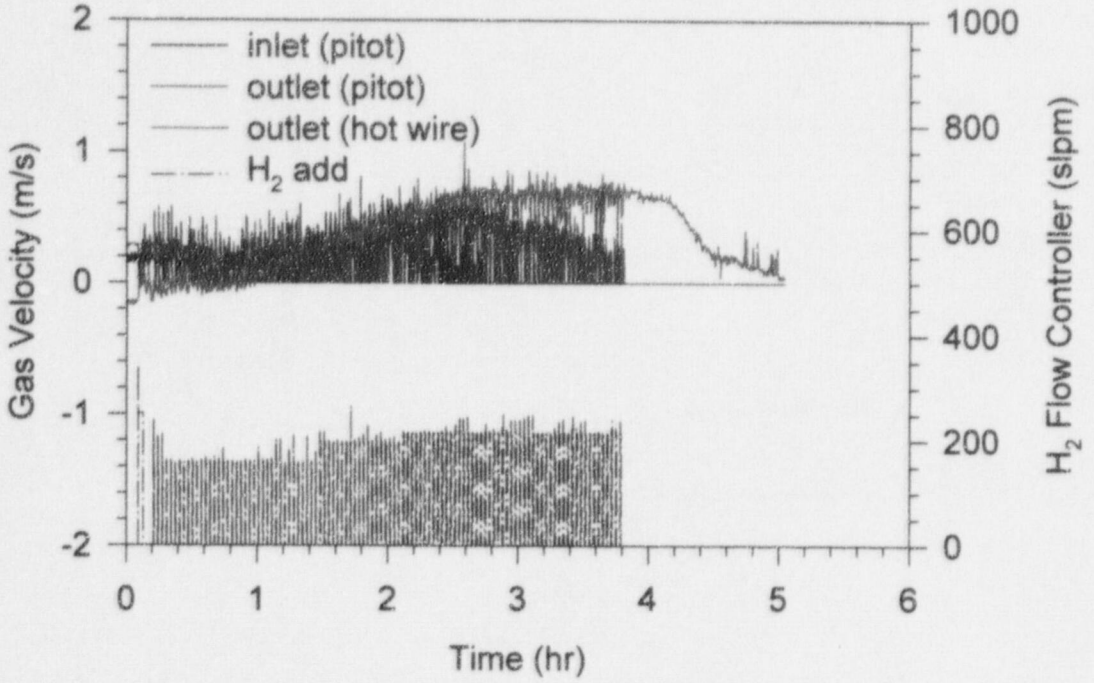

Figure 53. PAR gas velocity in PAR-4.

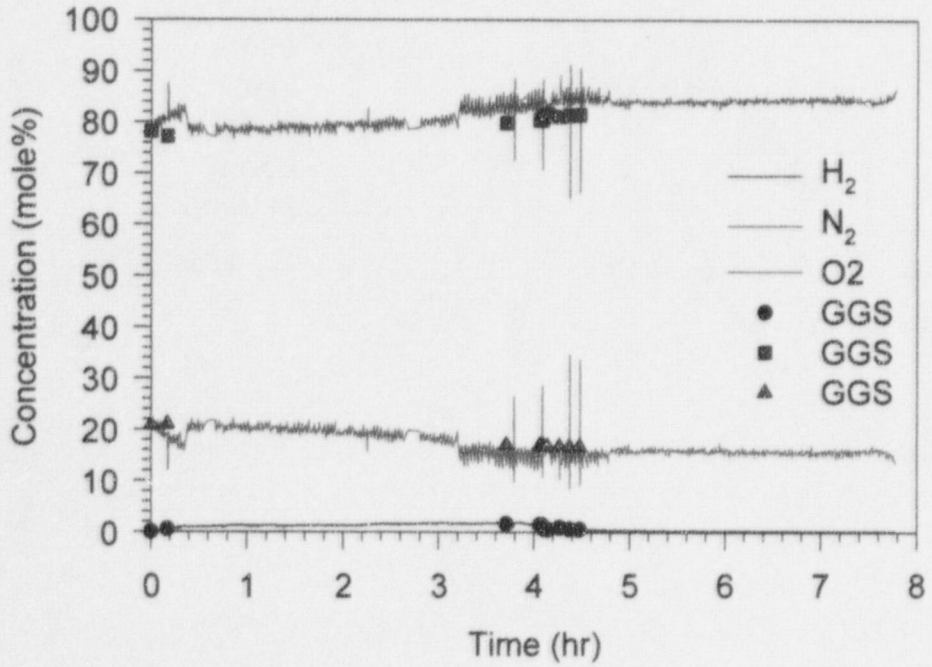

Figure 54. Gas concentrations (dry-basis) in PAR-4.

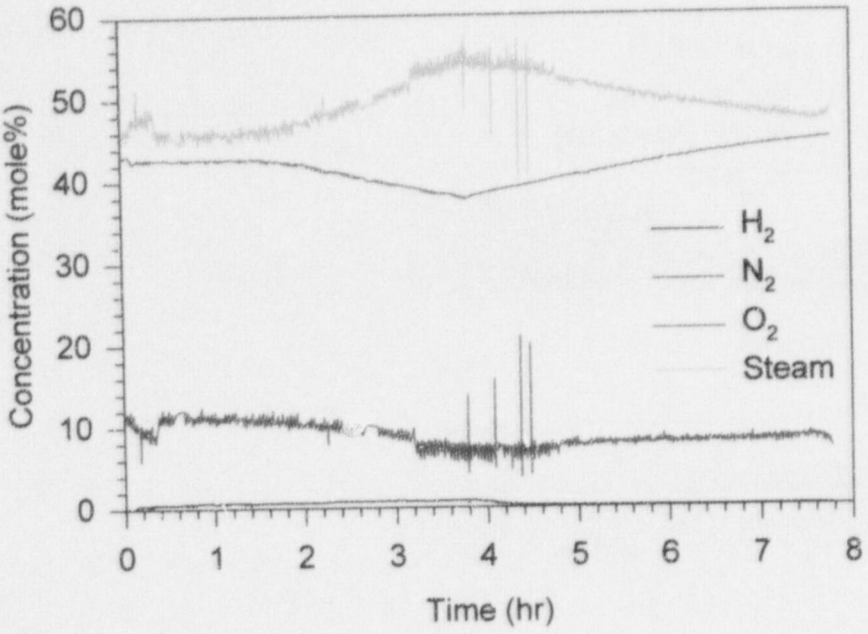

Figure 55. Gas concentrations (wet-basis) in PAR-4.

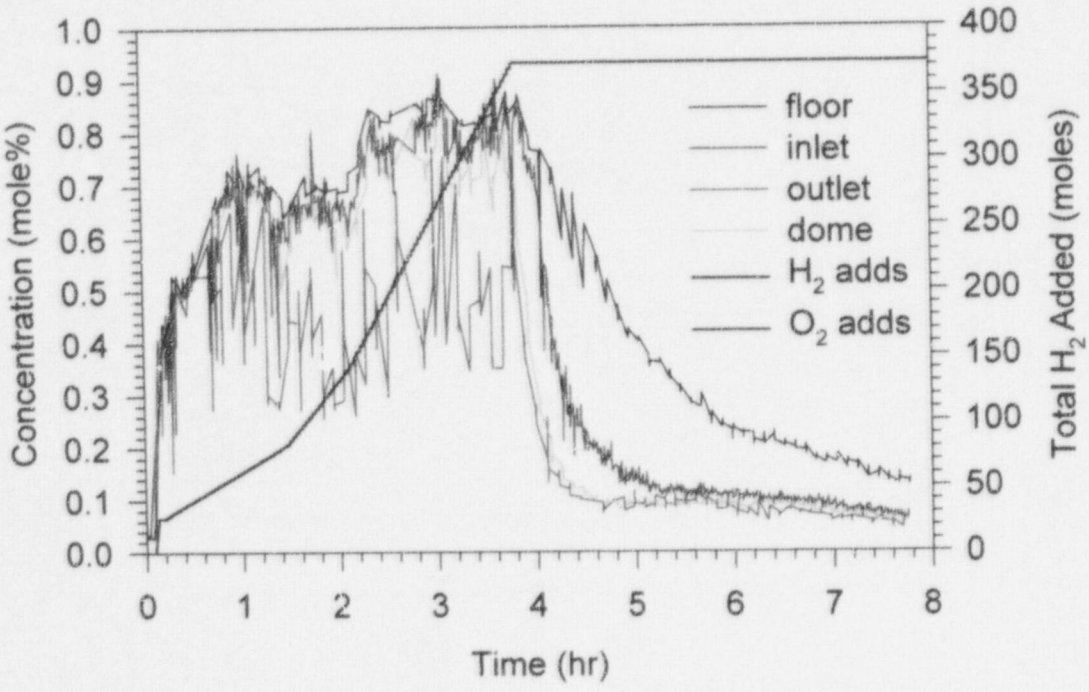

Figure 56. H_2 concentrations (wet-basis) in PAR-4.

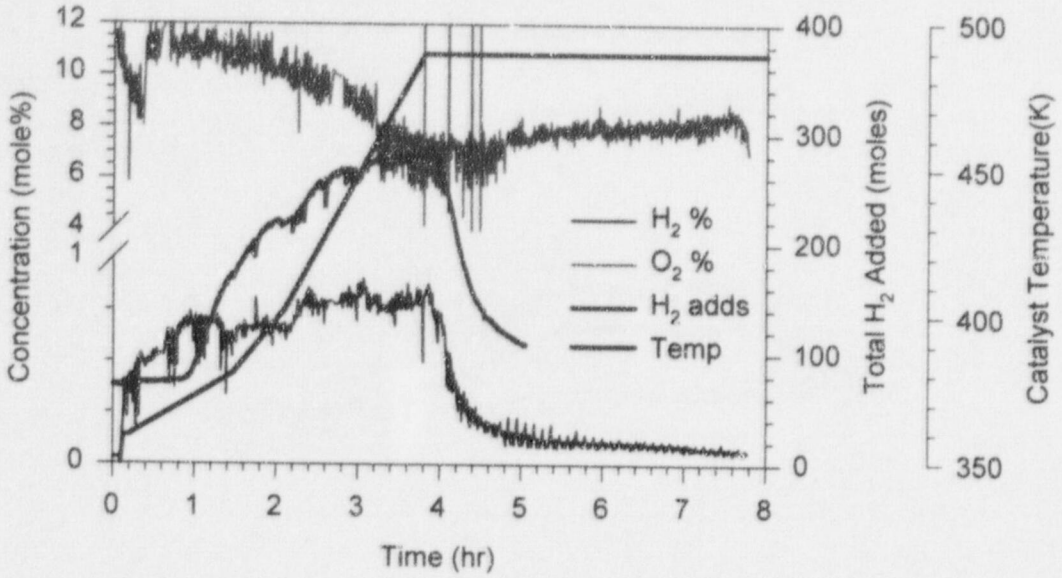

Figure 57. Catalyst temperature compared to gas additions and concentrations in PAR-4.

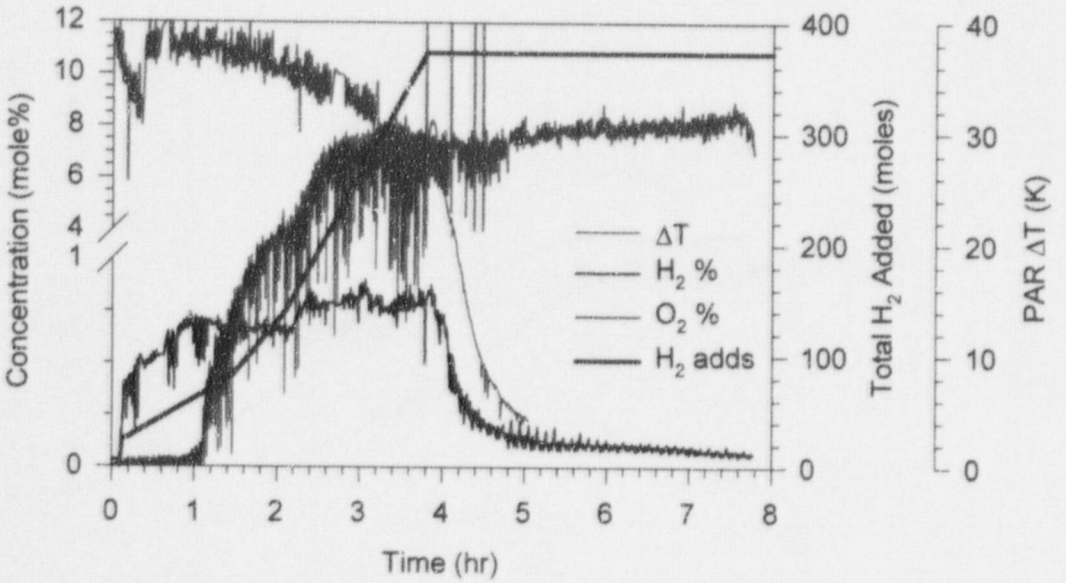

Figure 58. PAR ΔT temperature compared to gas additions and concentrations in PAR-4.

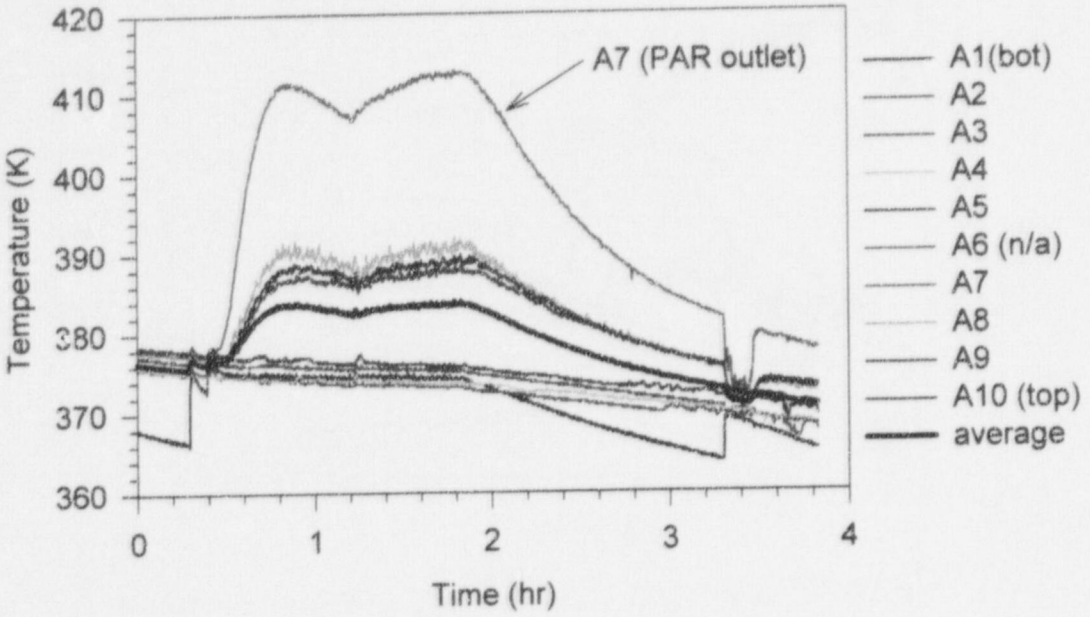

Figure 59. Surtsey vessel centerline gas temperatures from TC array A in PAR-5.

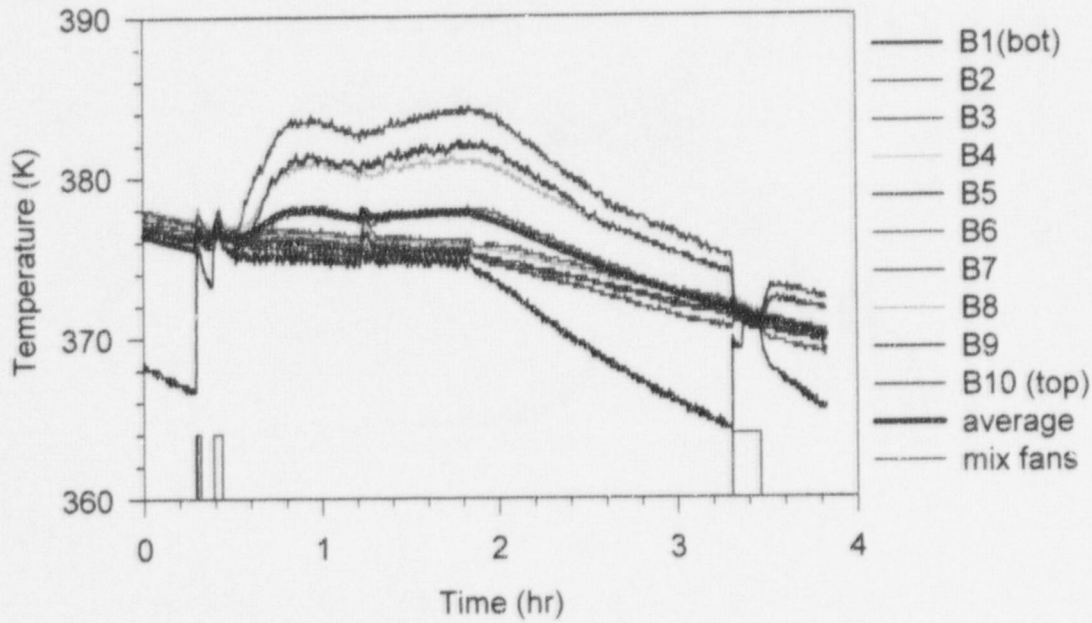

Figure 60. Surtsey vessel wall gas temperatures from TC array B in PAR-5.

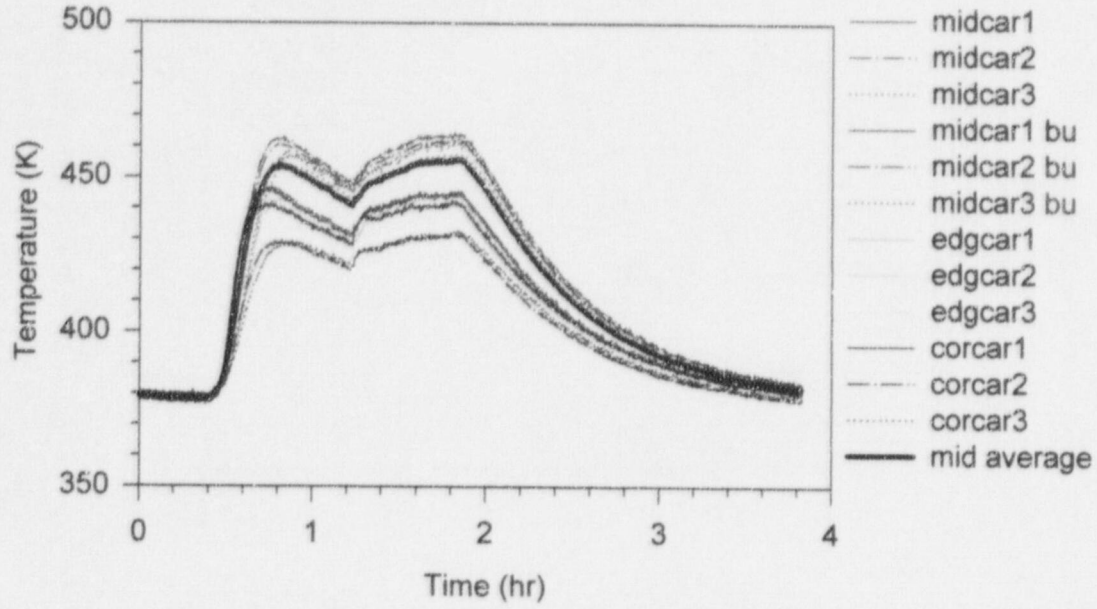

Figure 61. Catalyst cartridge temperatures in PAR-5.

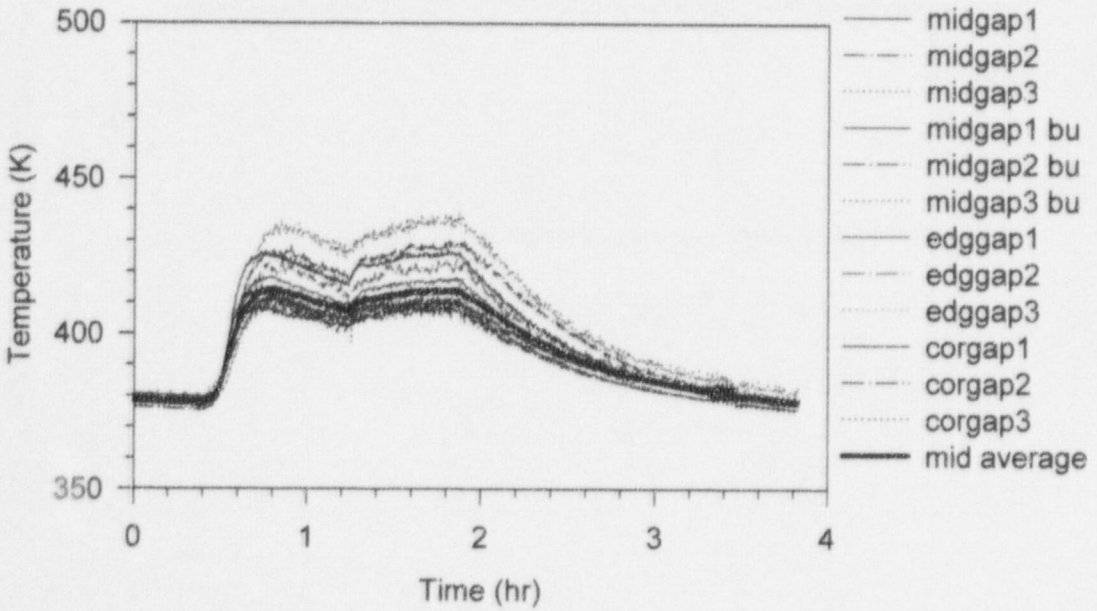

Figure 62. Catalyst gap temperatures in PAR-5.

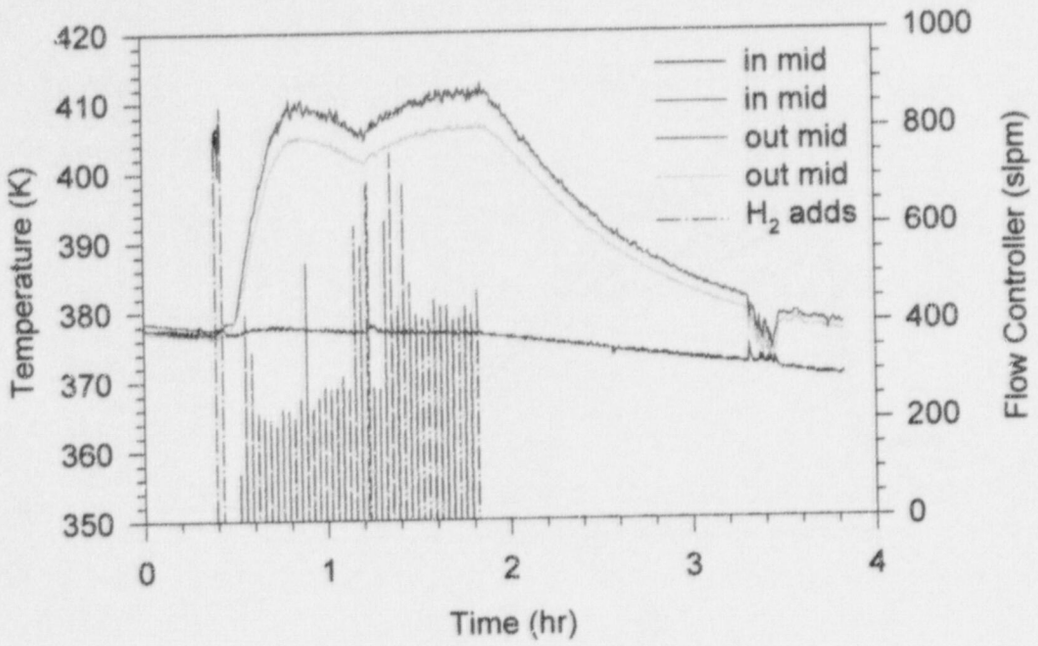

Figure 63. Inlet and outlet temperatures in PAR-5.

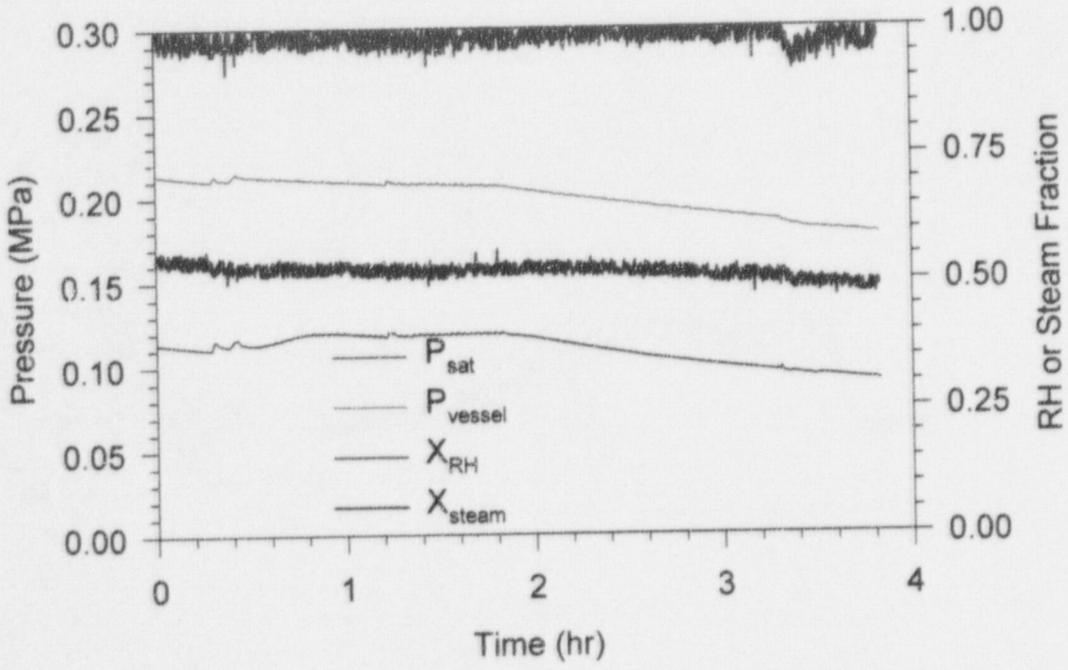

Figure 64. Saturation pressure, vessel pressure, relative humidity, and steam fraction in PAR-5.

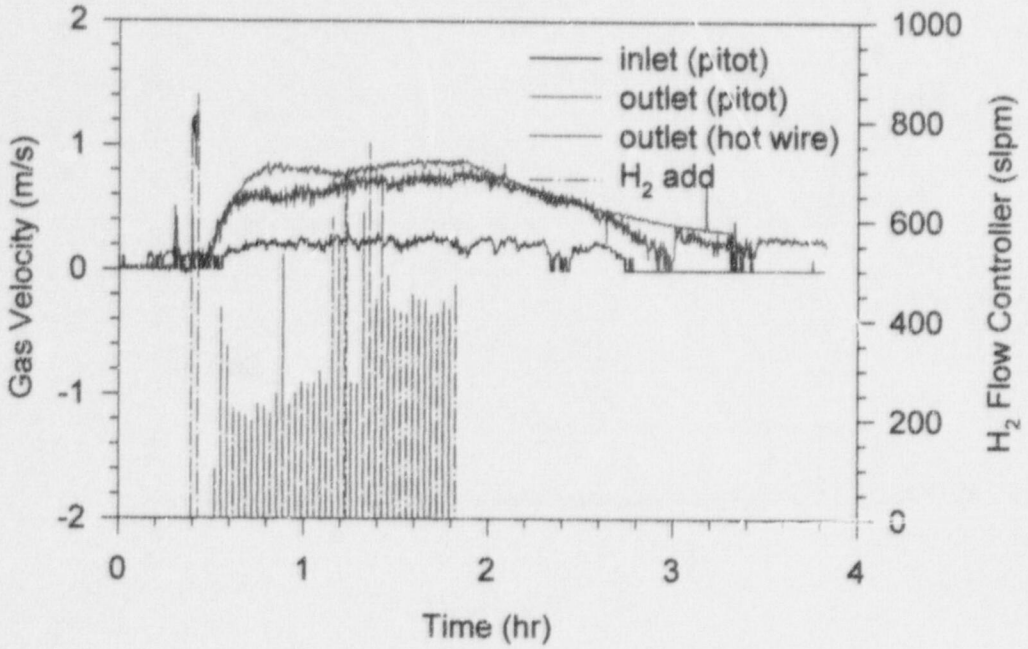

Figure 65. PAR gas velocity in PAR-5.

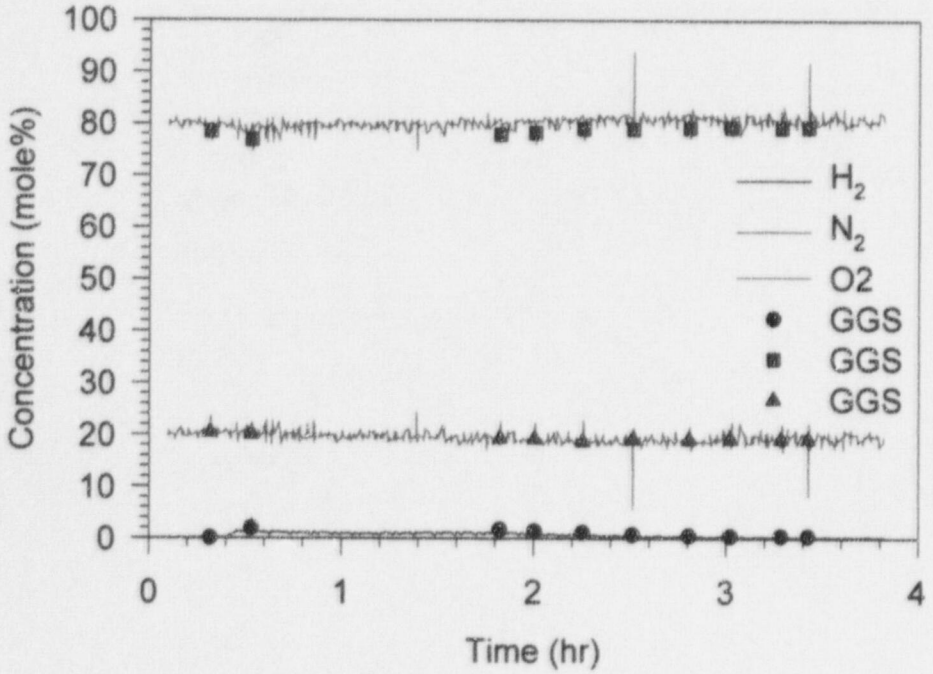

Figure 66. Gas concentrations (dry-basis) in PAR-5.

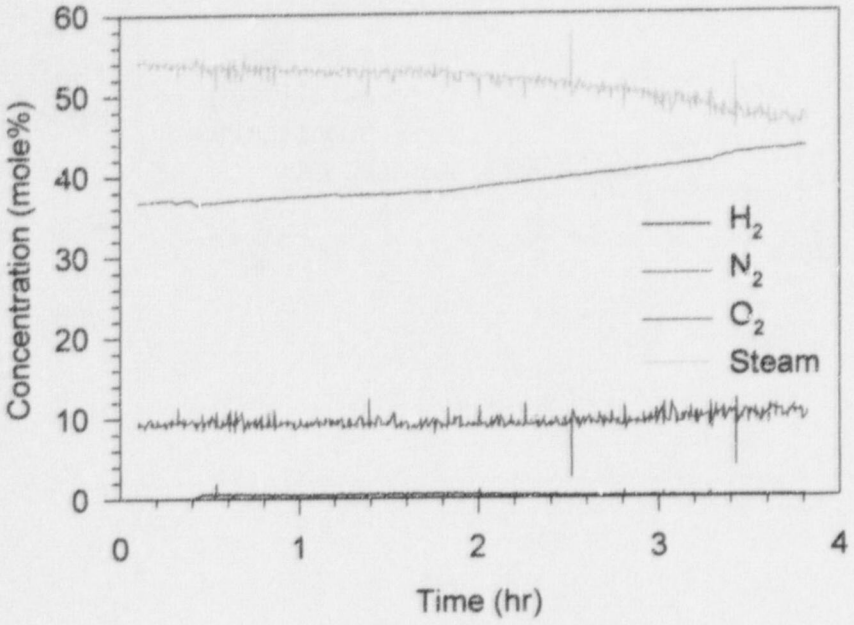

Figure 67. Gas concentrations (wet-basis) in PAR-5.

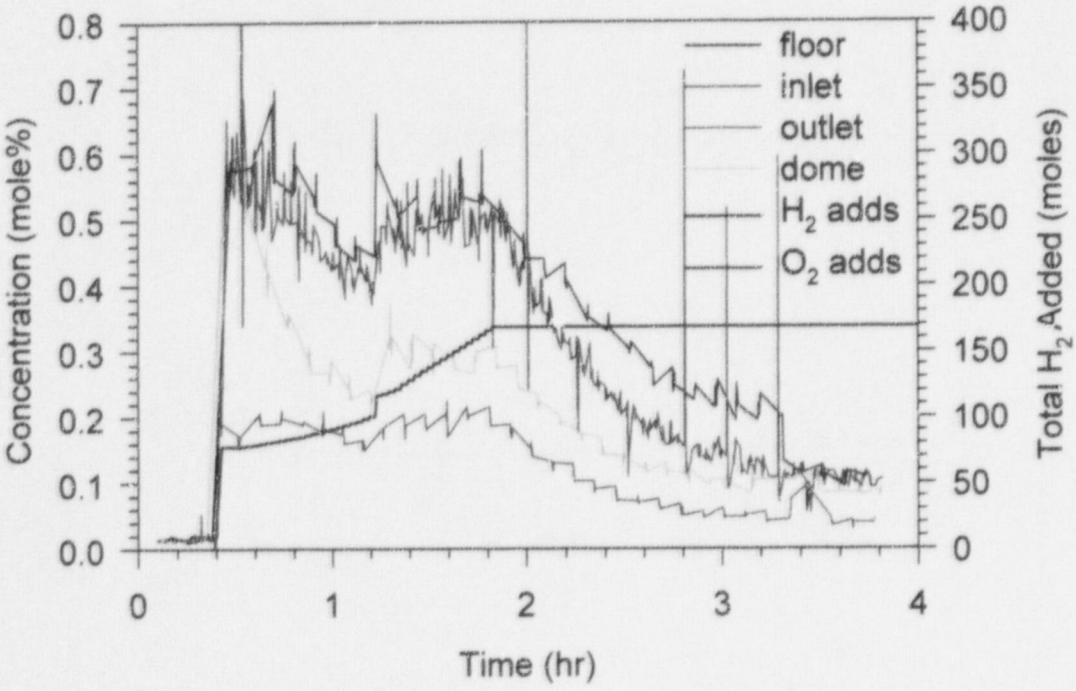

Figure 68. H_2 concentrations (wet-basis) in PAR-5.

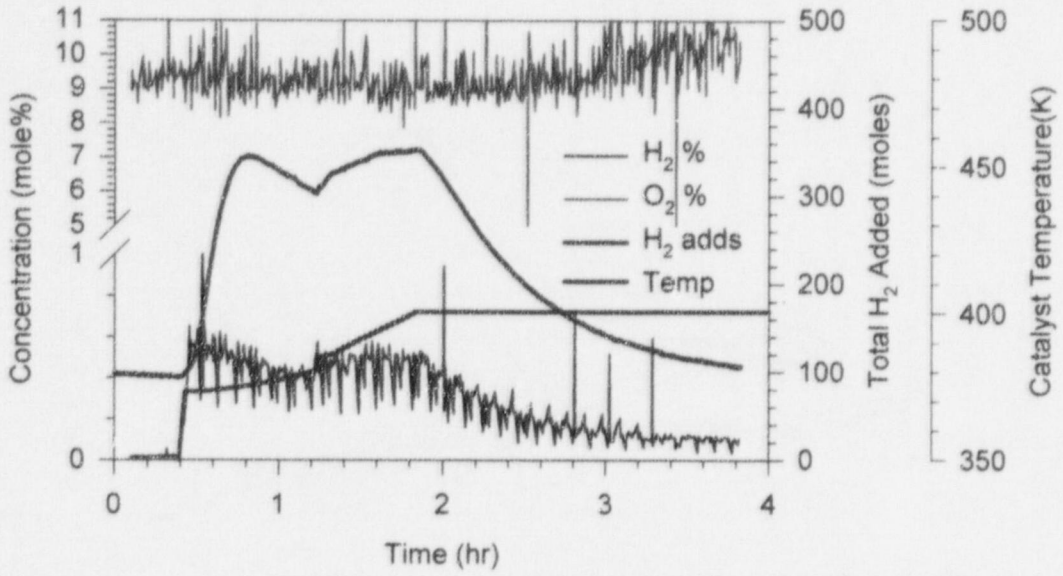

Figure 69. Catalyst temperature compared to gas additions and concentrations in PAR-5.

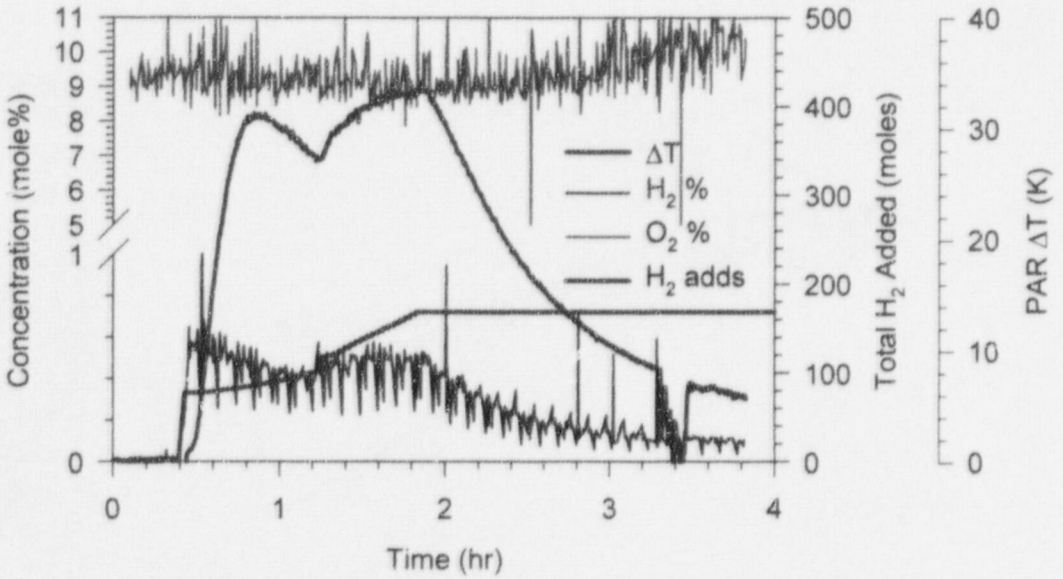

Figure 70. PAR ΔT temperature compared to gas additions and concentrations in PAR-5.

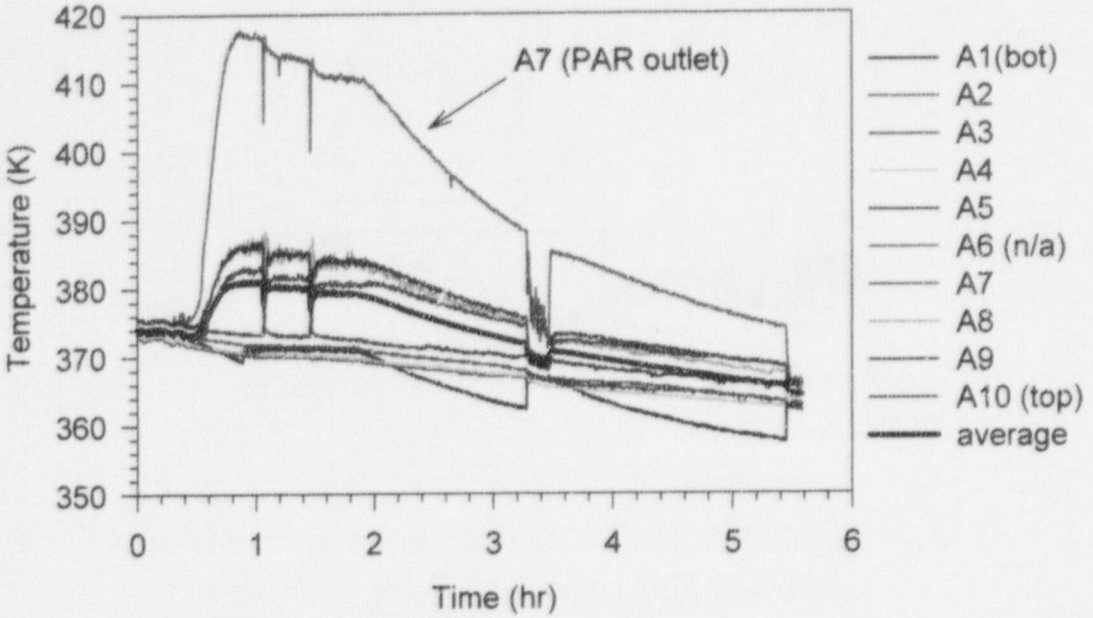

Figure 71. Surtsey vessel centerline gas temperatures from TC array A in PAR-6.

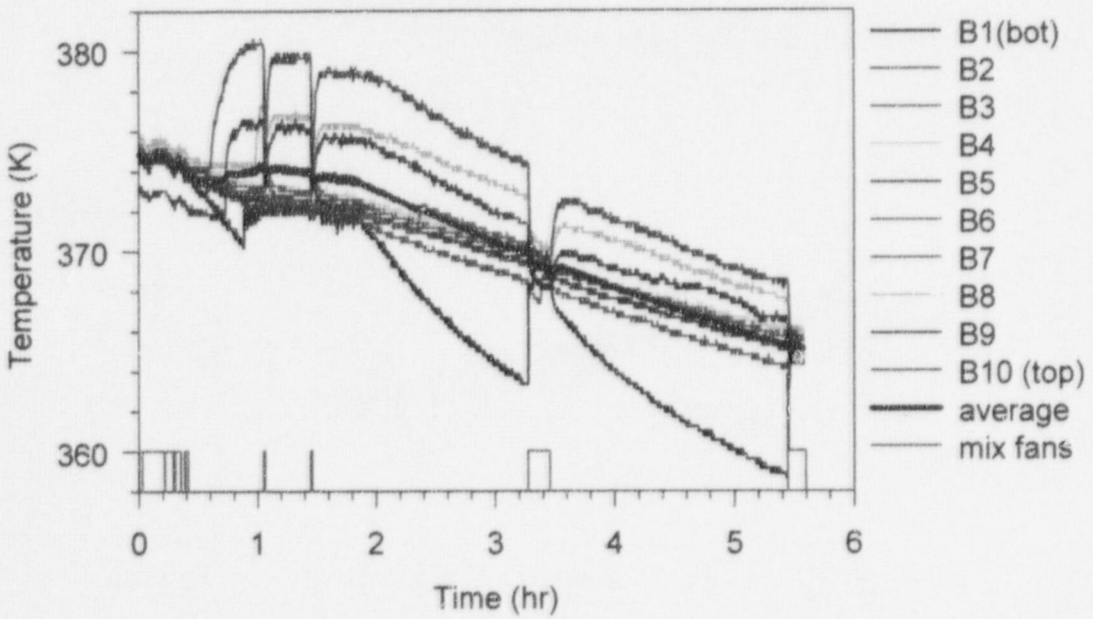

Figure 72. Surtsey vessel wall gas temperatures from TC array B in PAR-6.

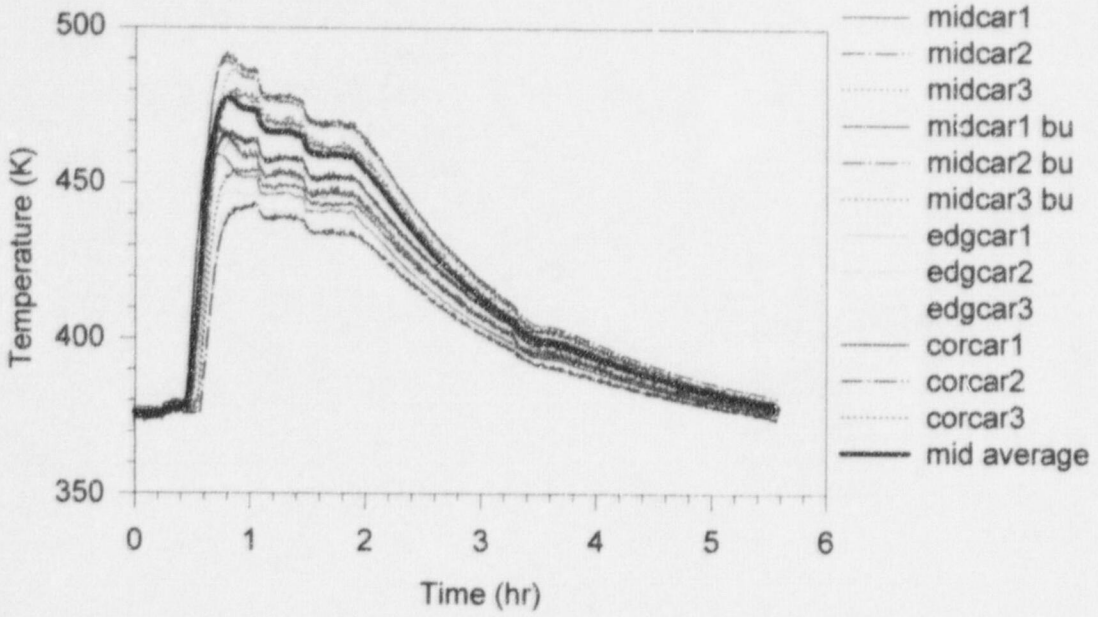

Figure 73. Catalyst cartridge temperatures in PAR-6.

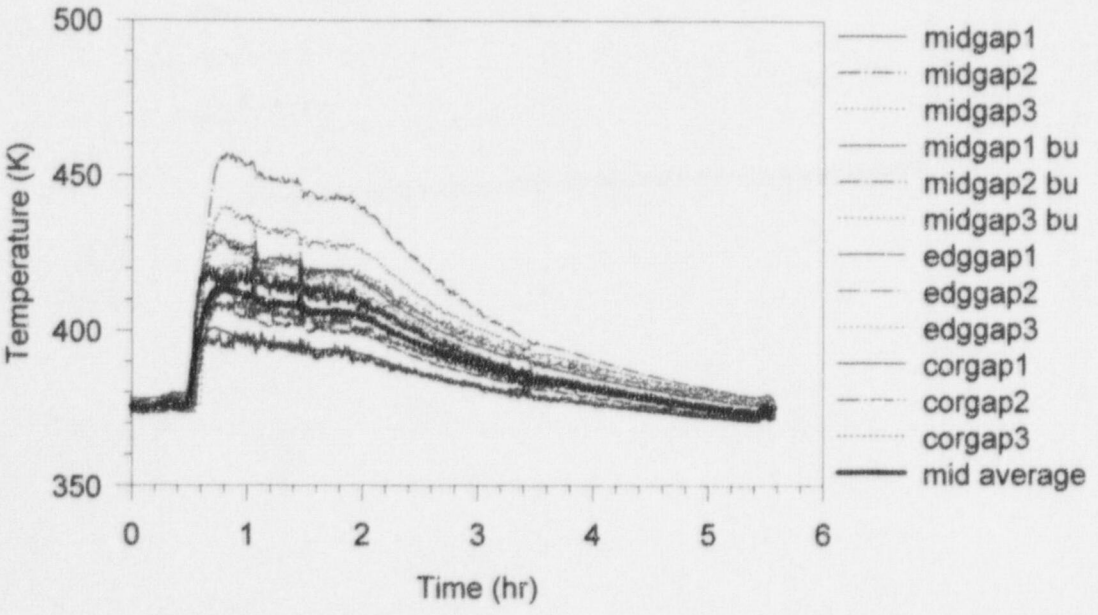

Figure 74. Catalyst gap temperatures in PAR-6.

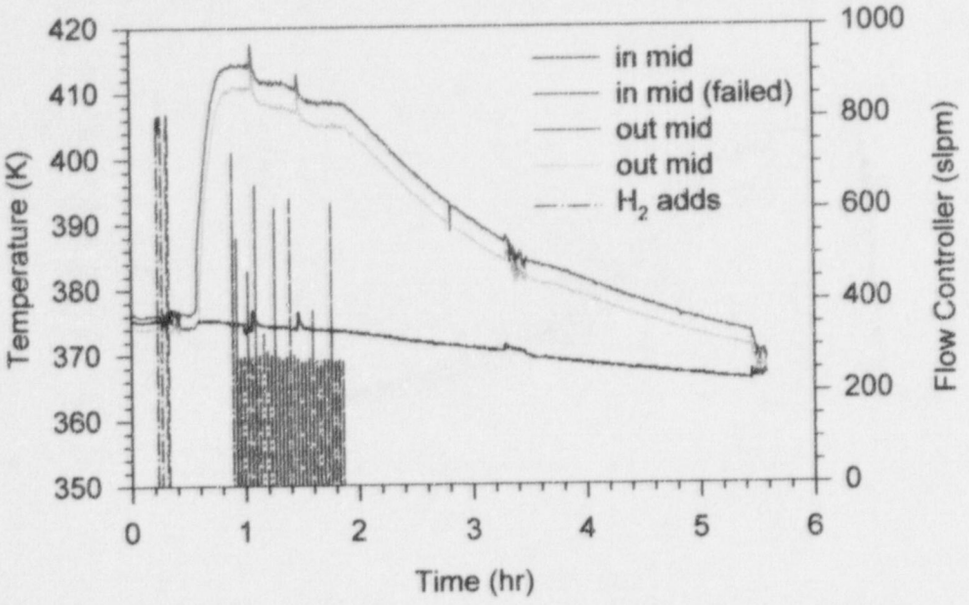

Figure 75. Inlet and outlet temperatures in PAR-6.

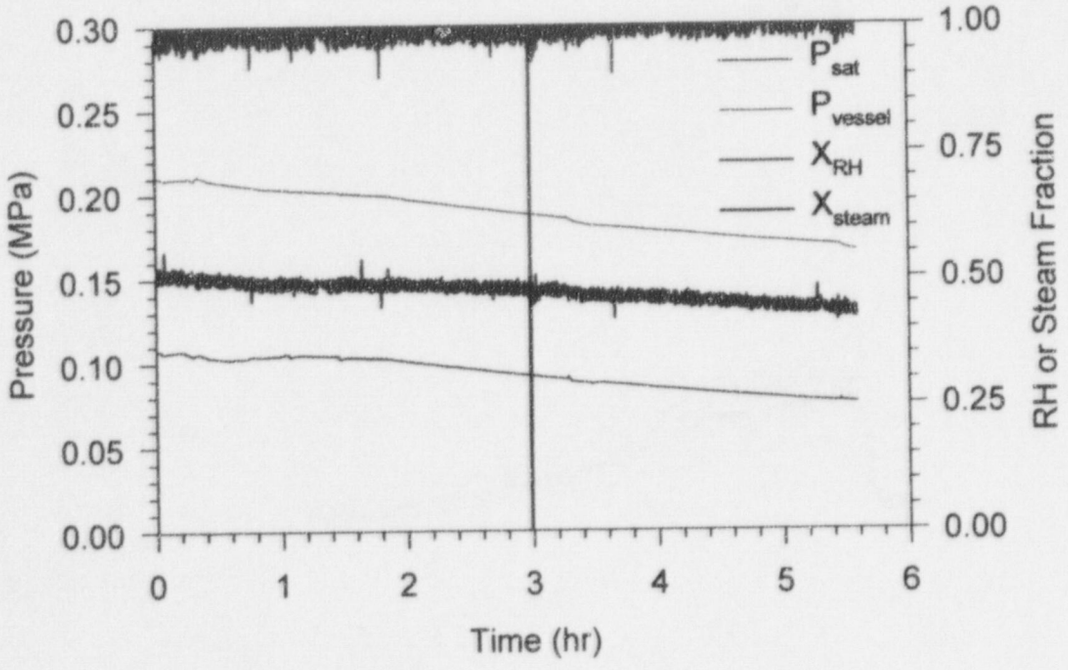

Figure 76. Saturation pressure, vessel pressure, relative humidity, and steam fraction in PAR-6.

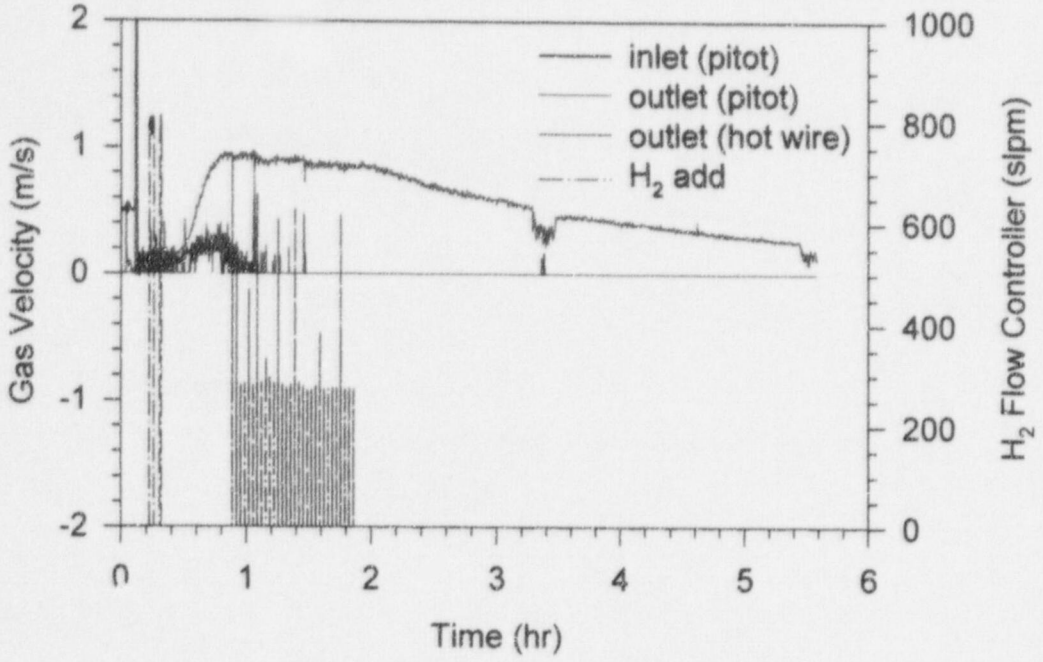

Figure 77. PAR gas velocity in PAR-6.

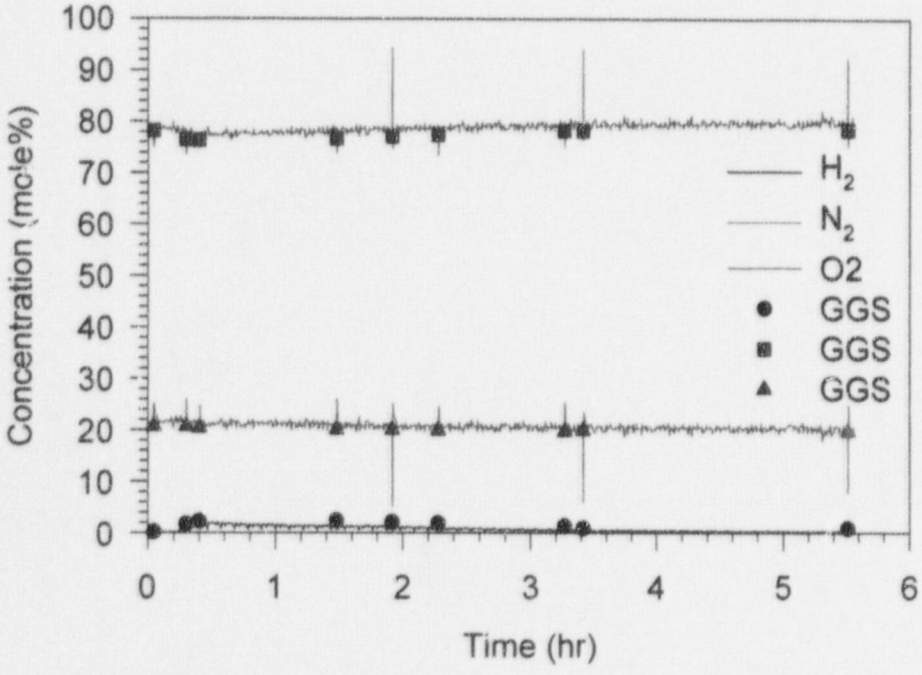

Figure 78. Gas concentrations (dry-basis) in PAR-6.

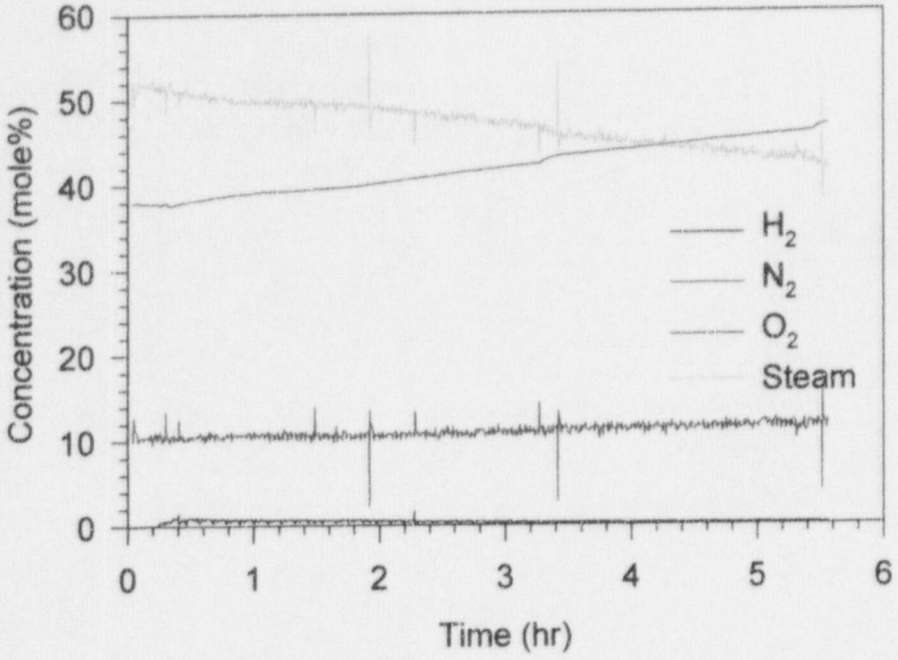

Figure 79. Gas concentrations (wet-basis) in PAR-6.

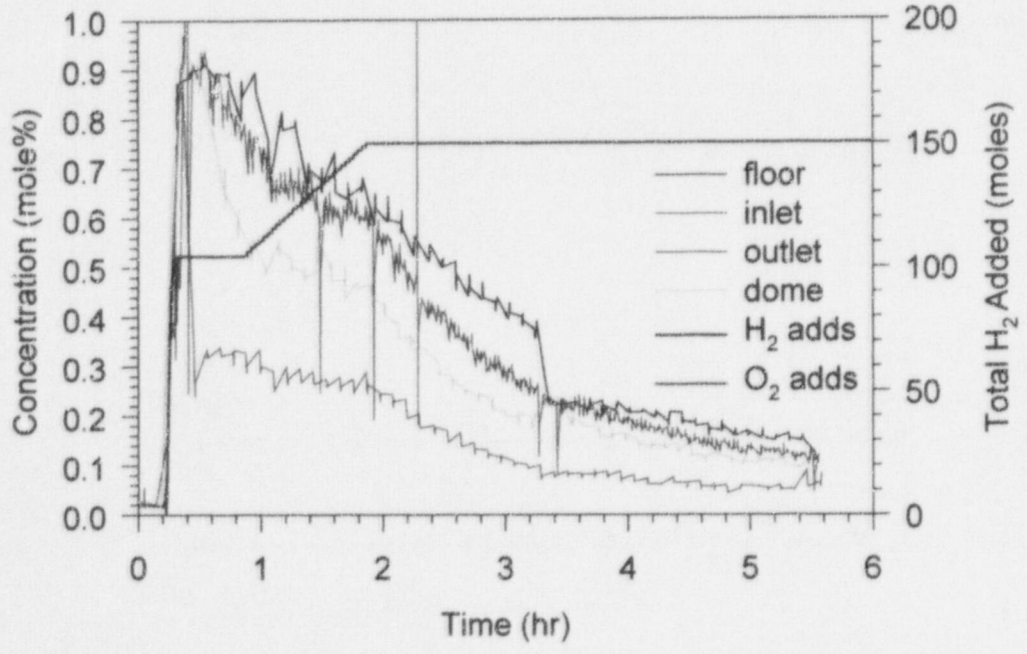

Figure 80. H_2 concentrations (wet-basis) in PAR-6.

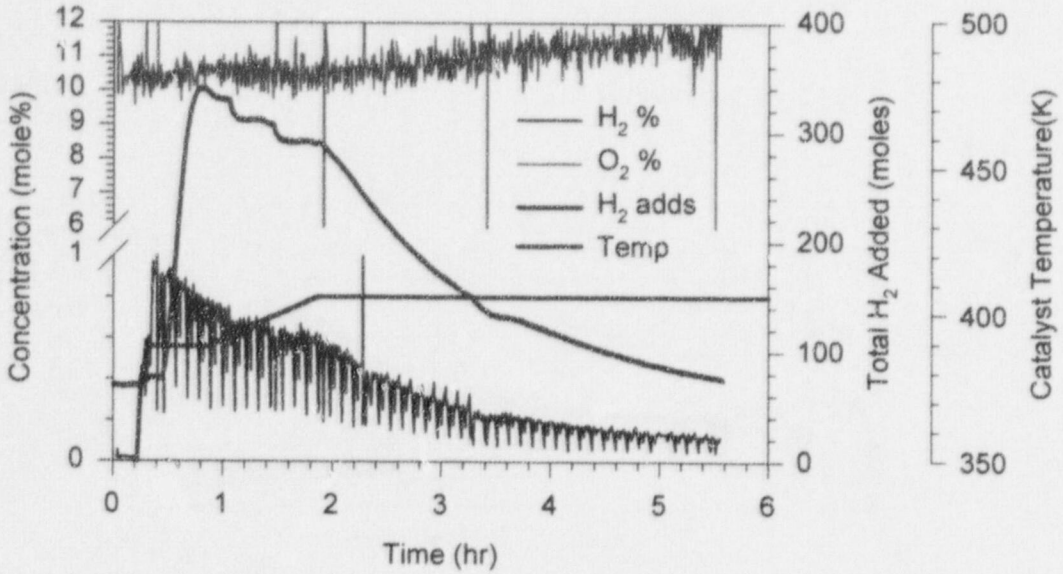

Figure 81. Catalyst temperature compared to gas additions and concentrations in PAR-6.

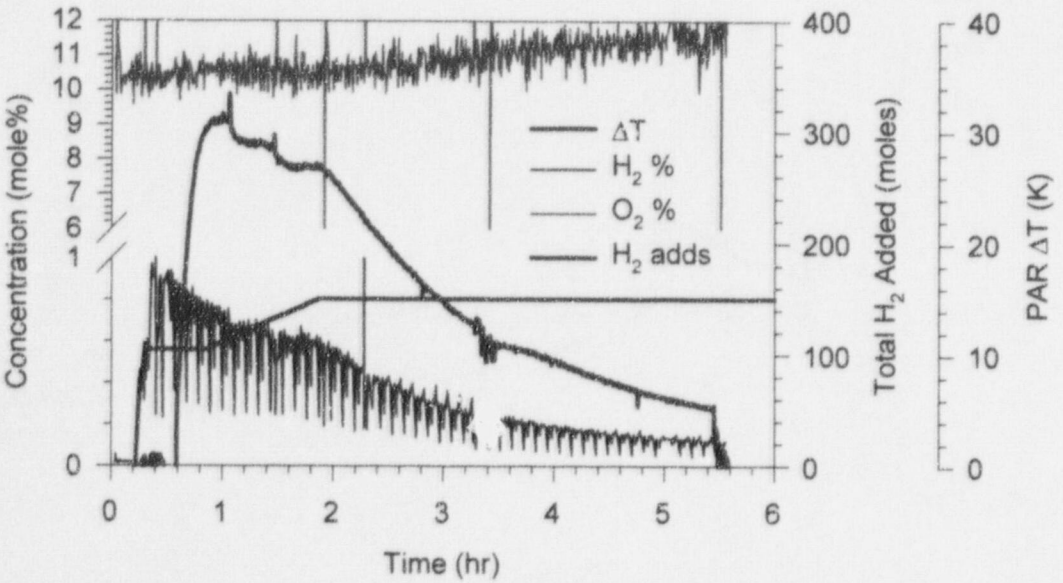

Figure 82. PAR ΔT temperature compared to gas additions and concentrations in PAR-6.

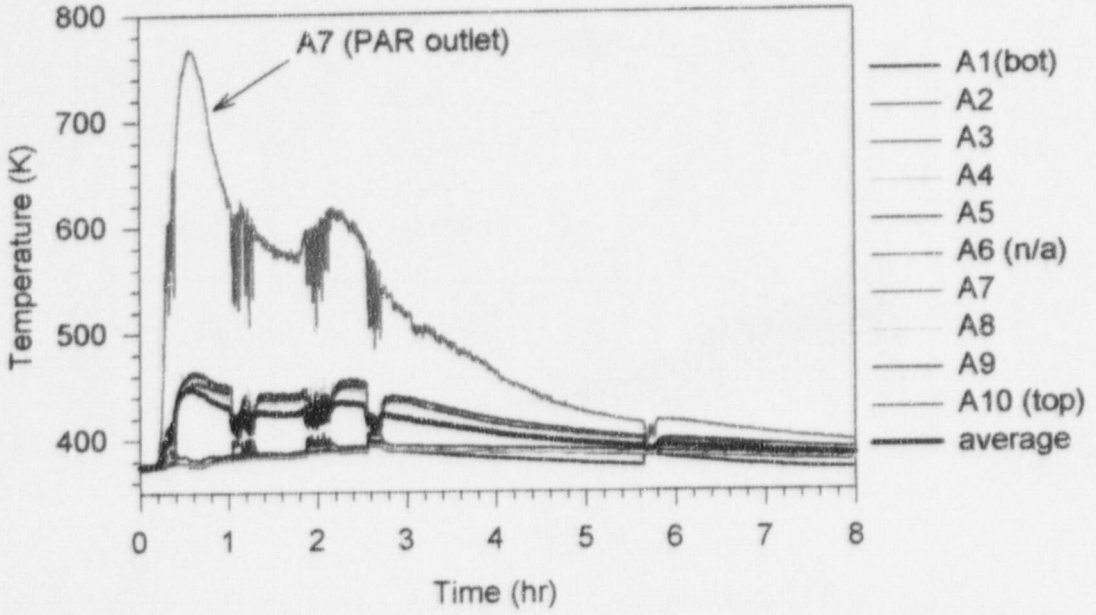

Figure 83. Surtsey vessel centerline gas temperatures from TC array A in PAR-7.

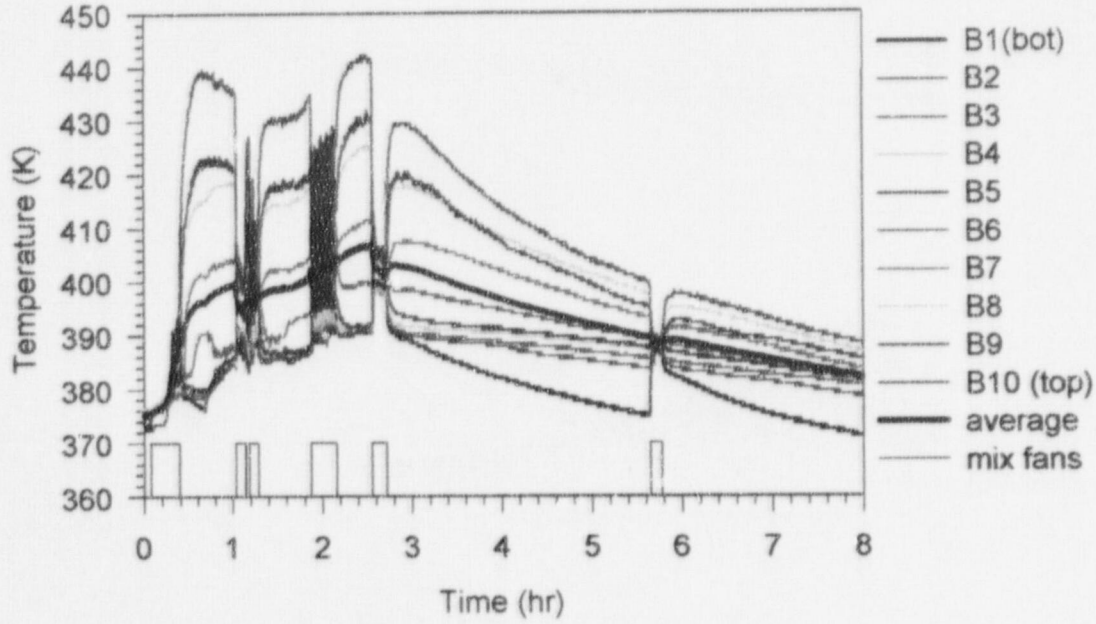

Figure 84. Surtsey vessel wall gas temperatures from TC array B in PAR-7.

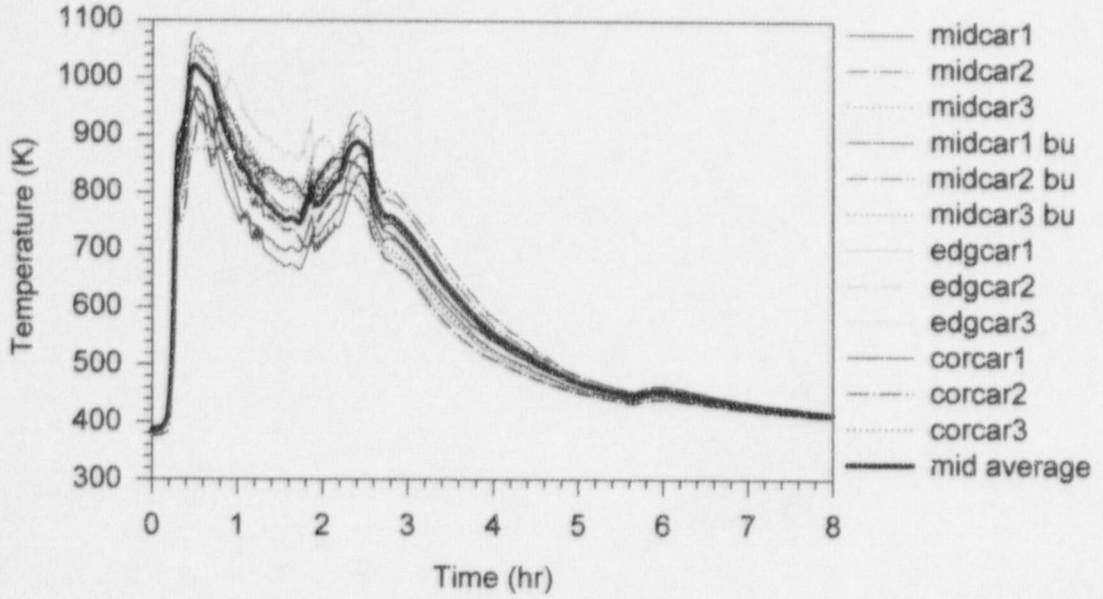

Figure 85. Catalyst cartridge temperatures in PAR-7.

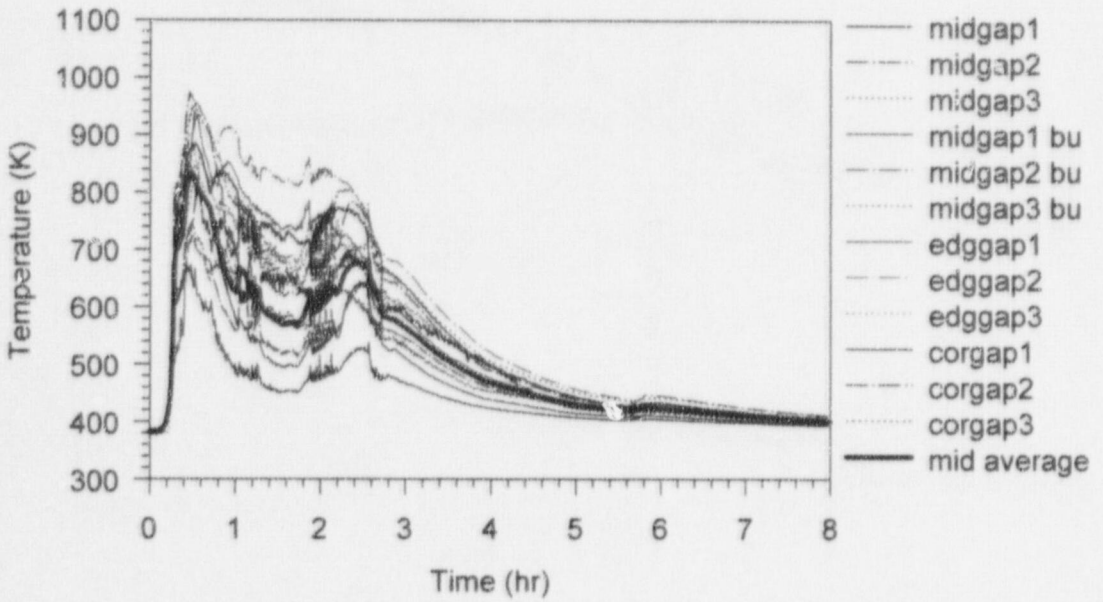

Figure 86. Catalyst gap temperatures in PAR-7.

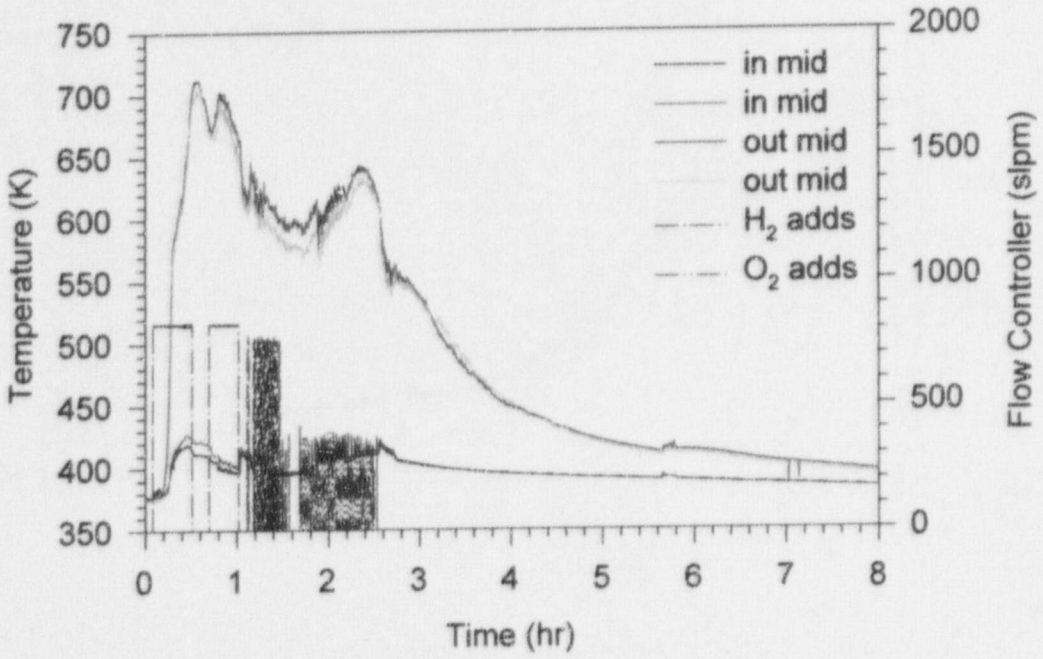

Figure 87. Inlet and outlet temperatures in PAR-7.

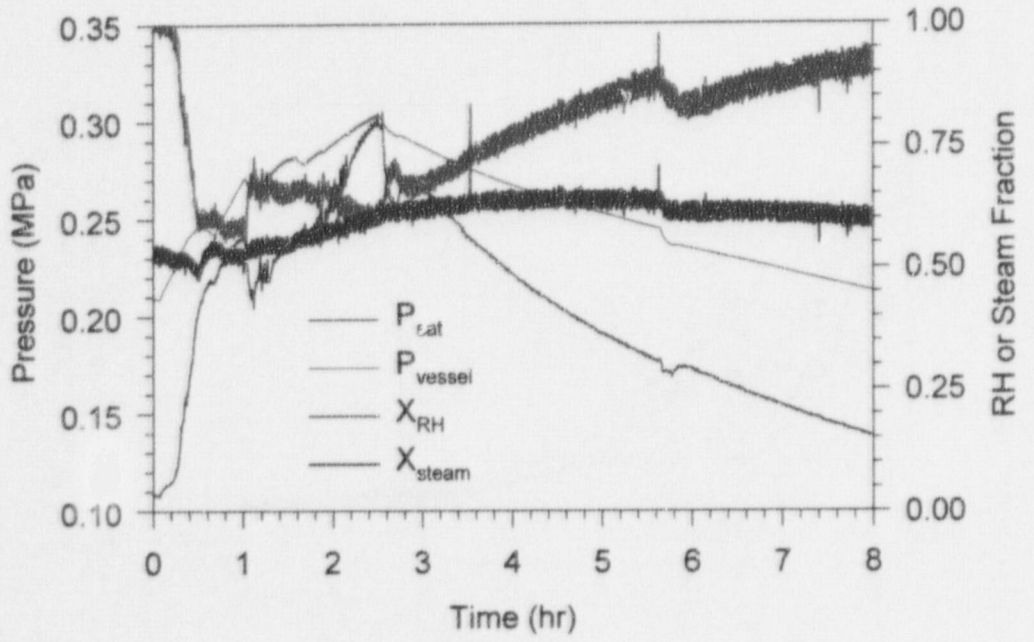

Figure 88. Saturation pressure, vessel pressure, relative humidity, and steam fraction in PAR-7.

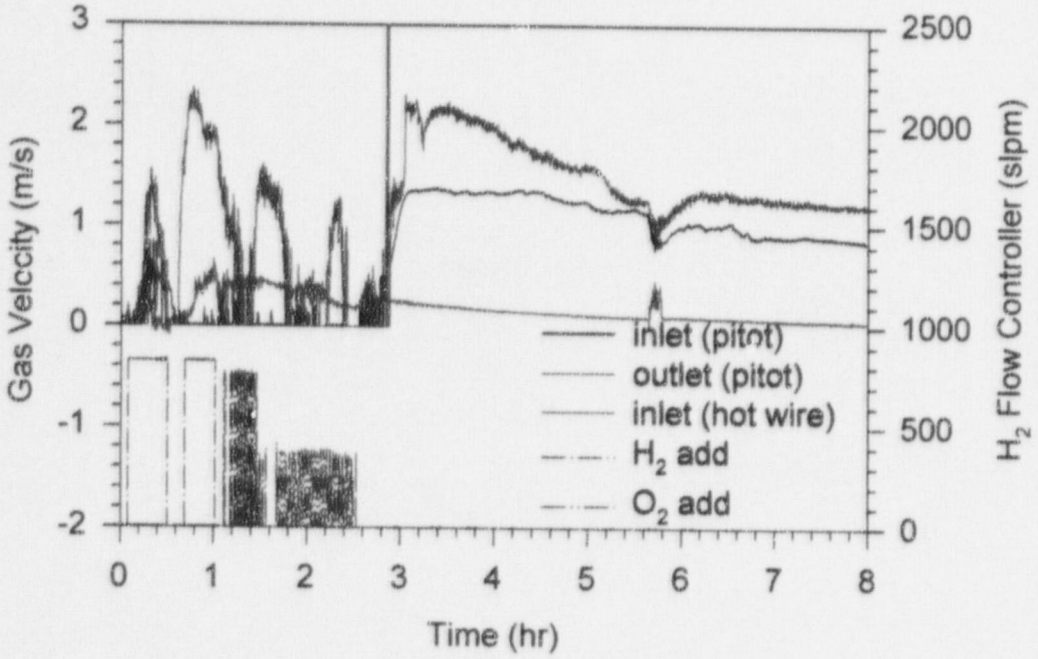

Figure 89. PAR gas velocity in PAR-7.

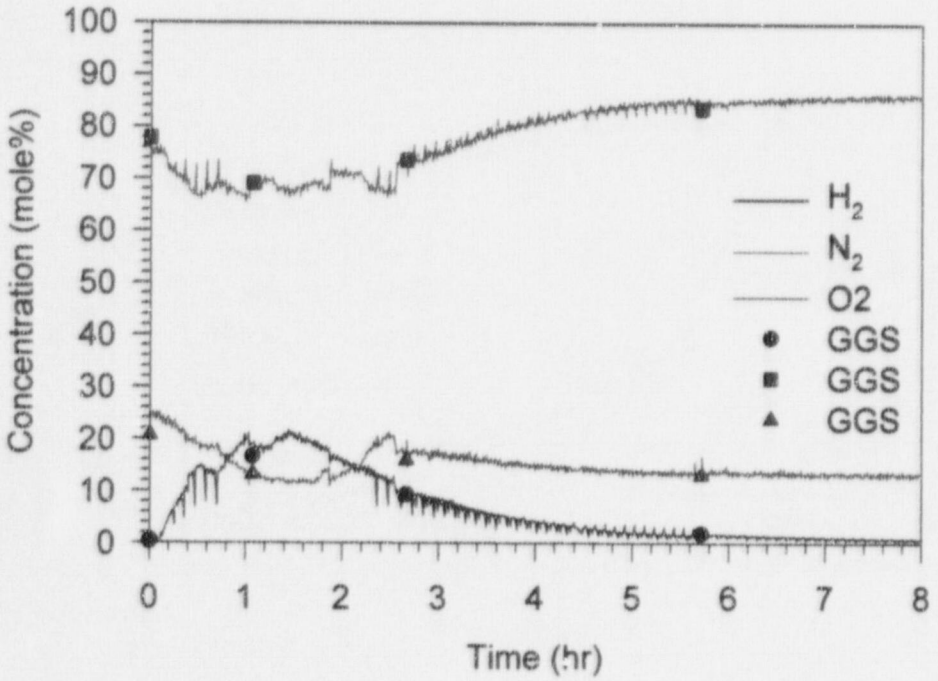

Figure 90. Gas concentrations (dry-basis) in PAR-7.

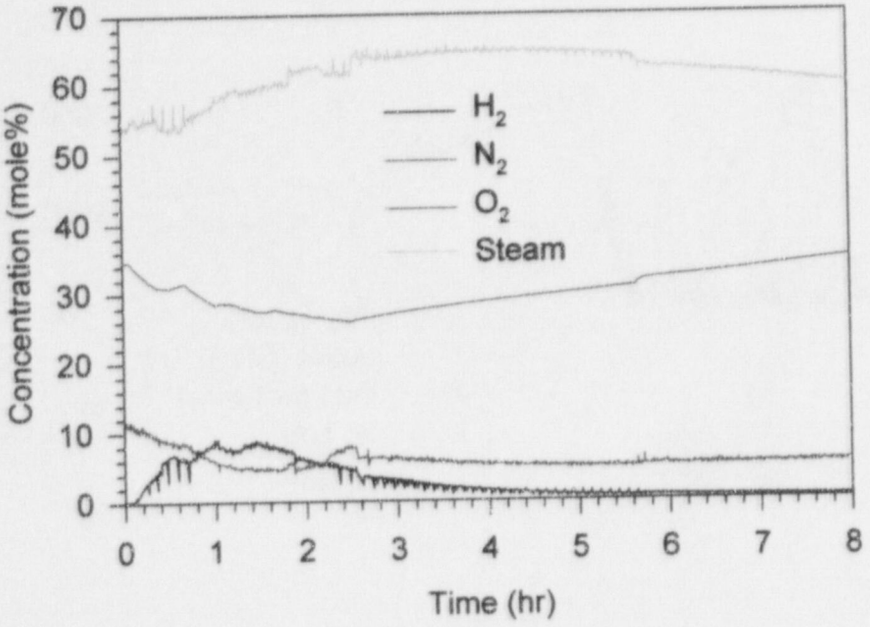

Figure 91. Gas concentrations (wet-basis) in PAR-7.

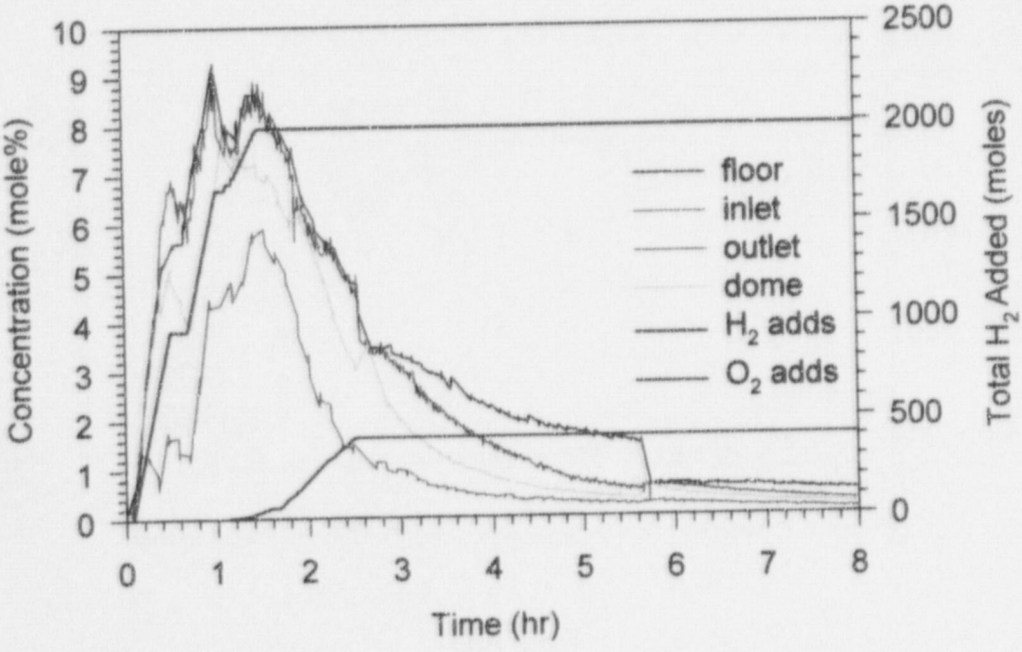

Figure 92. H_2 concentrations (wet-basis) in PAR-7.

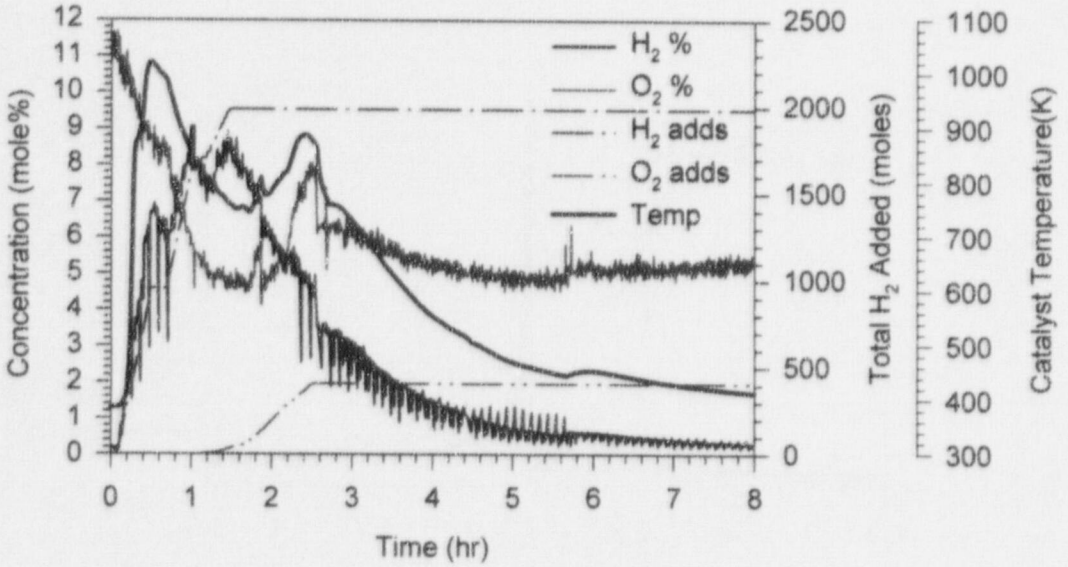

Figure 93. Catalyst temperature compared to gas additions and concentrations in PAR-7.

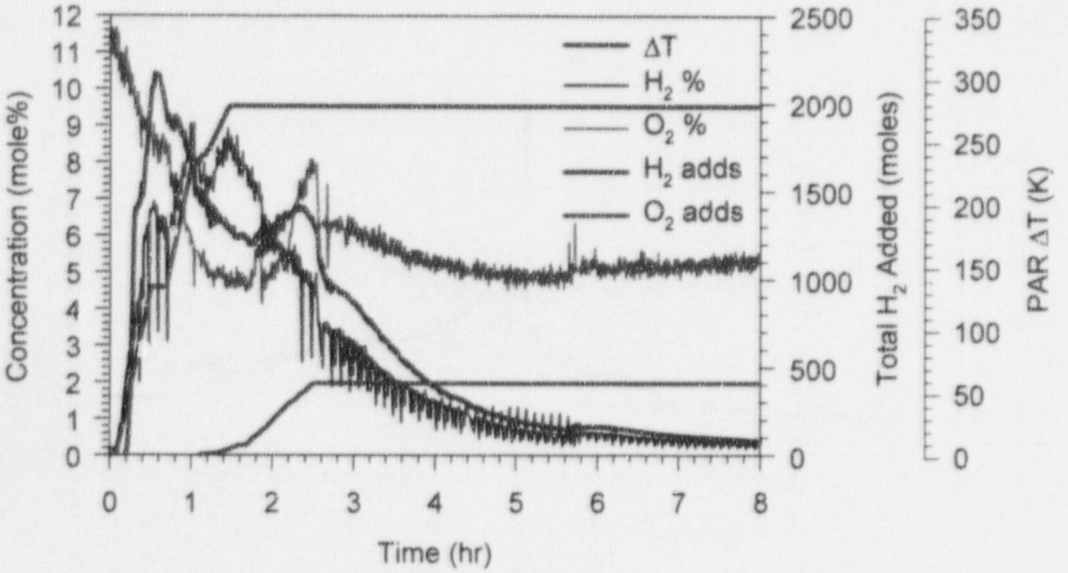

Figure 94. PAR ΔT temperature compared to gas additions and concentrations in PAR-7.

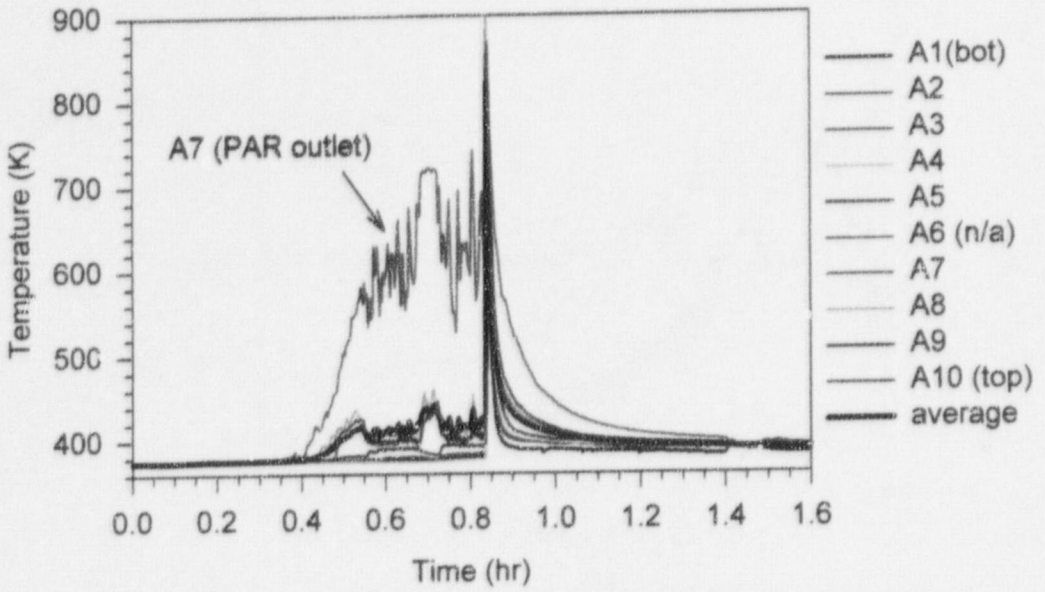

Figure 95. Surtsey vessel centerline gas temperatures from TC array A in PAR-8.

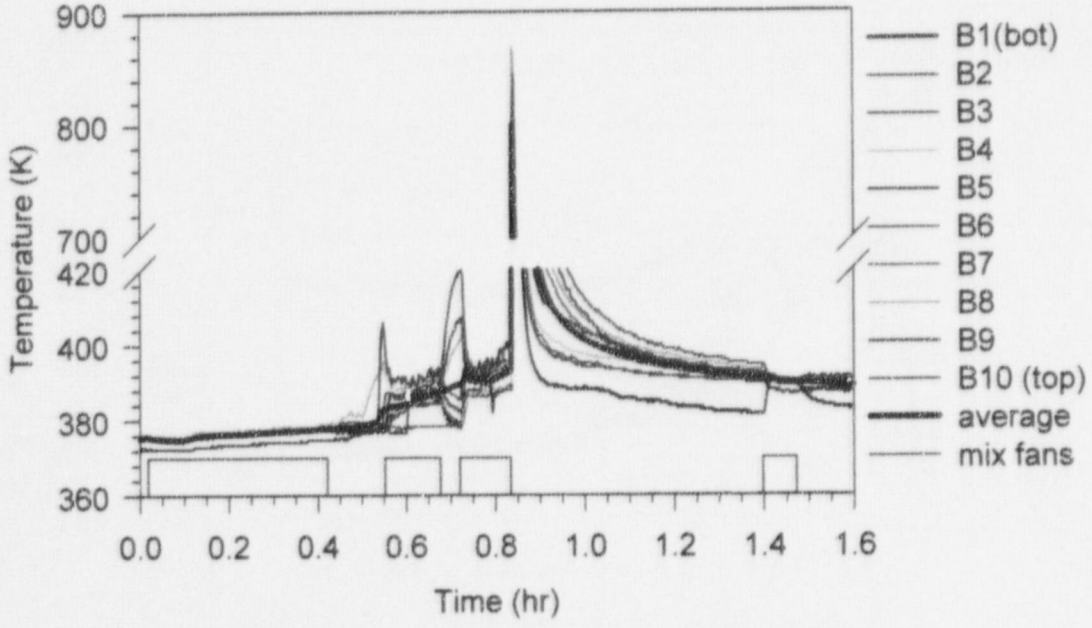

Figure 96. Surtsey vessel wall gas temperatures from TC array B in PAR-8.

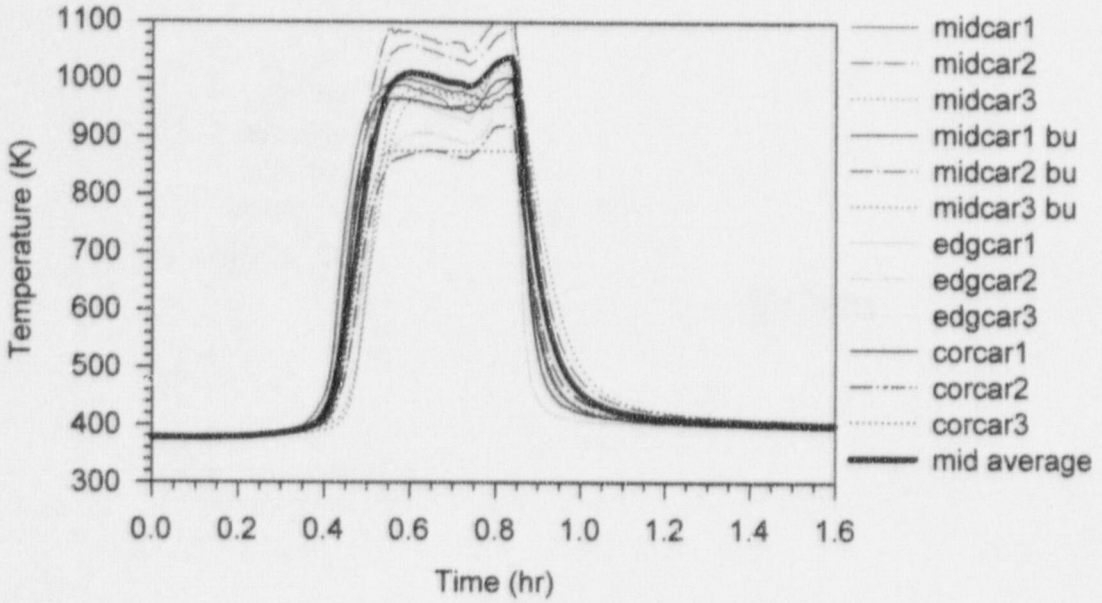

Figure 97. Catalyst cartridge temperatures in PAR-8.

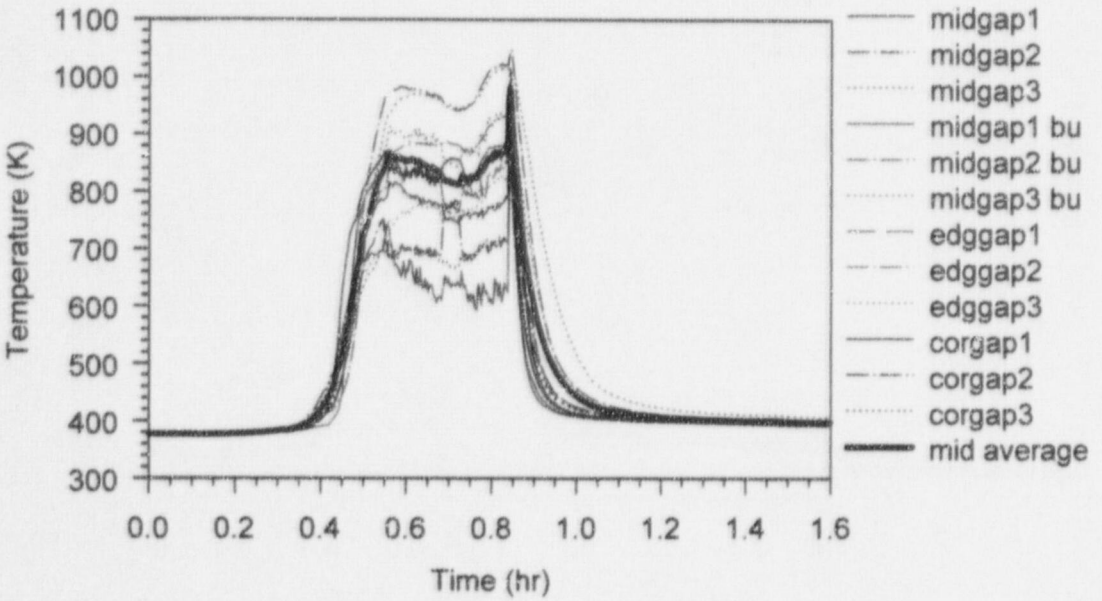

Figure 98. Catalyst gap temperatures in PAR-8.

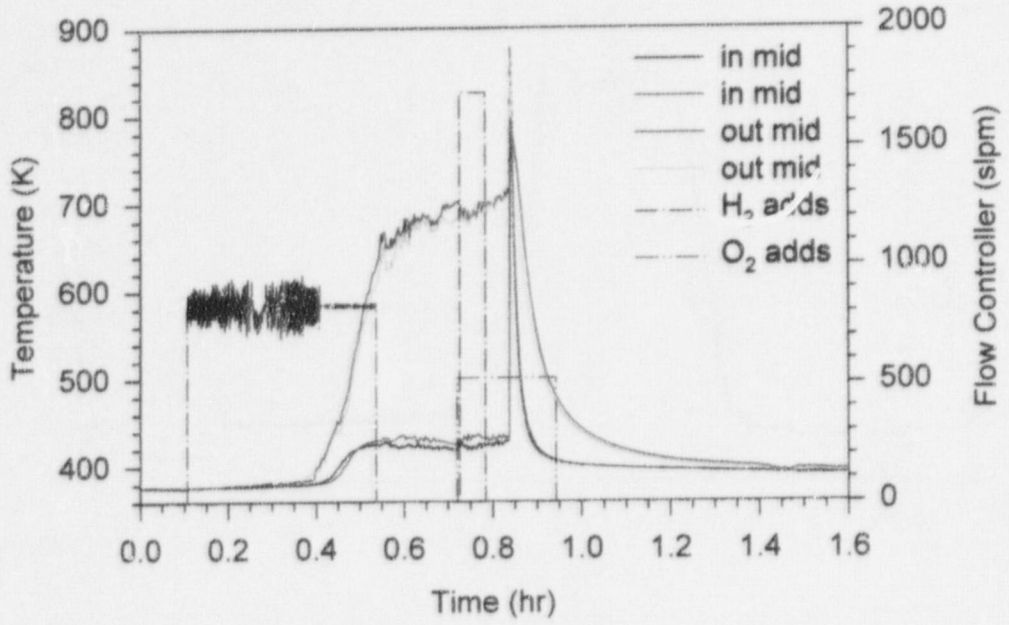

Figure 99. Inlet and outlet temperatures in PAR-8.

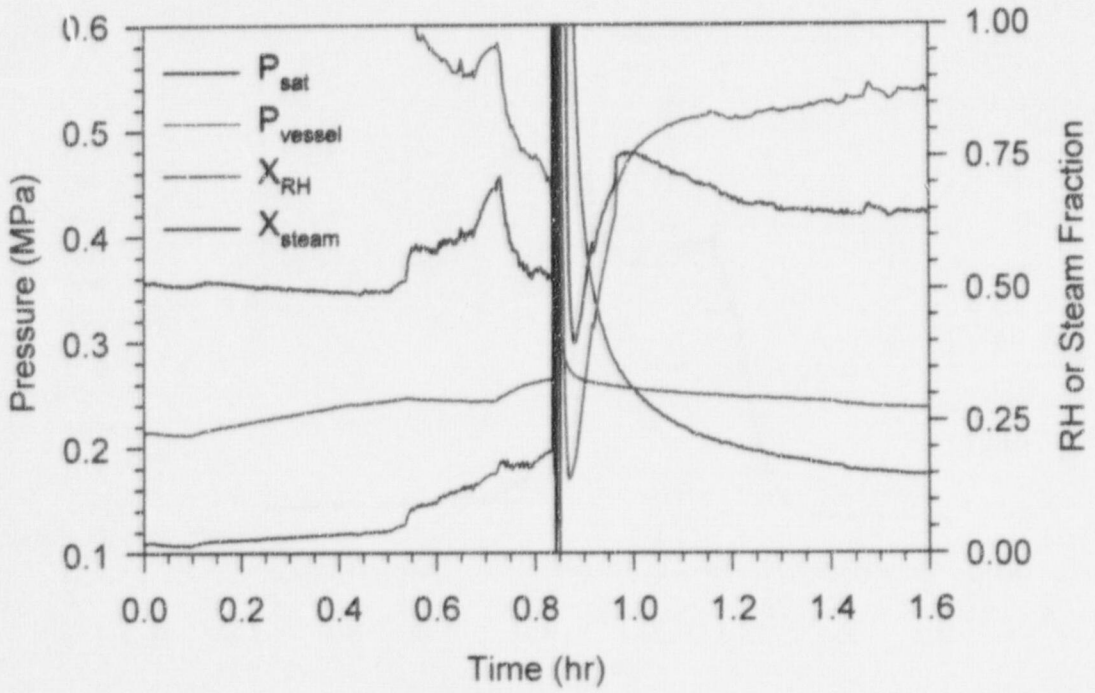

Figure 100. Saturation pressure, vessel pressure, relative humidity, and steam fraction in PAR-8.

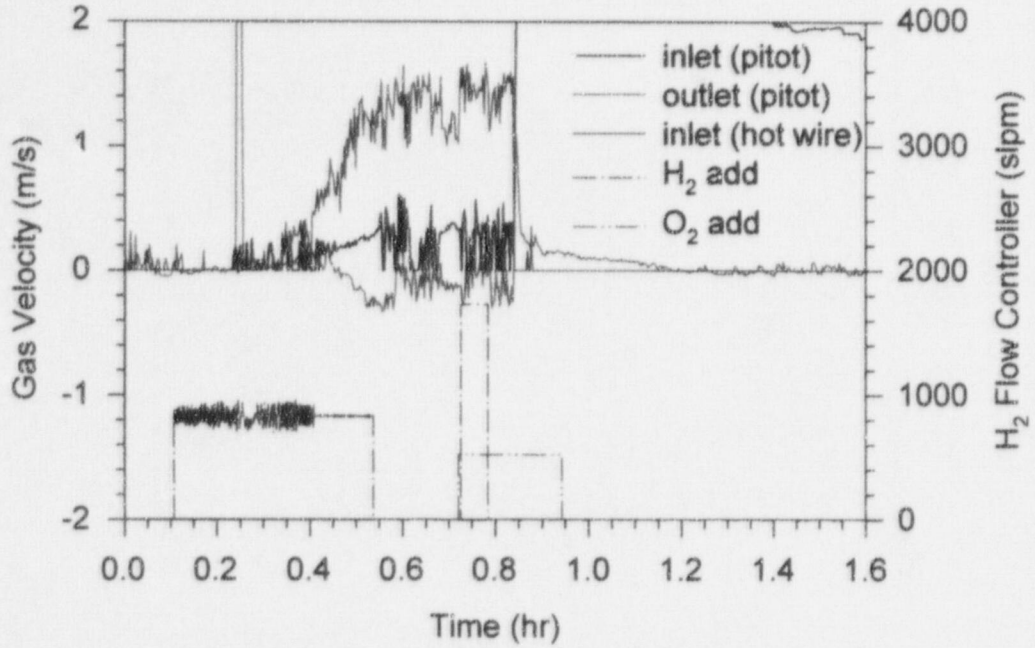

Figure 101. PAR gas velocity in PAR-8.

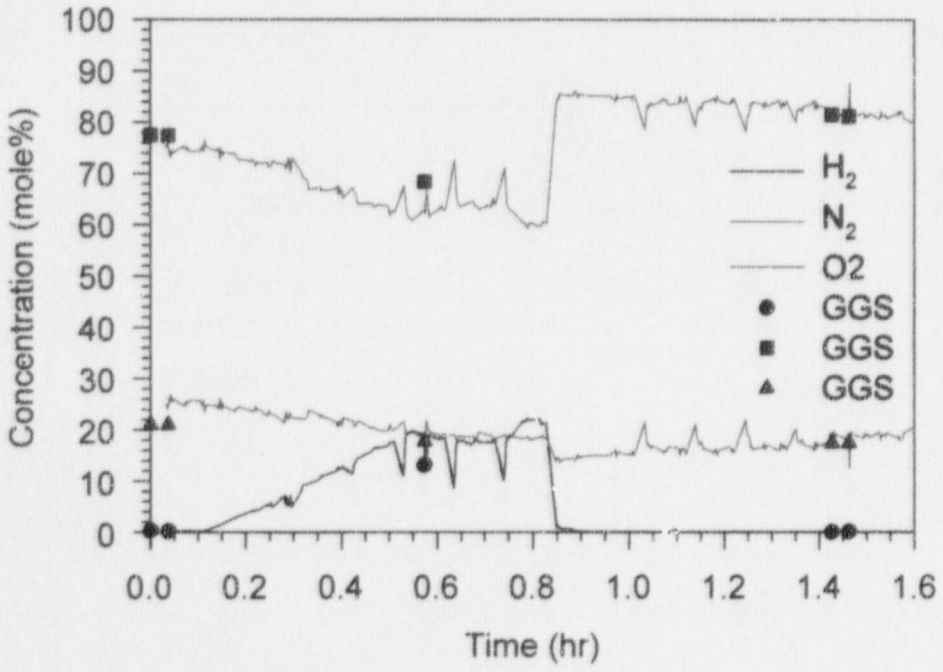

Figure 102. Gas concentrations (dry-basis) in PAR-8.

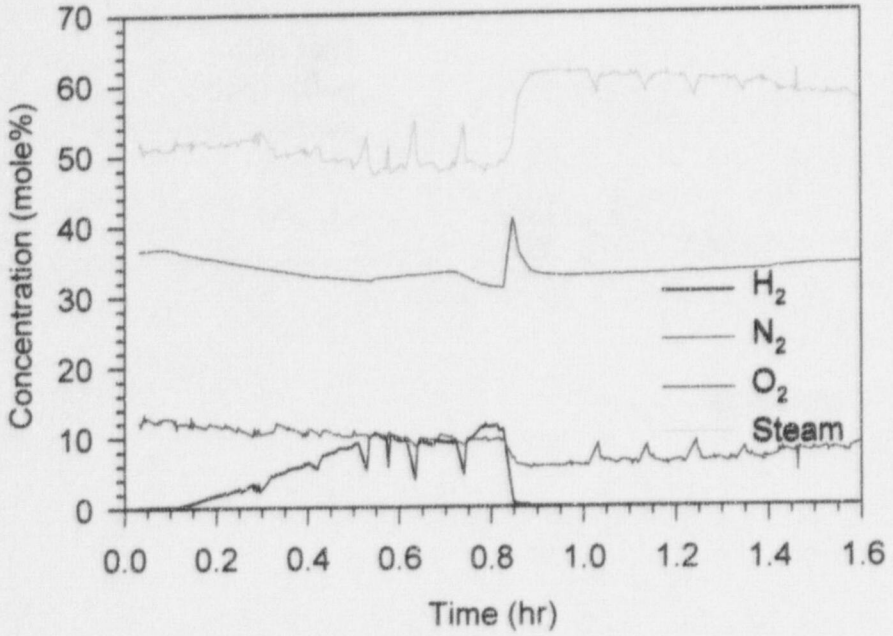

Figure 103. Gas concentrations (wet-basis) in PAR-8.

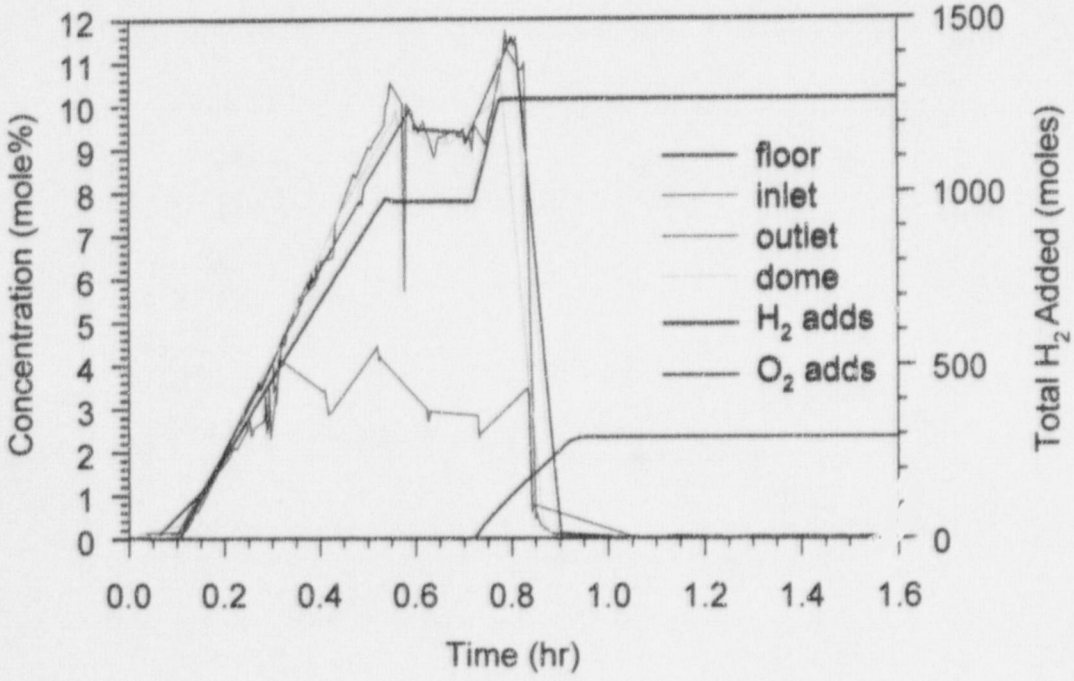

Figure 104. H_2 concentrations (wet-basis) in PAR-8.

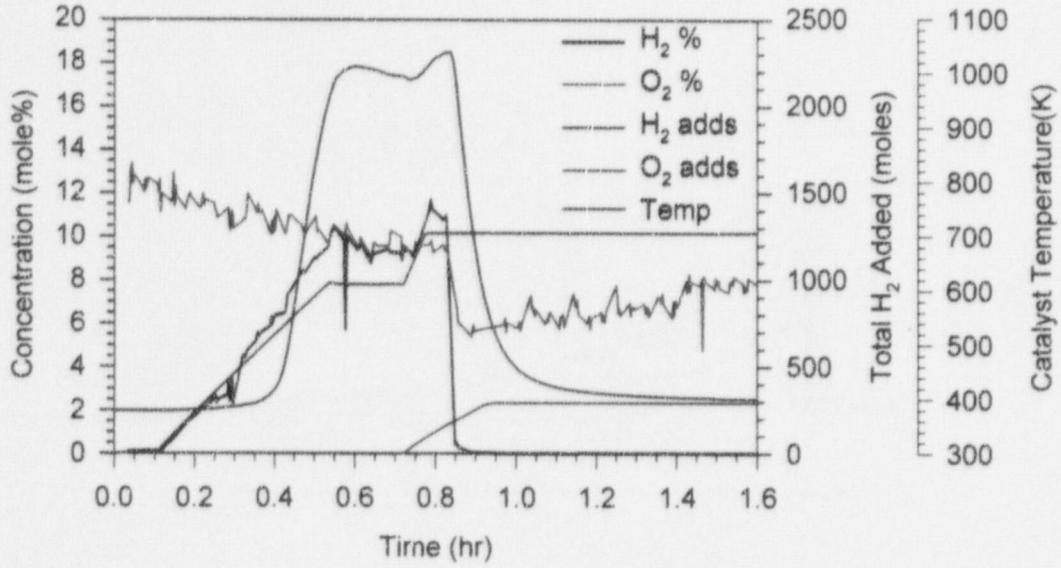

Figure 105. Catalyst temperature compared to gas additions and concentrations in PAR-8.

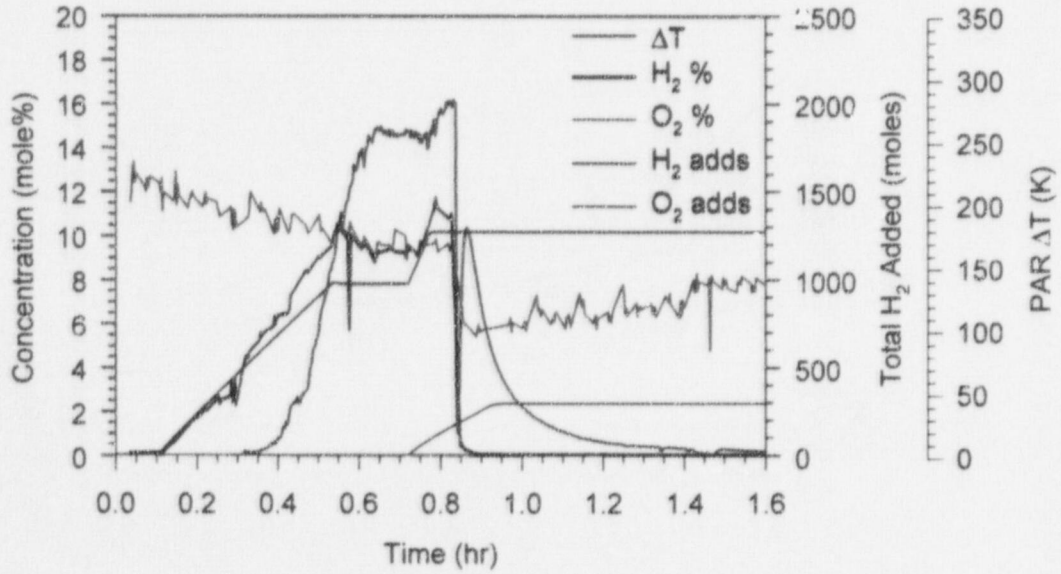

Figure 106. PAR ΔT temperature compared to gas additions and concentrations in PAR-8.

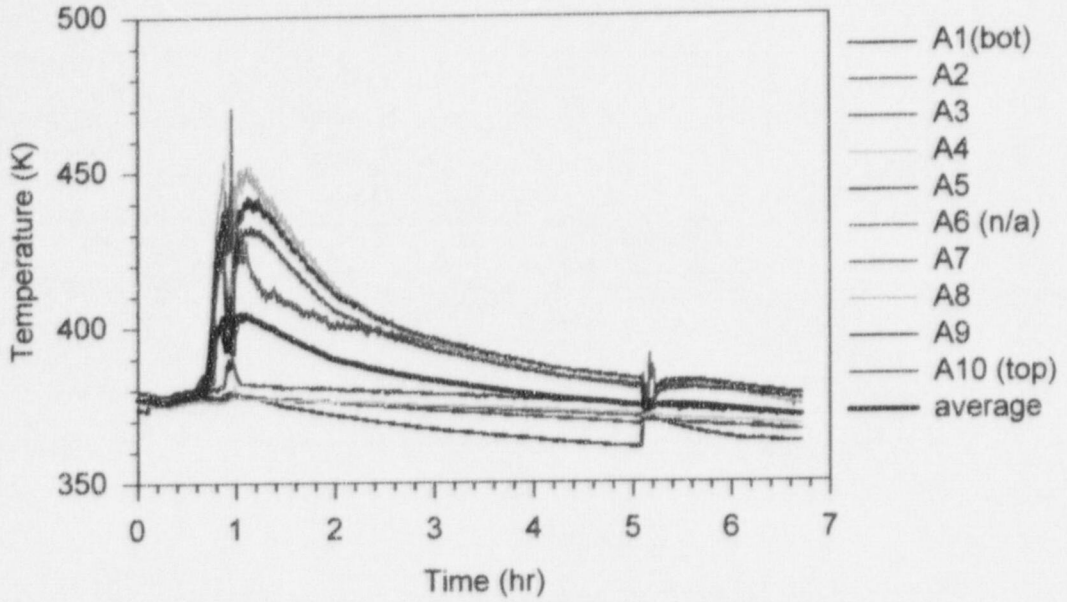

Figure 107. Surtsey vessel centerline gas temperatures from TC array A in PAR-8R.

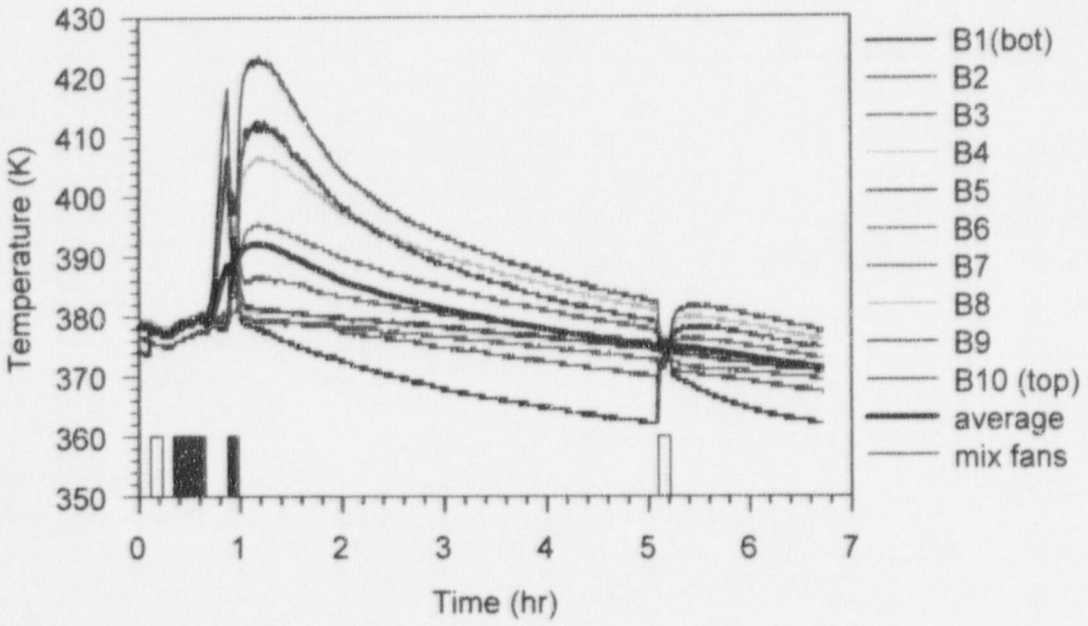

Figure 108. Surtsey vessel wall gas temperatures from TC array B in PAR-8R.

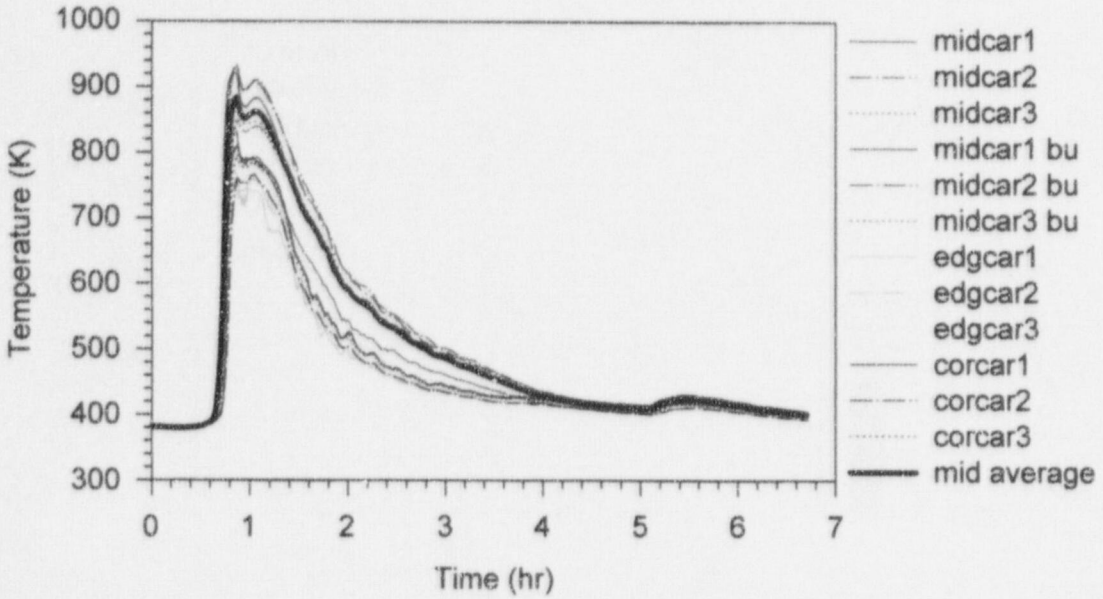

Figure 109. Catalyst cartridge temperatures in PAR-8R.

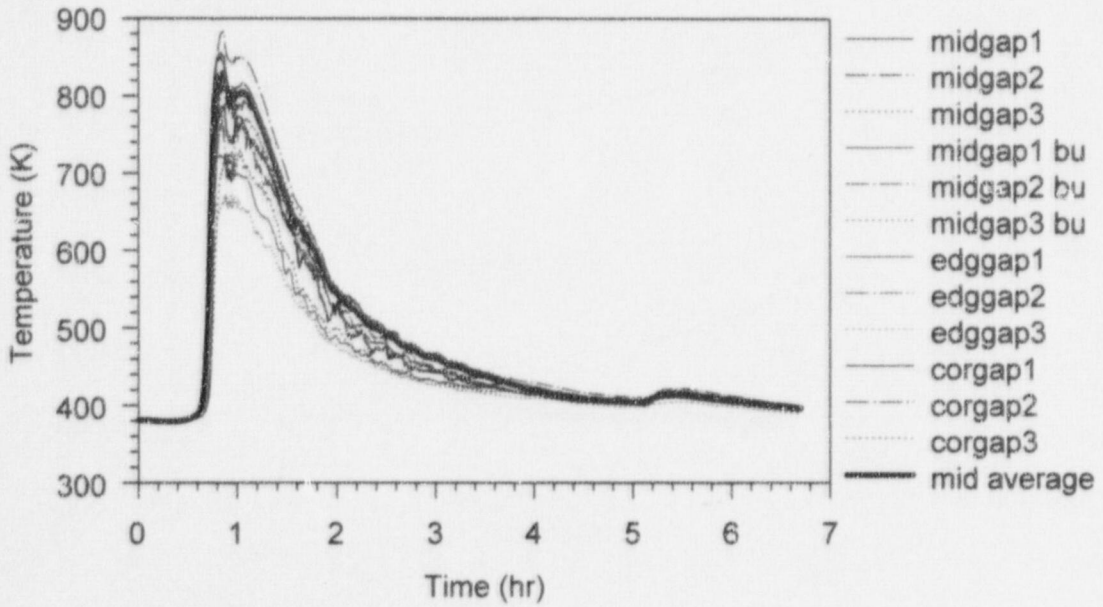

Figure 110. Catalyst gap temperatures in PAR-8R.

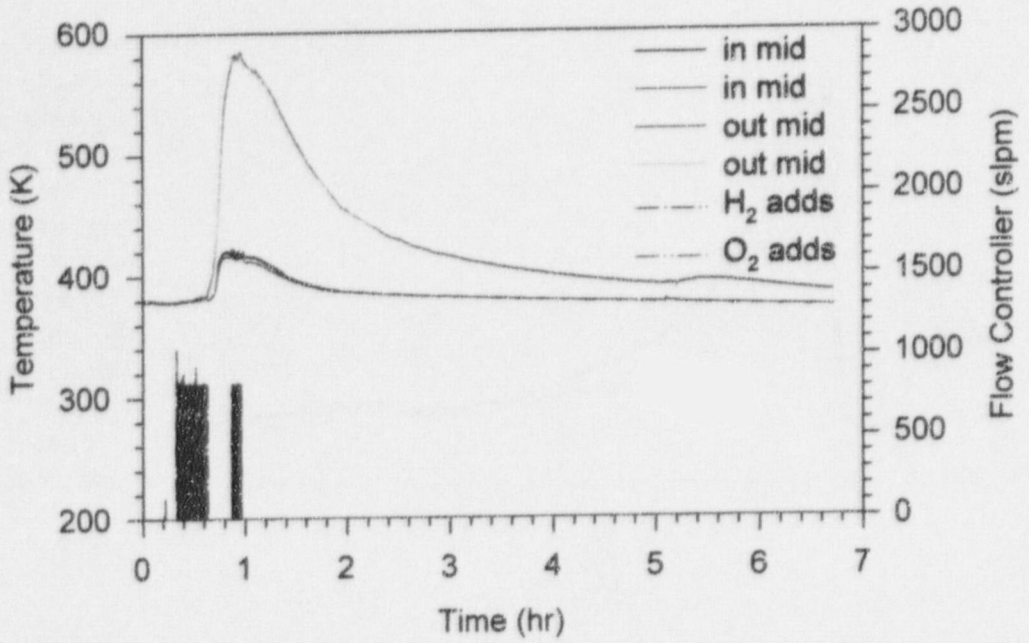

Figure 111. Inlet and outlet temperatures in PAR-8R.

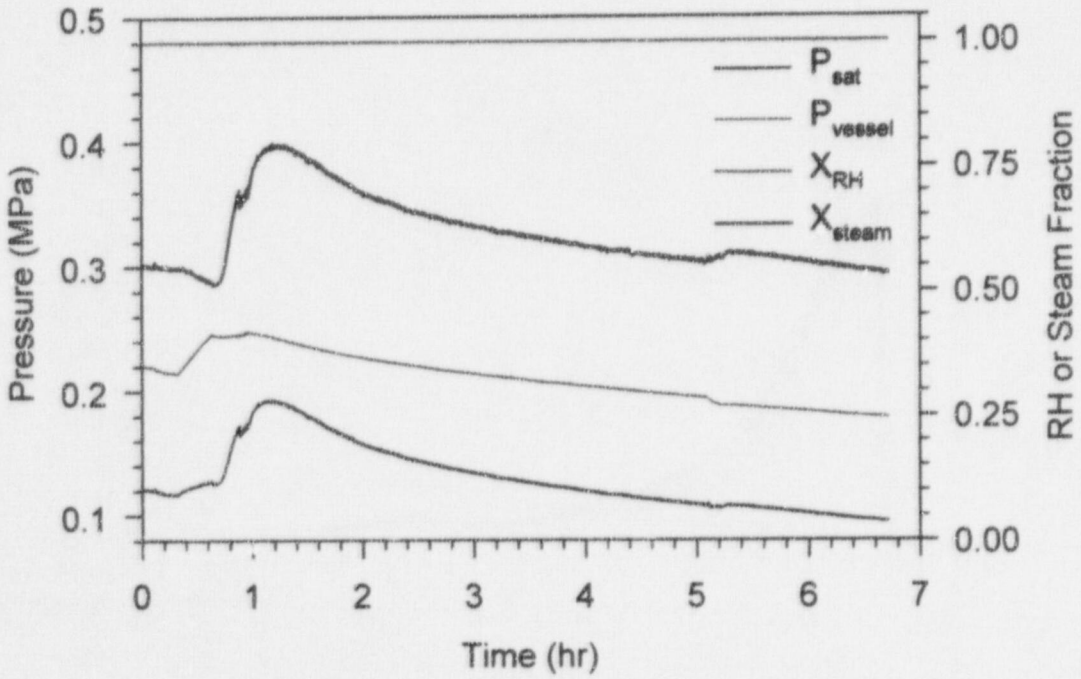

Figure 112. Saturation pressure, vessel pressure, relative humidity, and steam fraction in PAR-8R.

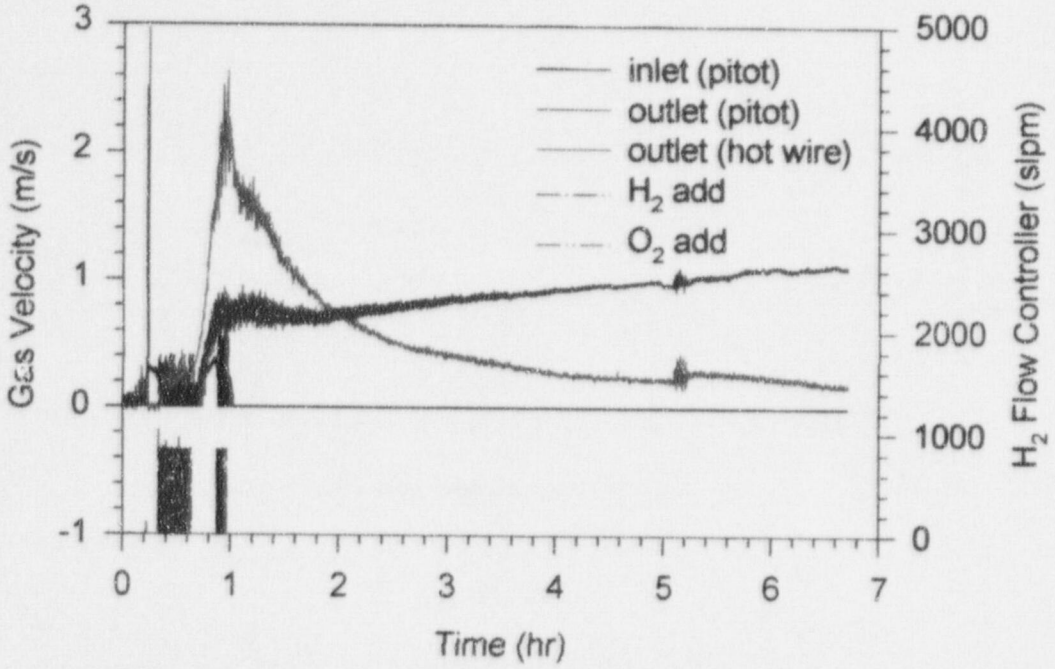

Figure 113. PAR gas velocity in PAR-8R.

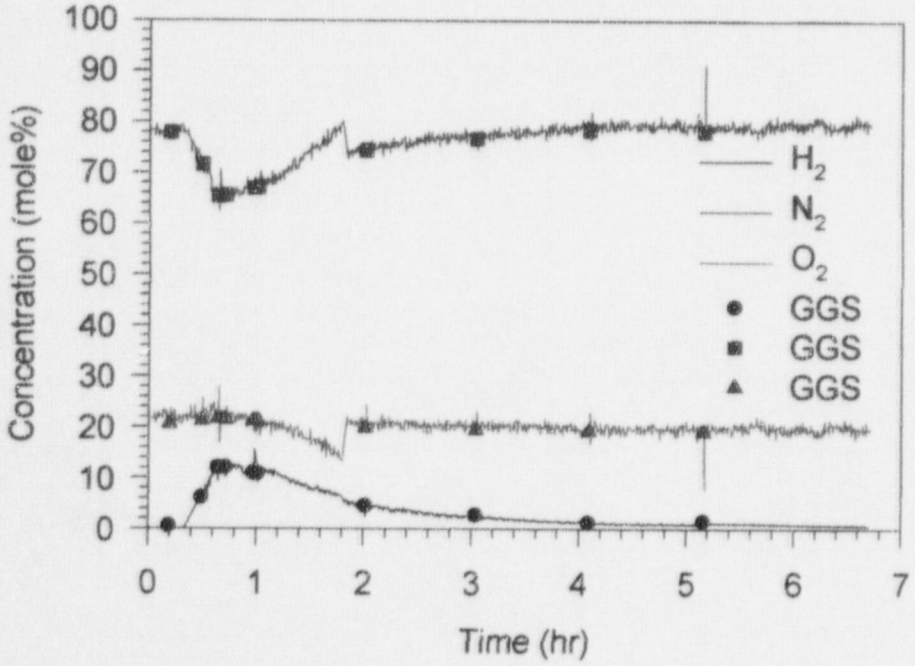

Figure 114. Gas concentrations (dry-basis) in PAR-8R.

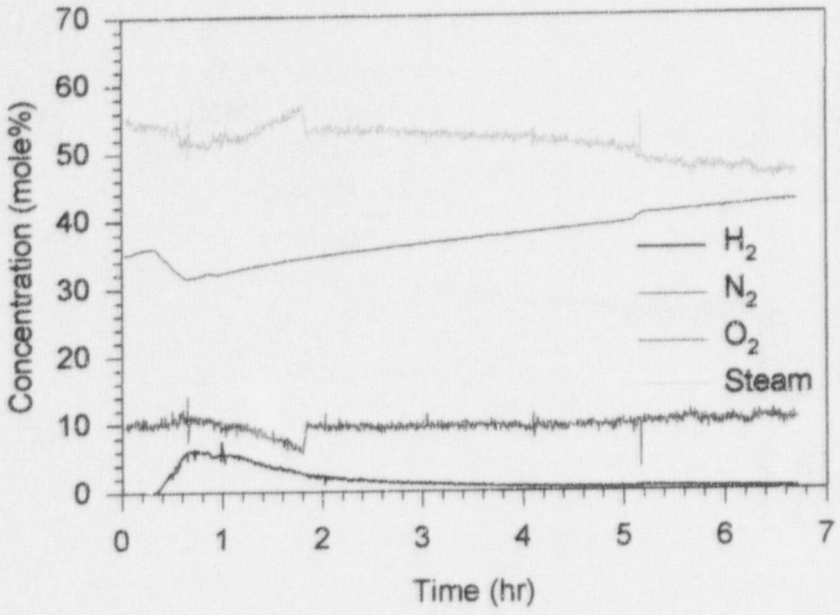

Figure 115. Gas concentrations (wet-basis) in PAR-8R.

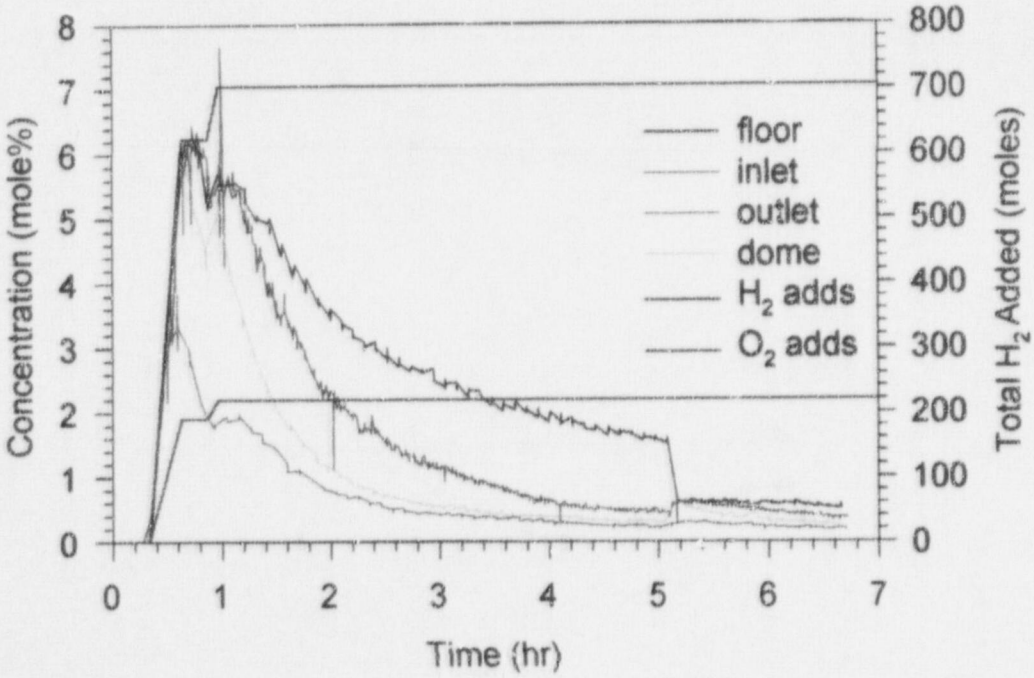

Figure 116. H_2 concentrations (wet-basis) in PAR-8R.

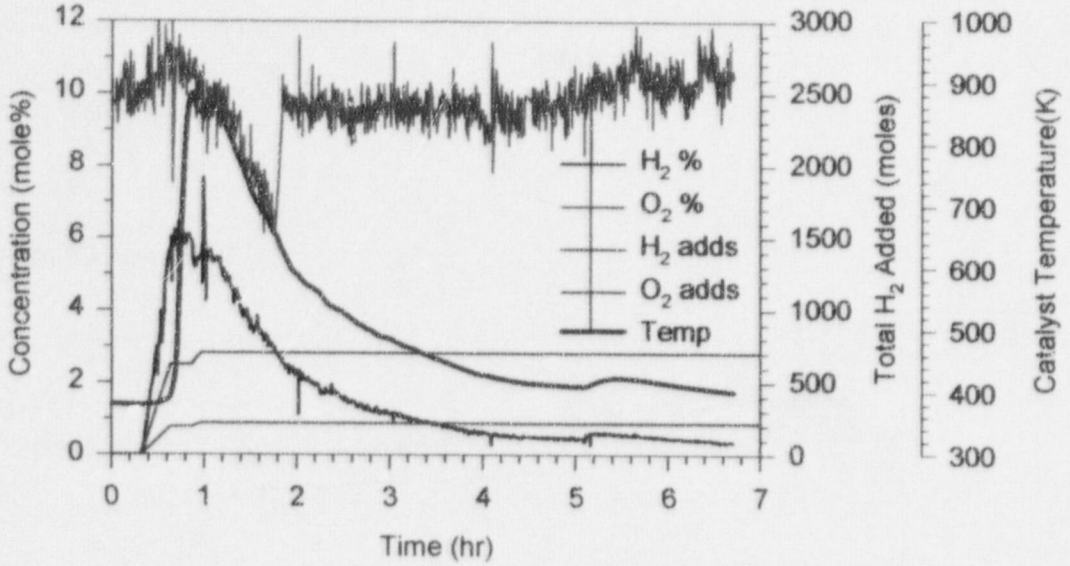

Figure 117. Catalyst temperature compared to gas additions and concentrations in PAR-8R.

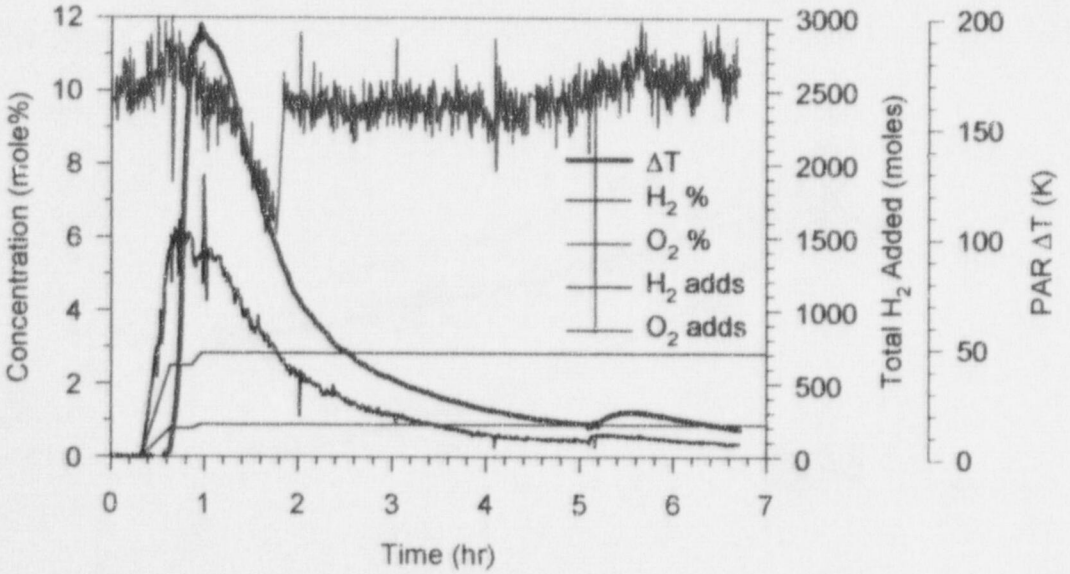

Figure 118. PAR ΔT temperature compared to gas additions and concentrations in PAR-8R.

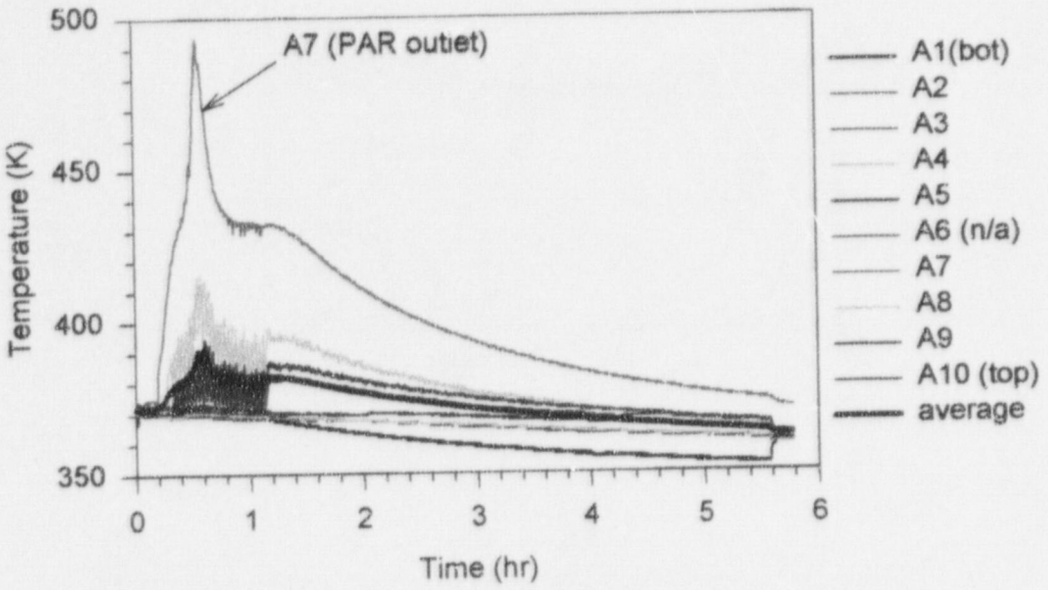

Figure 119. Surtsey vessel centerline gas temperatures from TC array A in PAR-9.

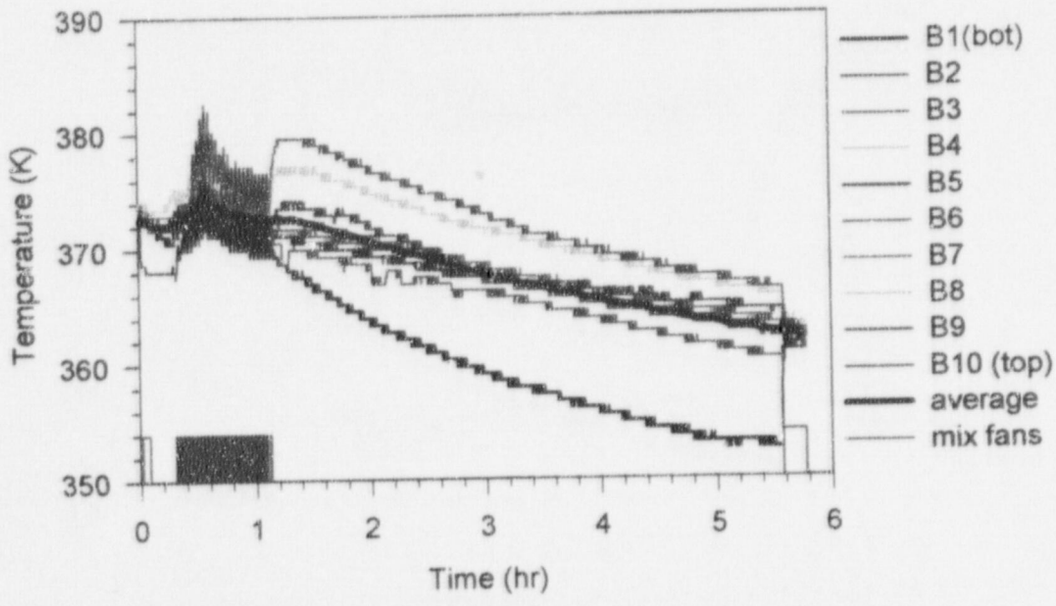

Figure 120. Surtsey vessel wall gas temperatures from TC array B in PAR-9.

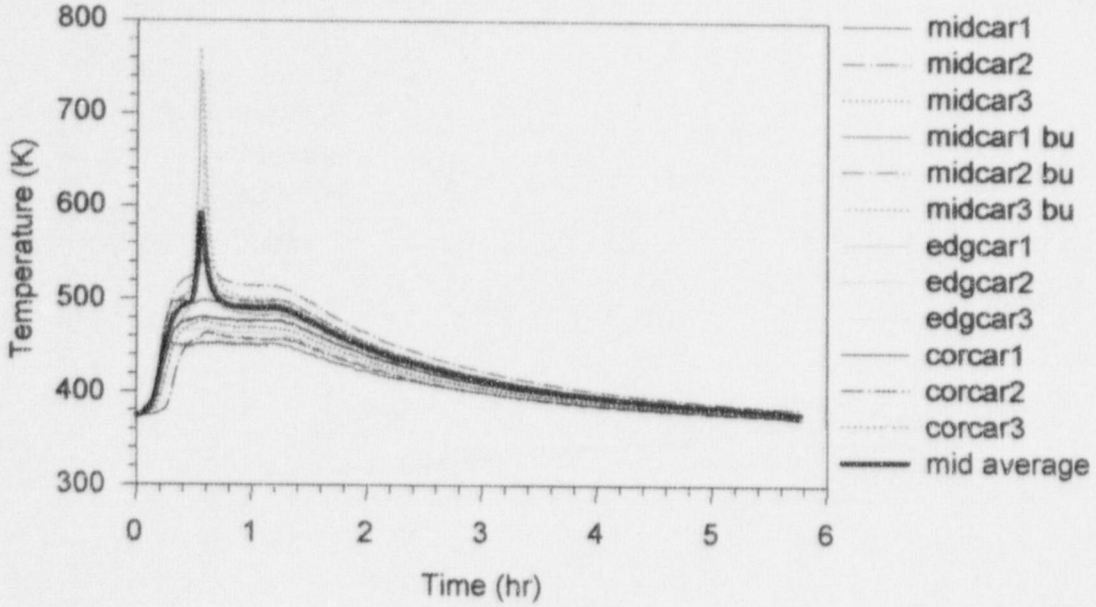

Figure 121. Catalyst cartridge temperatures in PAR-9.

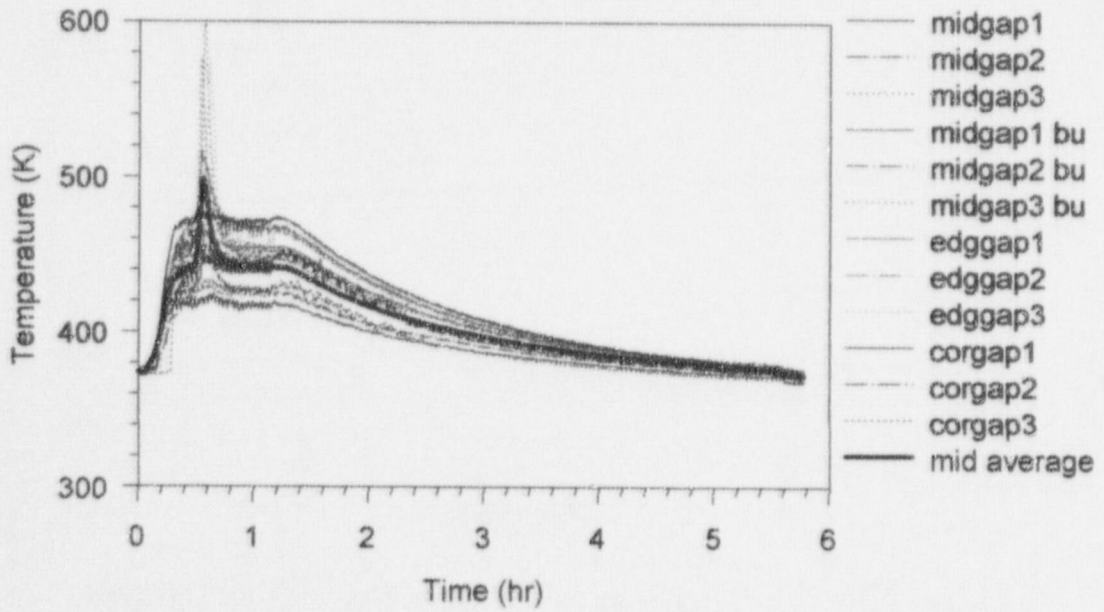

Figure 122. Catalyst gap temperatures in PAR-9.

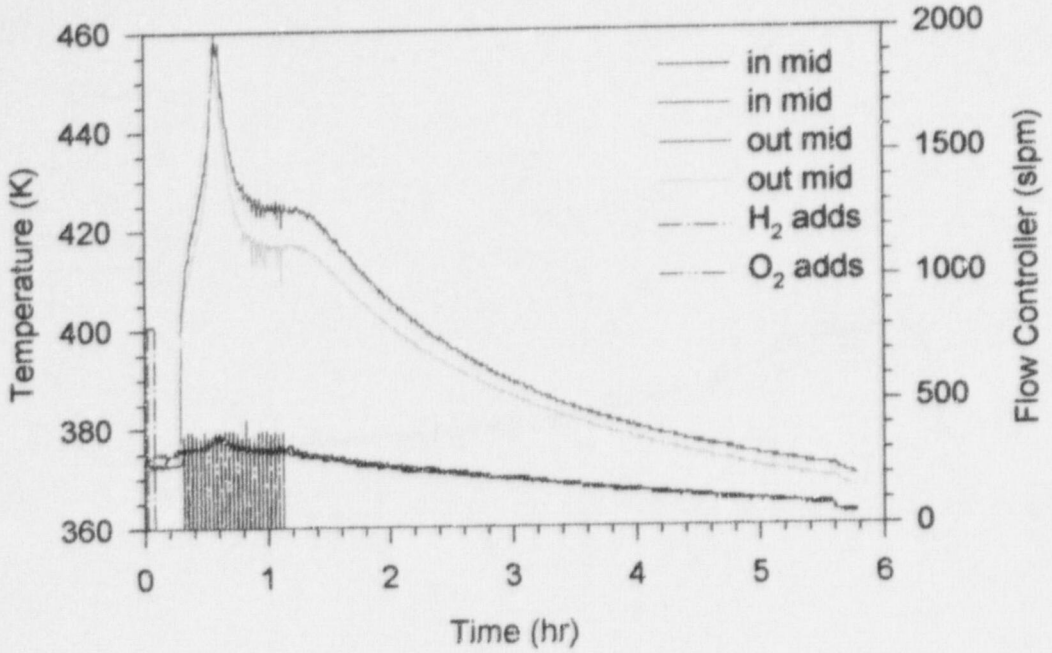

Figure 123. Inlet and outlet temperatures in PAR-9.

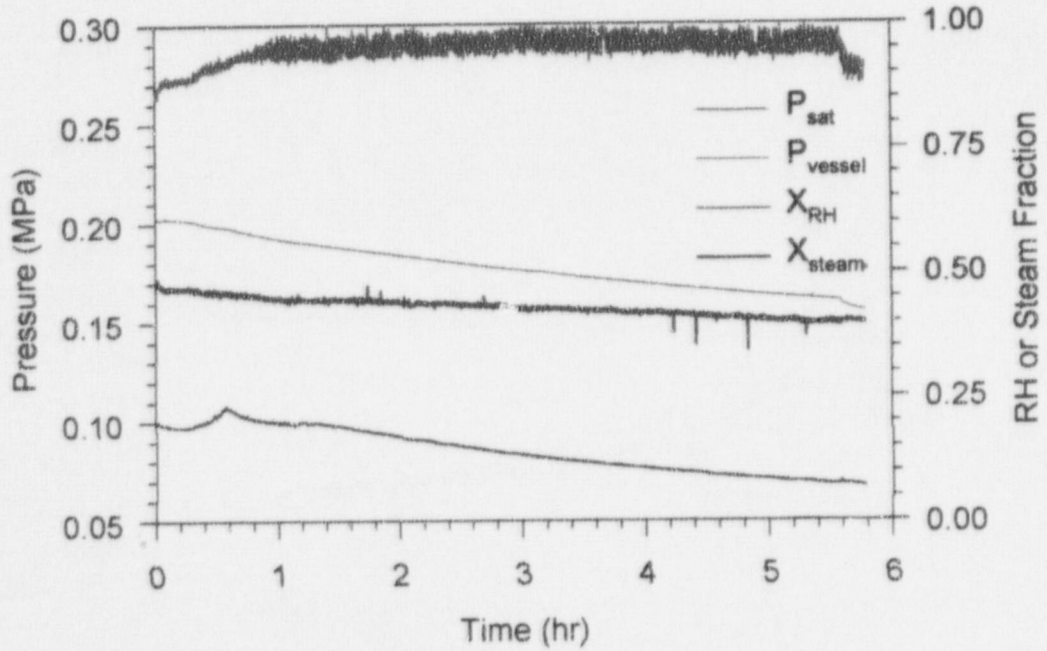

Figure 124. Saturation pressure, vessel pressure, relative humidity, and steam fraction in PAR-9.

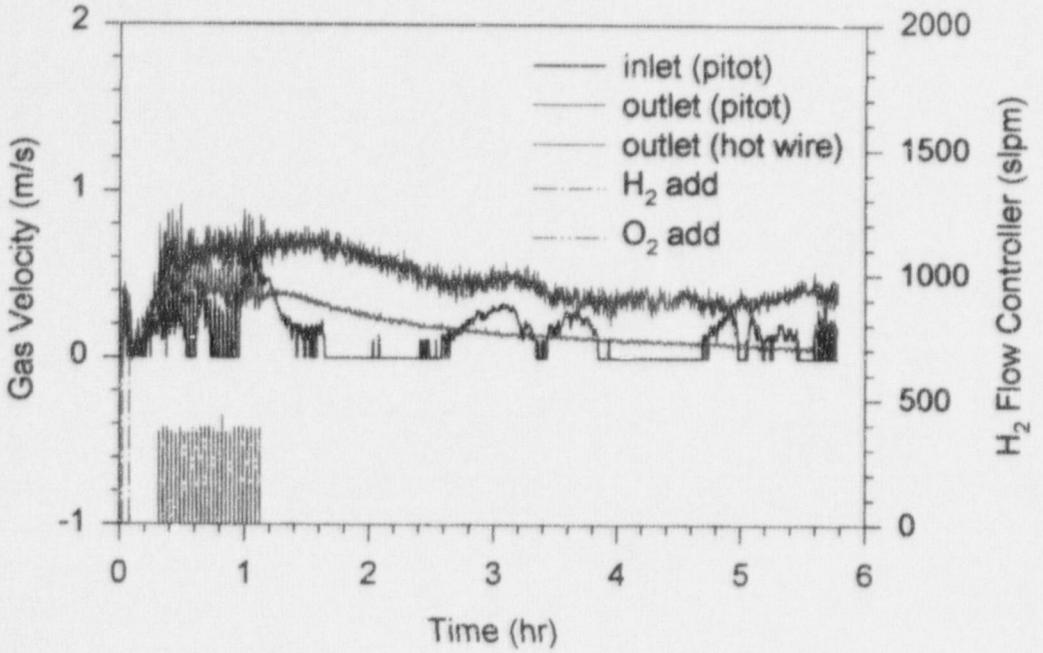

Figure 125. PAR gas velocity in PAR-9.

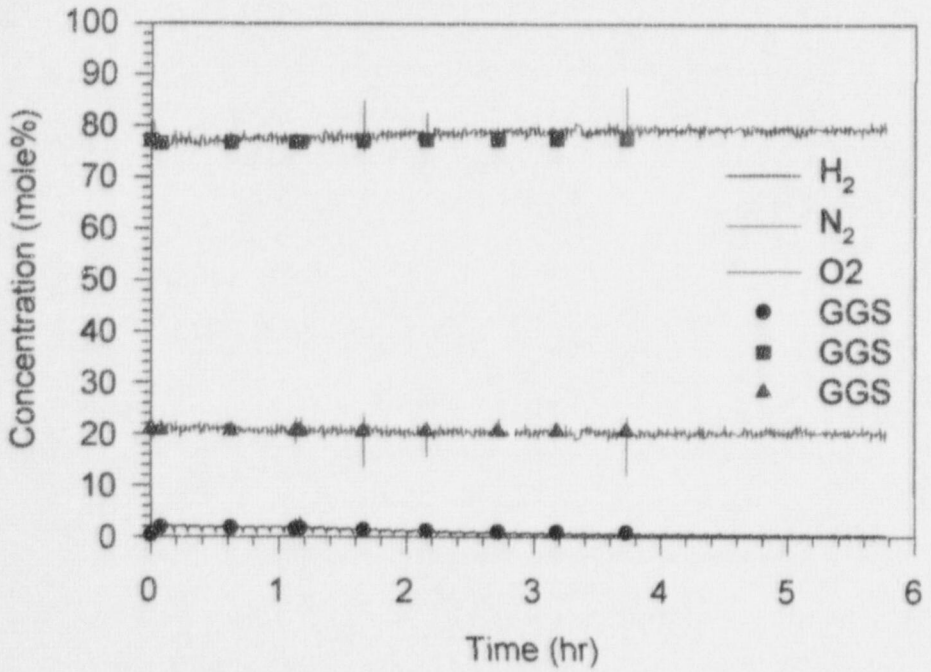

Figure 126. Gas concentrations (dry-basis) in PAR-9.

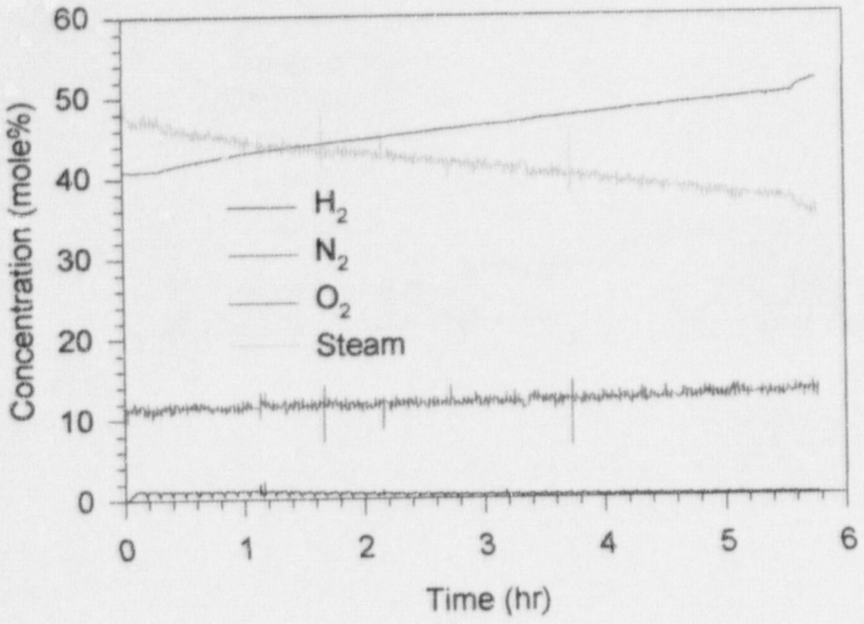

Figure 127. Gas concentrations (wet-basis) in PAR-9.

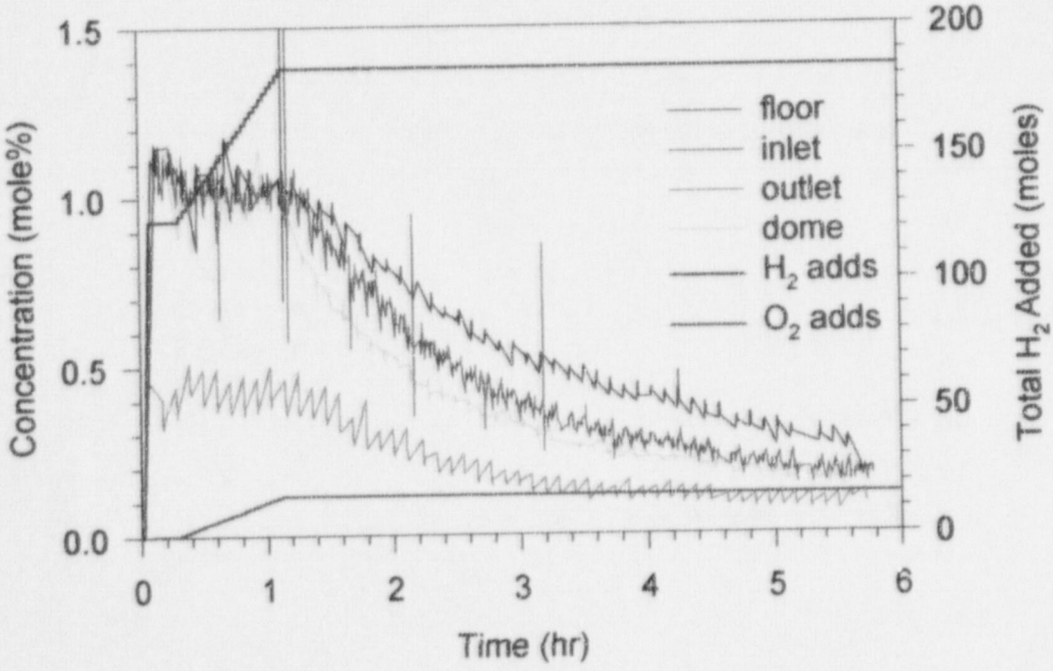

Figure 128. H_2 concentrations (wet-basis) in PAR-9.

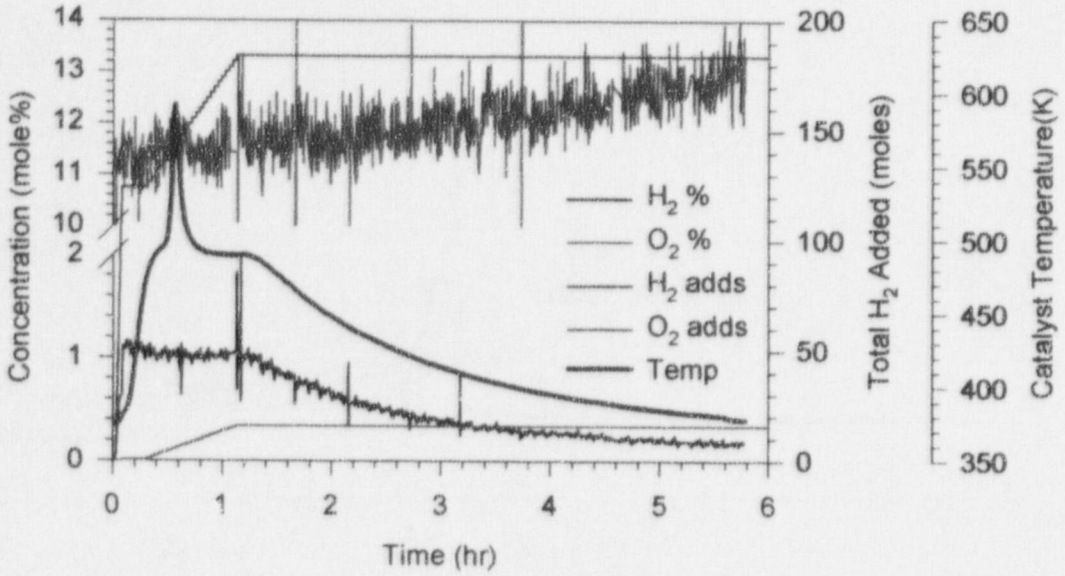

Figure 129. Catalyst temperature compared to gas additions and concentrations in PAR-9.

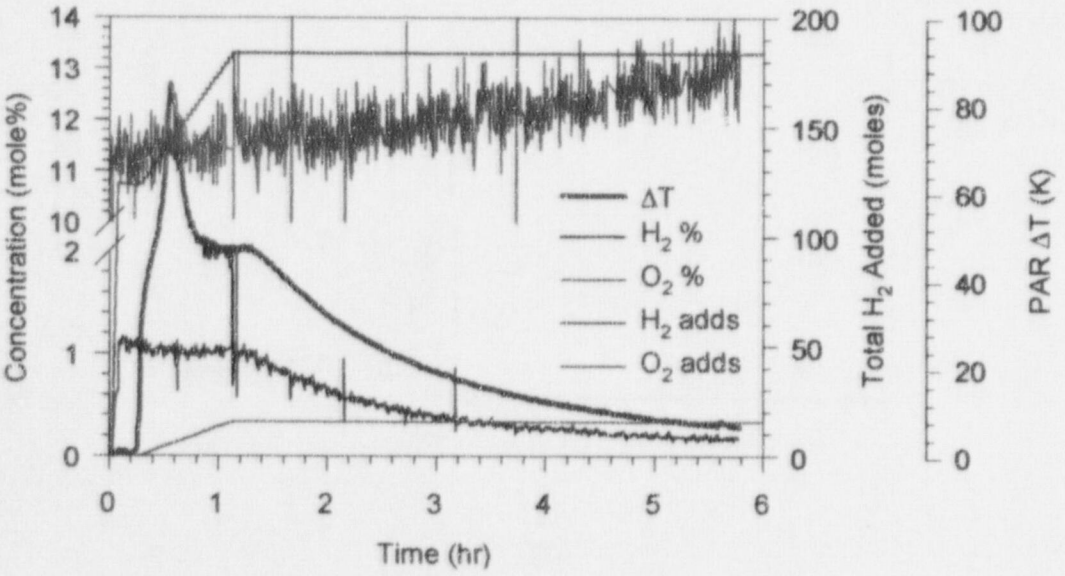

Figure 130. PAR ΔT temperature compared to gas additions and concentrations in PAR-9.

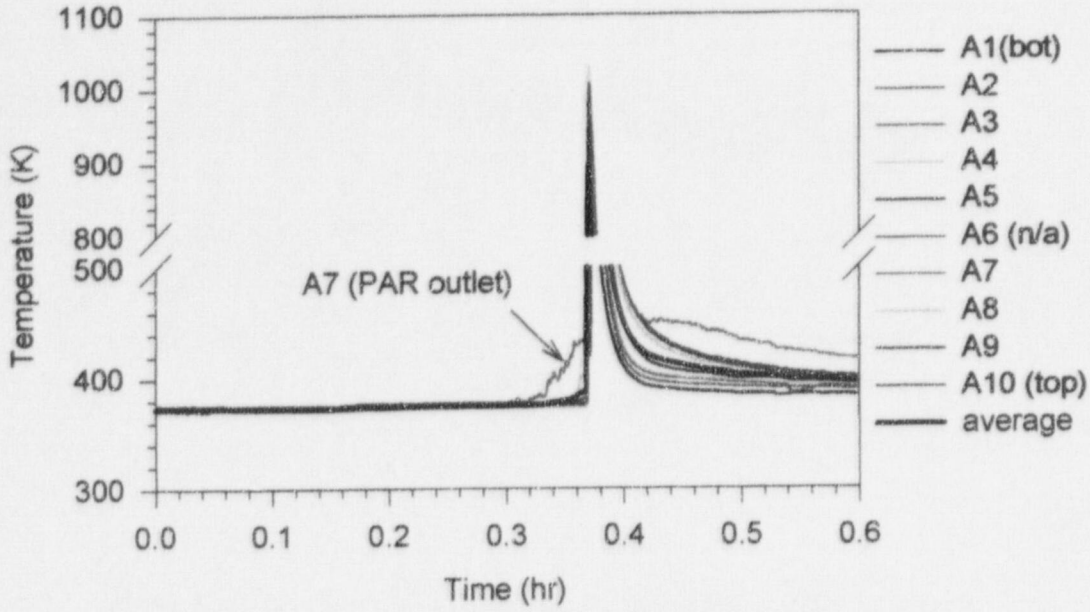

Figure 131. Surtsey vessel centerline gas temperatures from TC array A in PAR-10.

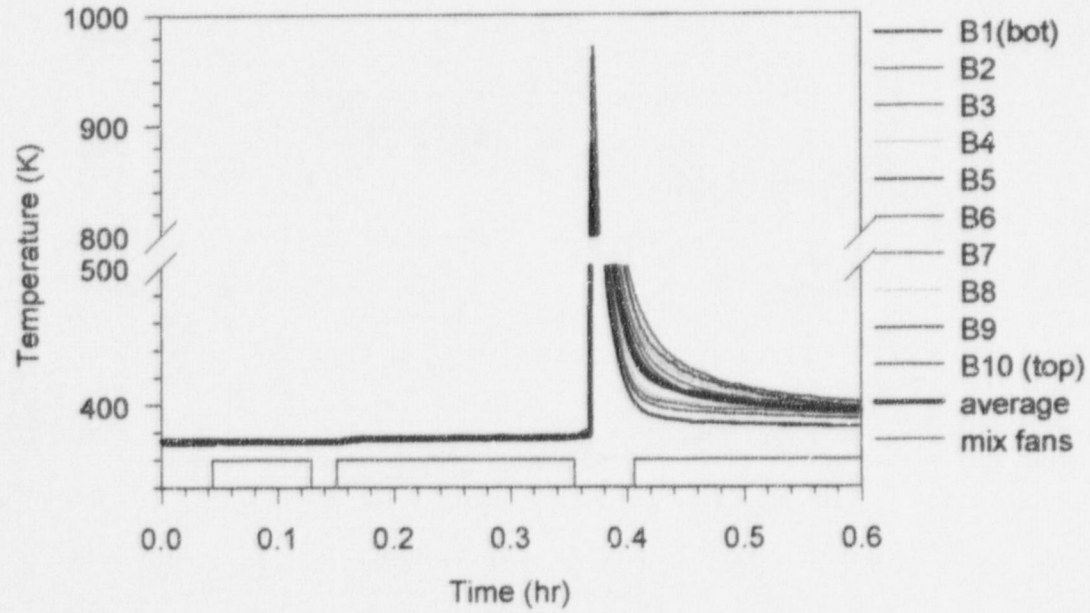

Figure 132. Surtsey vessel wall gas temperatures from TC array B in PAR-10.

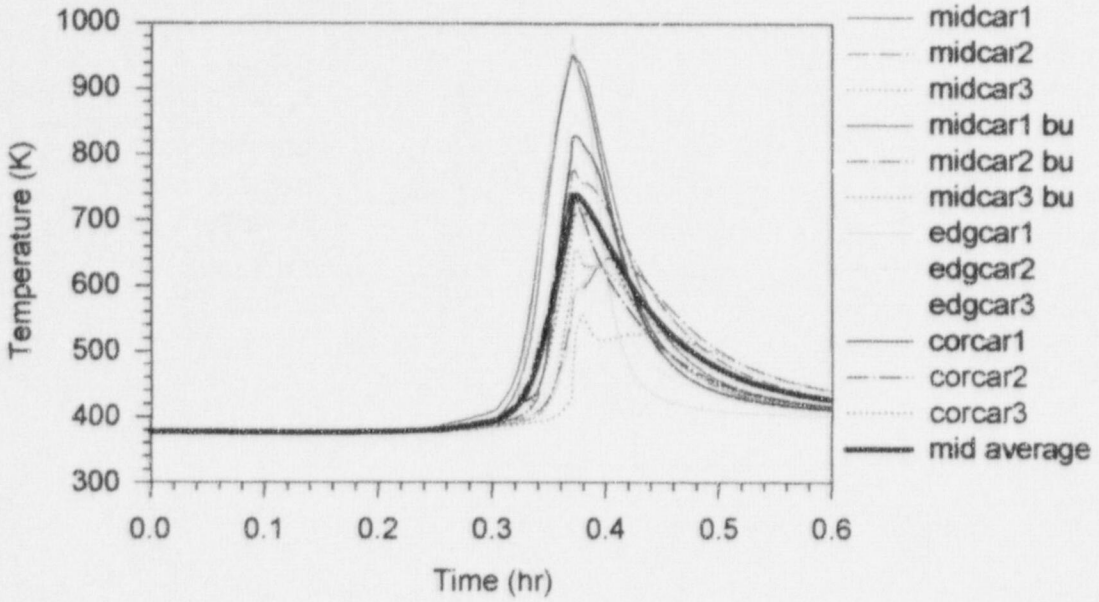

Figure 133. Catalyst cartridge temperatures in PAR-10.

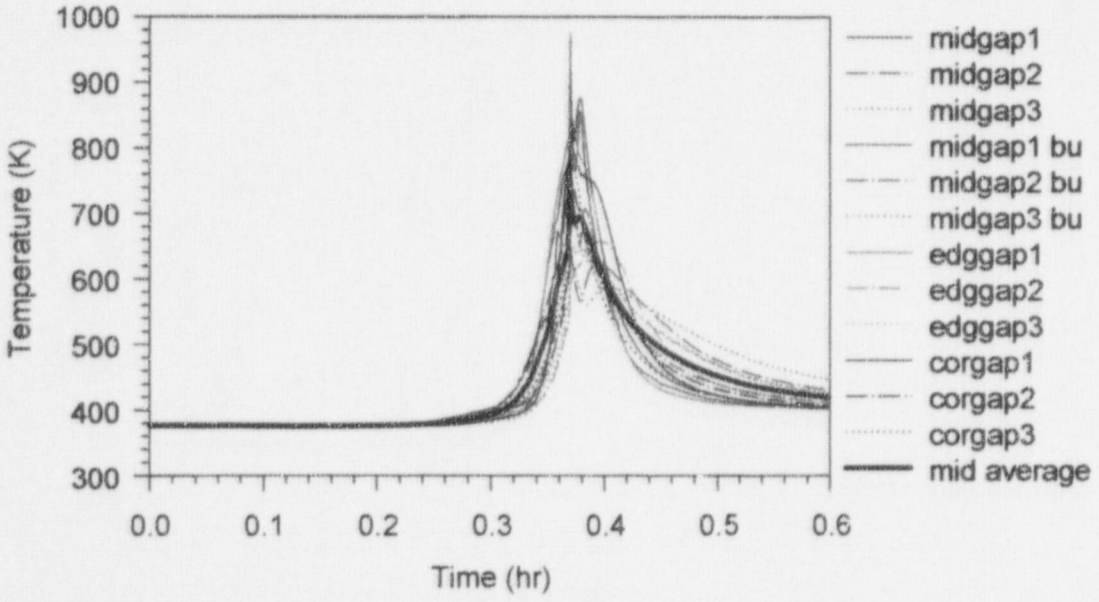

Figure 134. Catalyst gap temperatures in PAR-10.

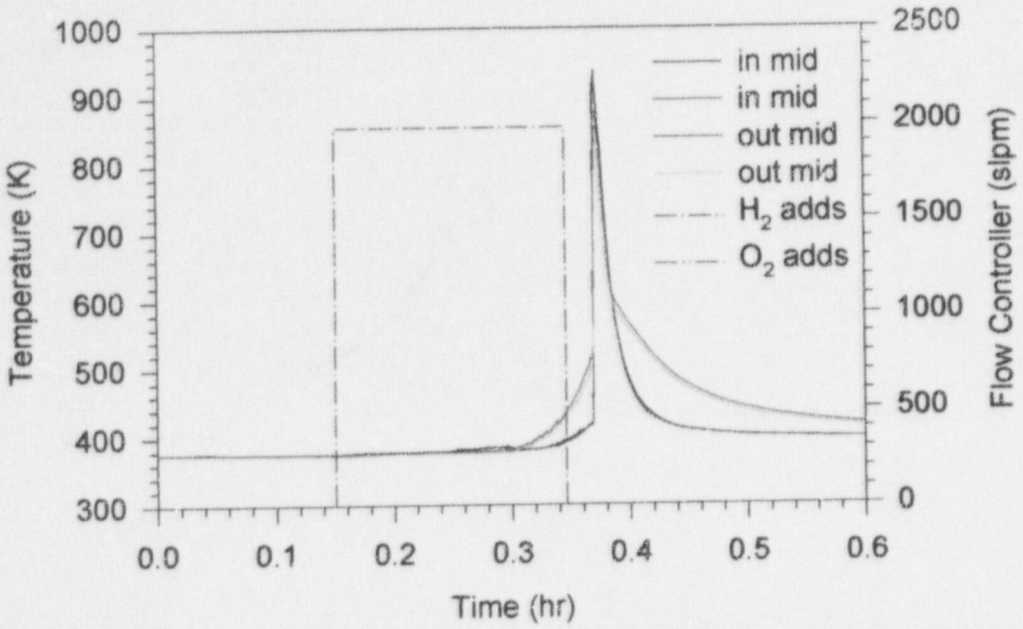

Figure 135. Inlet and outlet temperatures in PAR-10.

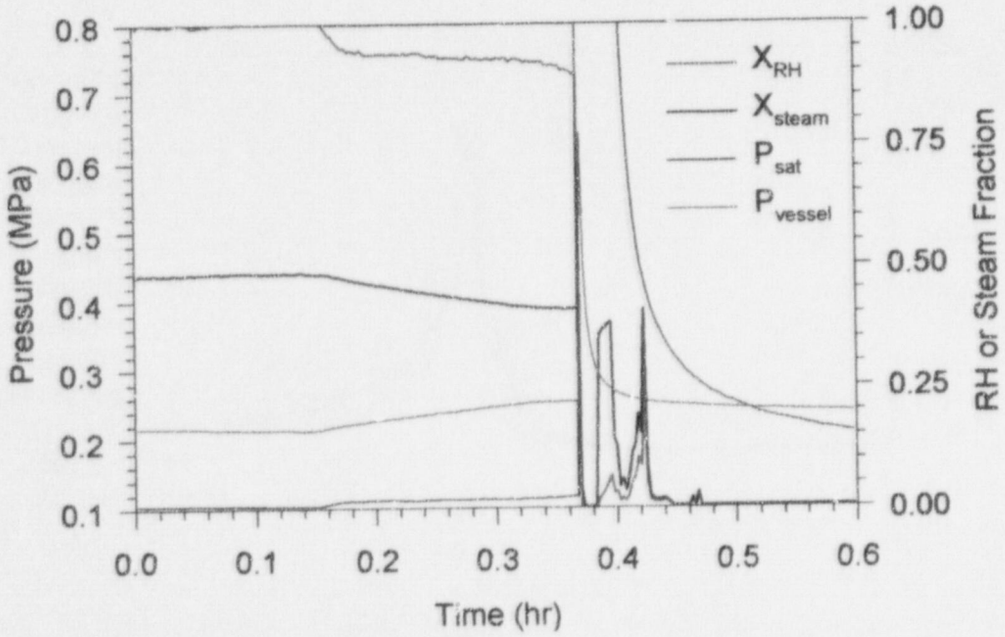

Figure 136. Saturation pressure, vessel pressure, relative humidity, and steam fraction in PAR-10.

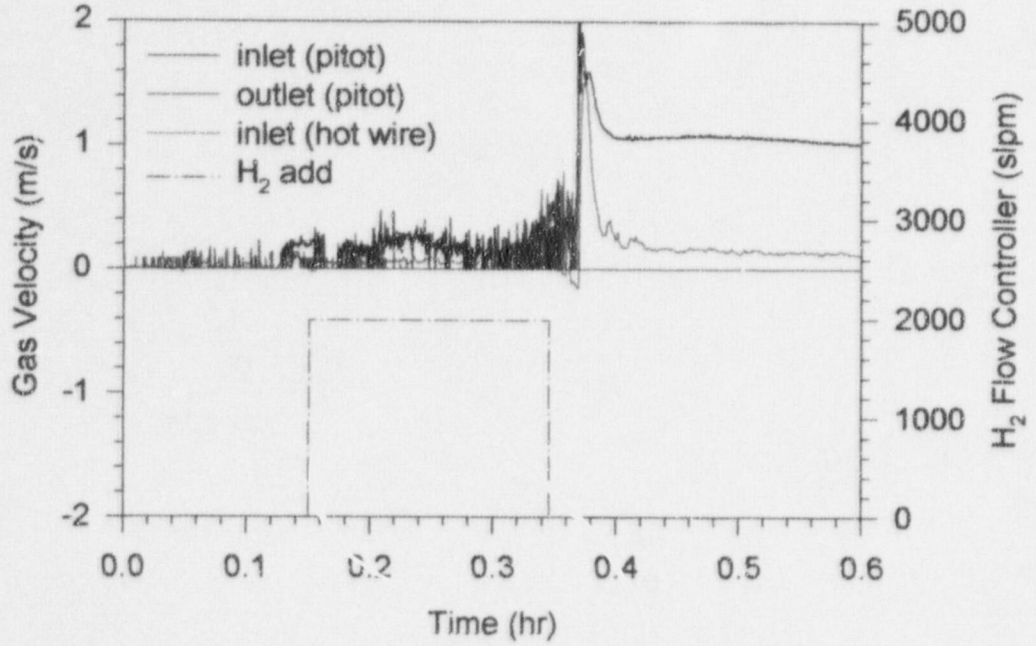

Figure 137. PAR gas velocity in PAR-10.

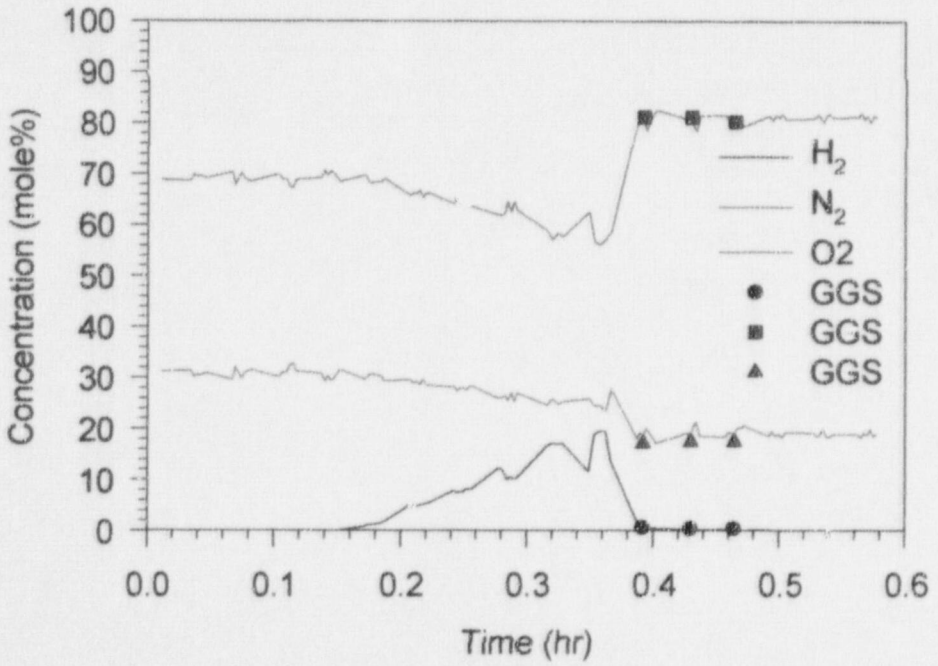

Figure 138. Gas concentrations (dry-basis) in PAR-10.

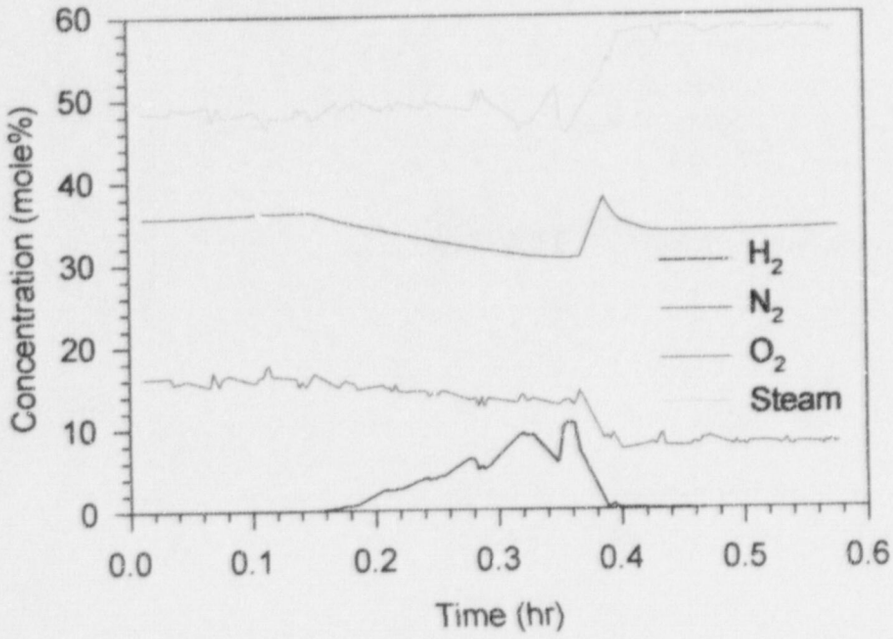

Figure 139. Gas concentrations (wet-basis) in PAR-10.

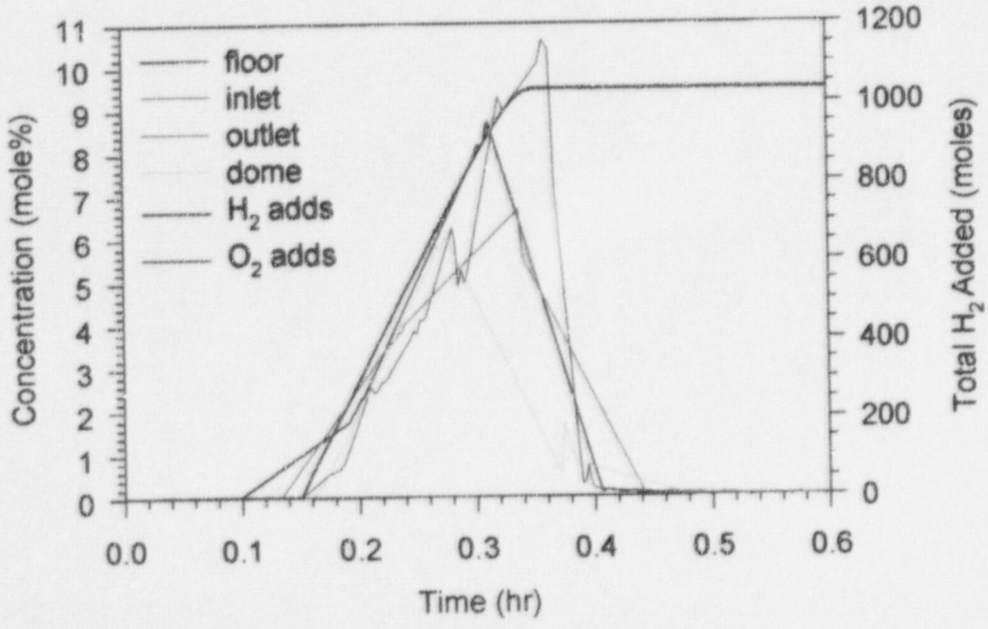

Figure 140. H_2 concentrations (wet-basis) in PAR-10.

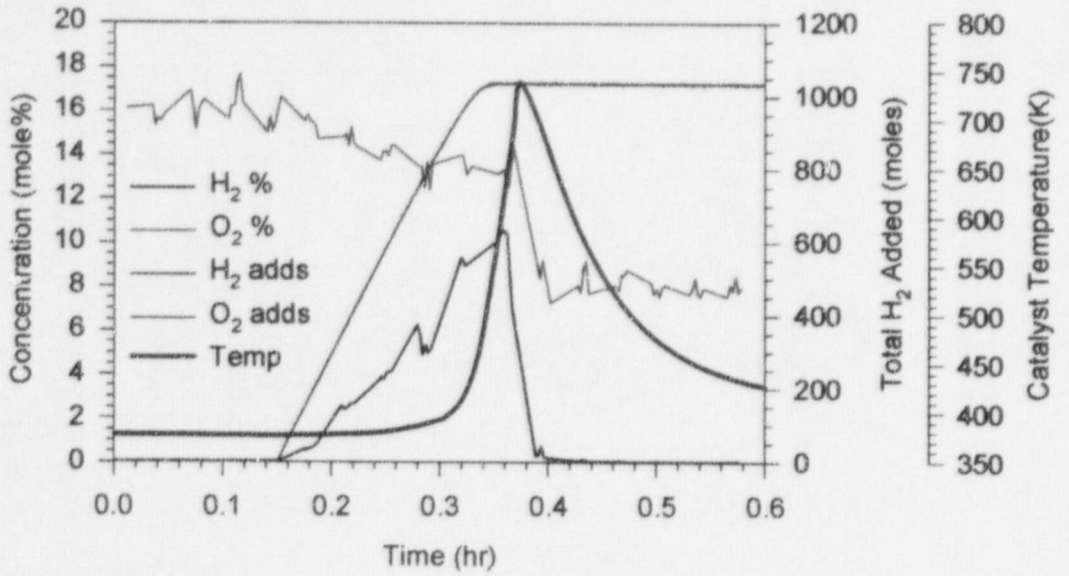

Figure 141. Catalyst temperature compared to gas additions and concentrations in PAR-10.

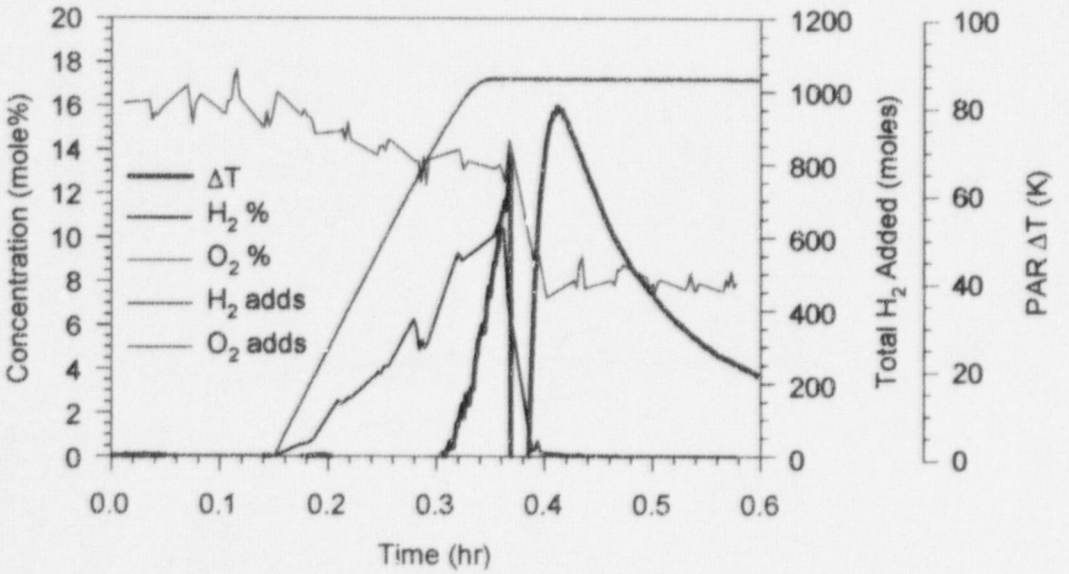

Figure 142. PAR ΔT temperature compared to gas additions and concentrations in PAR-10.

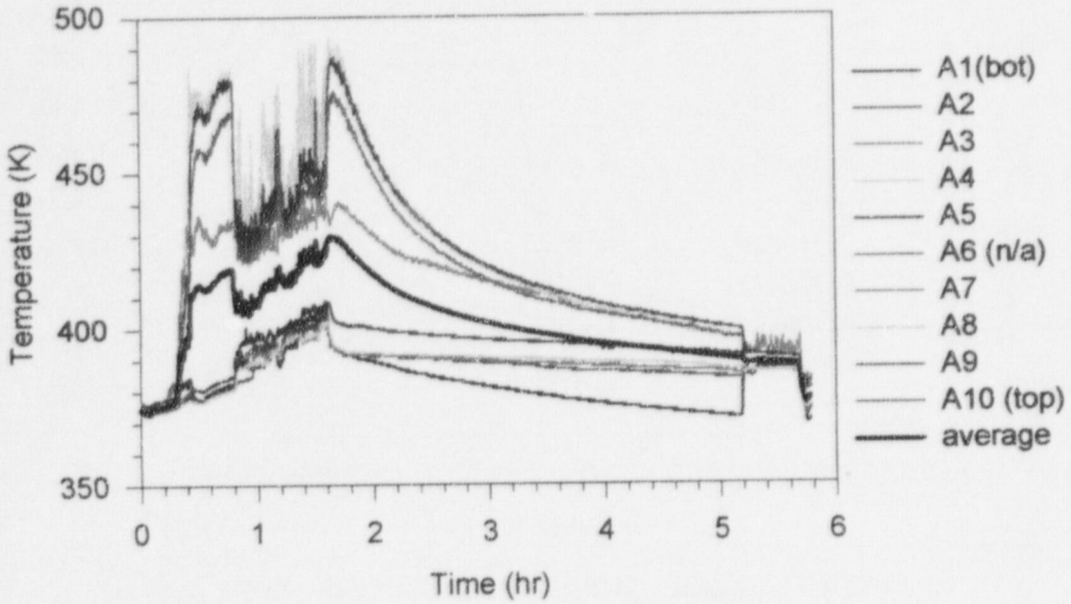

Figure 143. Surtsey vessel centerline gas temperatures from TC array A in PAR-12.

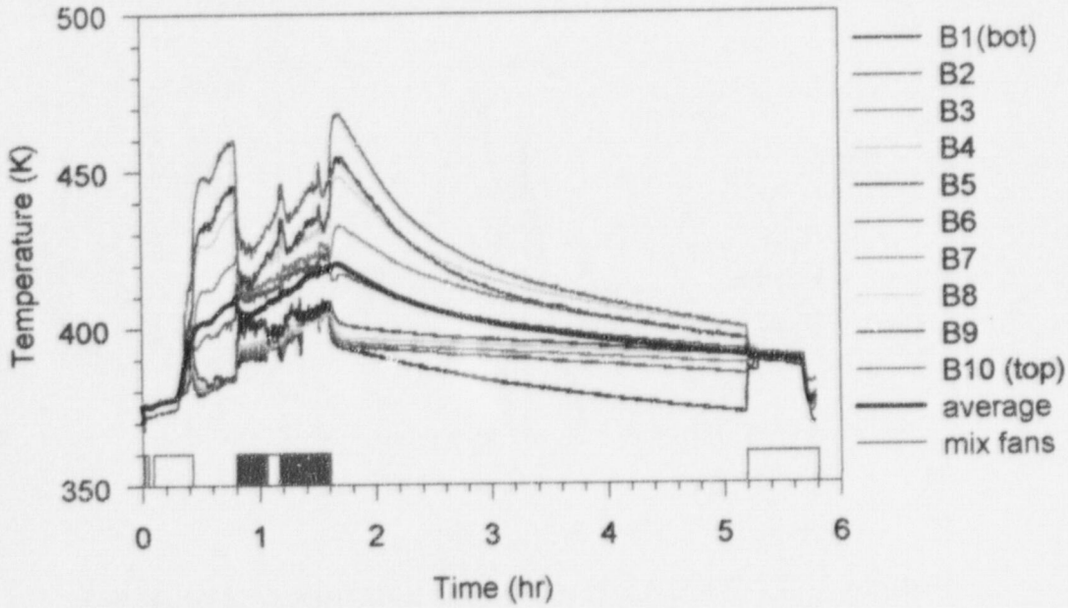

Figure 144. Surtsey vessel wall gas temperatures from TC array B in PAR-12.

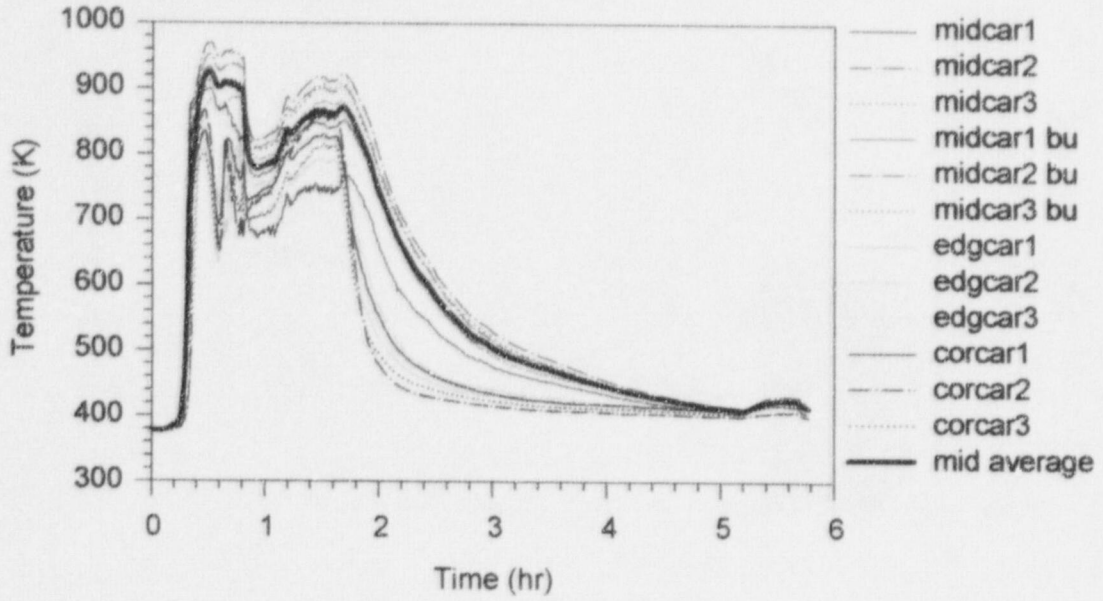

Figure 145. Catalyst cartridge temperatures in PAR-12.

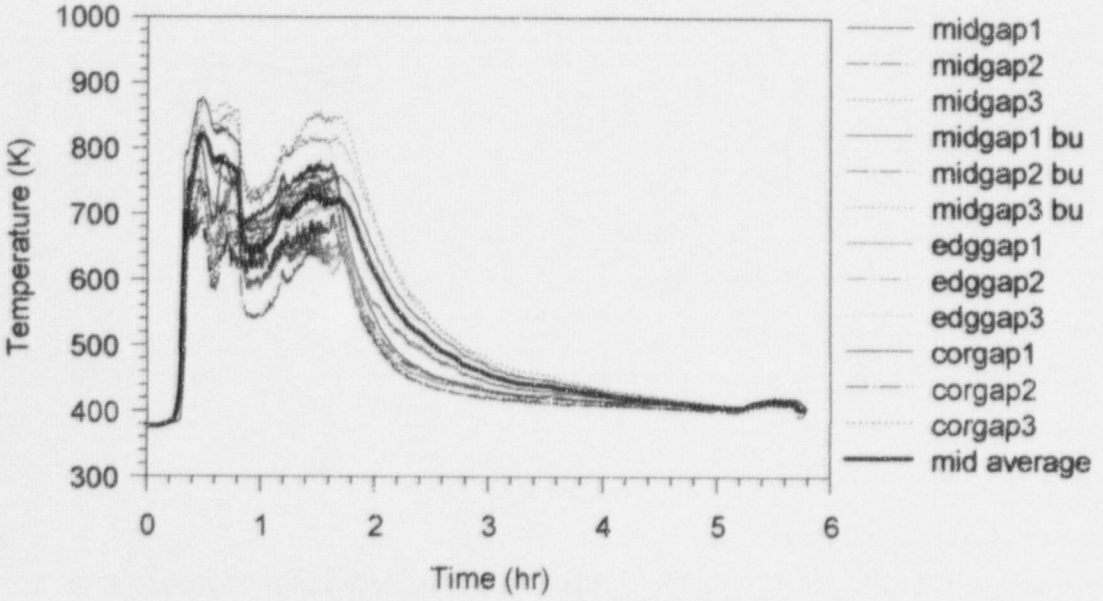

Figure 146. Catalyst gap temperatures in PAR-12.

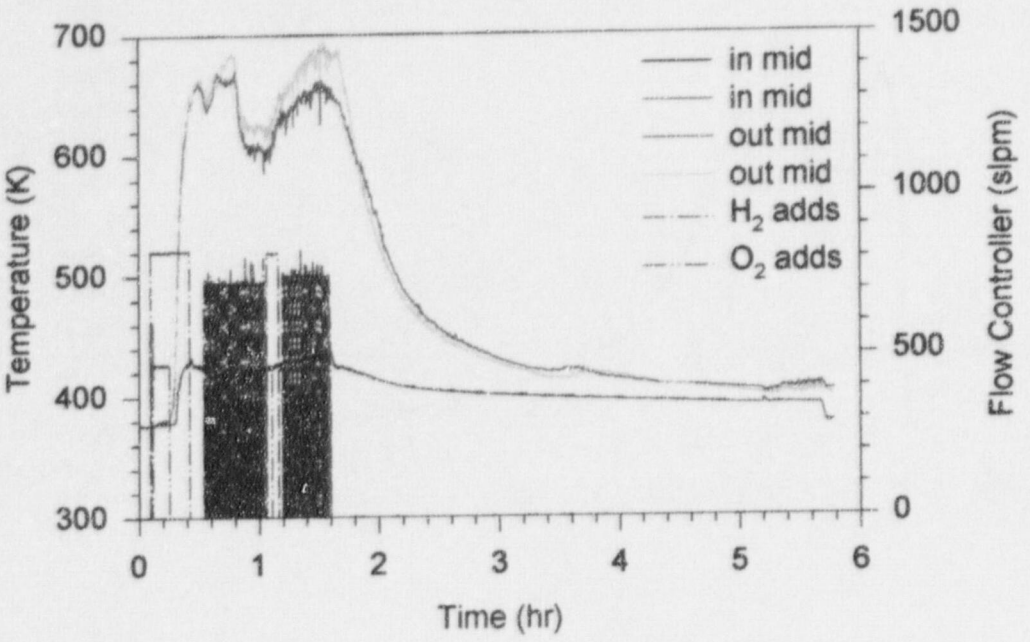

Figure 147. Inlet and outlet temperatures in PAR-12.

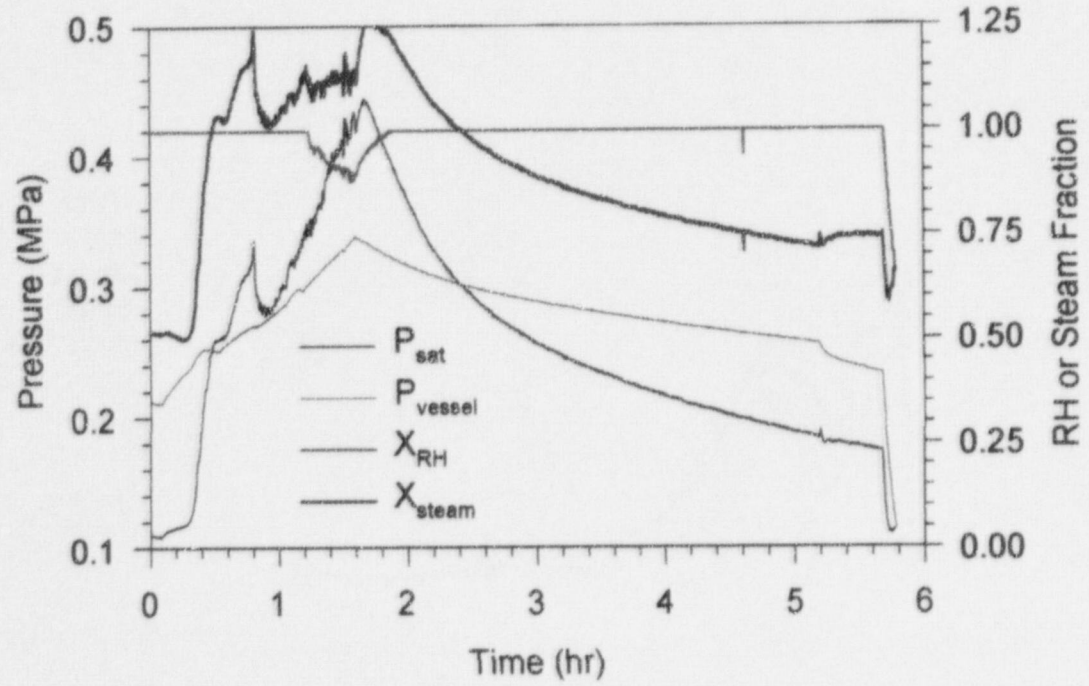

Figure 148. Saturation pressure, vessel pressure, relative humidity, and steam fraction in PAR-12.

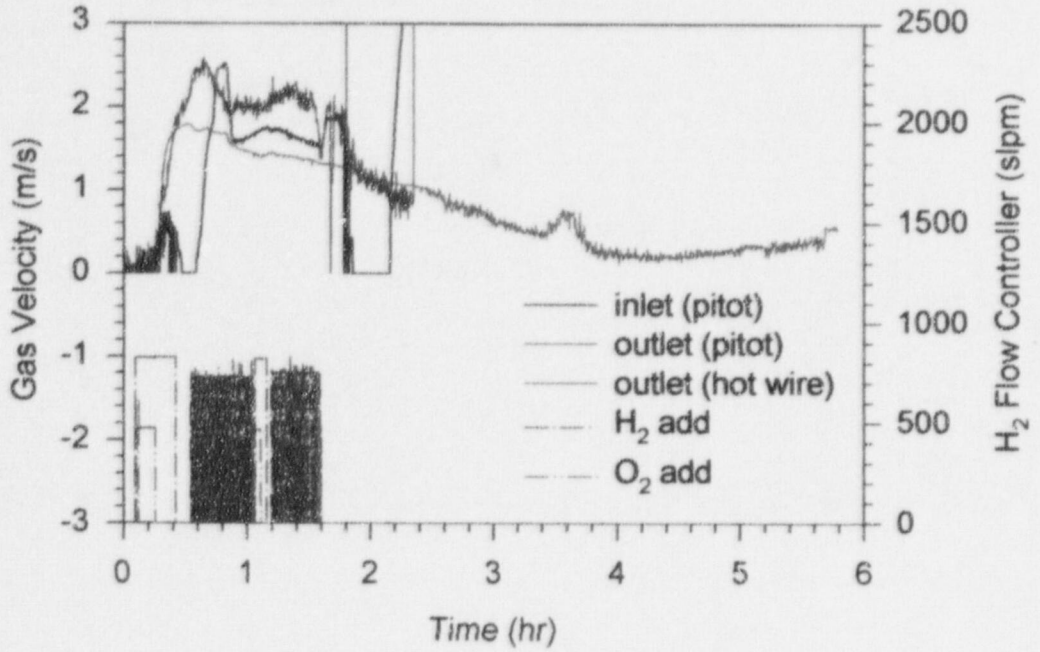

Figure 149. PAR gas velocity in PAR-12.

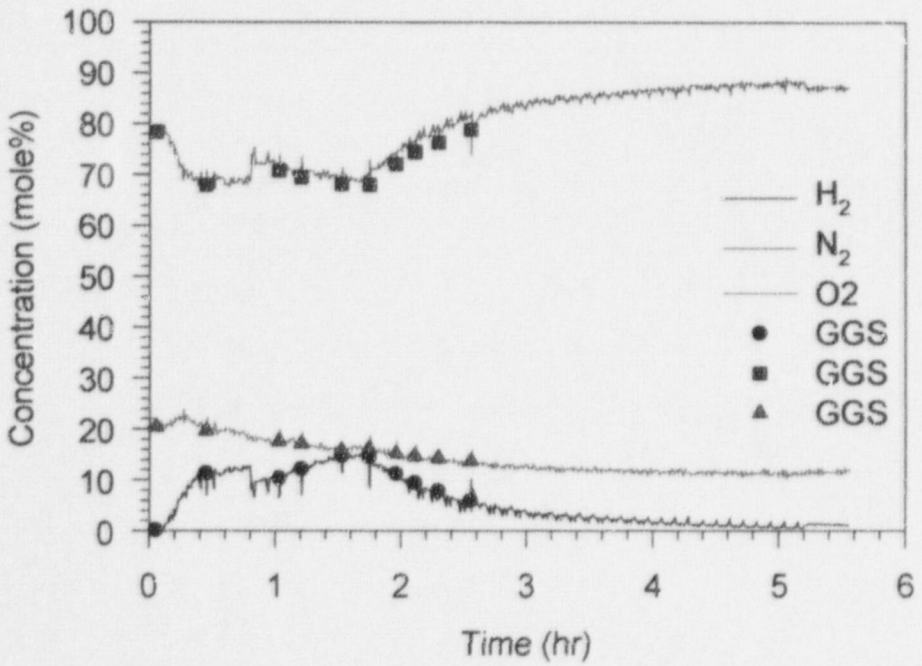

Figure 150. Gas concentrations (dry-basis) in PAR-12.

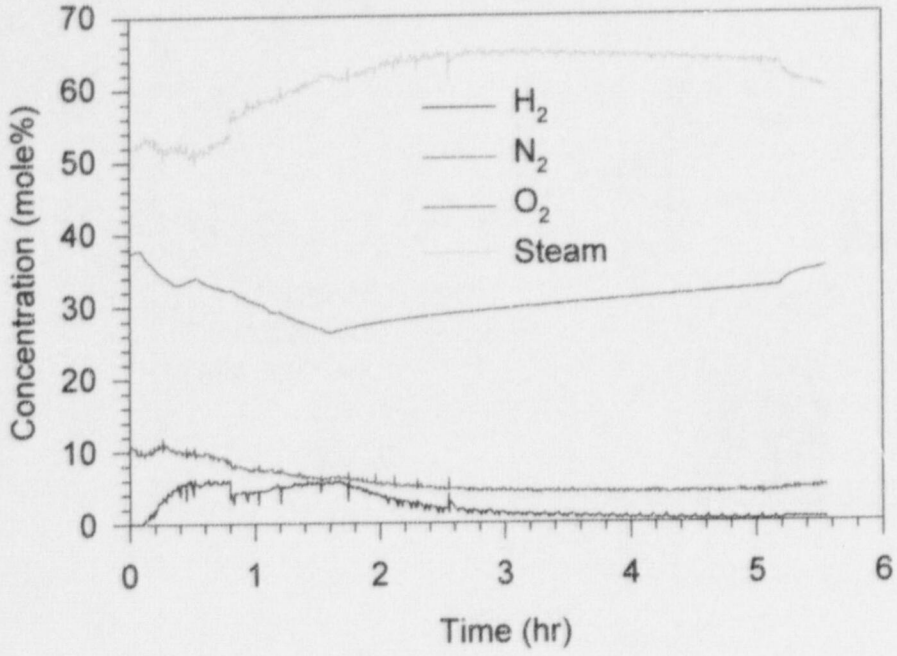

Figure 151. Gas concentrations (wet-basis) in PAR-12.

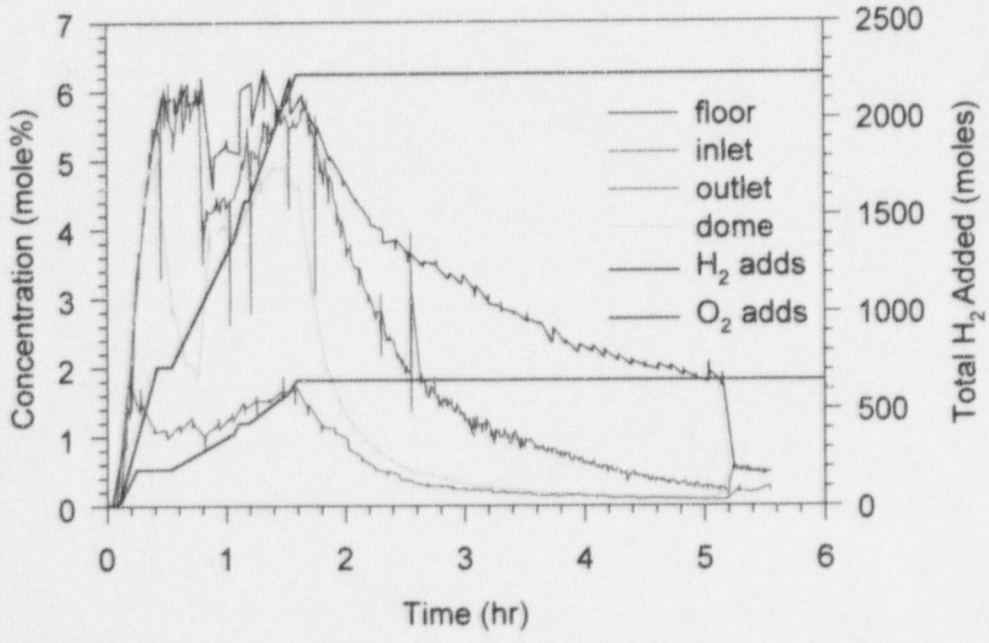

Figure 152. H_2 concentrations (wet-basis) in PAR-12.

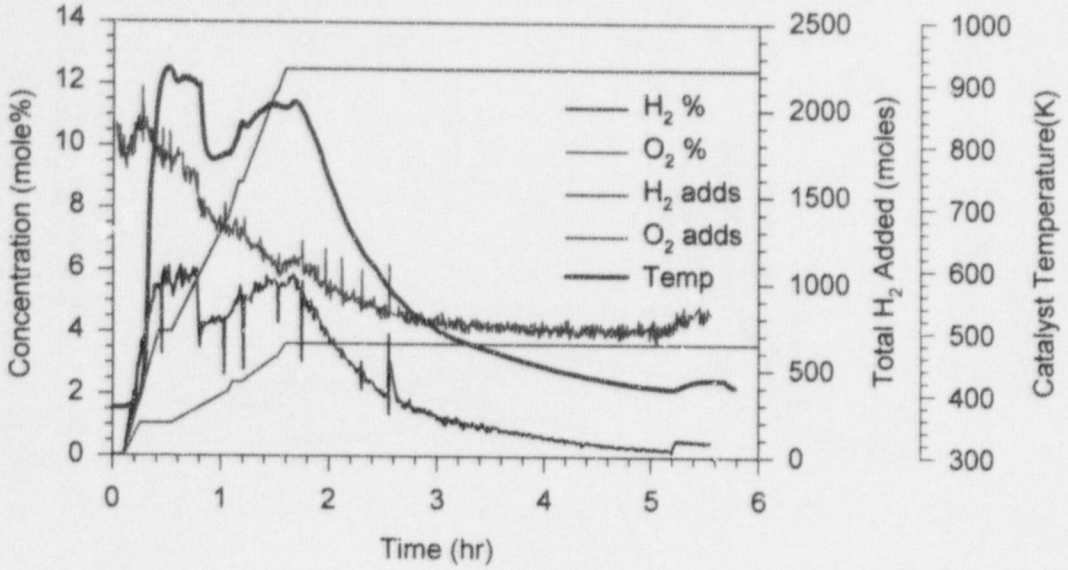

Figure 153. Catalyst temperature compared to gas additions and concentrations in PAR-12.

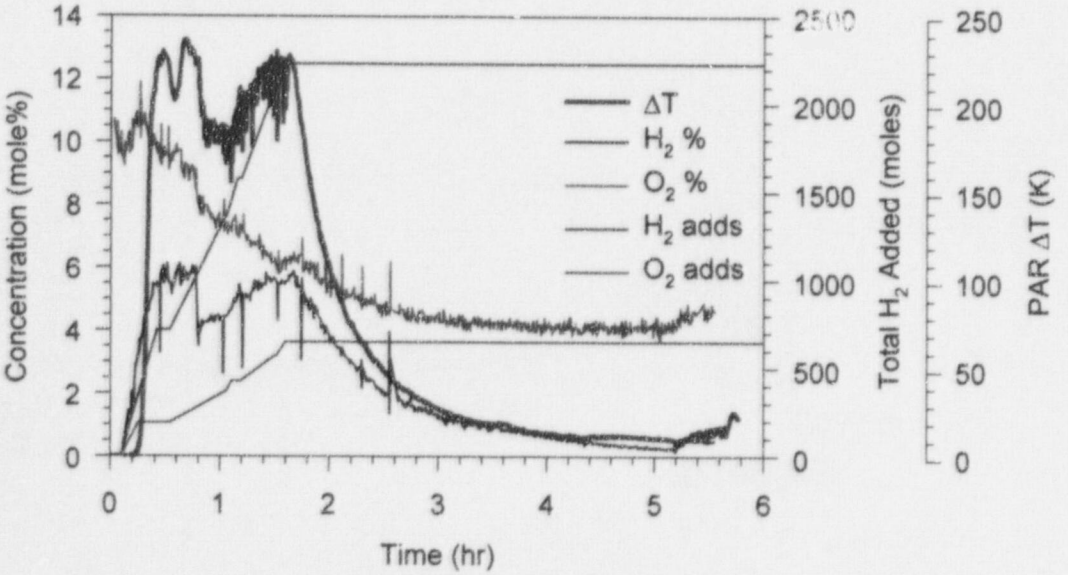

Figure 154. PAR ΔT temperature compared to gas additions and concentrations in PAR-12.

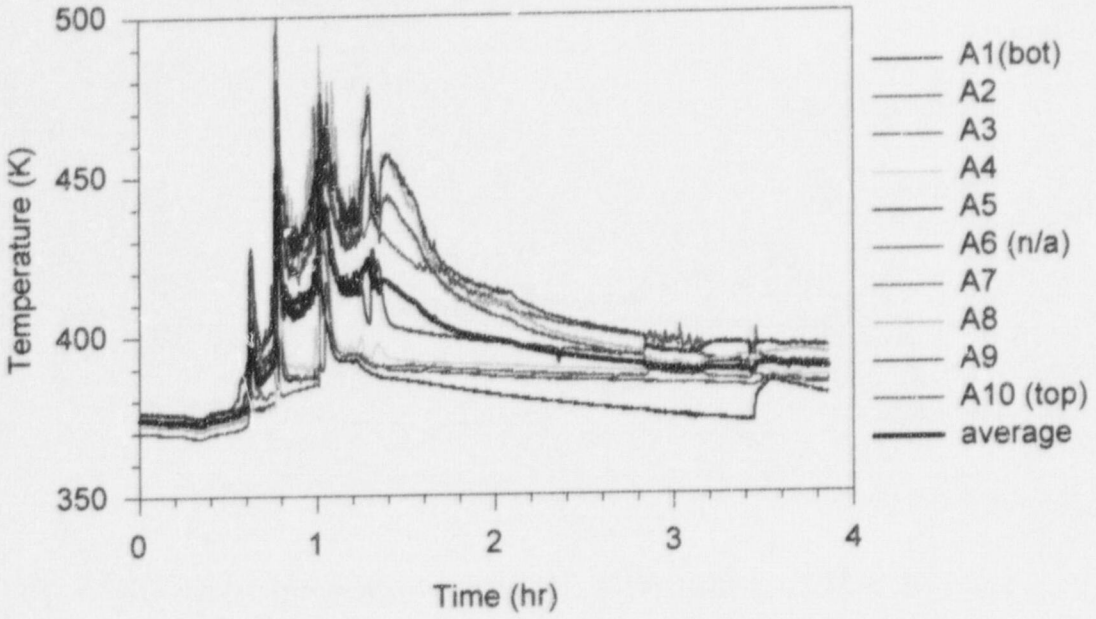

Figure 155. Surtsey vessel centerline gas temperatures from TC array A in PAR-13.

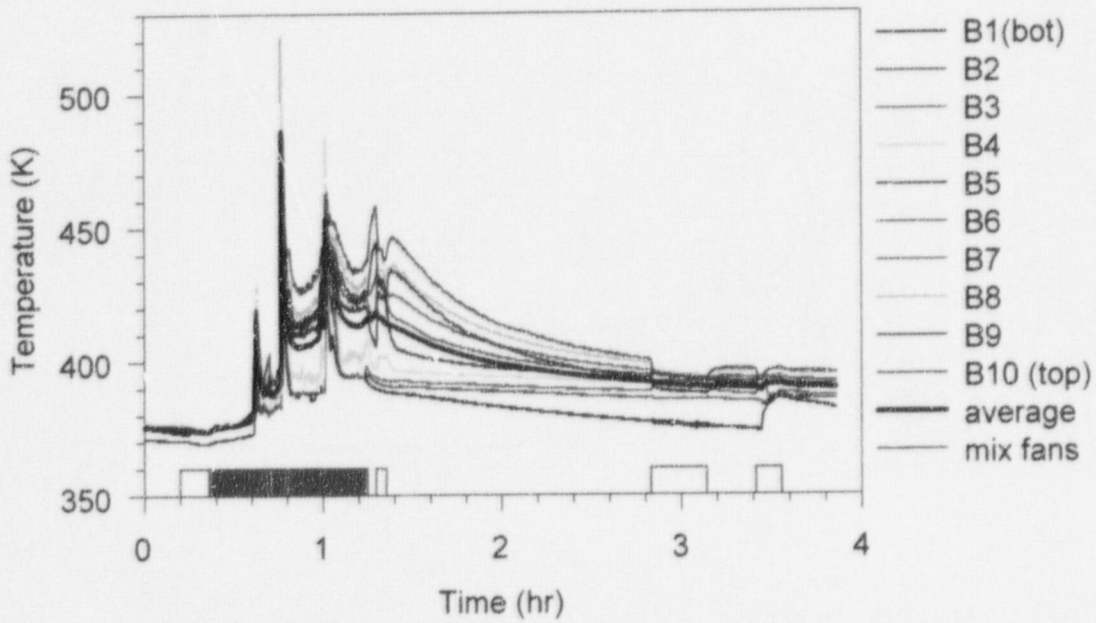

Figure 156. Surtsey vessel wall gas temperatures from TC array B in PAR-13.

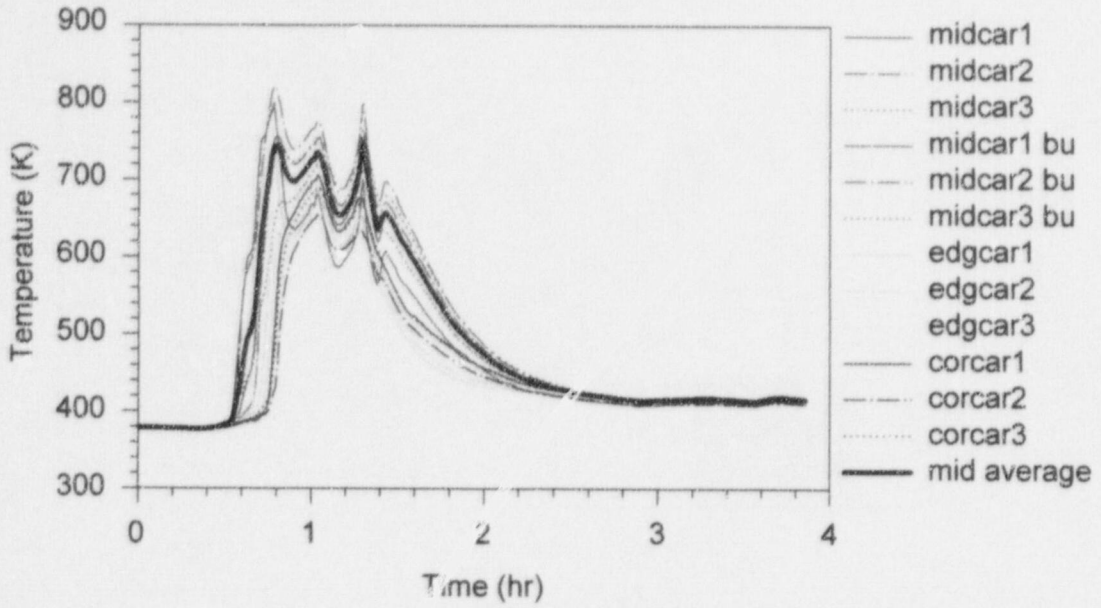

Figure 157. Catalyst cartridge temperatures in PAR-13.

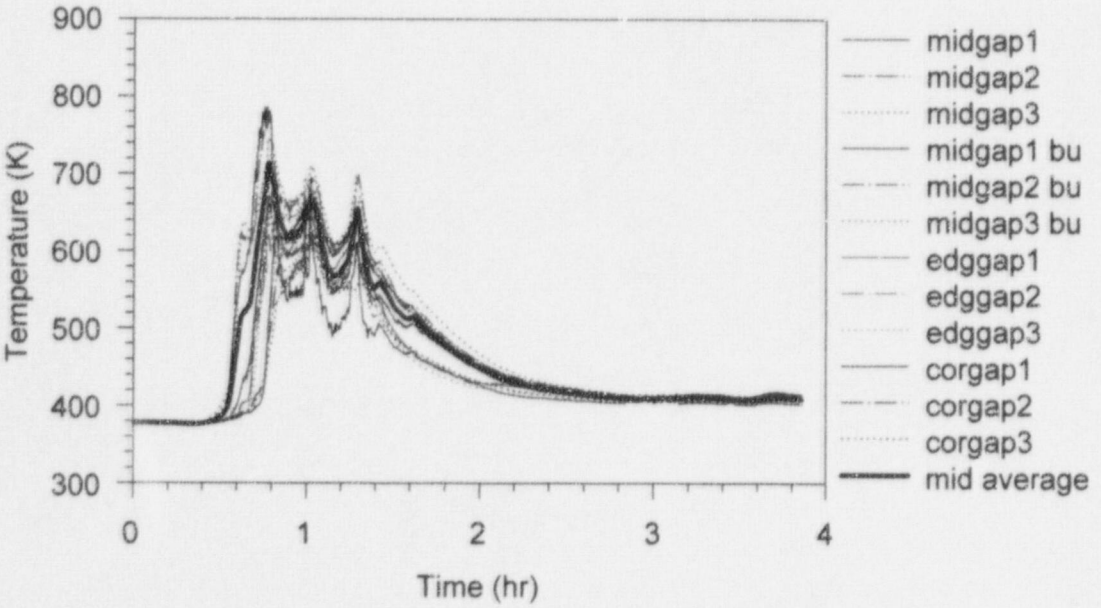

Figure 158. Catalyst gap temperatures in PAR-13.

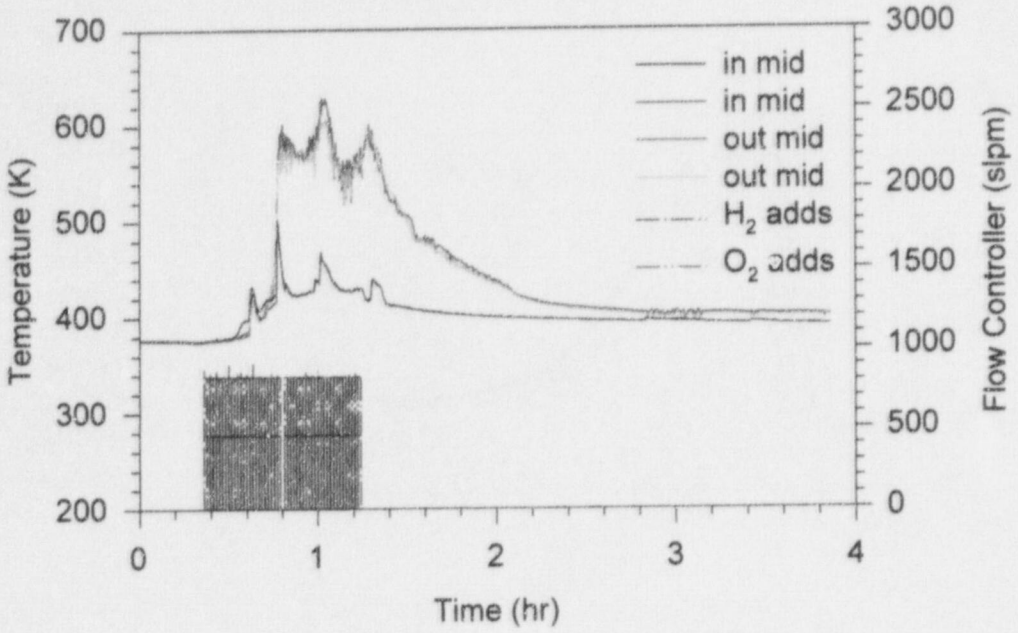

Figure 159. Inlet and outlet temperatures in PAR-13.

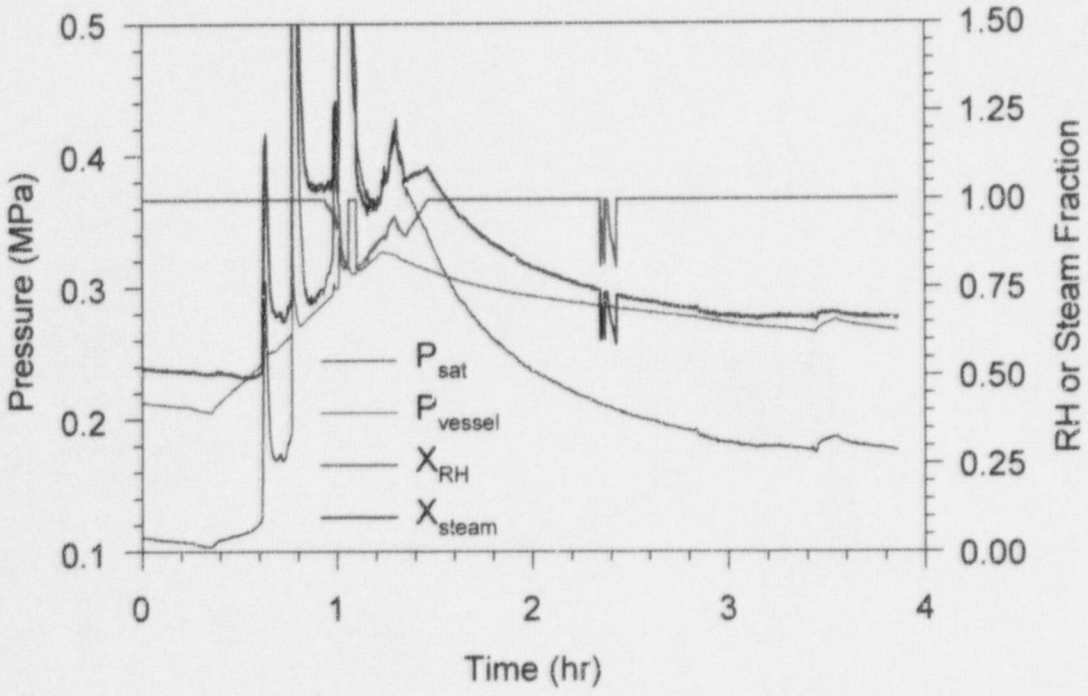

Figure 160. Saturation pressure, vessel pressure, relative humidity, and steam fraction in PAR-13.

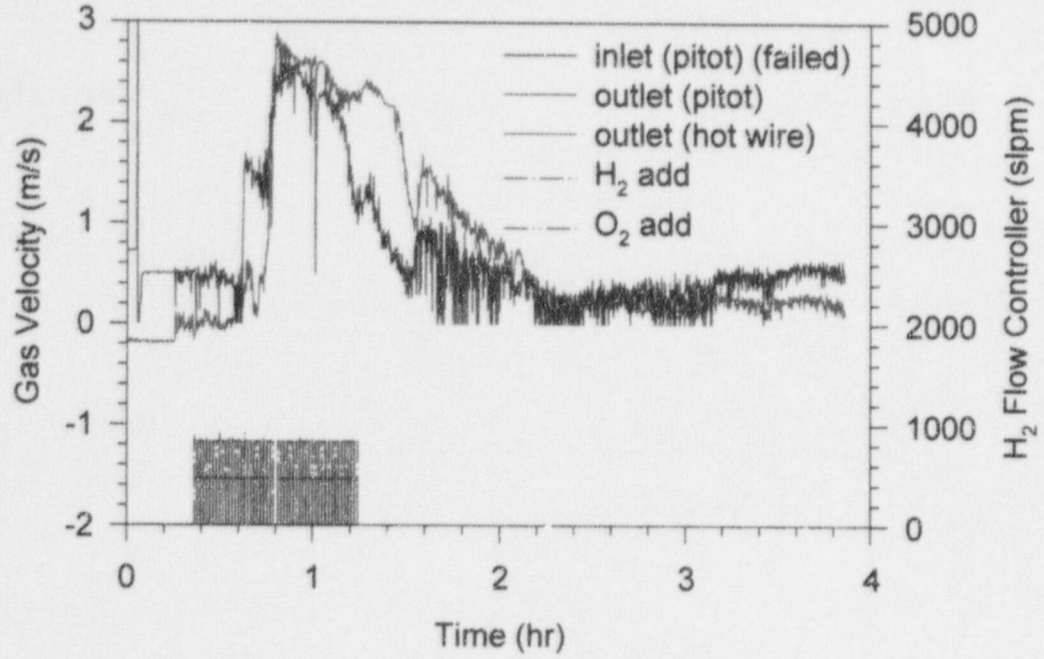

Figure 161. PAR gas velocity in PAR-13.

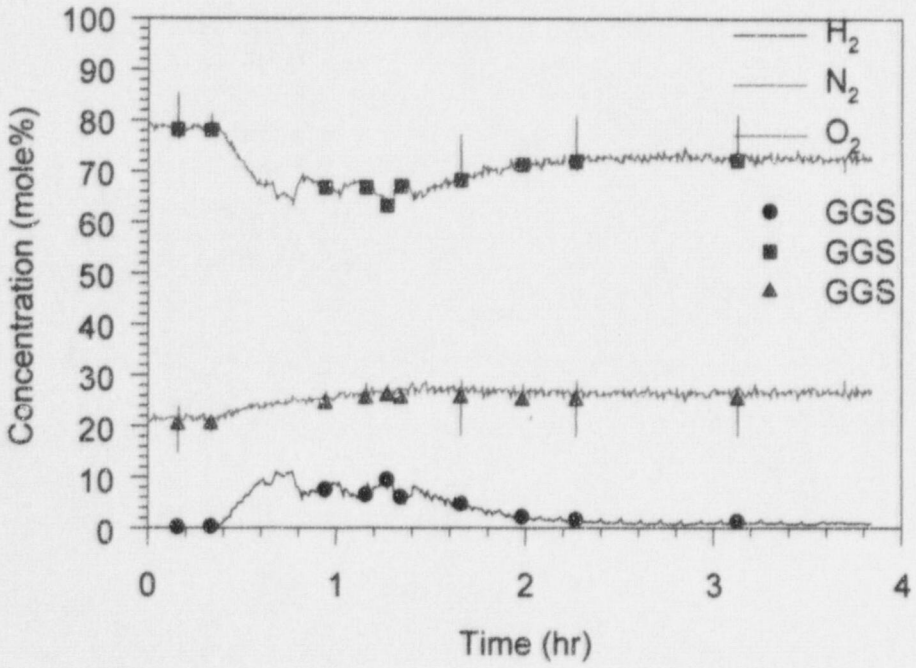

Figure 162. Gas concentrations (dry-basis) in PAR-13.

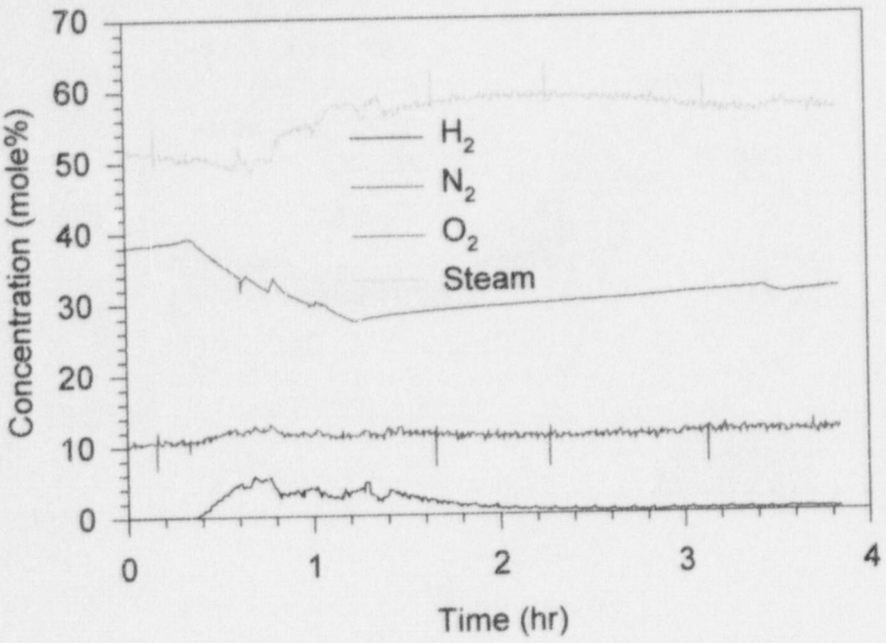

Figure 163. Gas concentrations (wet-basis) in PAR-13.

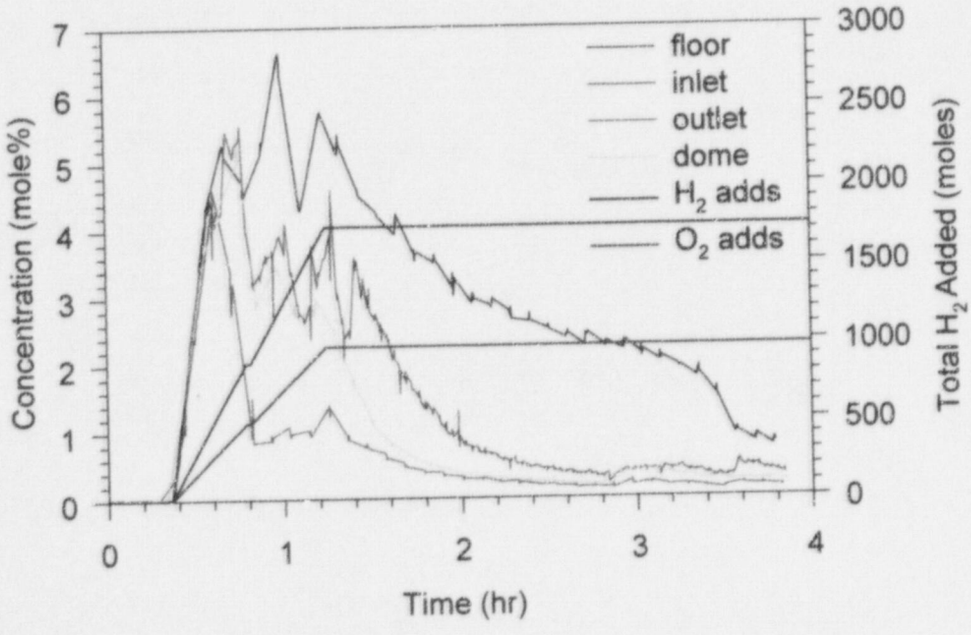

Figure 164. H_2 concentrations (wet-basis) in PAR-13.

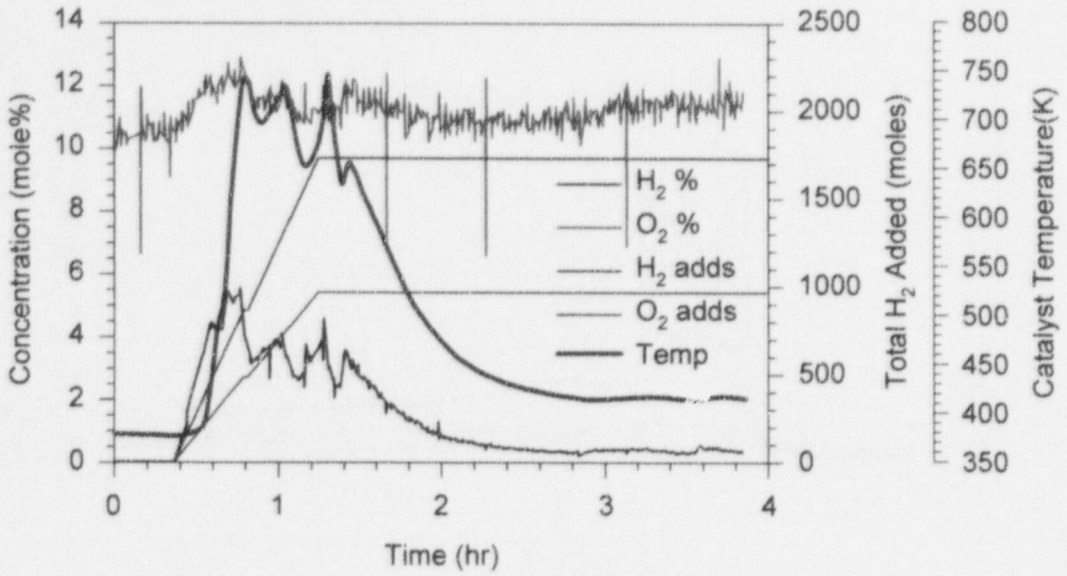

Figure 165. Catalyst temperature compared to gas additions and concentrations in PAR-13.

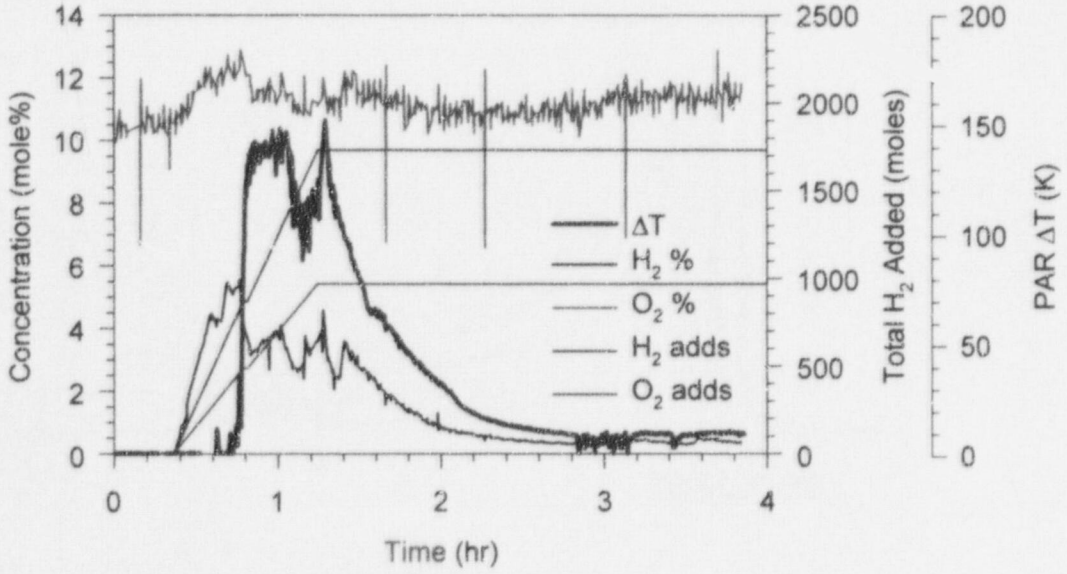

Figure 166. PAR ΔT temperature compared to gas additions and concentrations in PAR-13.

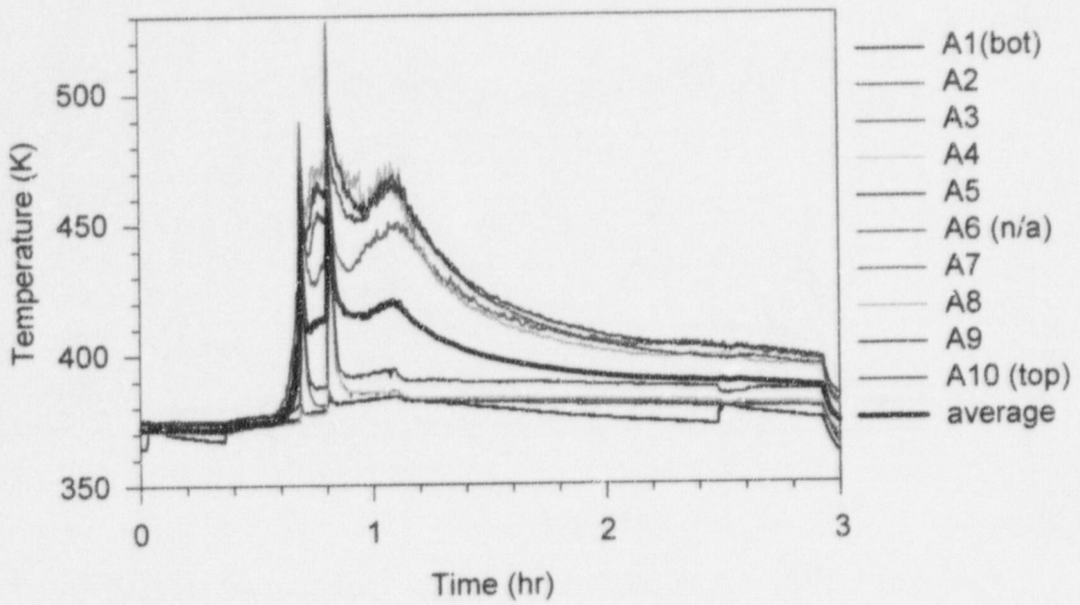

Figure 167. Surtsey vessel centerline gas temperatures from TC array A in PAR-13R.

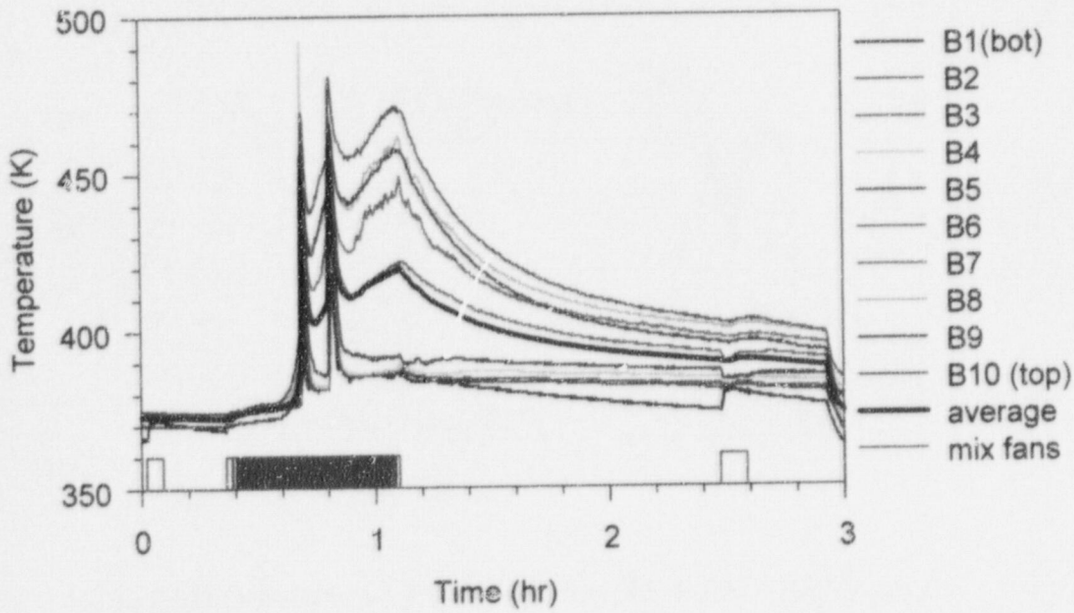

Figure 168. Surtsey vessel wall gas temperatures from TC array B in PAR-13R.

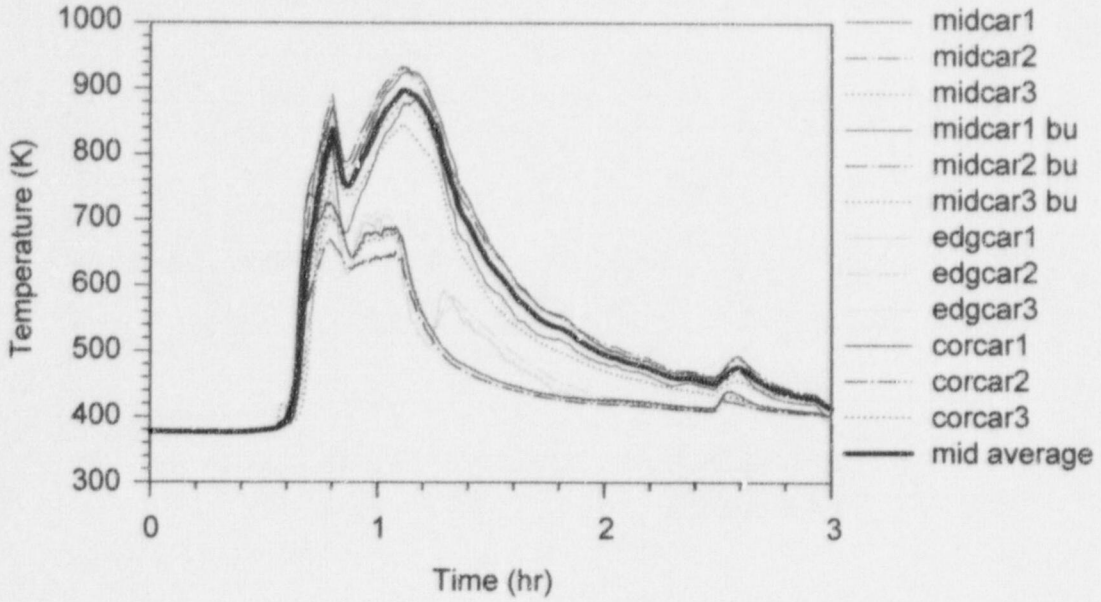

Figure 169. Catalyst cartridge temperatures in PAR-13R.

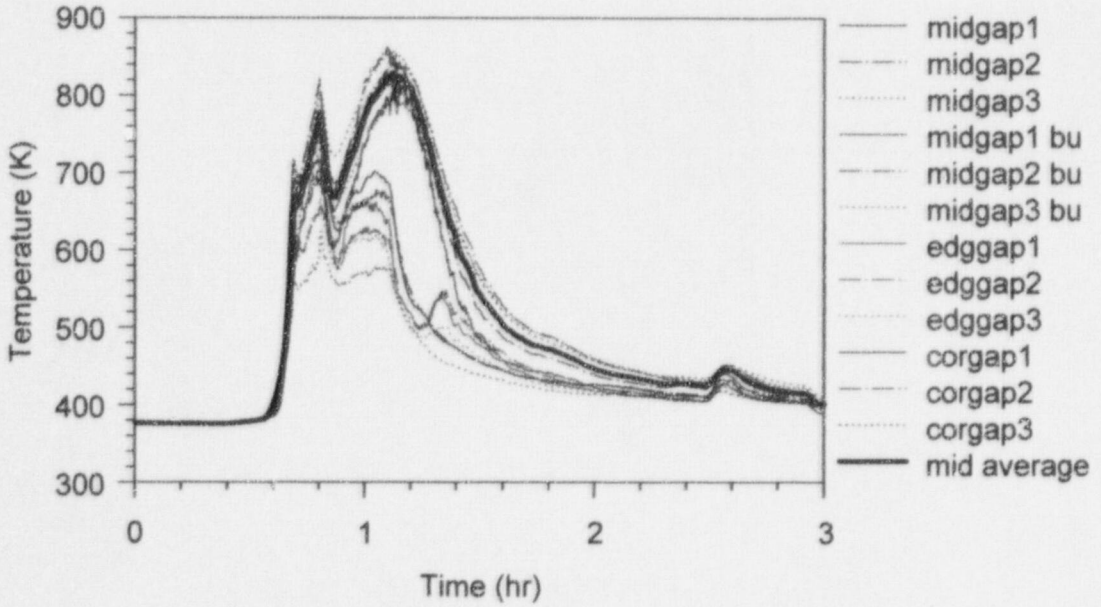

Figure 170. Catalyst gap temperatures in PAR-13R.

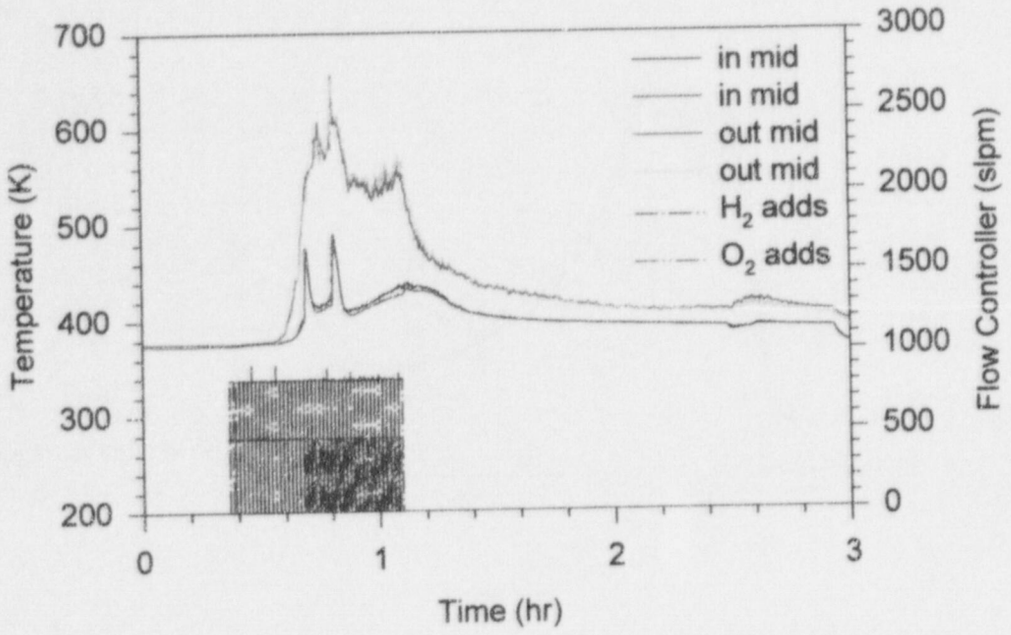

Figure 171. Inlet and outlet temperatures in PAR-13R.

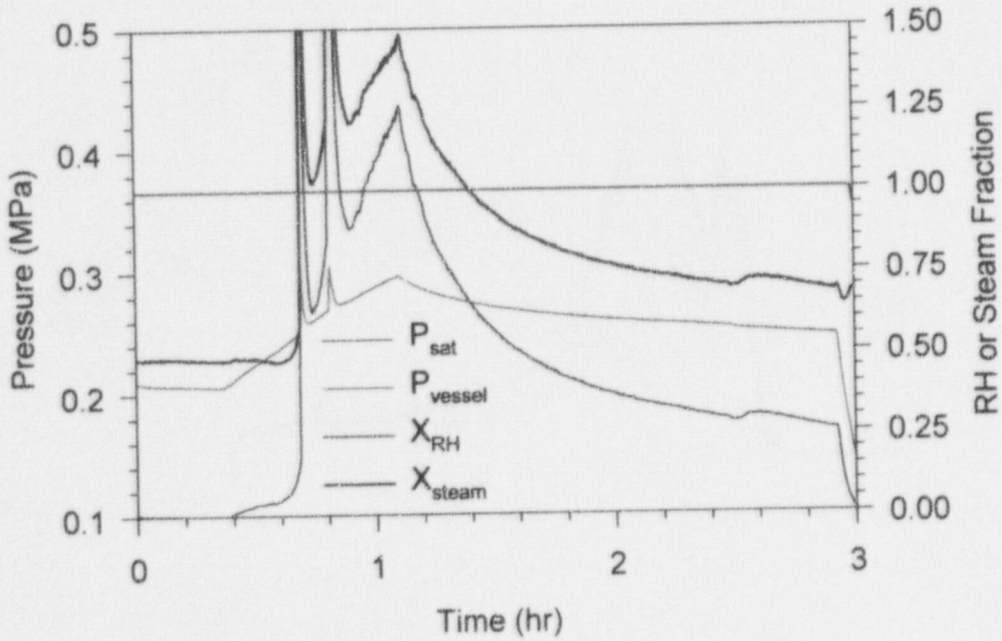

Figure 172. Saturation pressure, vessel pressure, relative humidity, and steam fraction in PAR-13R.

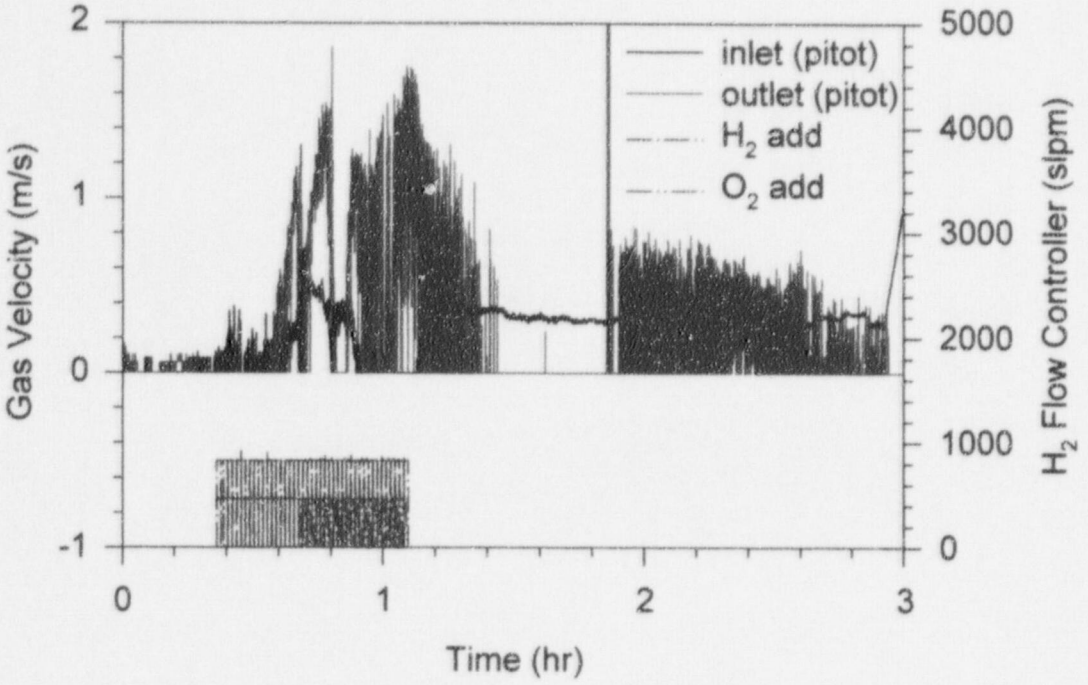

Figure 173. PAR gas velocity in PAR-13R.

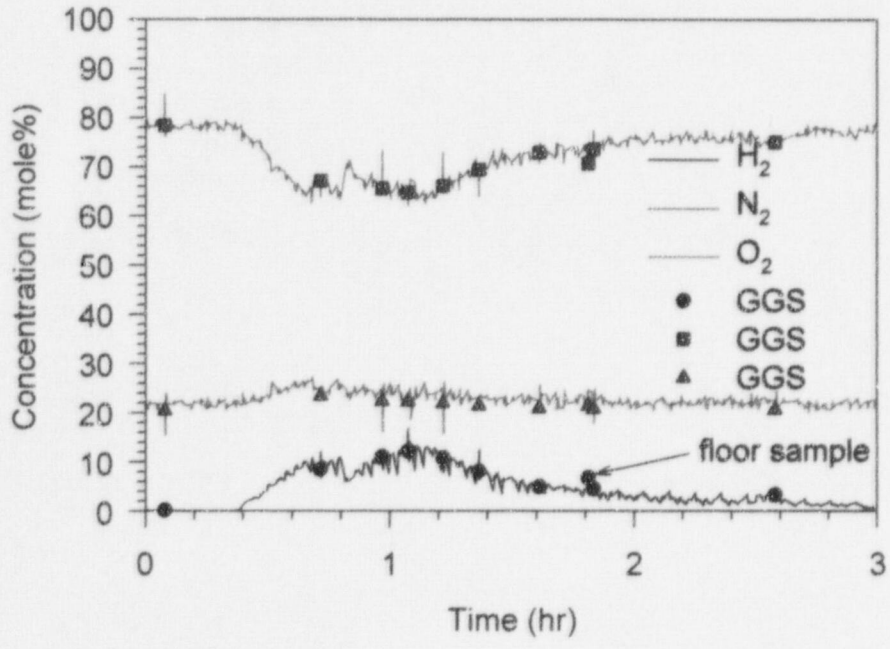

Figure 174. Gas concentrations (dry-basis) in PAR-13R.

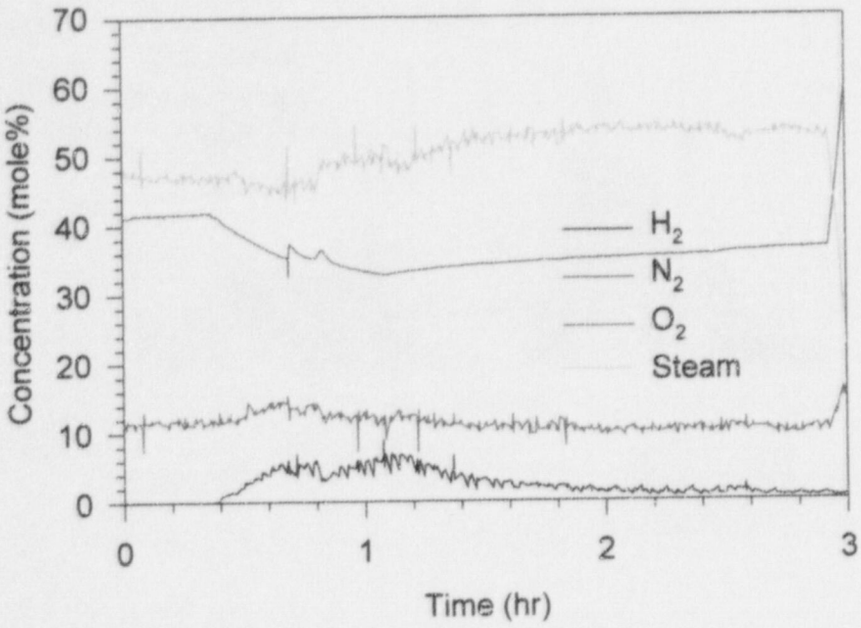

Figure 175. Gas concentrations (wet-basis) in PAR-13R.

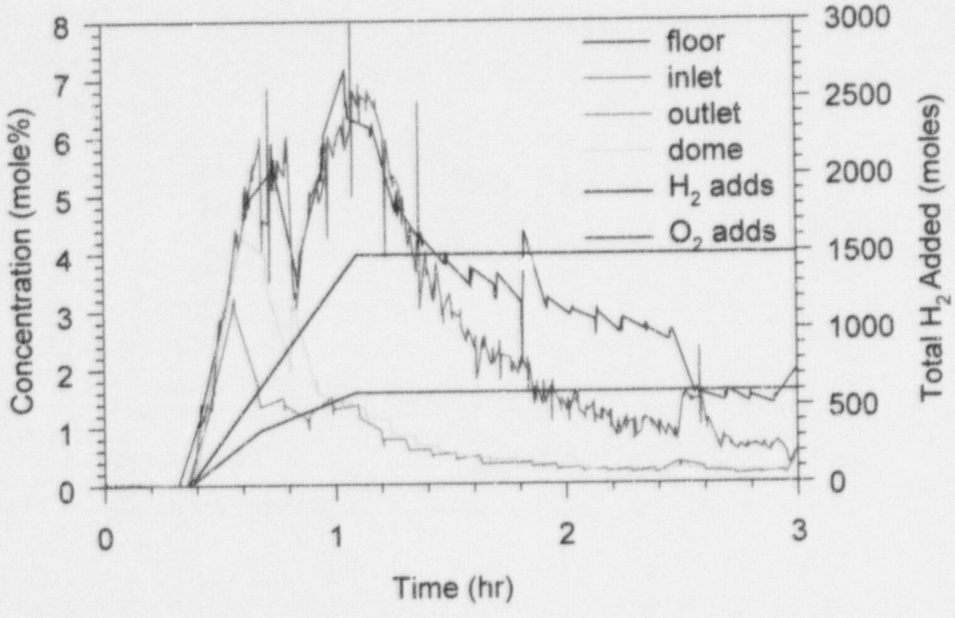

Figure 176. H_2 concentrations (wet-basis) in PAR-13R.

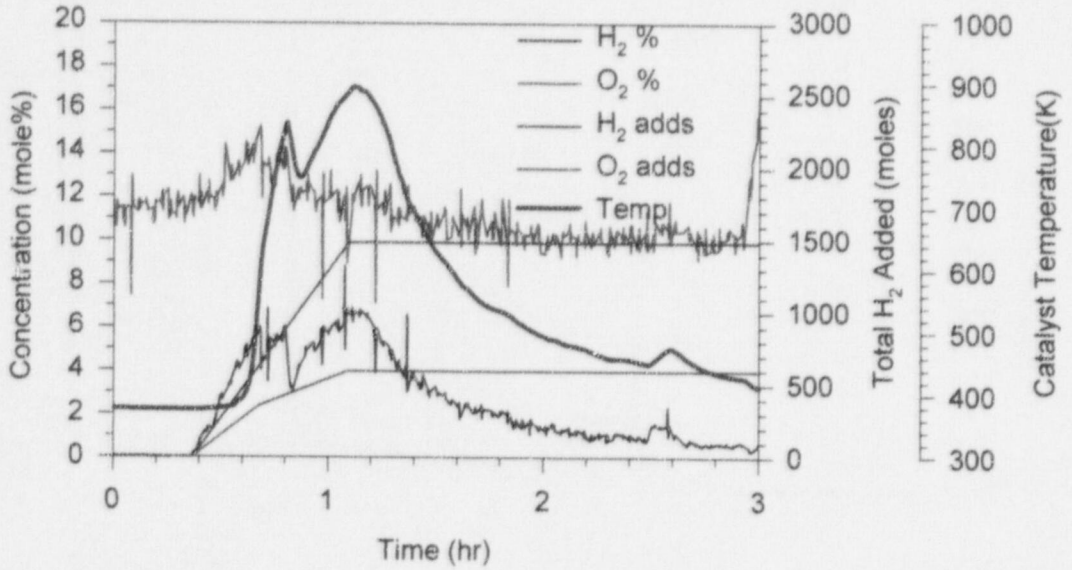

Figure 177. Catalyst temperature compared to gas additions and concentrations in PAR-13R.

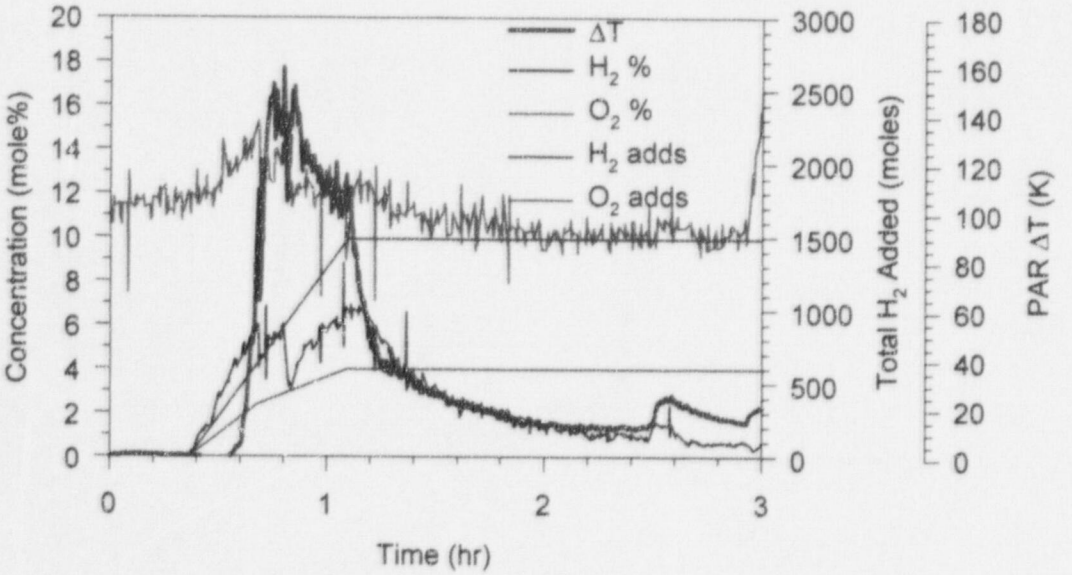

Figure 178. PAR ΔT temperature compared to gas additions and concentrations in PAR-13R.

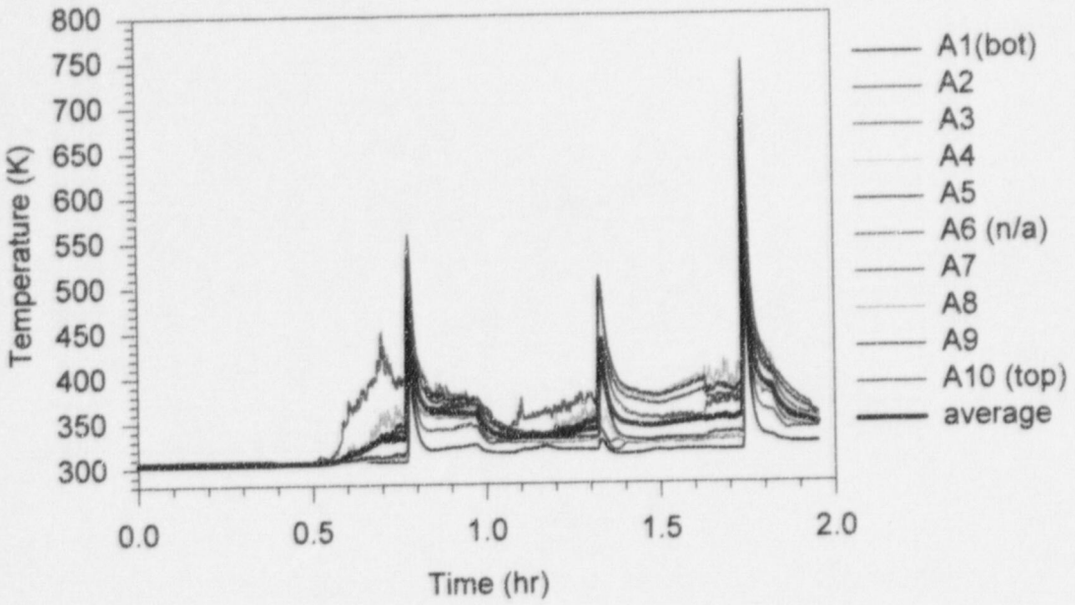

Figure 179. Surtsey vessel centerline gas temperatures from TC array A in PAR-demo1.

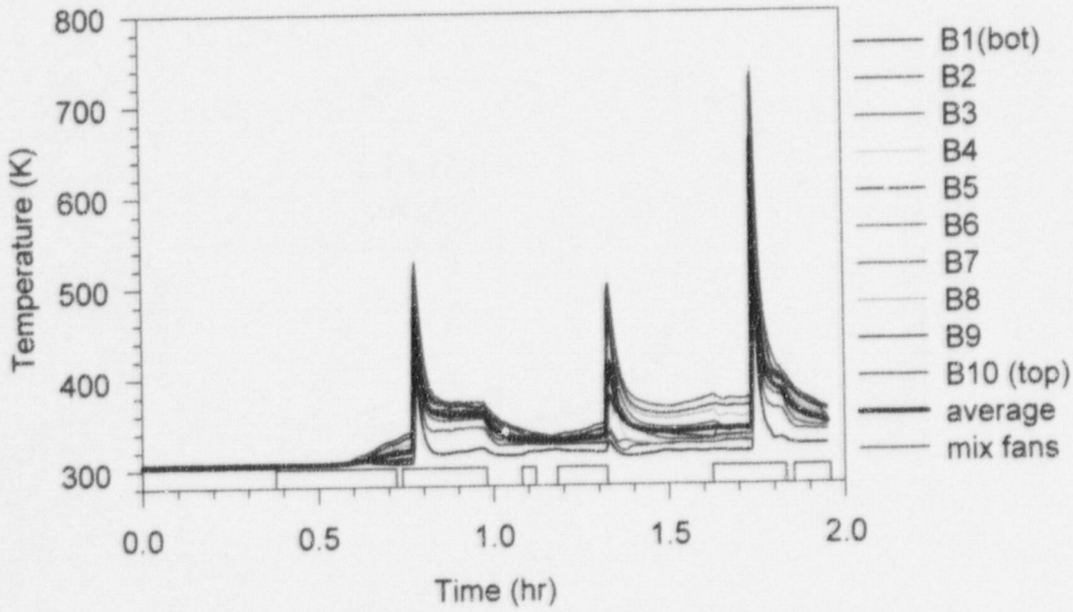

Figure 180. Surtsey vessel wall gas temperatures from TC array B in PAR-demo1.

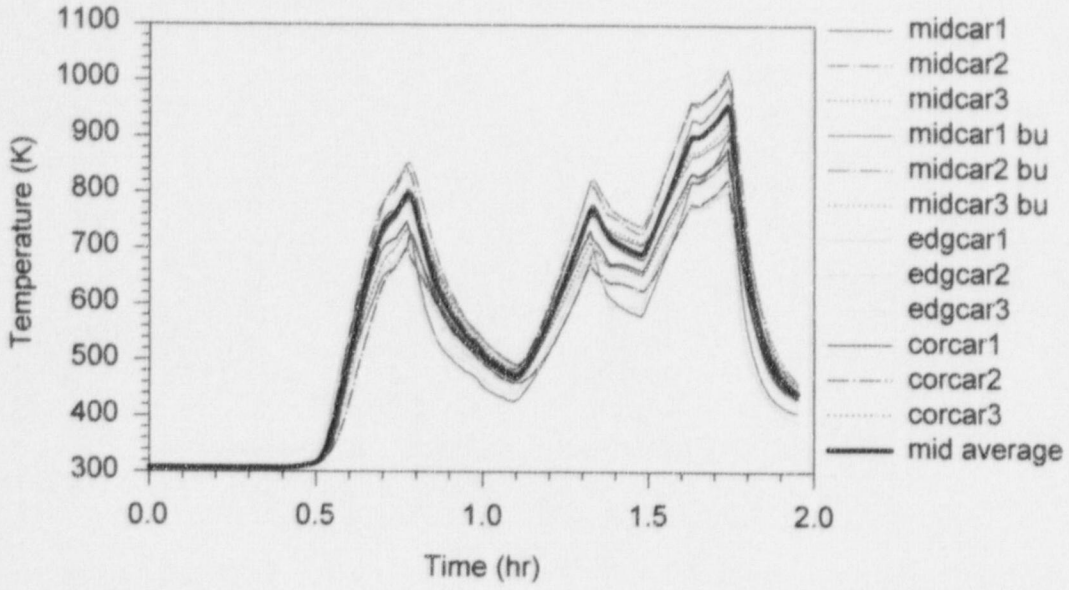

Figure 181. Catalyst cartridge temperatures in PAR-demo1.

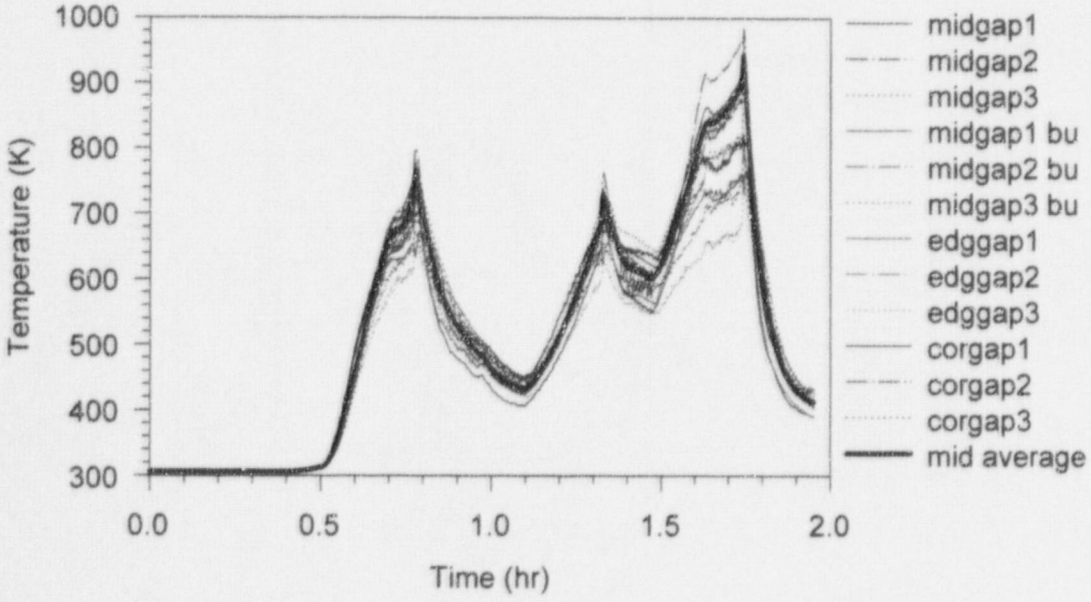

Figure 182. Catalyst gap temperatures in PAR-demo1.

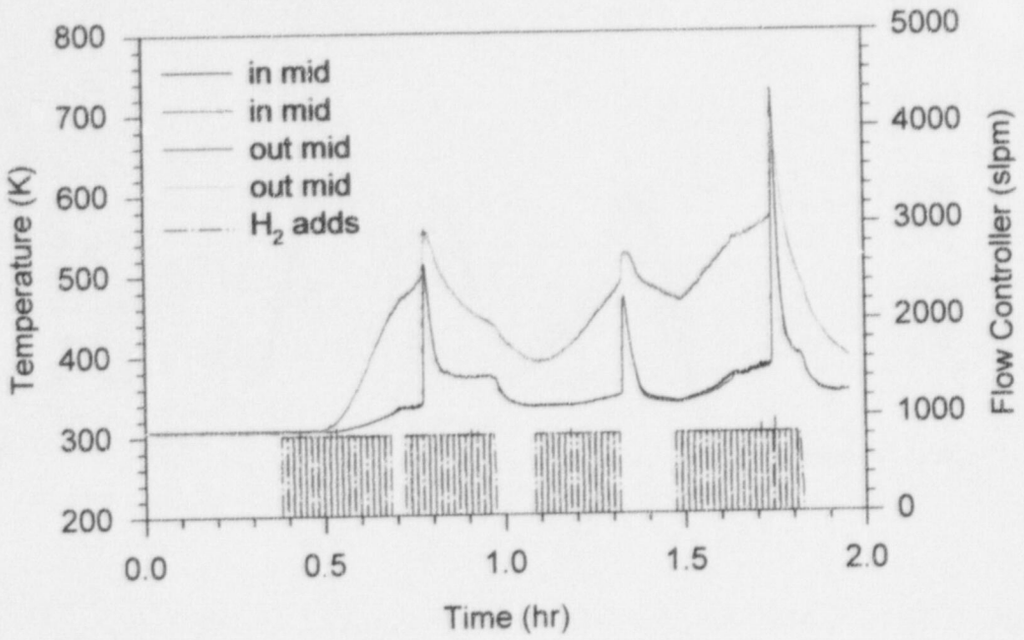

Figure 183. Inlet and outlet temperatures in PAR-demo1.

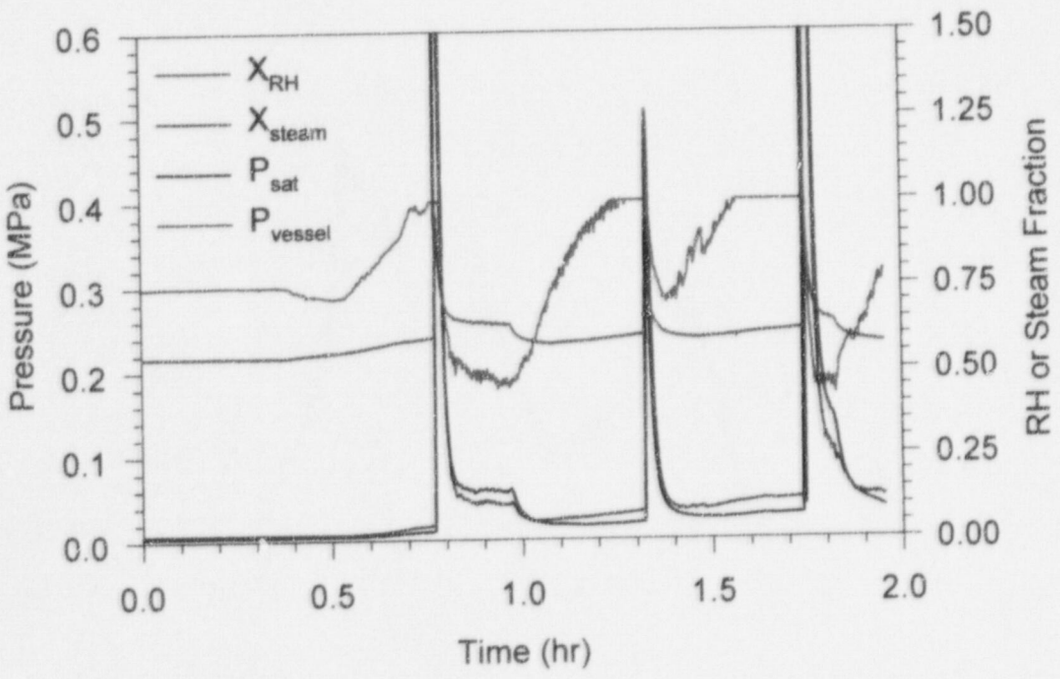

Figure 184. Saturation pressure, vessel pressure, relative humidity, and steam fraction in PAR-demo1.

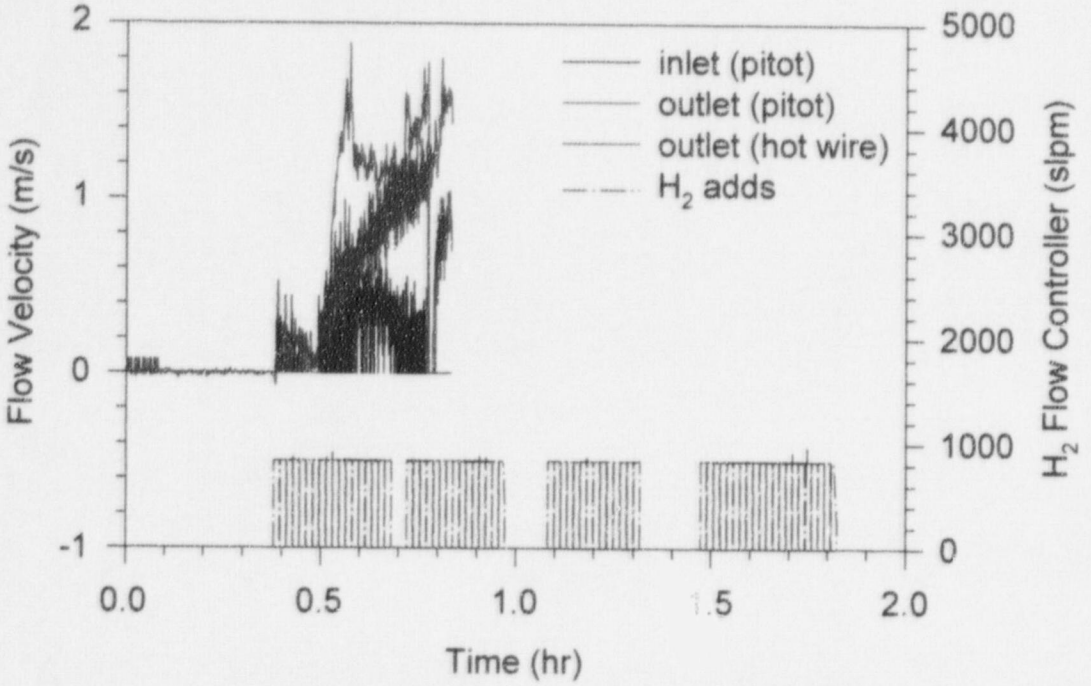

Figure 185. PAR gas velocity in PAR-demo1.

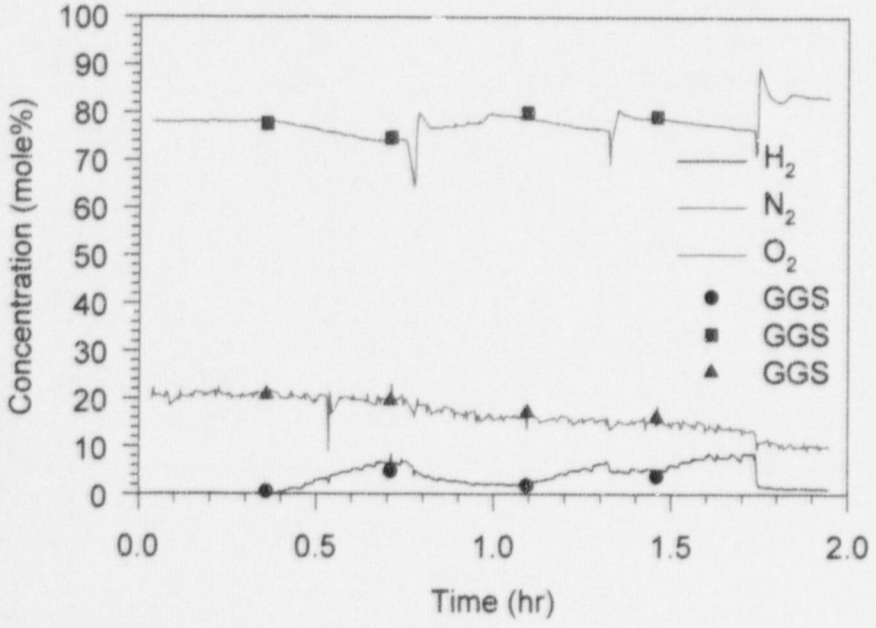

Figure 186. Gas concentrations (dry-basis) in PAR-demo1.

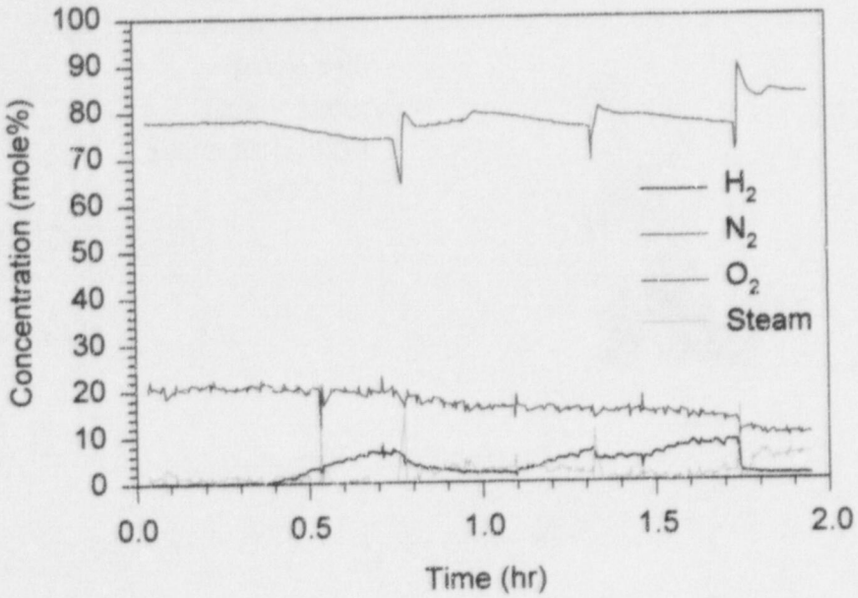

Figure 187. Gas concentrations (wet-basis) in PAR-demo1.

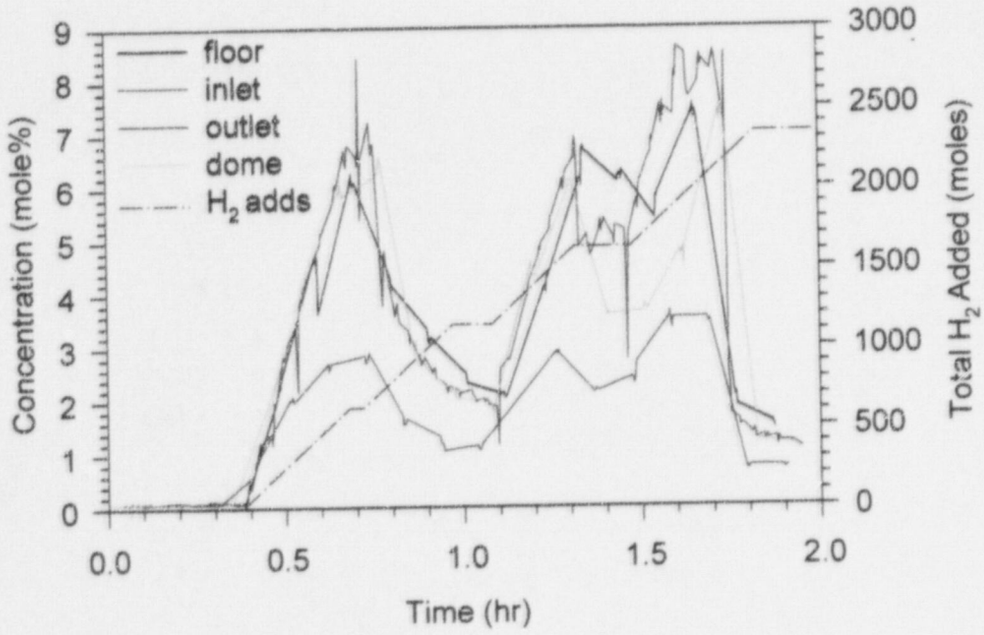

Figure 188. H_2 concentrations (wet-basis) in PAR-demo1.

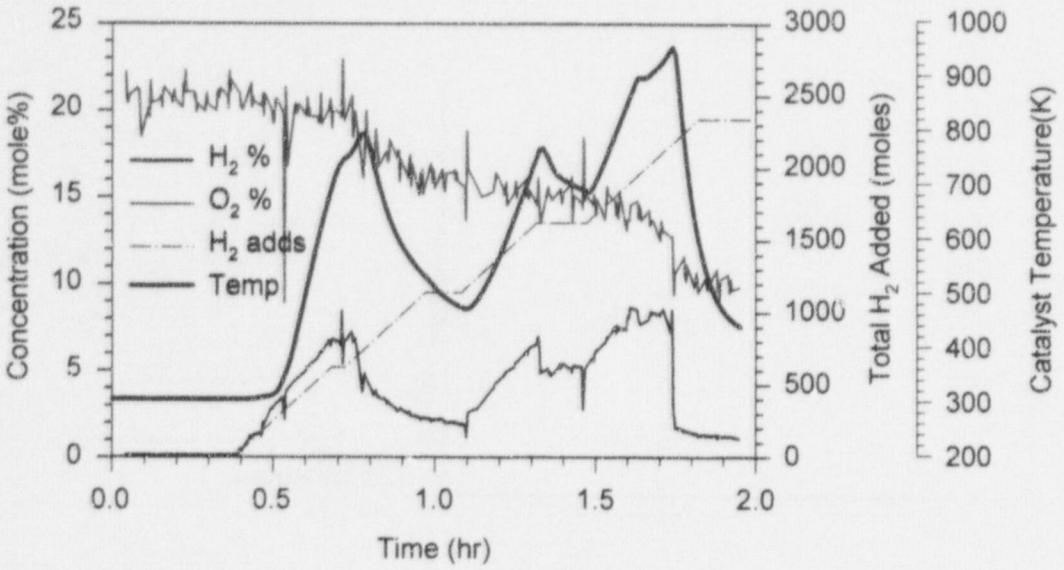

Figure 189. Catalyst temperature compared to gas additions and concentrations in PAR-demo1.

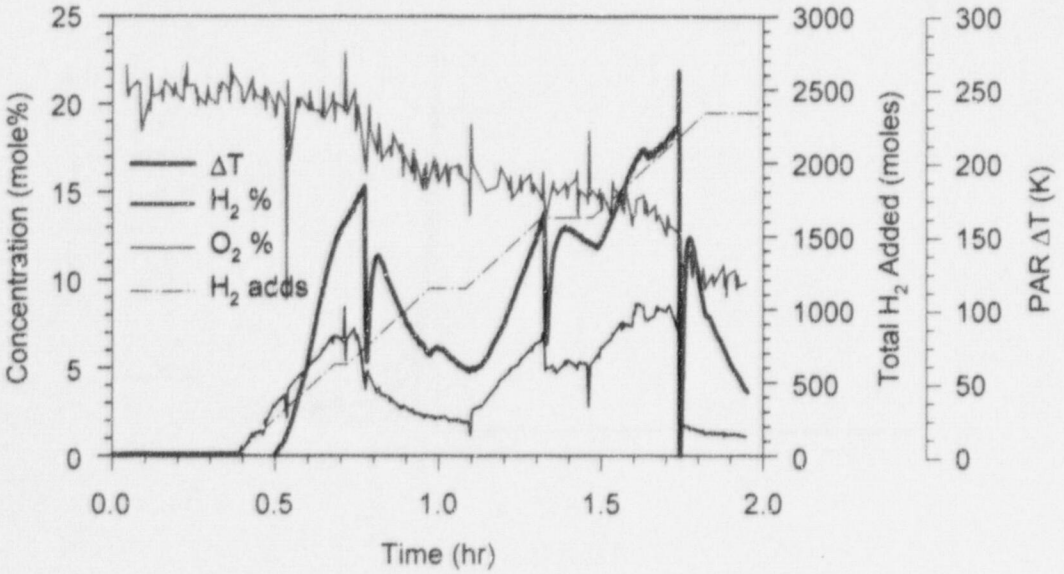

Figure 190. PAR ΔT temperature compared to gas additions and concentrations in PAR-demo1.

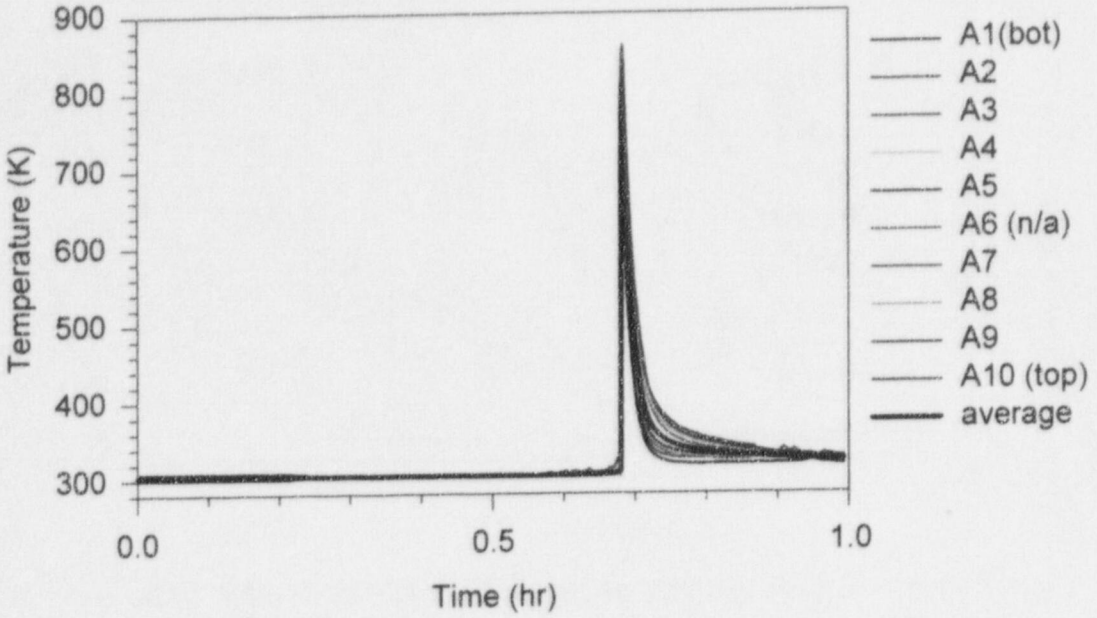

Figure 191. Surtsey vessel centerline gas temperatures from TC array A in PAR-demo2.

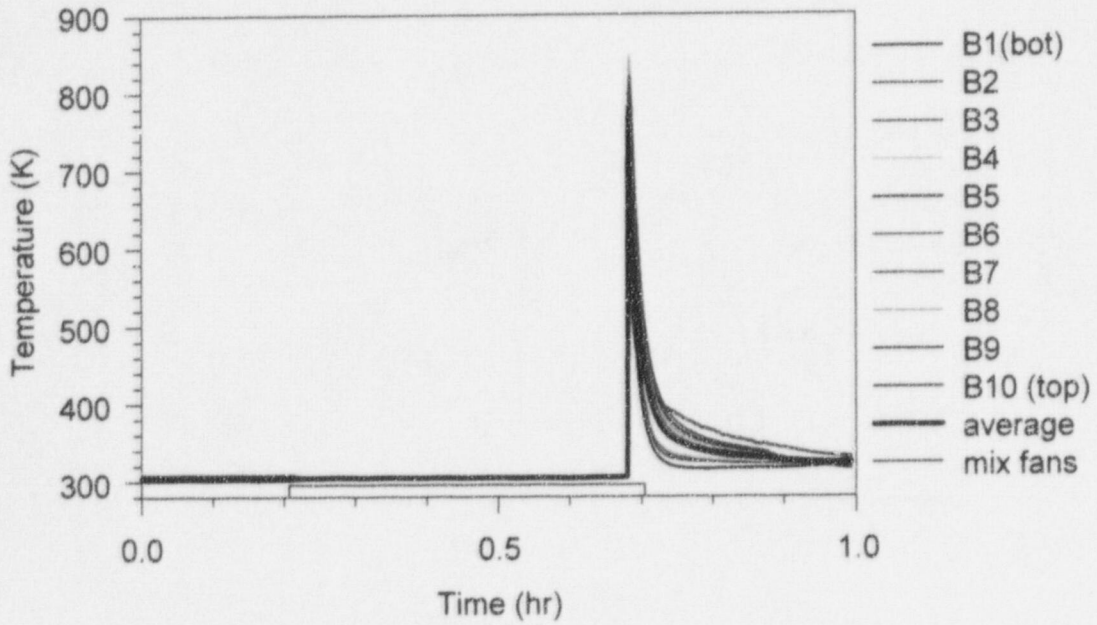

Figure 192. Surtsey vessel wall gas temperatures from TC array B in PAR-demo2.

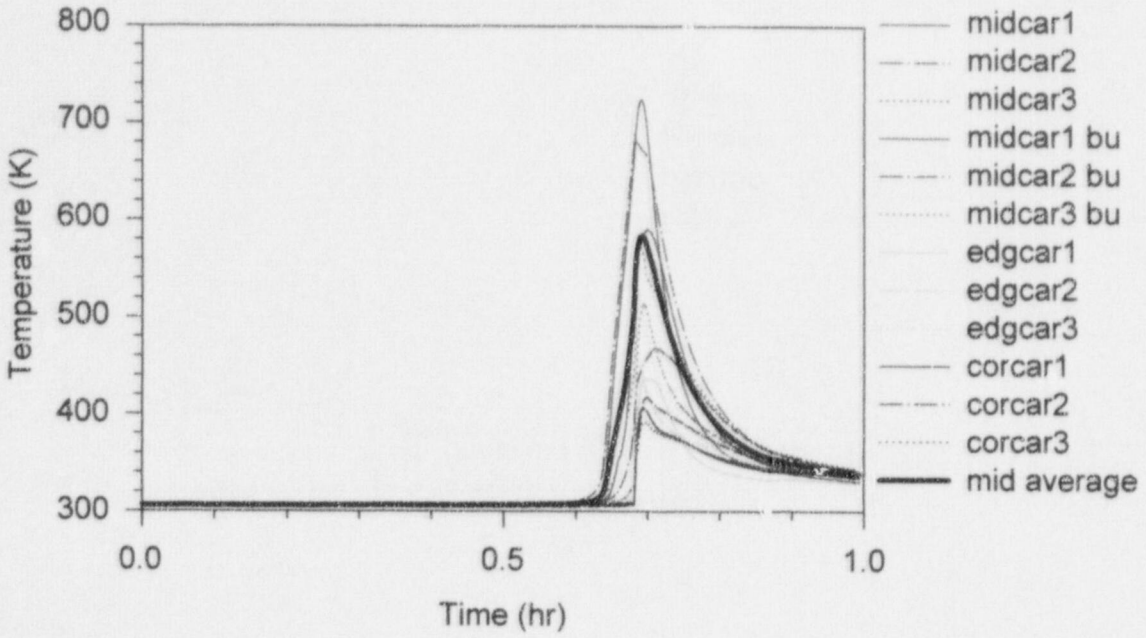

Figure 193. Catalyst cartridge temperatures in PAR-demo2.

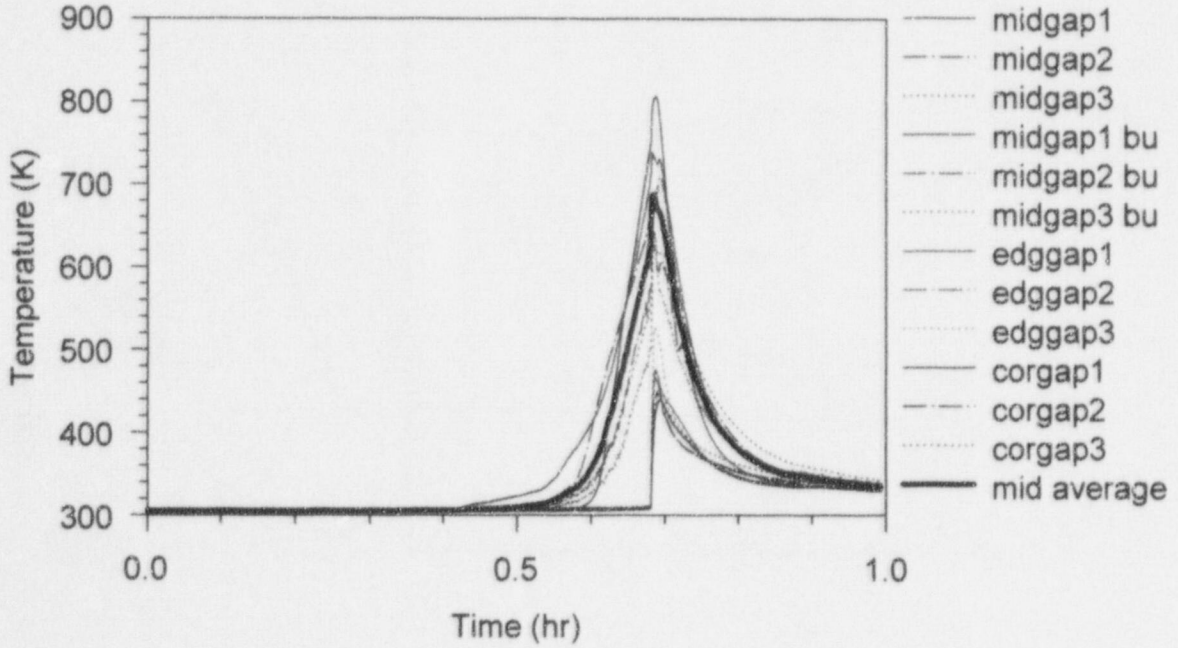

Figure 194. Catalyst gap temperatures in PAR-demo2.

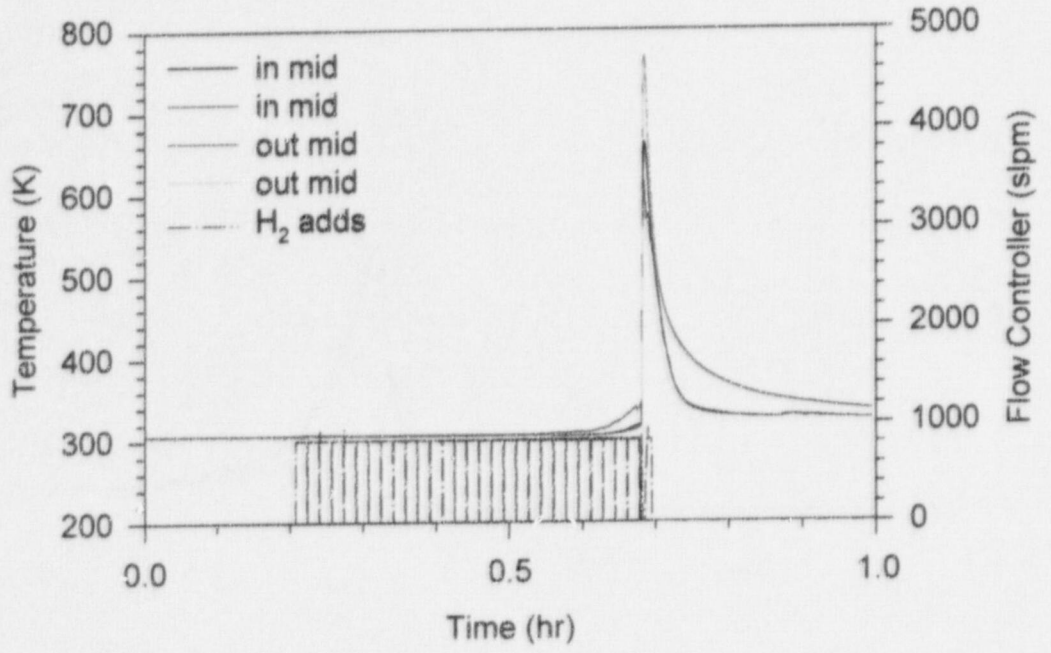

Figure 195. Inlet and outlet temperatures in PAR-demo2.

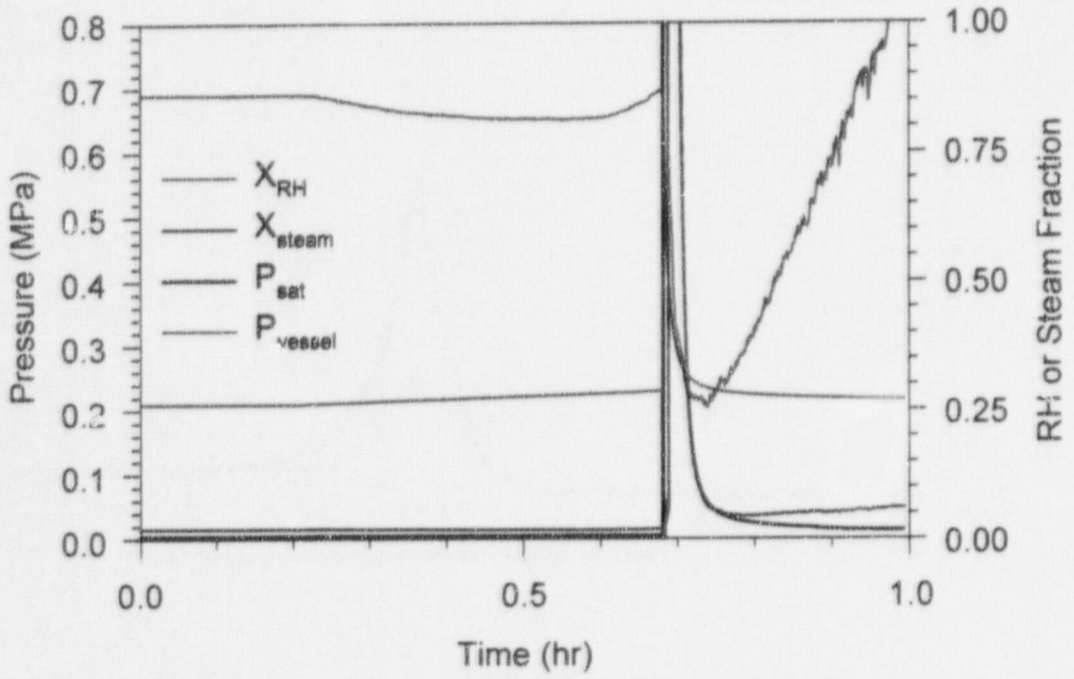

Figure 196. Saturation pressure, vessel pressure, relative humidity, and steam fraction in PAR-demo2.

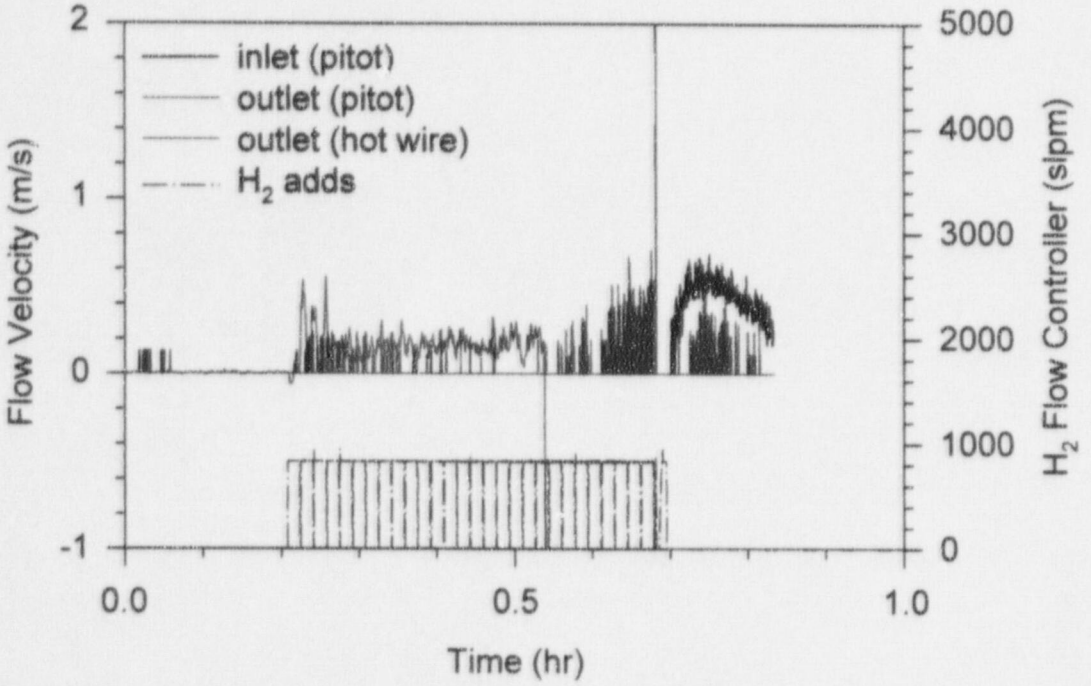

Figure 197. PAR gas velocity in PAR-demo2.

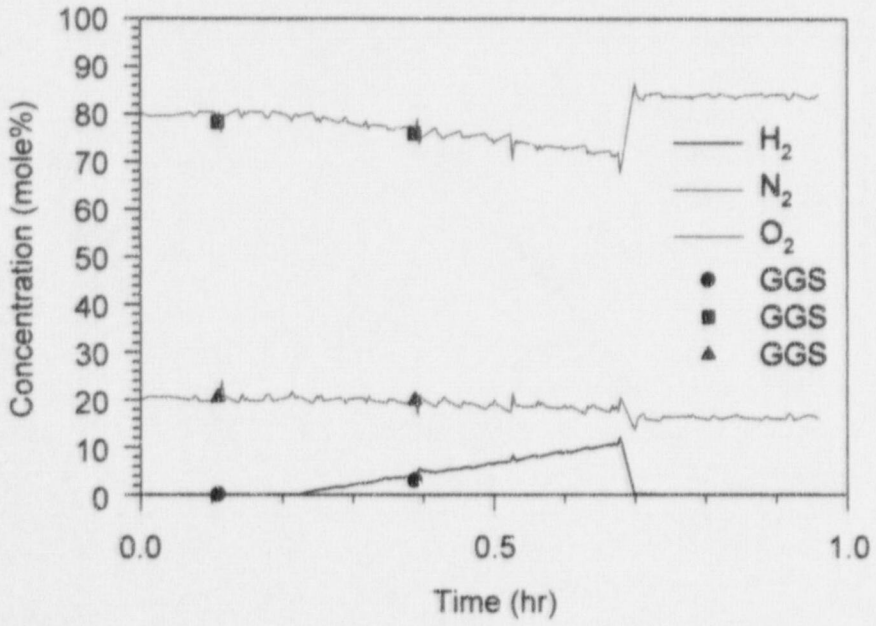

Figure 198. Gas concentrations (dry-basis) in PAR-demo2.

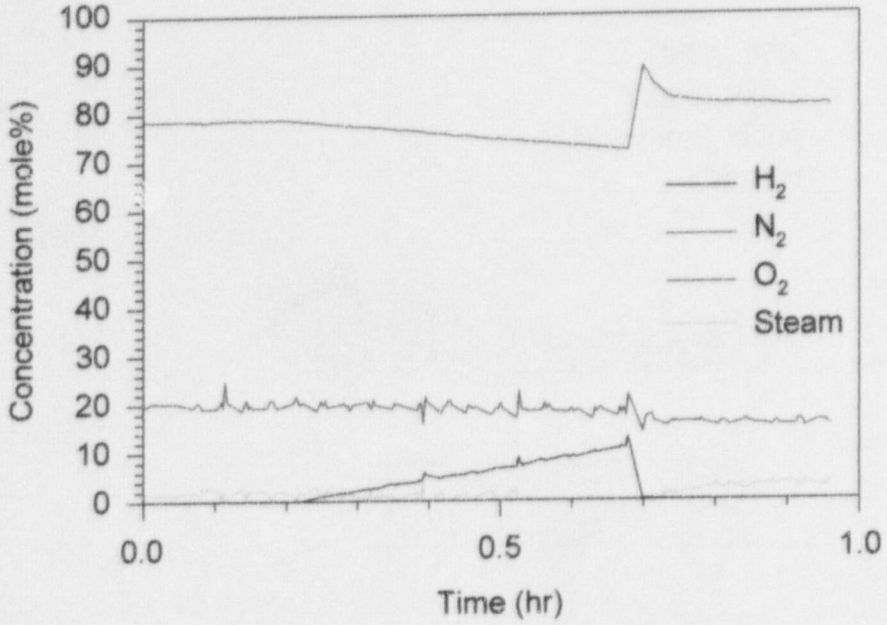

Figure 199. Gas concentrations (wet-basis) in PAR-demo2.

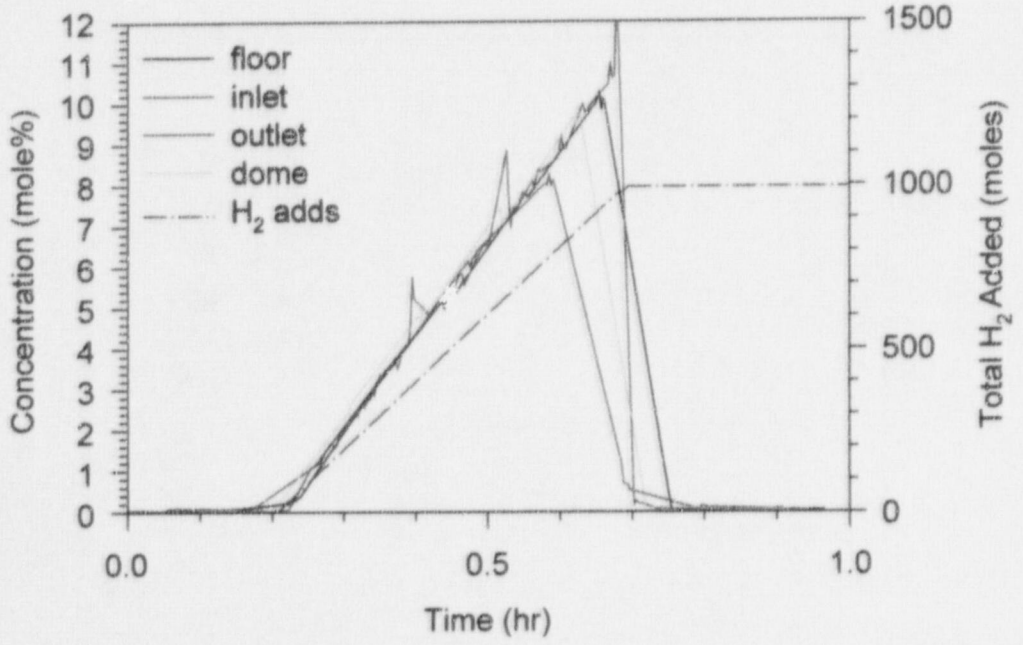

Figure 200. H_2 concentrations (wet-basis) in PAR-demo2.

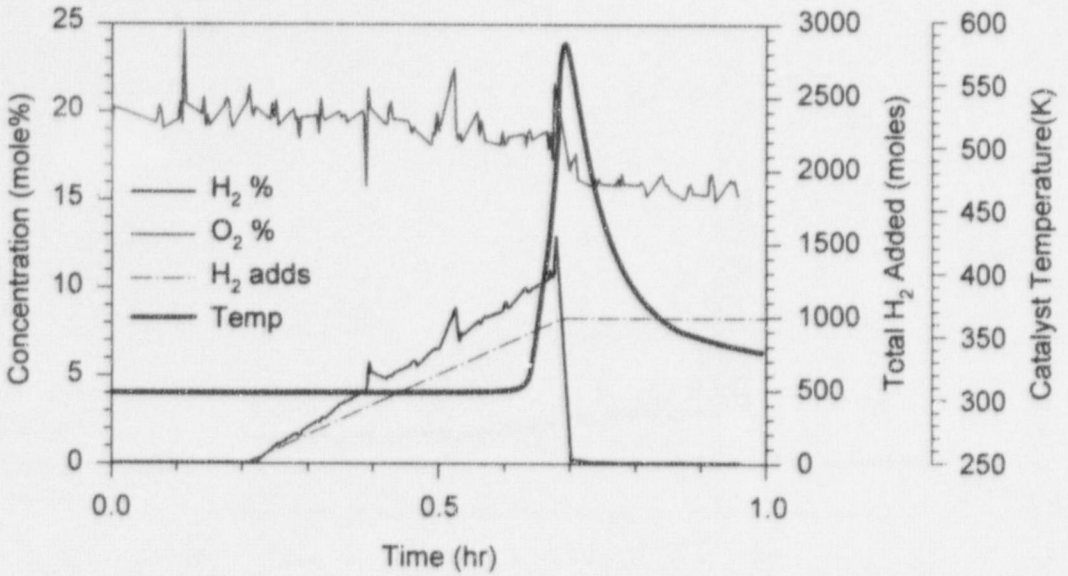

Figure 201. Catalyst temperature compared to gas additions and concentrations in PAR-demo2.

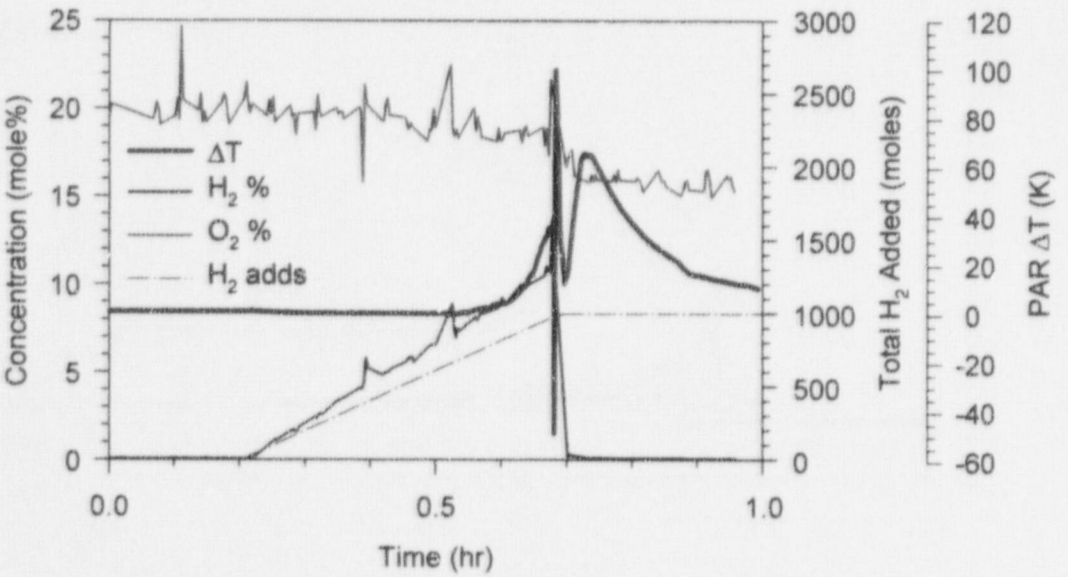

Figure 202. PAR ΔT temperature compared to gas additions and concentrations in PAR-demo2.

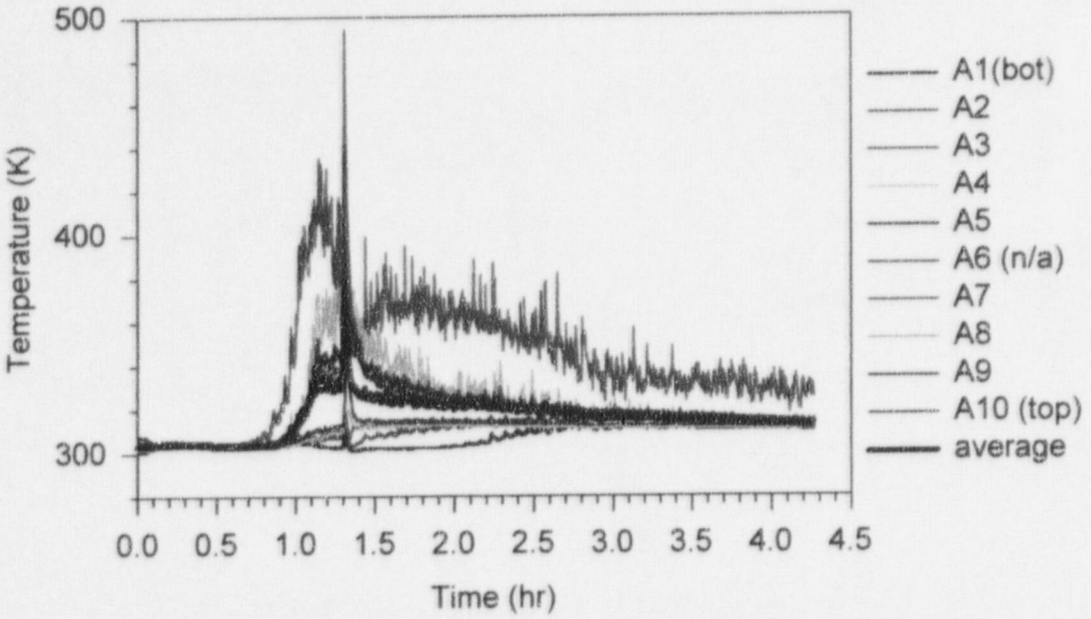

Figure 203. Surtsey vessel centerline gas temperatures from TC array A in PAR-demo3.

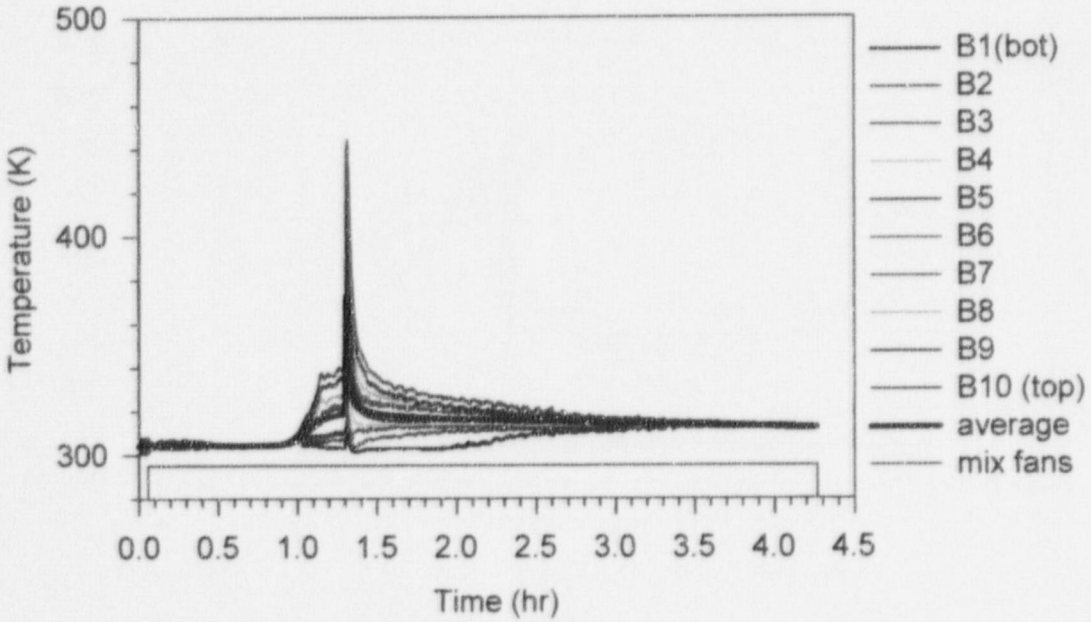

Figure 204. Surtsey vessel wall gas temperatures from TC array B in PAR-demo3.

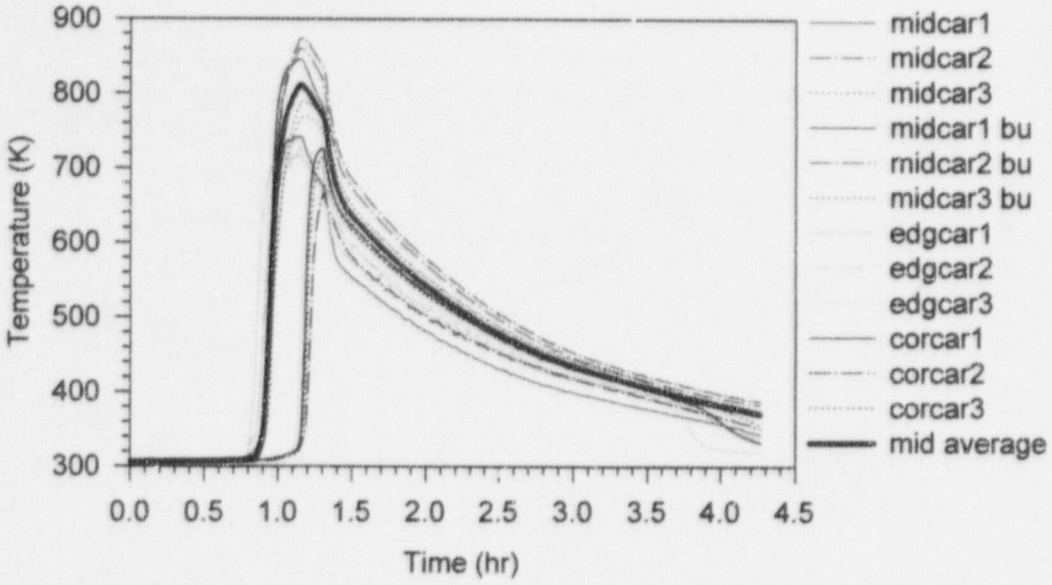

Figure 205. Catalyst cartridge temperatures in PAR-demo3.

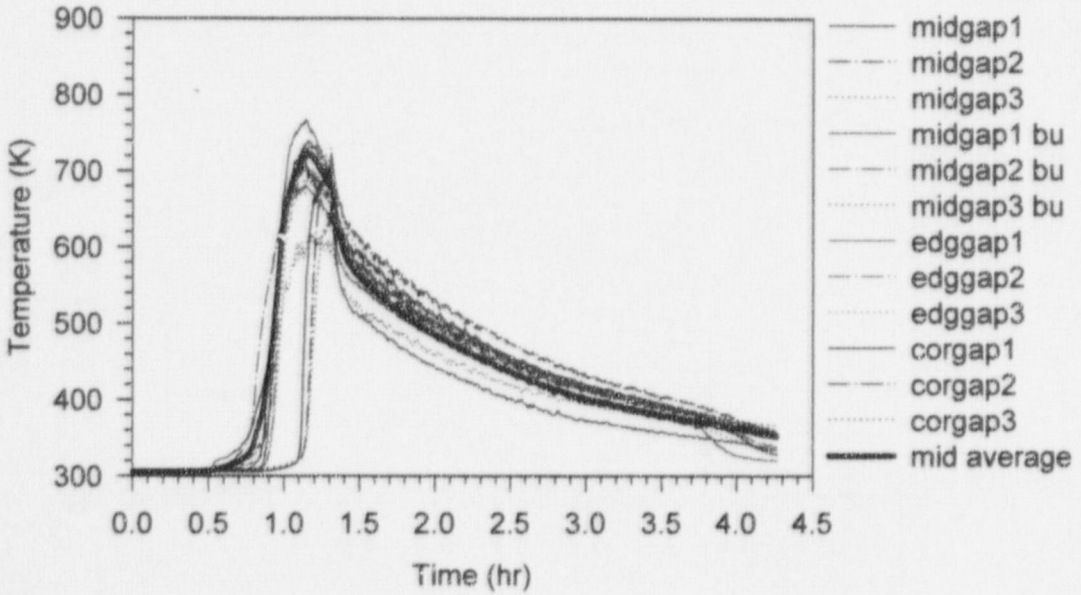

Figure 206. Catalyst gap temperatures in PAR-demo3.

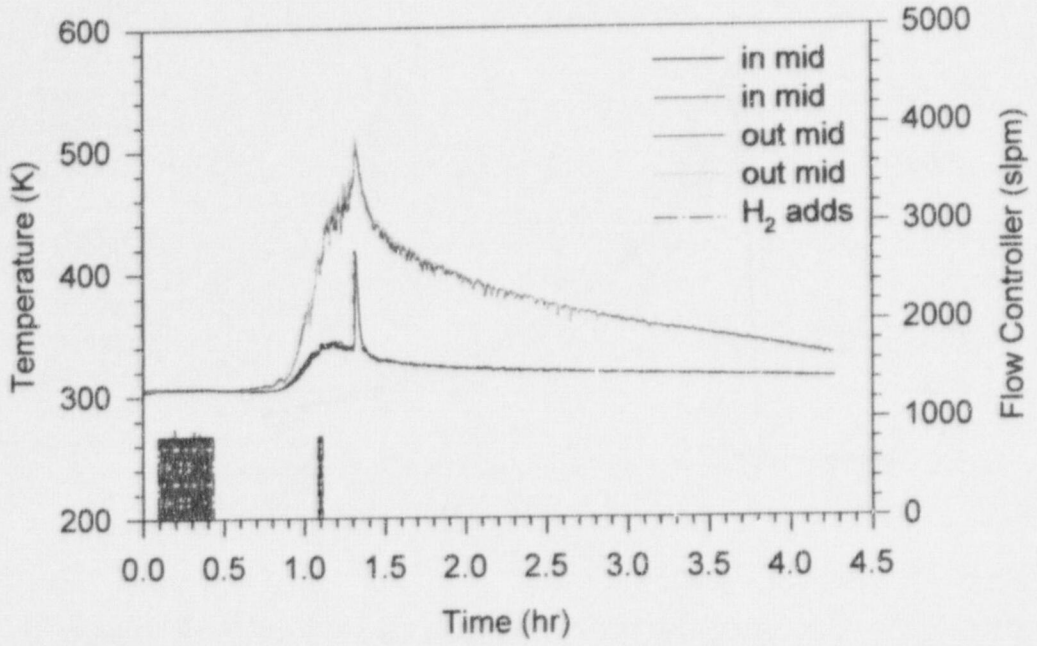

Figure 207. Inlet and outlet temperatures in PAR-demo3.

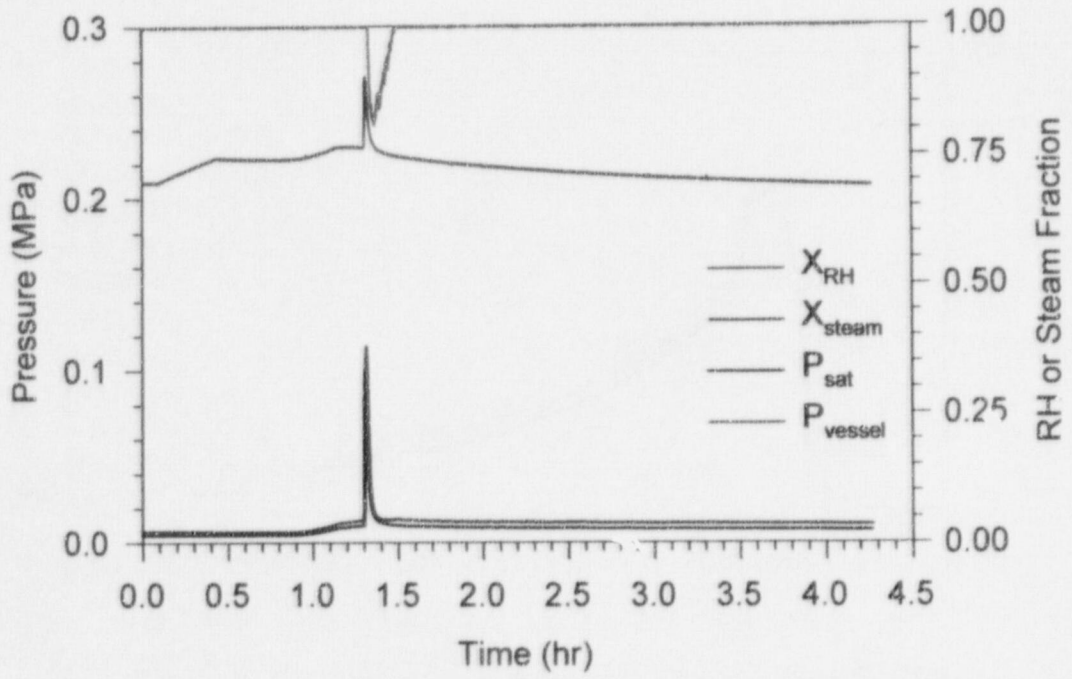

Figure 208. Saturation pressure, vessel pressure, relative humidity, and steam fraction in PAR-demo3.

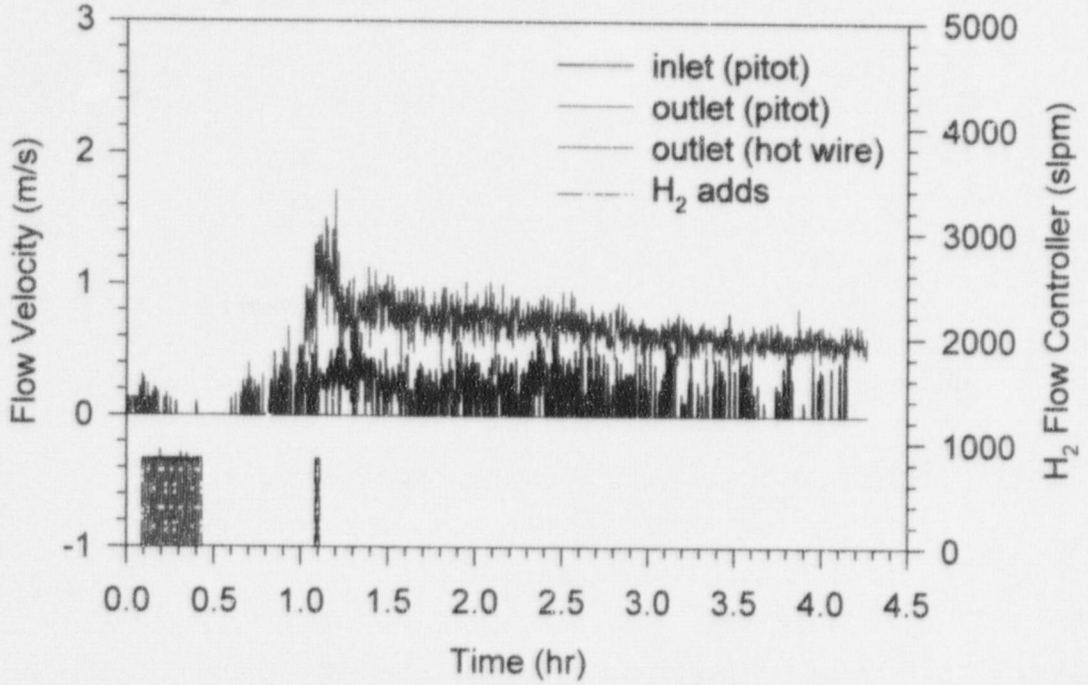

Figure 209. PAR gas velocity in PAR-demo3.

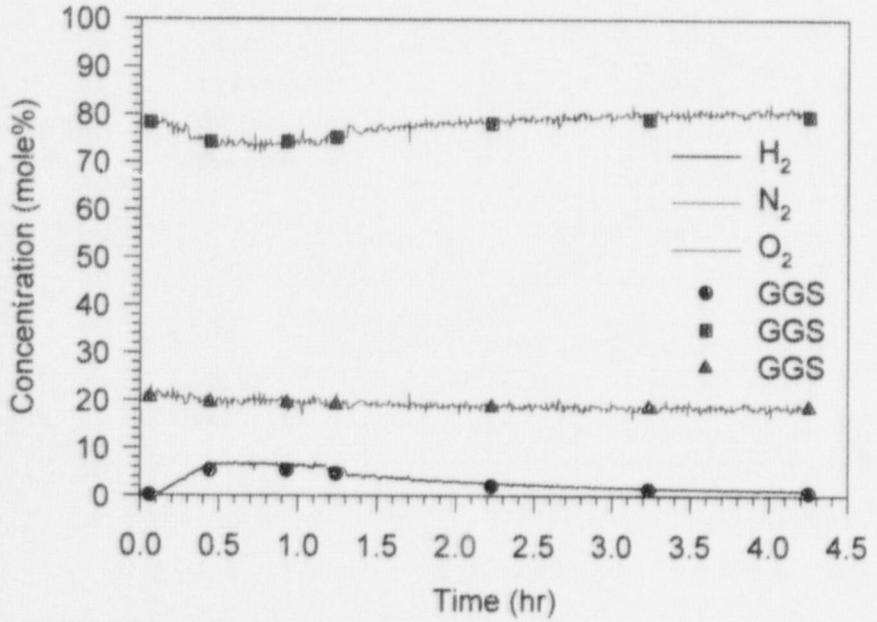

Figure 210. Gas concentrations (dry-basis) in PAR-demo3.

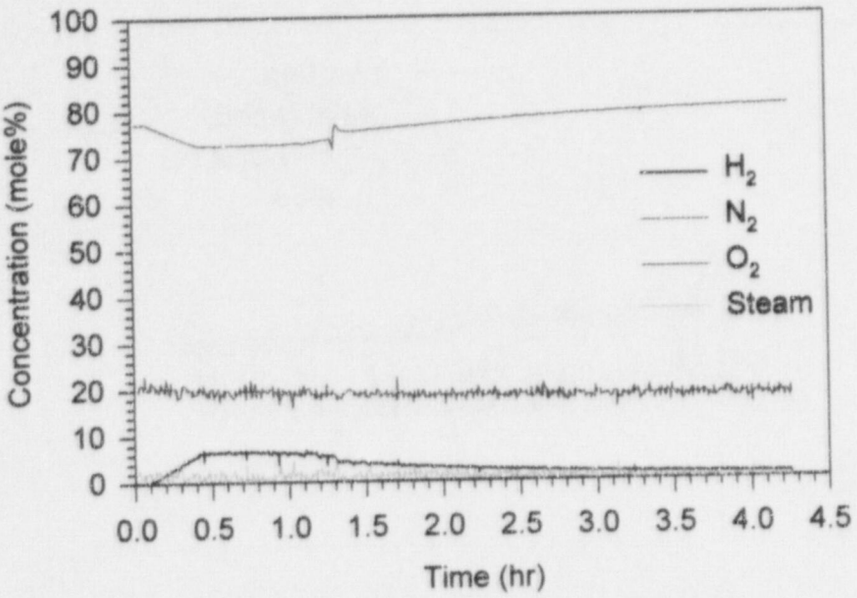

Figure 211. Gas concentrations (wet-basis) in PAR-demo3.

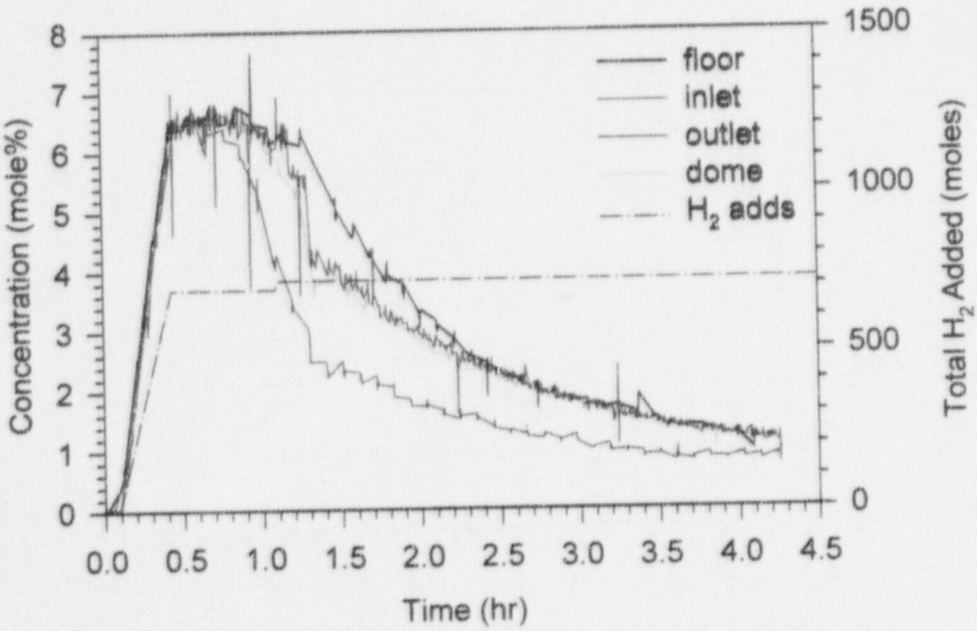

Figure 212. H_2 ccncentrations (wet-basis) in PAR-demo3.

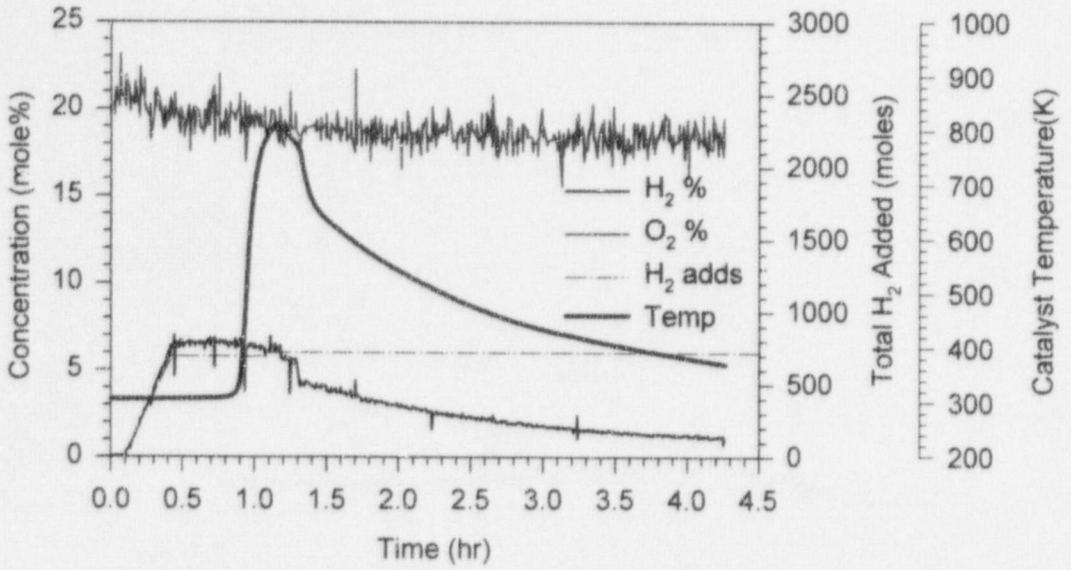

Figure 213. Catalyst temperature compared to gas additions and concentrations in PAR-demo3.

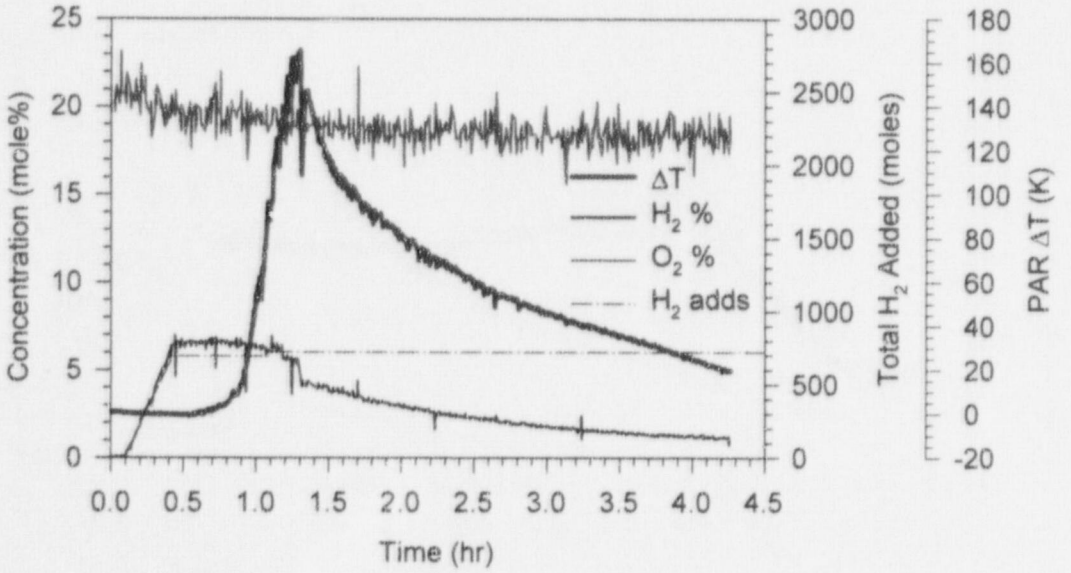

Figure 214. PAR ΔT temperature compared to gas additions and concentrations in PAR-demo3.

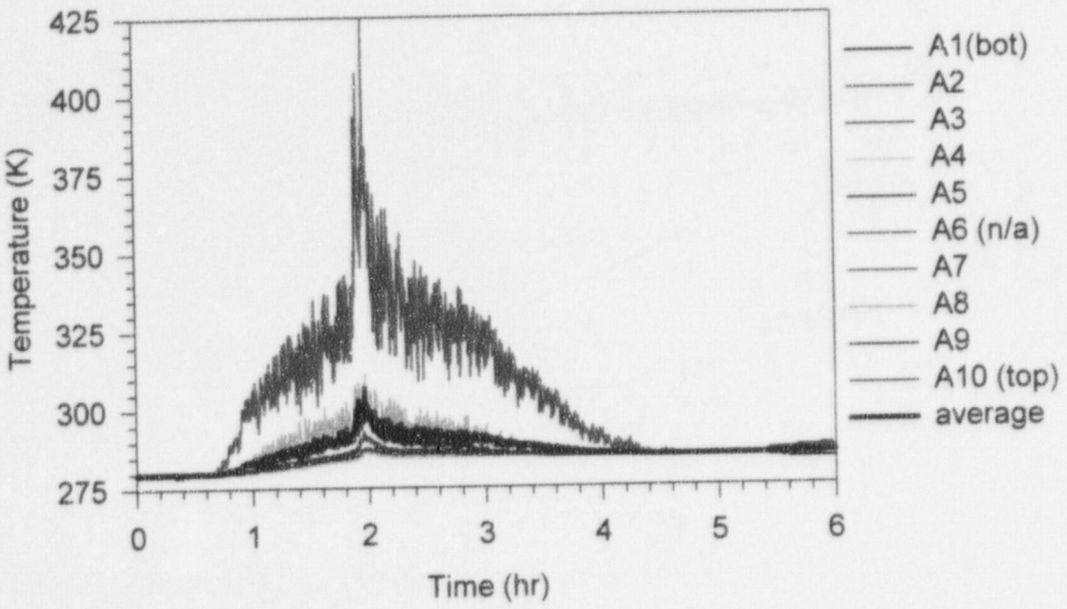

Figure 215. Surtsey vessel centerline gas temperatures from TC array A in PAR-14.

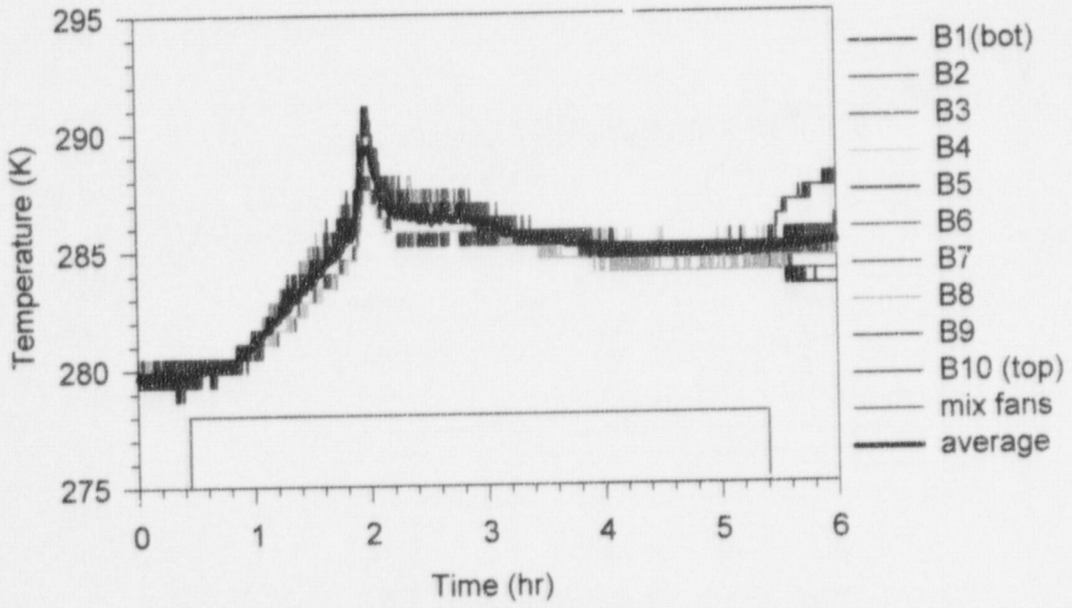

Figure 216. Surtsey vessel wall gas temperatures from TC array B in PAR-14.

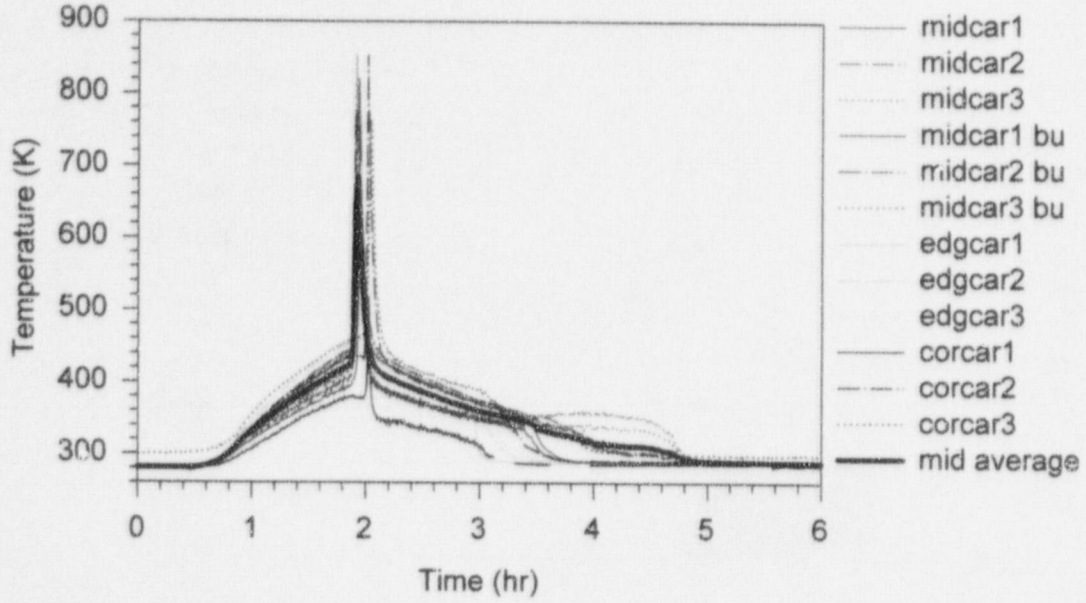

Figure 217. Catalyst cartridge temperatures in PAR-14.

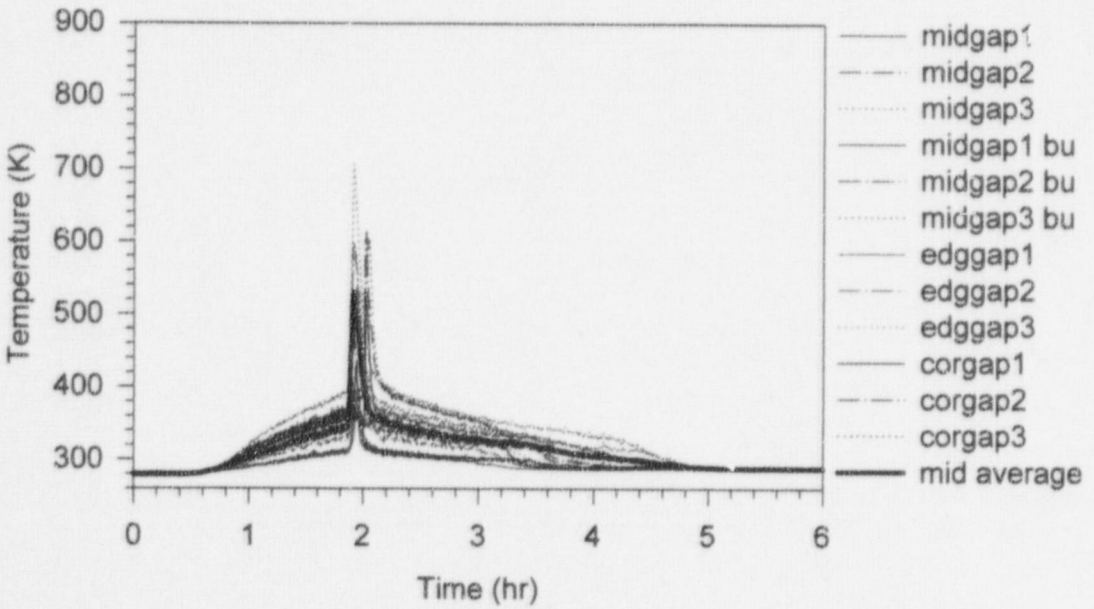

Figure 218. Catalyst gap temperatures in PAR-14.

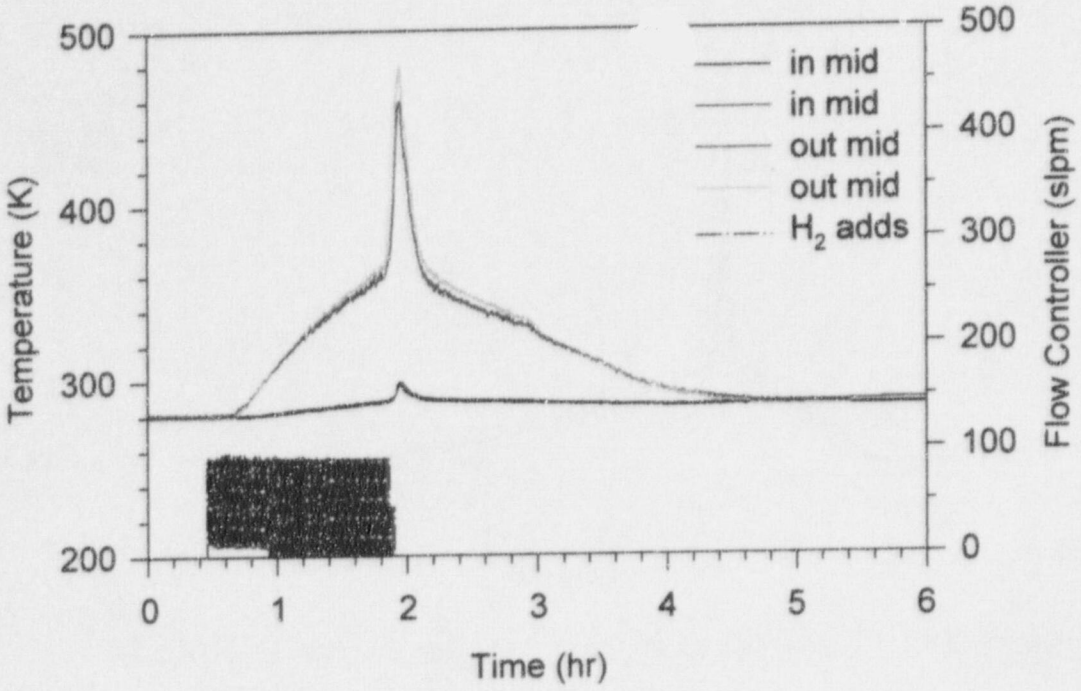

Figure 219. Inlet and outlet temperatures in PAR-14.

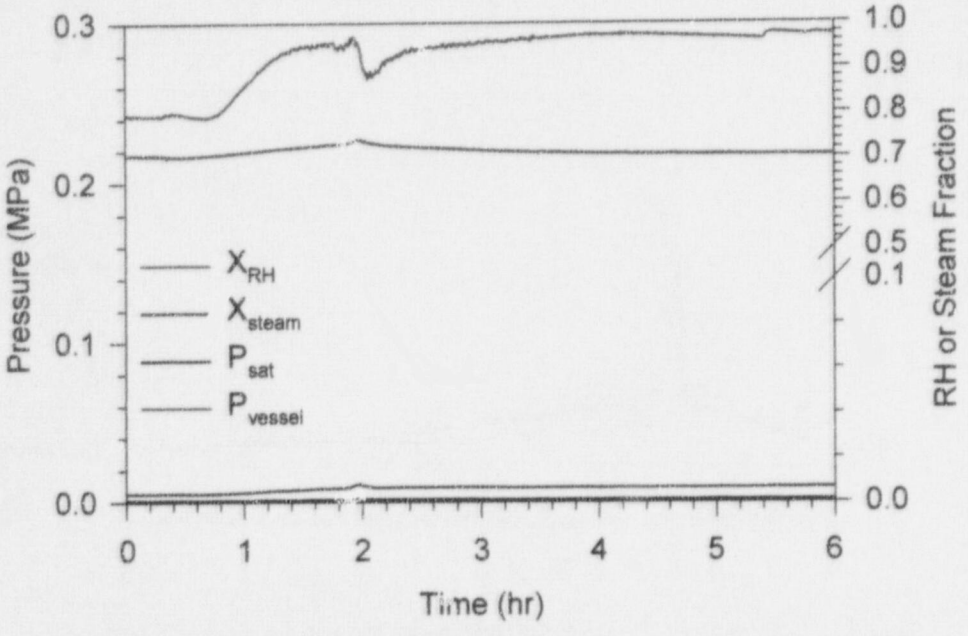

Figure 220. Saturation pressure, vessel pressure, relative humidity, and steam fraction in PAR-14.

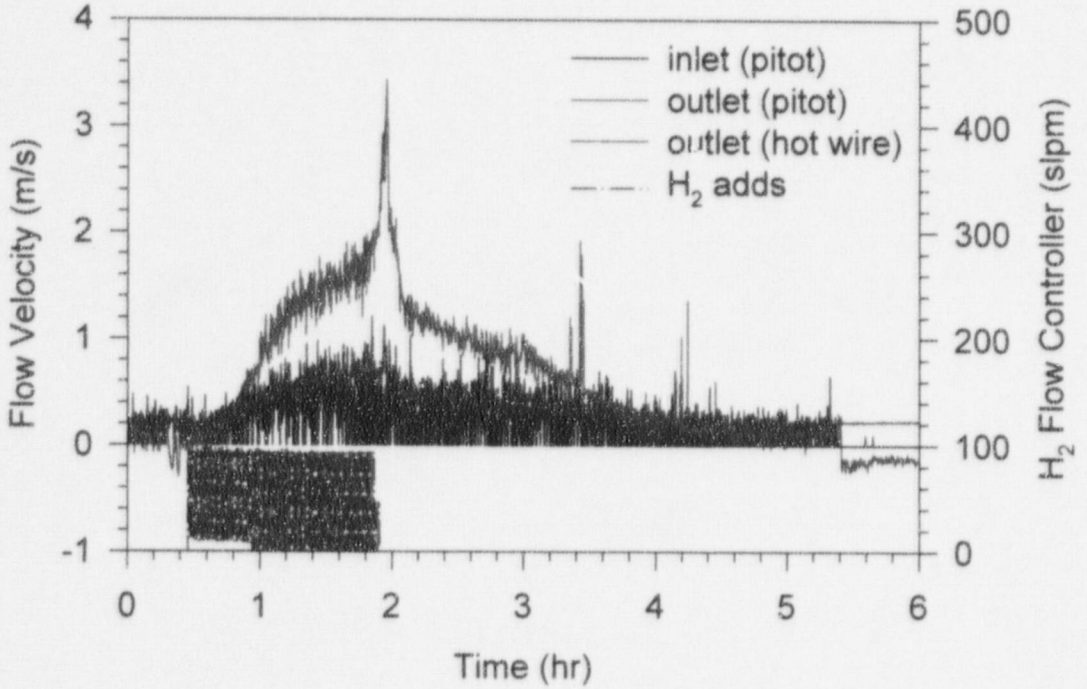

Figure 221. PAR gas velocity in PAR-14.

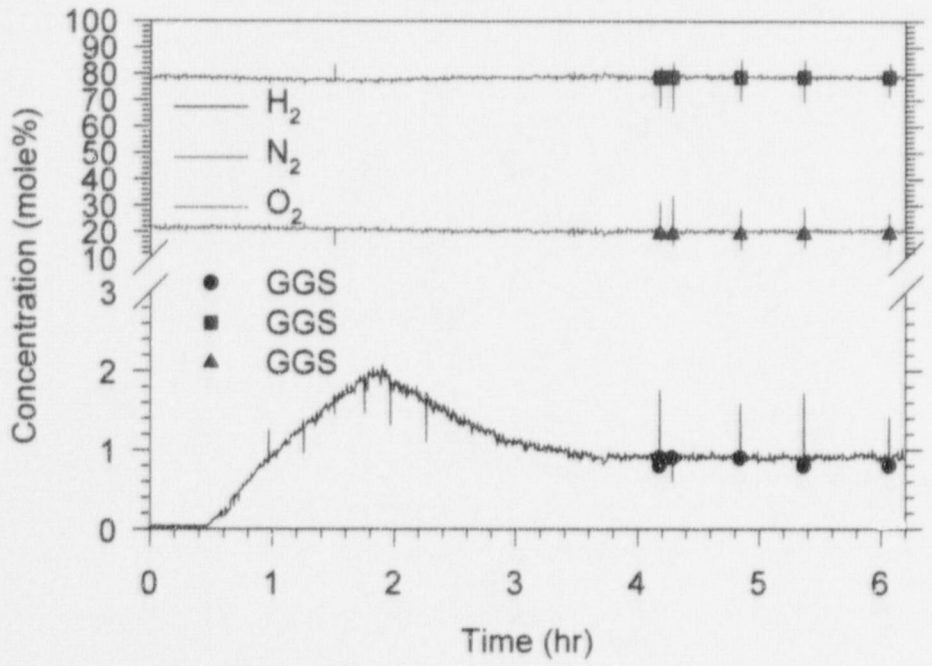

Figure 222. Gas concentrations (dry-basis) in PAR-14.

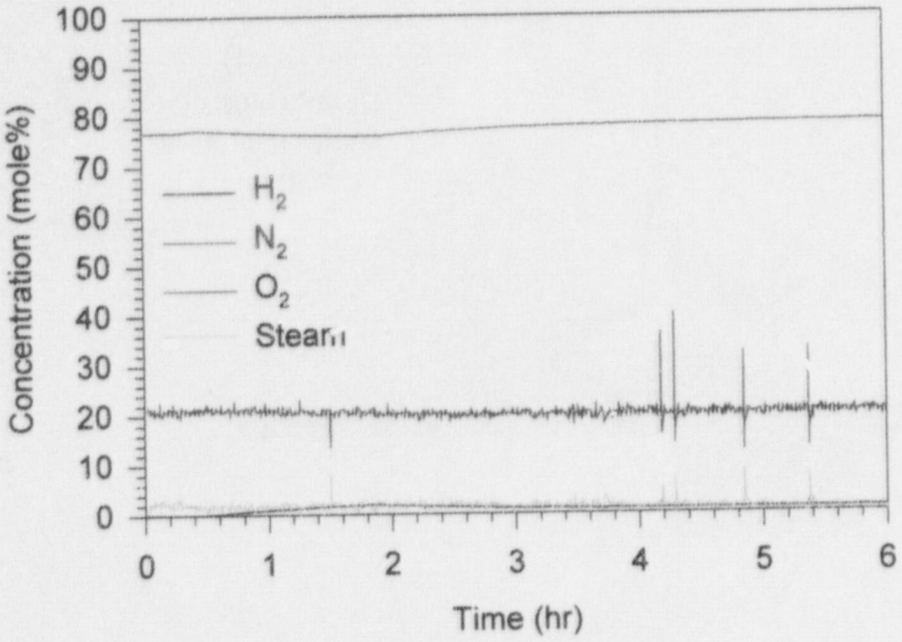

Figure 223. Gas concentrations (wet-basis) in PAR-14.

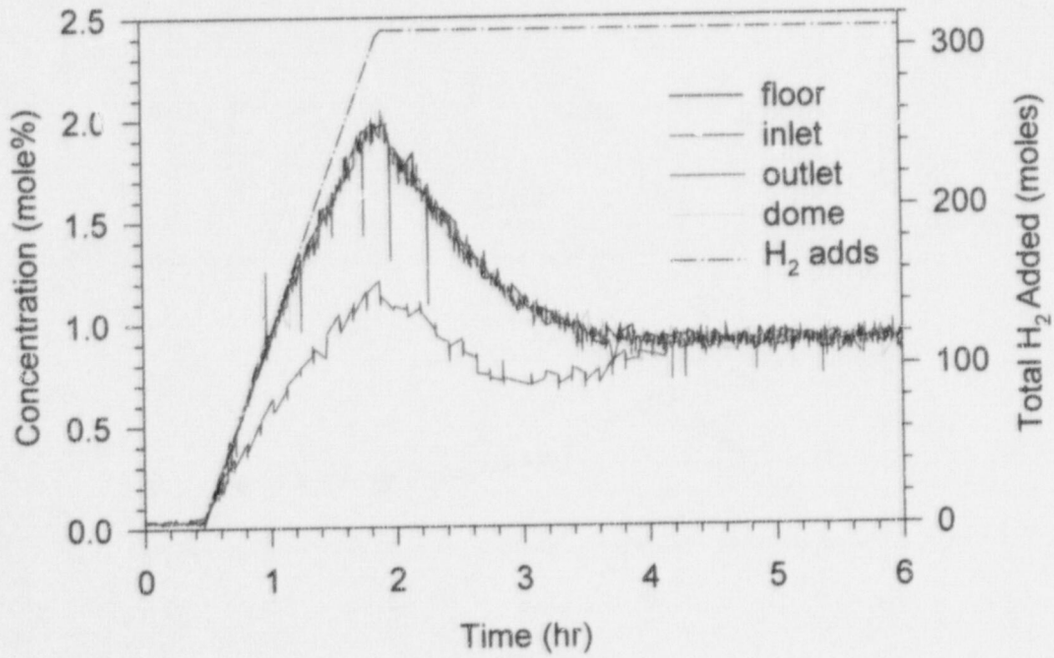

Figure 224. H_2 concentrations (wet-basis) in PAR-14.

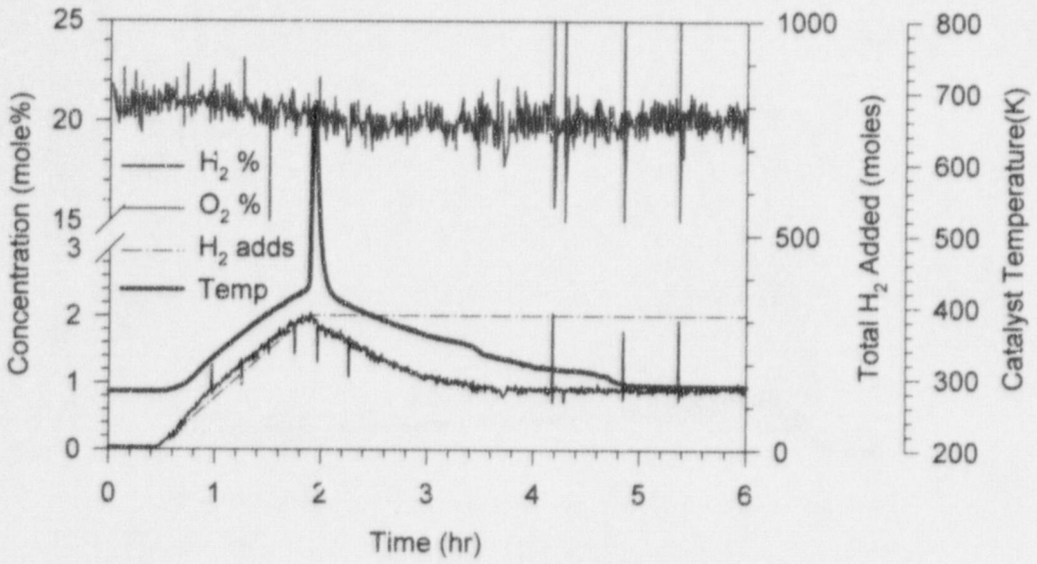

Figure 225. Catalyst temperature compared to gas additions and concentrations in PAR-14.

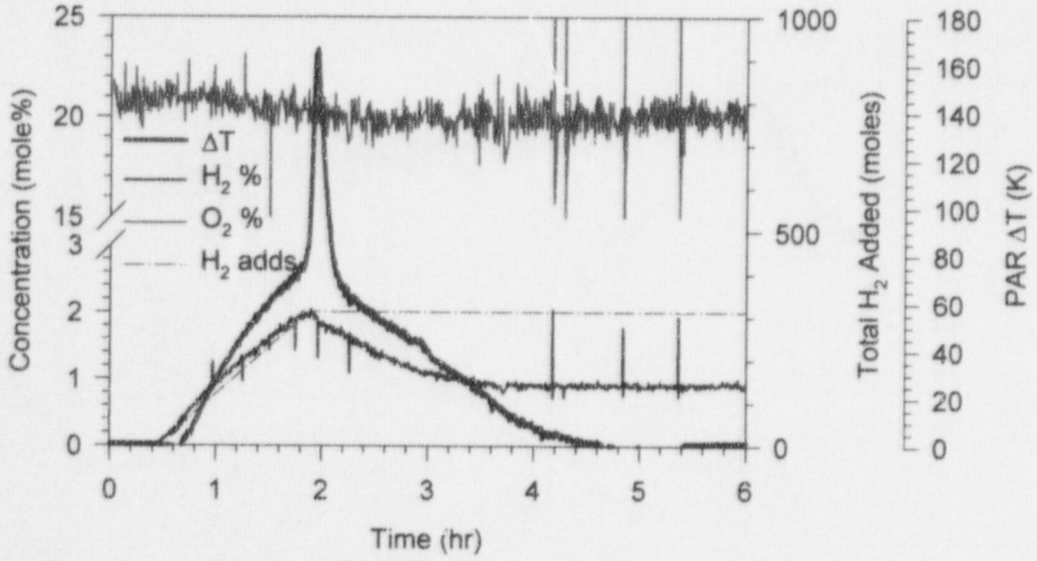

Figure 226. PAR ΔT temperature compared to gas additions and concentrations in PAR-14.

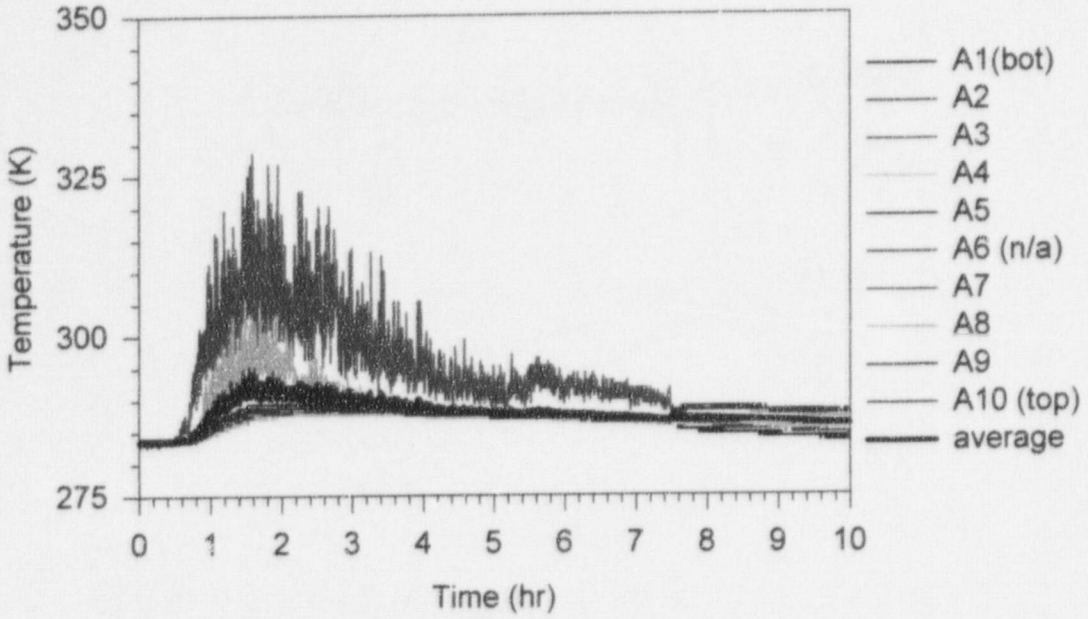

Figure 227. Surtsey vessel centerline gas temperatures from TC array A in PAR-15.

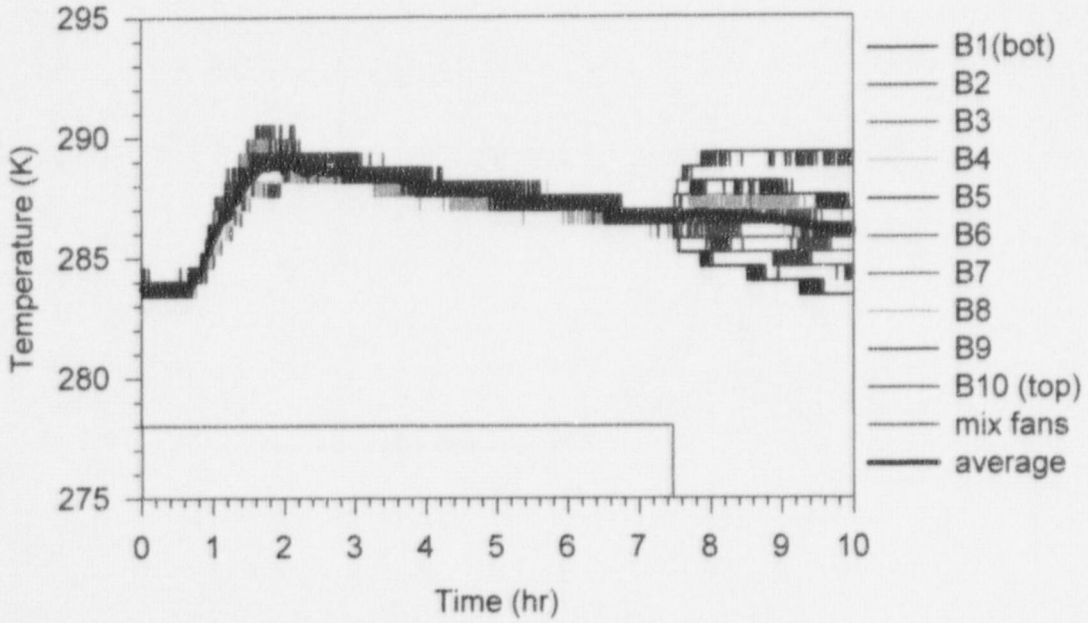

Figure 228. Surtsey vessel wall gas temperatures from TC array B in PAR-15.

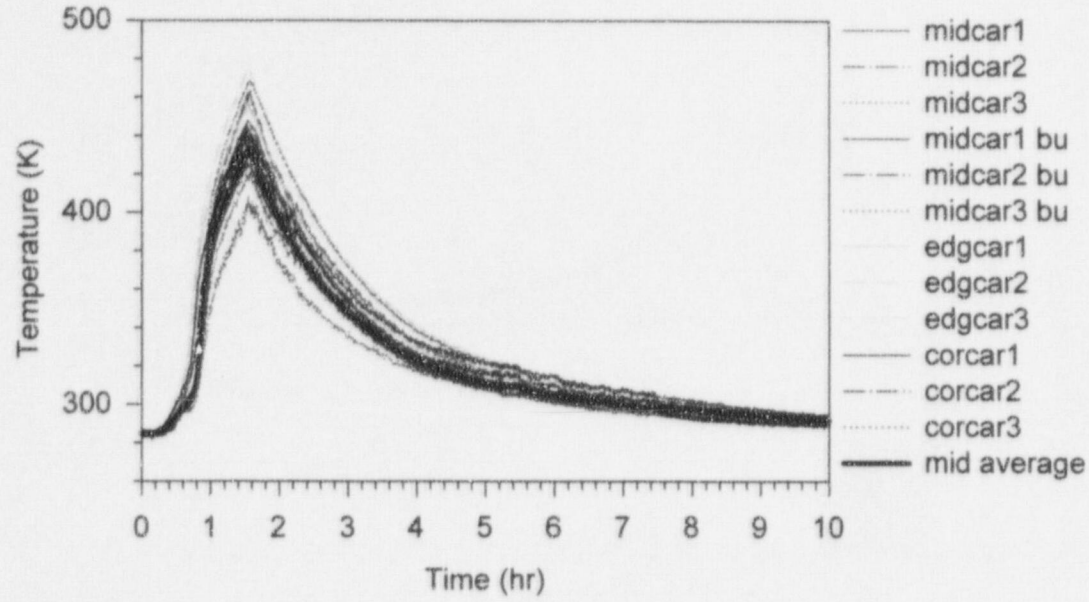

Figure 229. Catalyst cartridge temperatures in PAR-15.

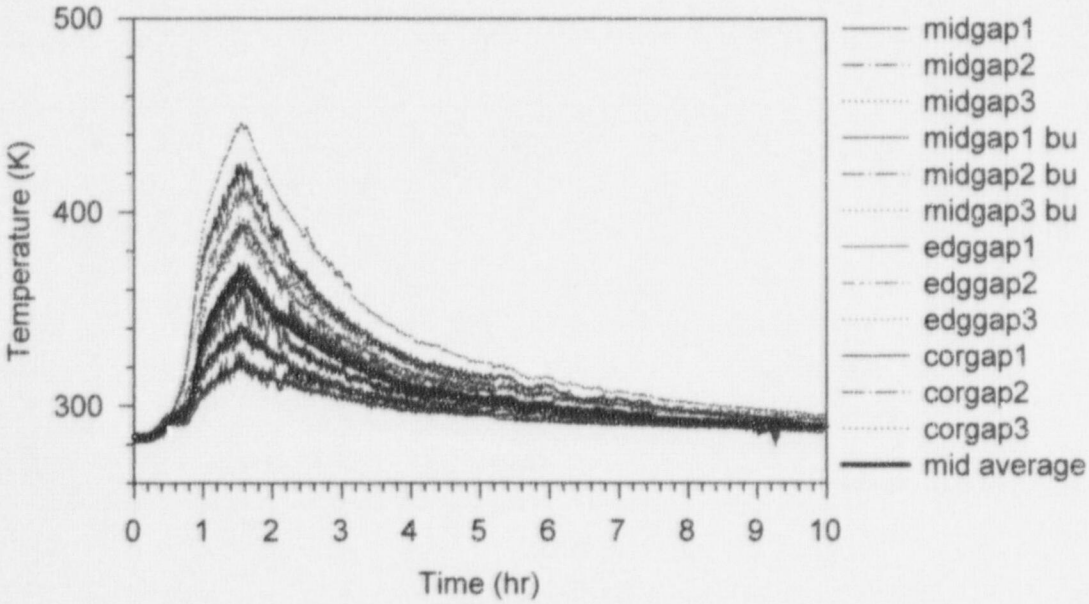

Figure 230. Catalyst gap temperatures in PAR-15.

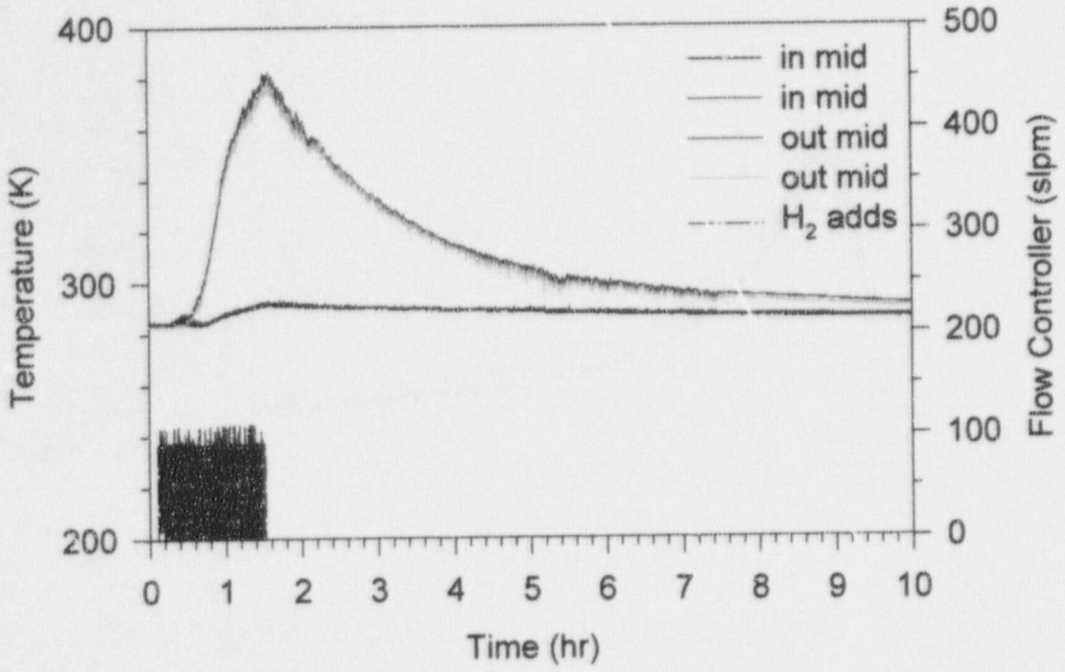

Figure 231. Inlet and outlet temperatures in PAR-15.

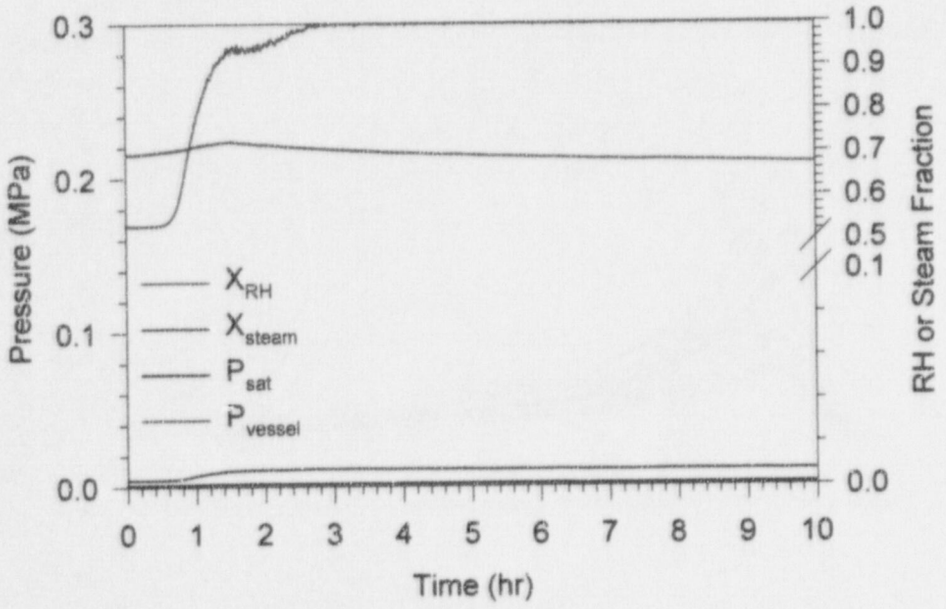

Figure 232. Saturation pressure, vessel pressure, relative humidity, and steam fraction in PAR-15.

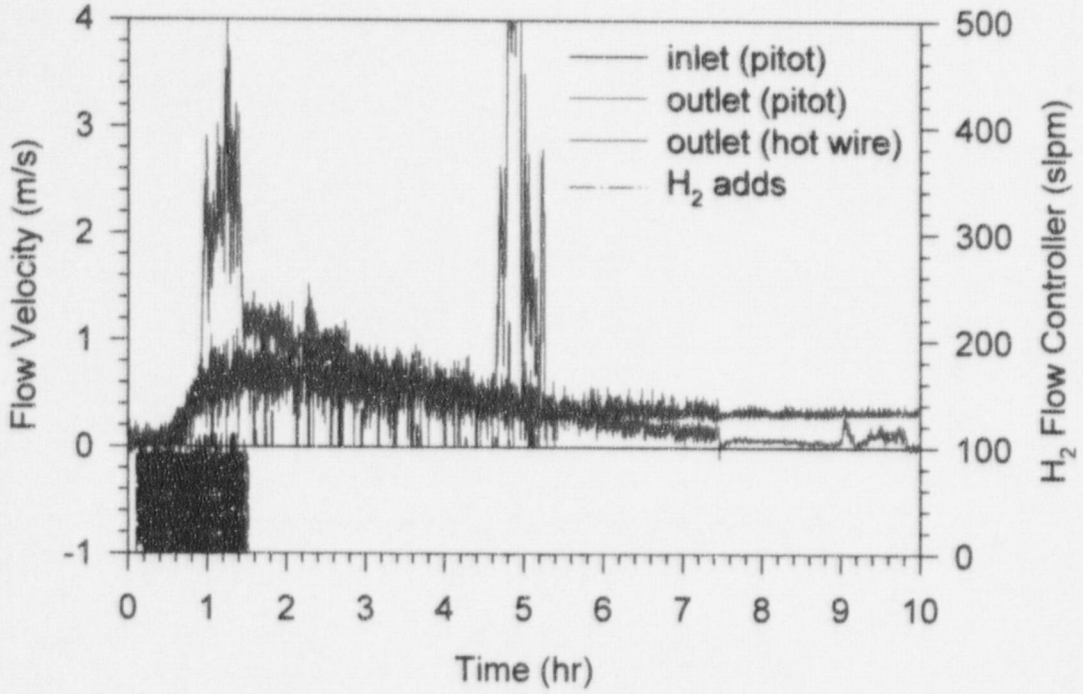

Figure 233. PAR gas velocity in PAR-15.

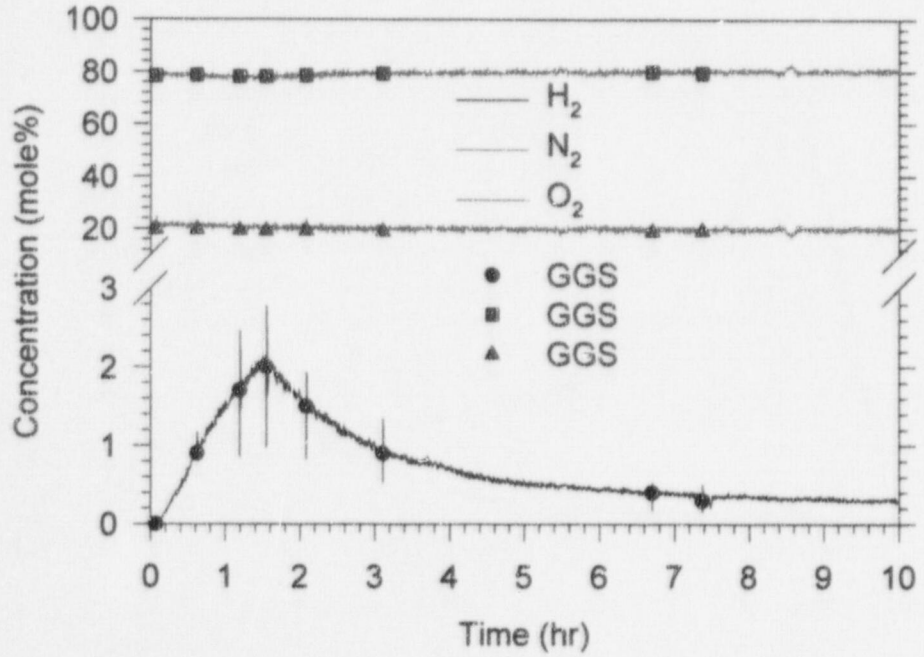

Figure 234. Gas concentrations (dry-basis) in PAR-15.

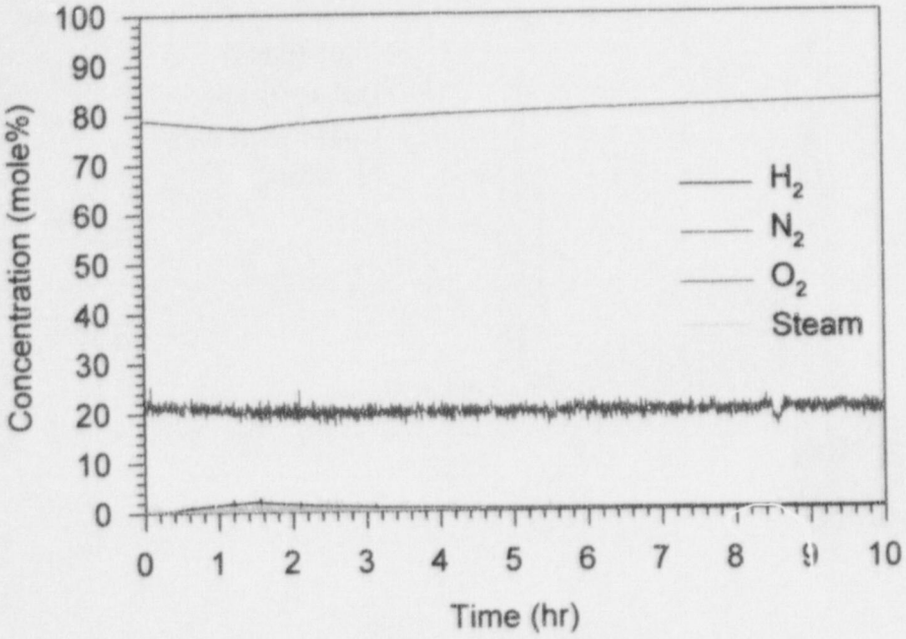

Figure 235. Gas concentrations (wet-basis) in PAR-15.

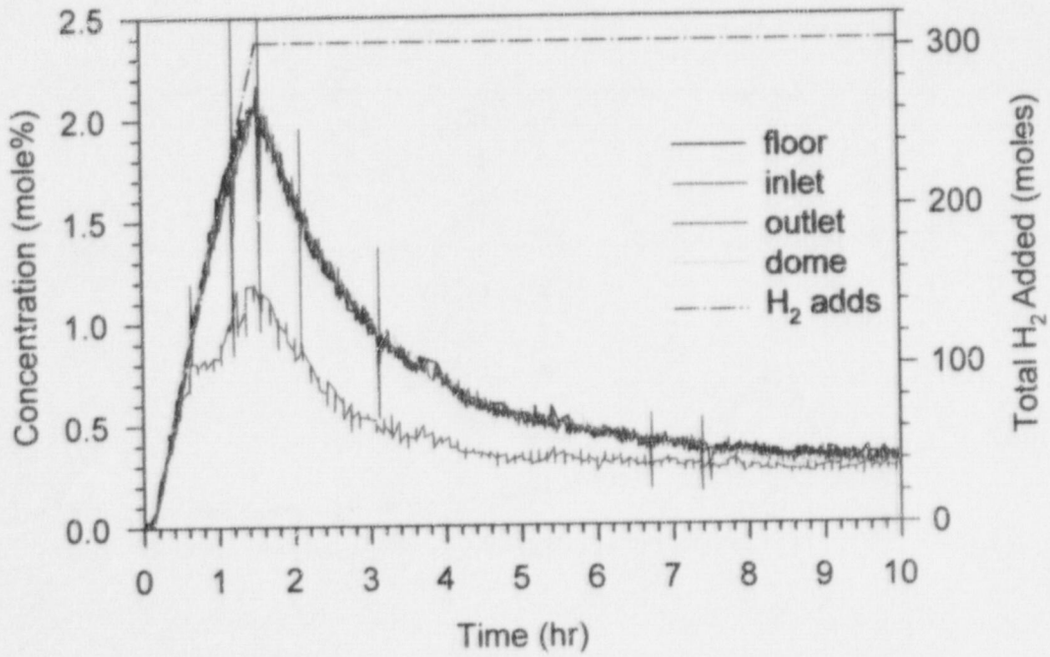

Figure 236. H_2 concentrations (wet-basis) in PAR-15.

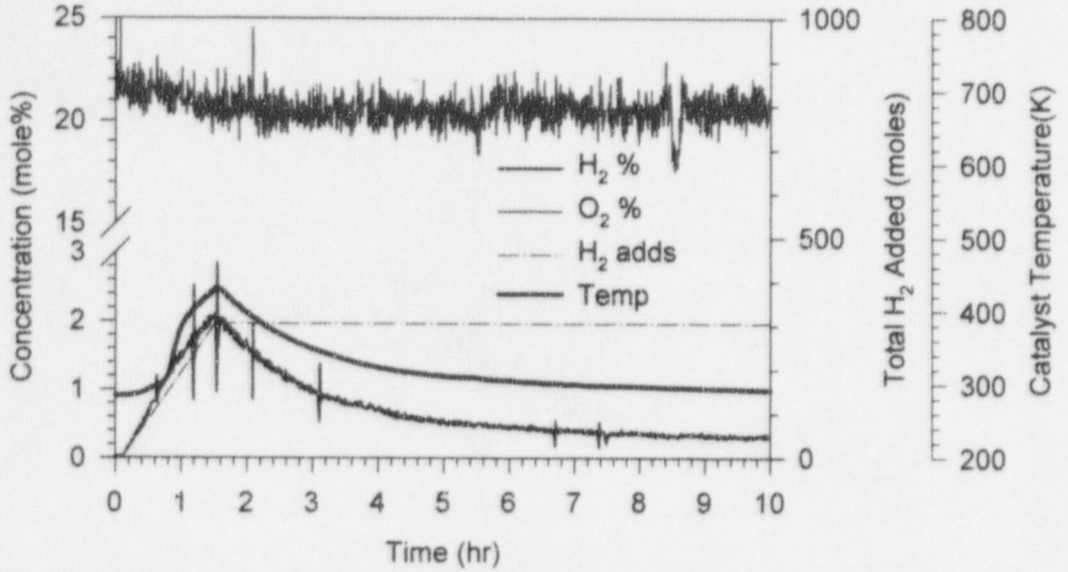

Figure 237. Catalyst temperature compared to gas additions and concentrations in PAR-15.

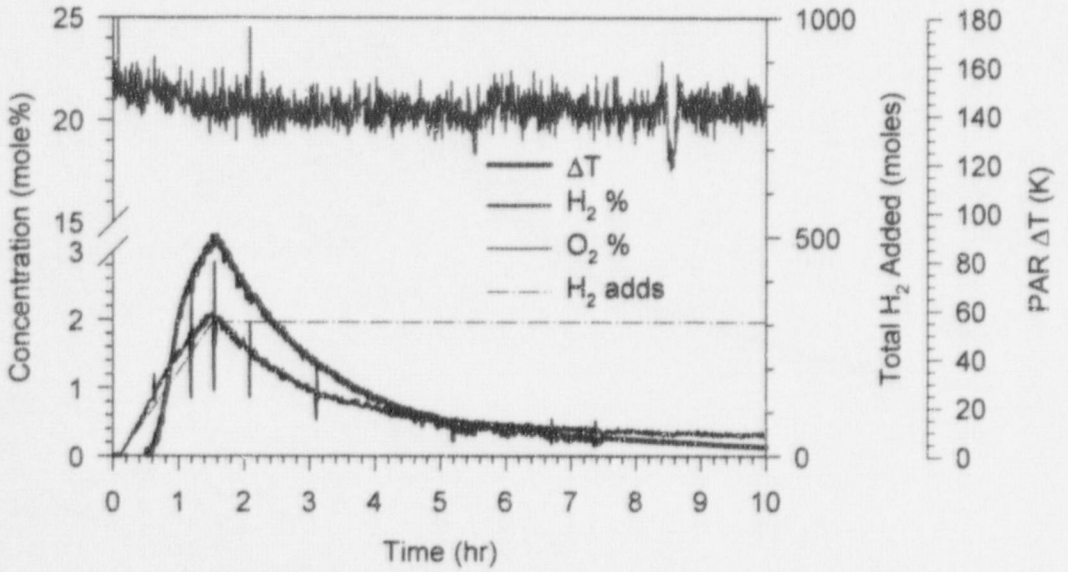

Figure 238. PAR ΔT temperature compared to gas additions and concentrations in PAR-15.

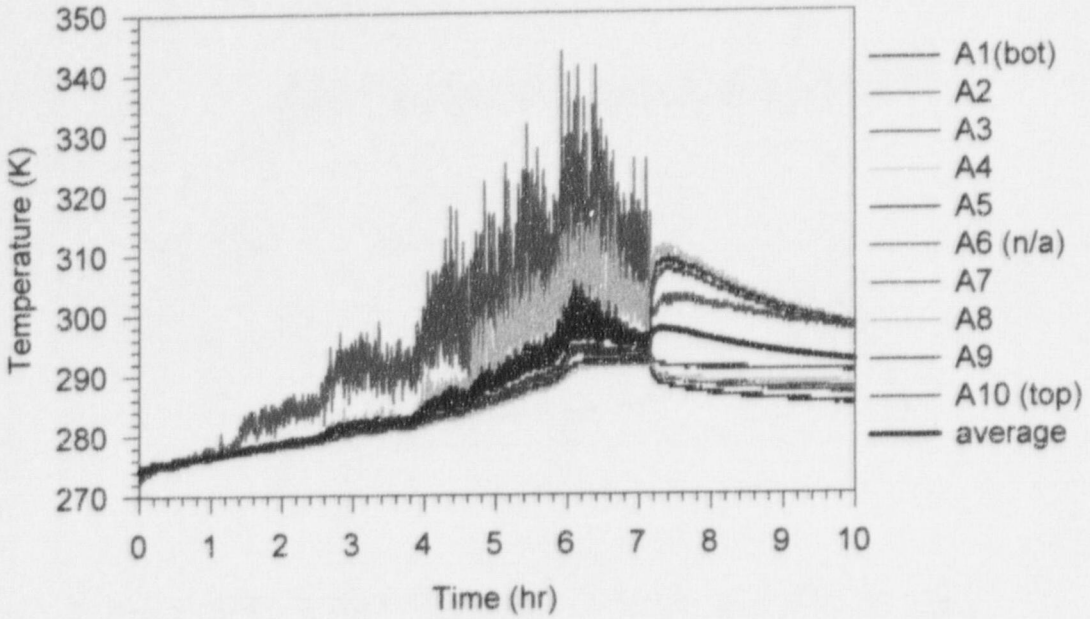

Figure 239. Surtsey vessel centerline gas temperatures from TC array A in PAR-16.

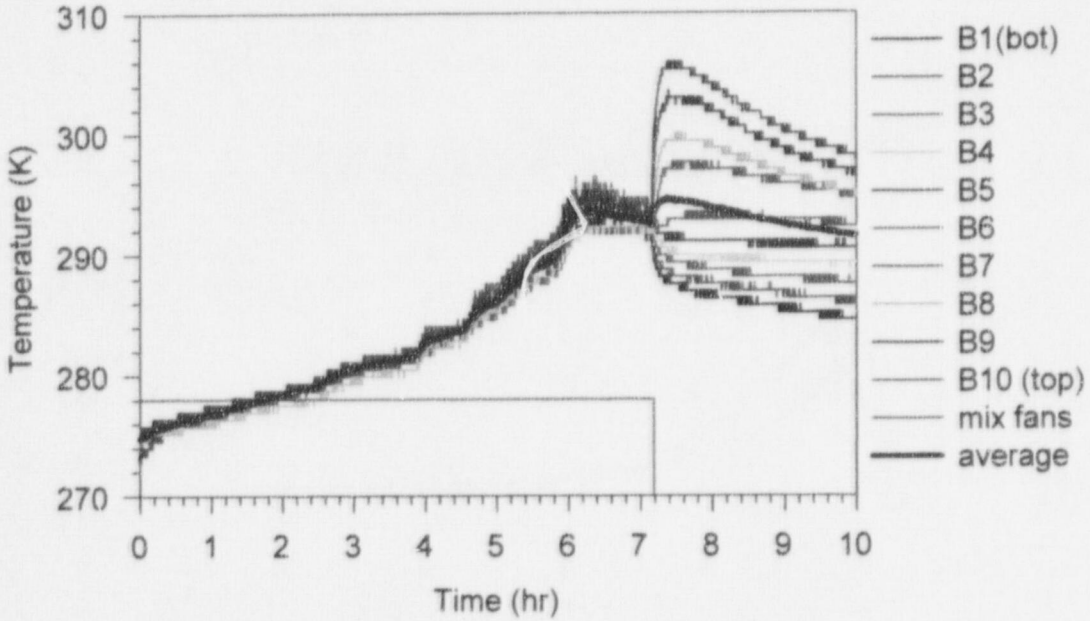

Figure 240. Surtsey vessel wall gas temperatures from TC array B in PAR-16.

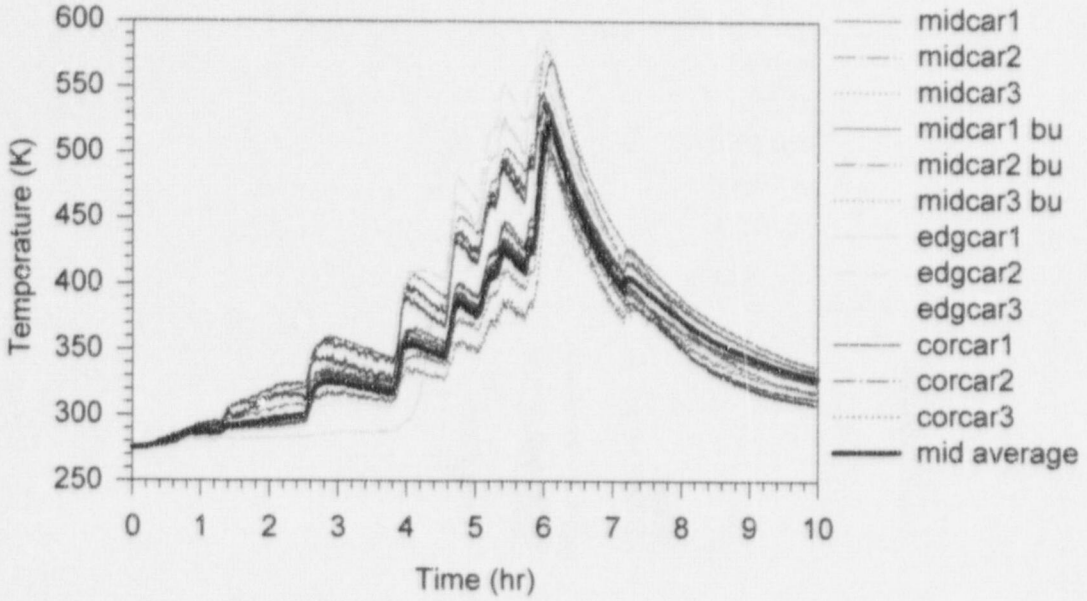

Figure 241. Catalyst cartridge temperatures in PAR-16.

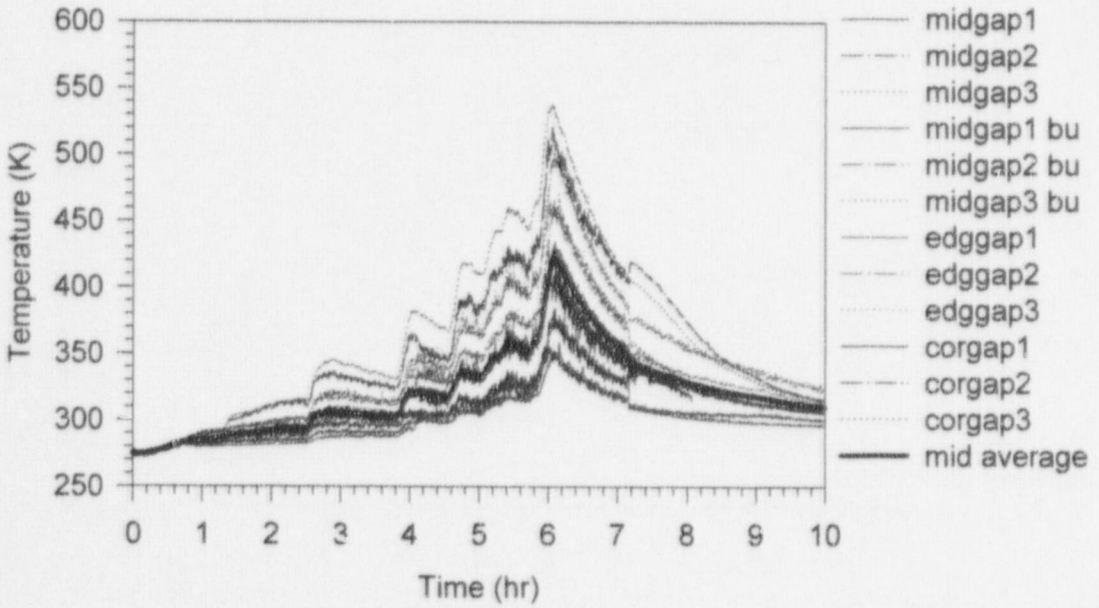

Figure 242. Catalyst gap temperatures in PAR-16.

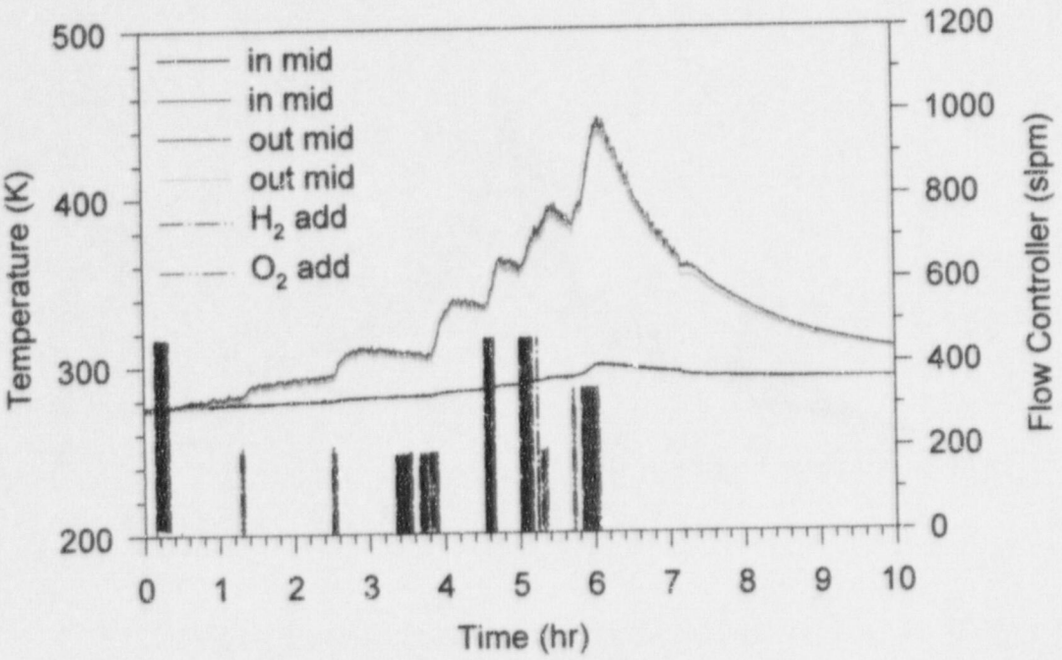

Figure 243. Inlet and outlet temperatures in PAR-16.

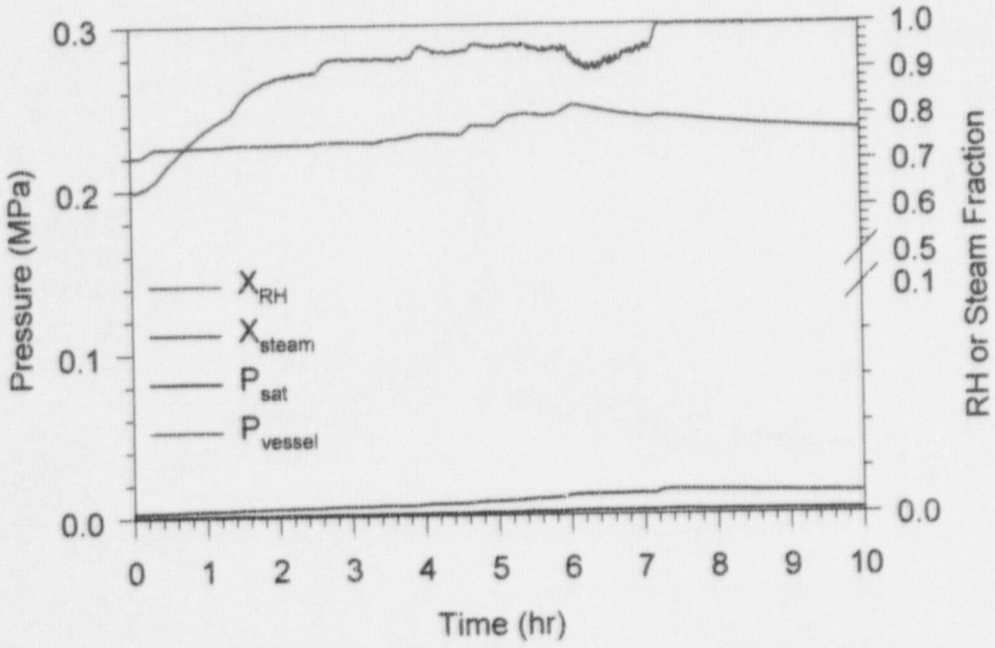

Figure 244. Saturation pressure, vessel pressure, relative humidity, and steam fraction in PAR-16.

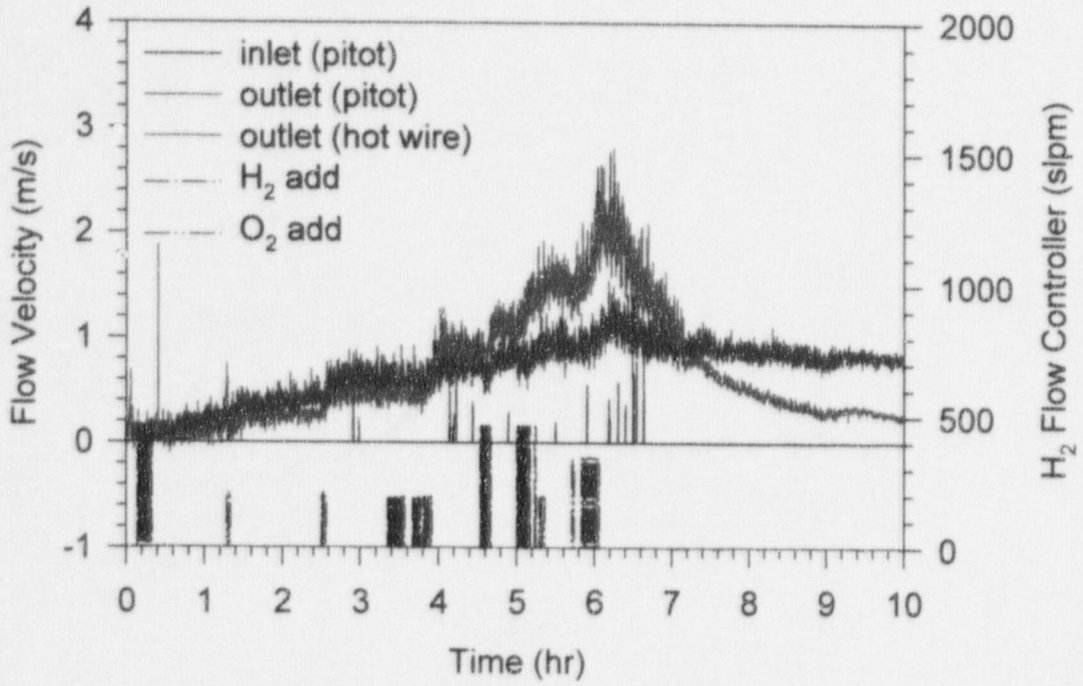

Figure 245. PAR gas velocity in PAR-16.

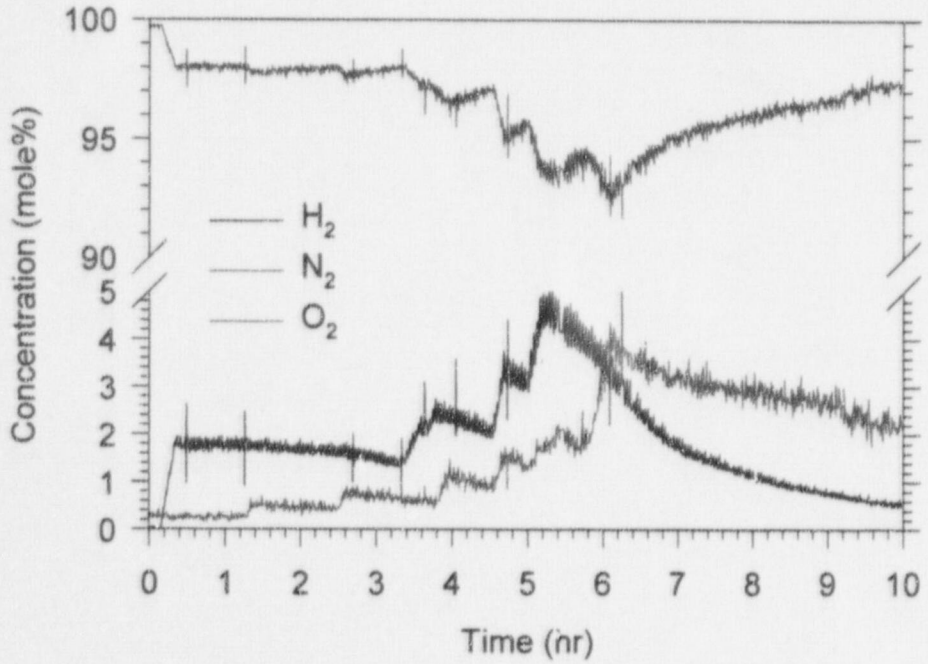

Figure 246. Gas concentrations (dry-basis) in PAR-16.

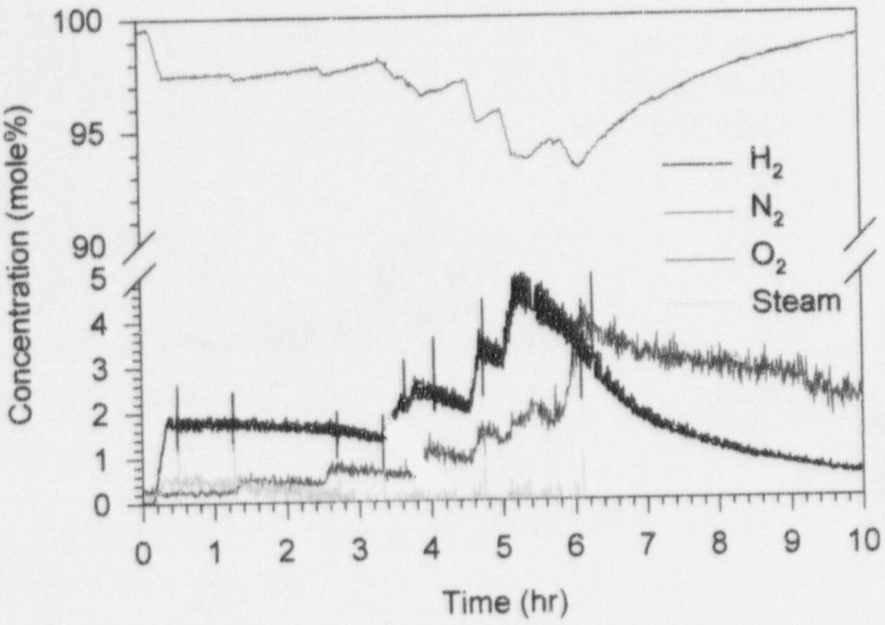

Figure 247. Gas concentrations (wet-basis) in PAR-16.

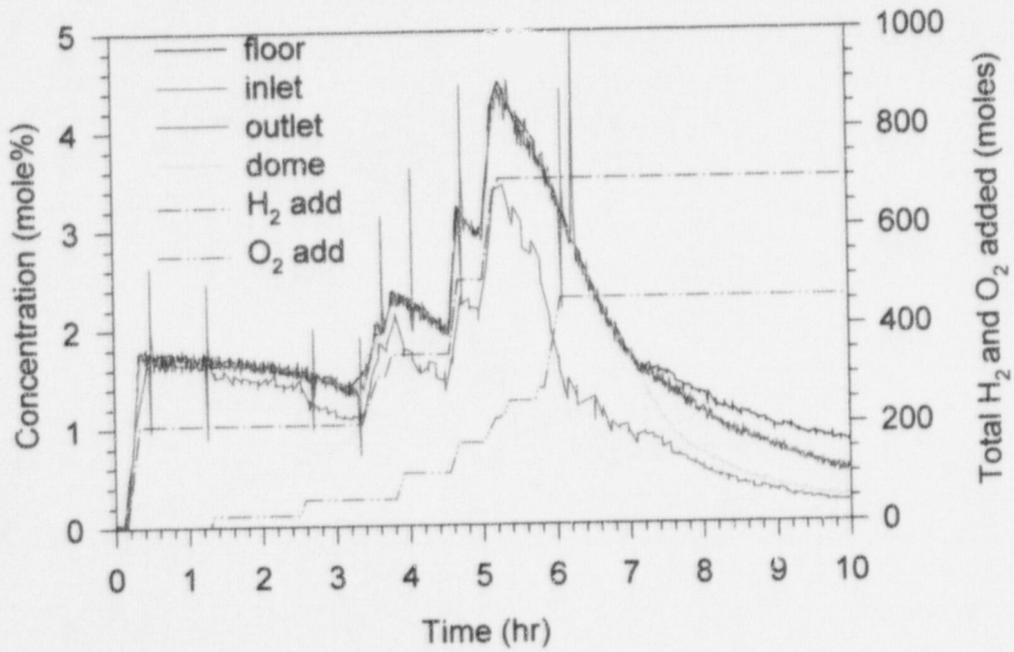

Figure 248. H_2 concentrations (wet-basis) in PAR-16.

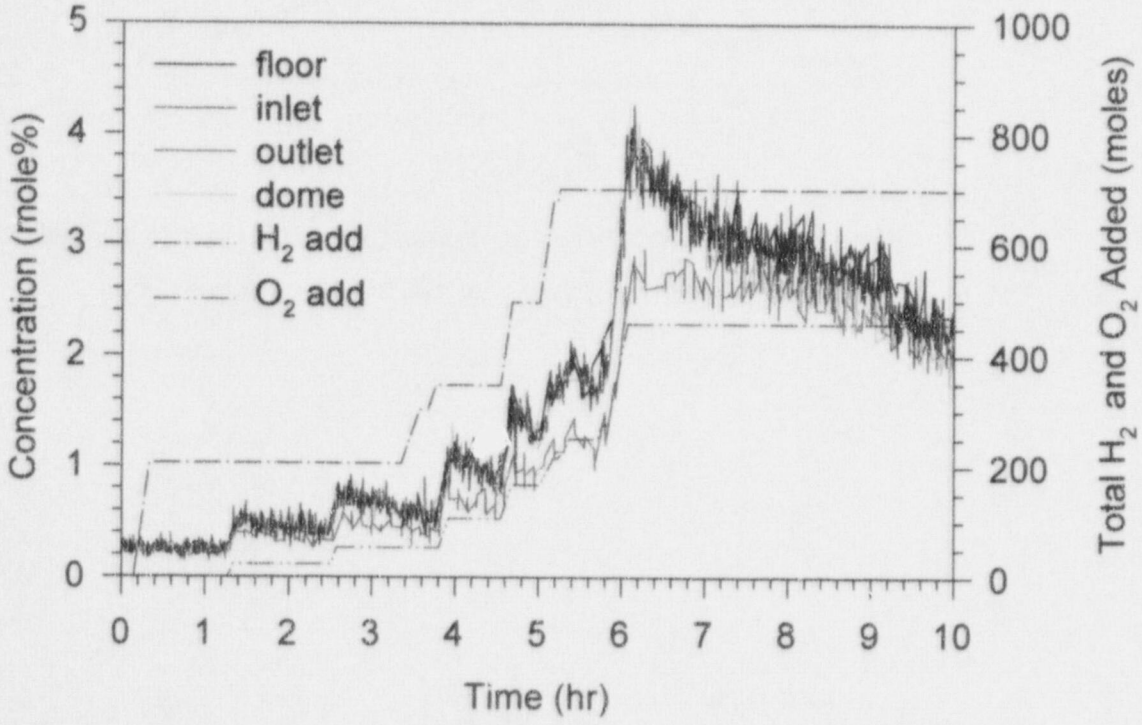

Figure 249. O_2 concentrations (wet-basis) in PAR-16.

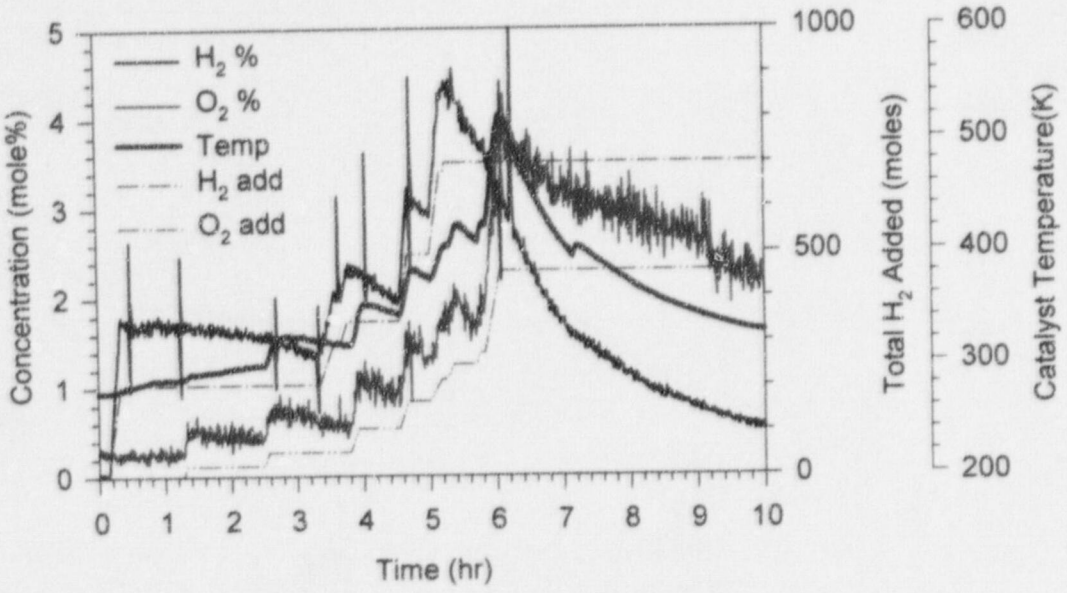

Figure 250. Catalyst temperature compared to gas additions and concentrations in PAR-16.

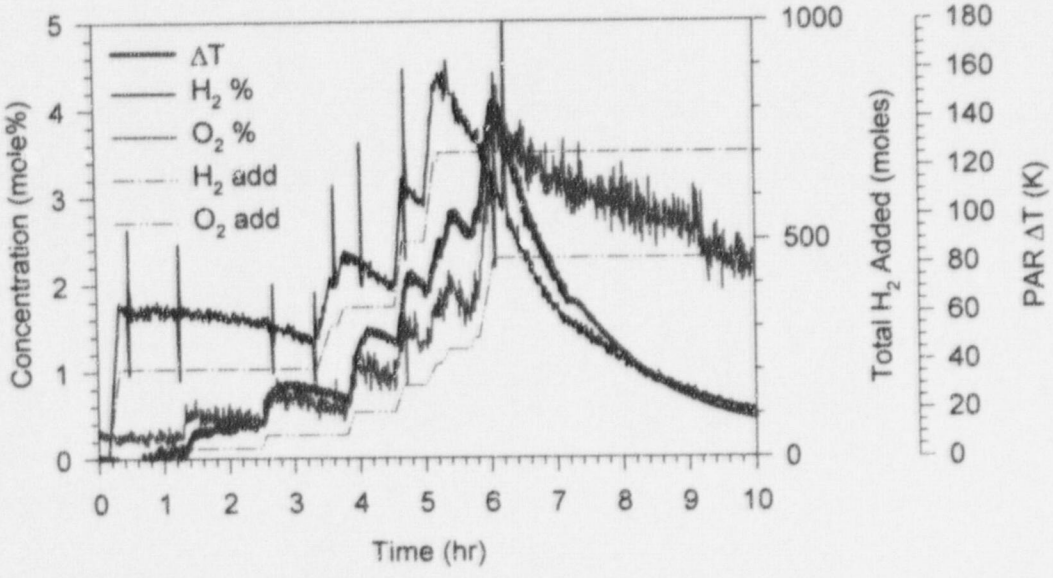

Figure 251. PAR ΔT temperature compared to gas additions and concentrations in PAR-16.

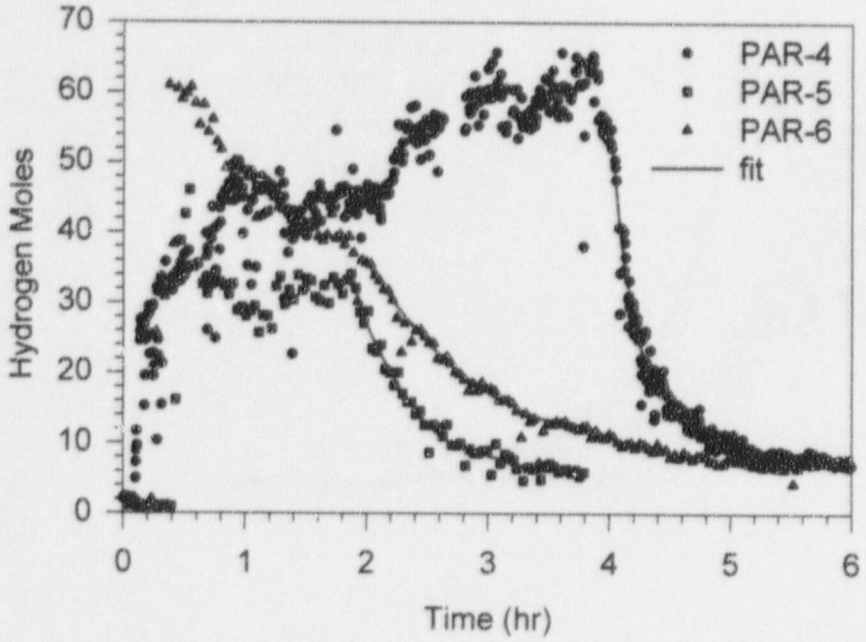

Figure 252. Hydrogen moles in Surtsey during tests with low hydrogen concentration.

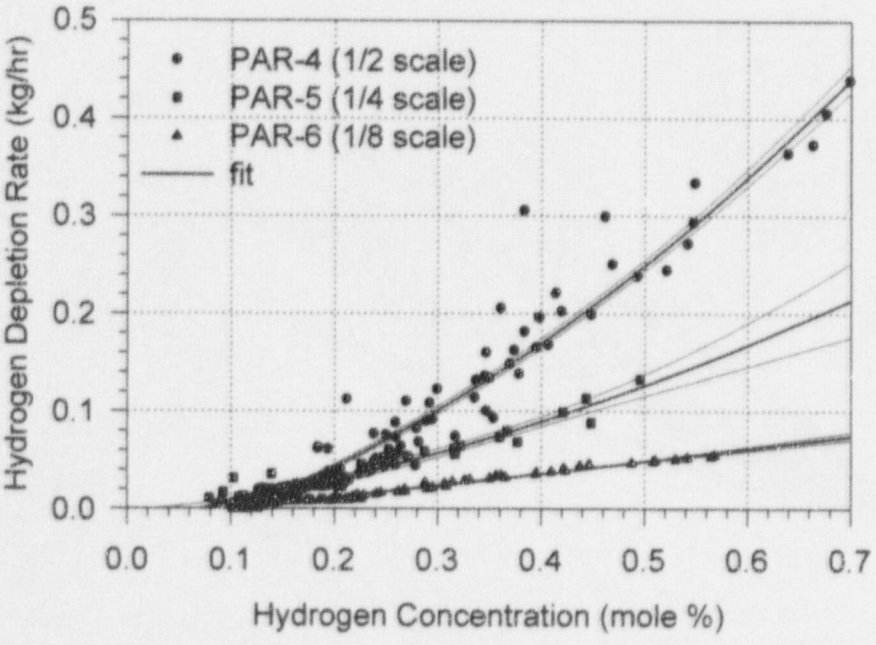

Figure 253. Hydrogen depletion rates at low hydrogen concentrations.

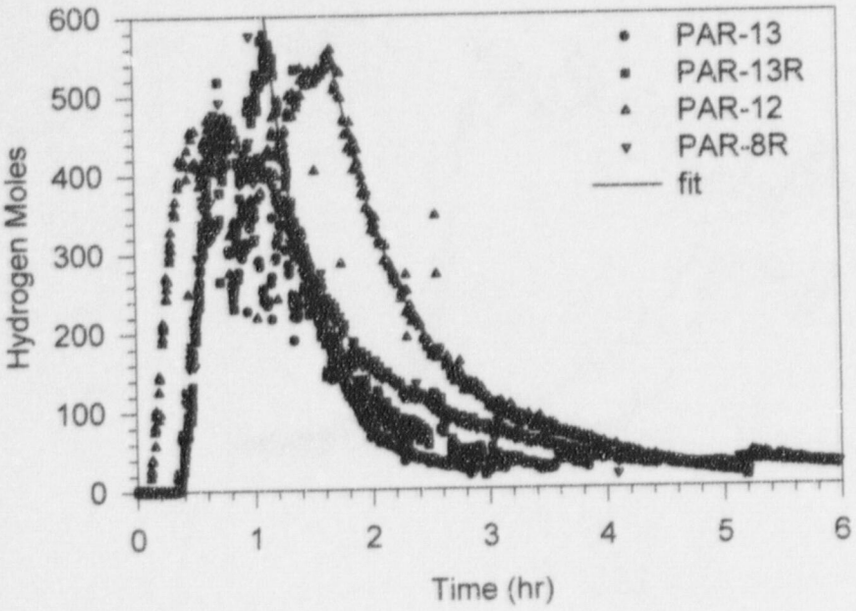

Figure 254. Hydrogen moles in Surtsey during tests with high hydrogen concentrations.

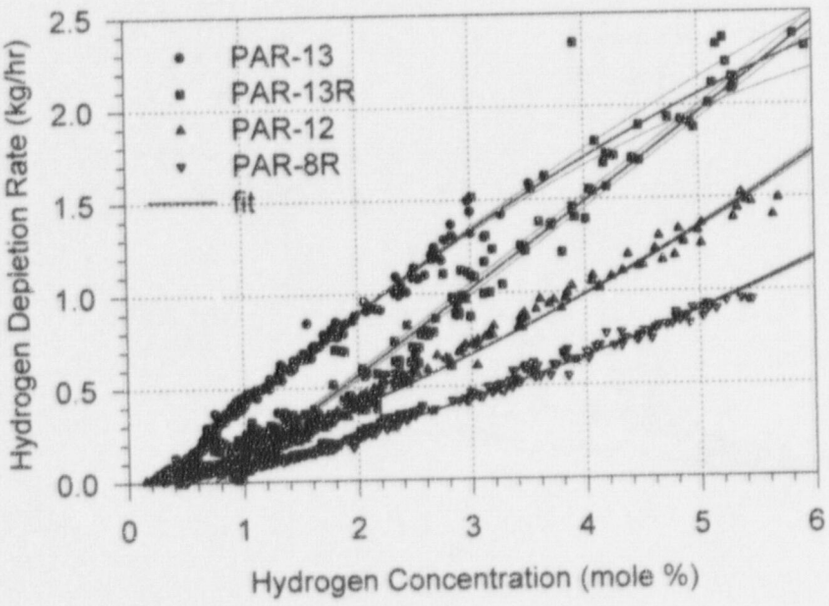

Figure 255. Hydrogen depletion rates at high hydrogen concentrations.

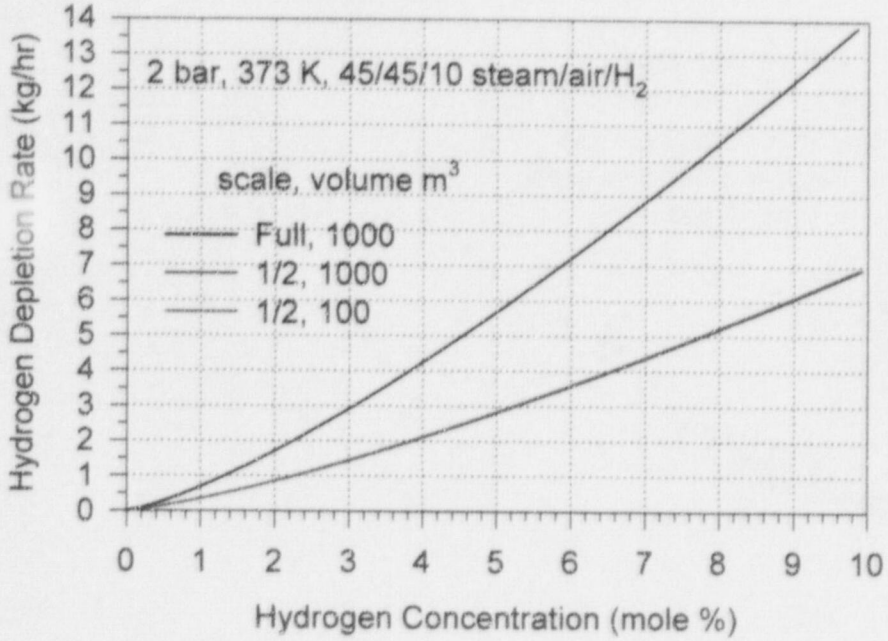

Figure 256. Predictions of hydrogen depletion rates versus hydrogen concentrations.

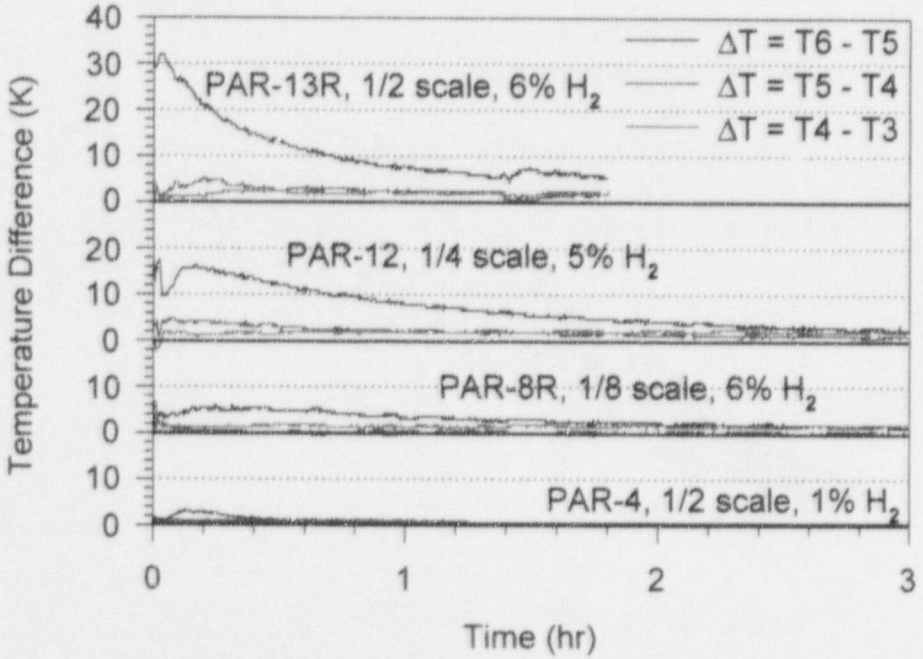

Figure 257. Temperature difference between successive array B thermocouples.

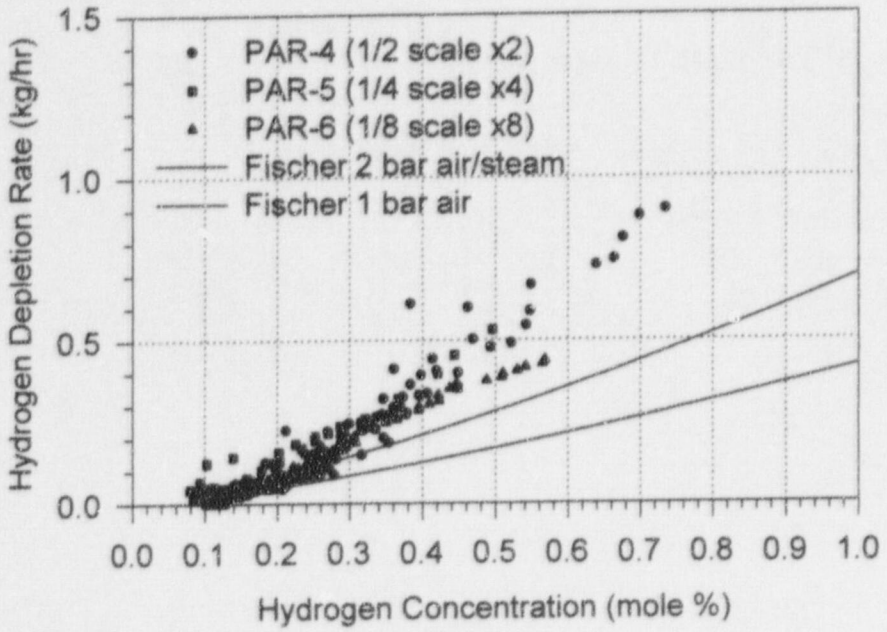

Figure 258. Normalized hydrogen depletion rates at low hydrogen concentrations.

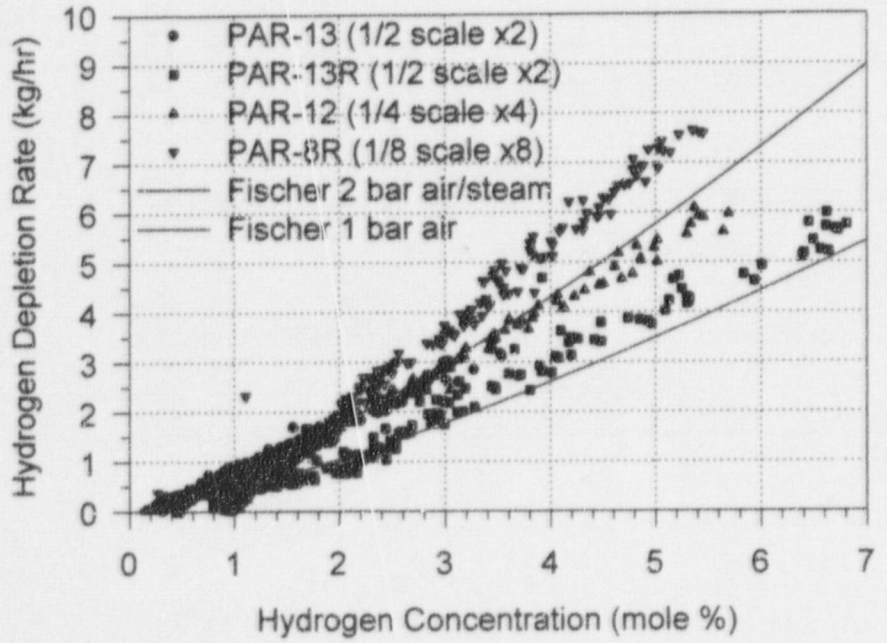

Figure 259. Normalized hydrogen depletion rates at high hydrogen concentrations.

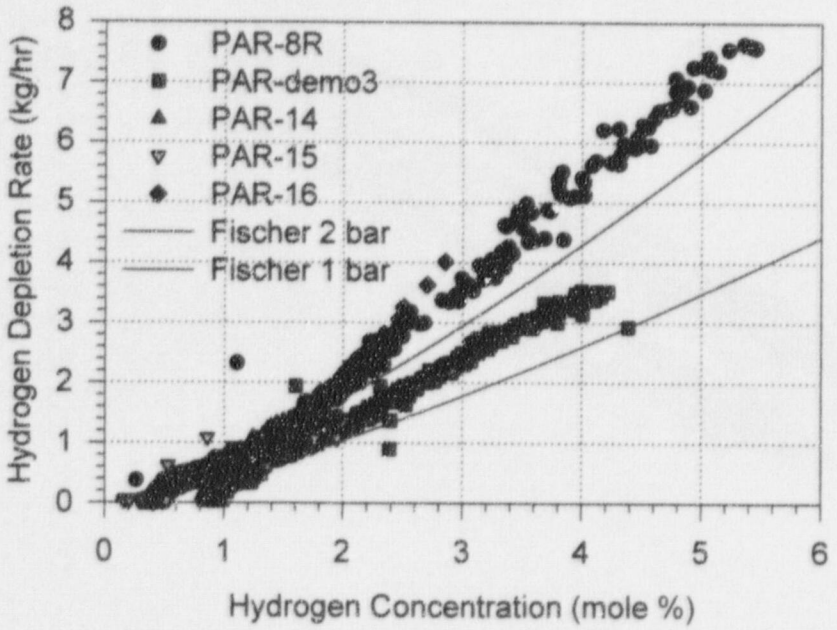

Figure 260. Normalized well-mixed hydrogen depletion rates at high hydrogen concentrations.

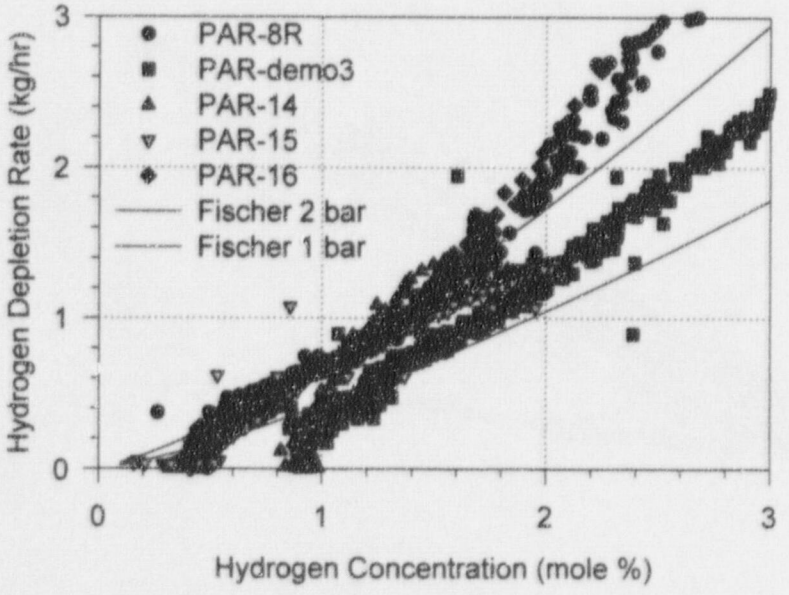

Figure 261. Normalized well-mixed hydrogen depletion rates at low hydrogen concentrations.

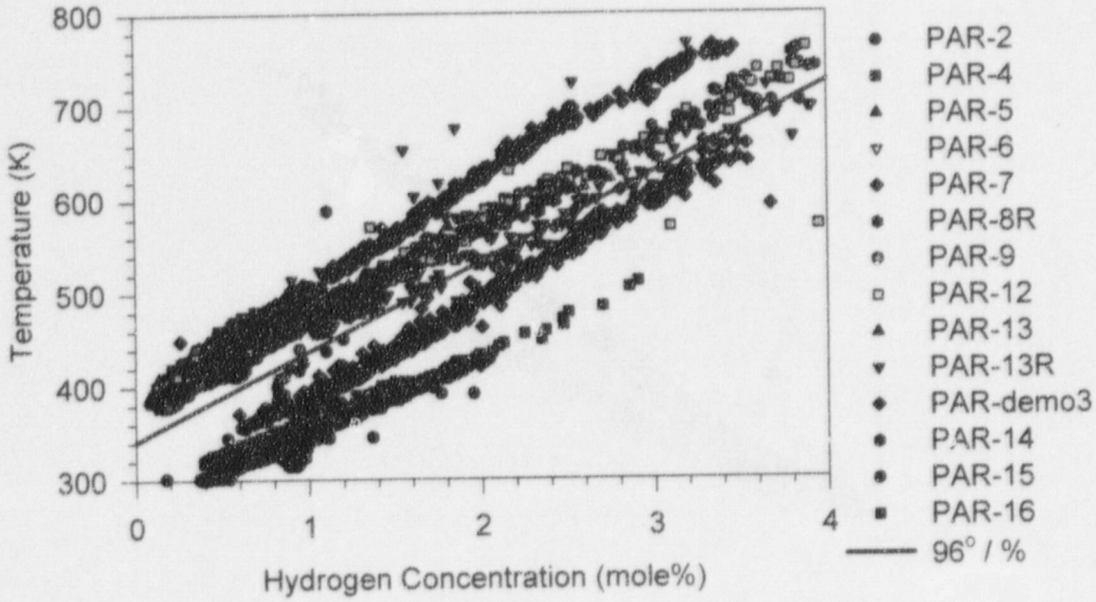

Figure 262. Cartridge temperature versus hydrogen concentration.

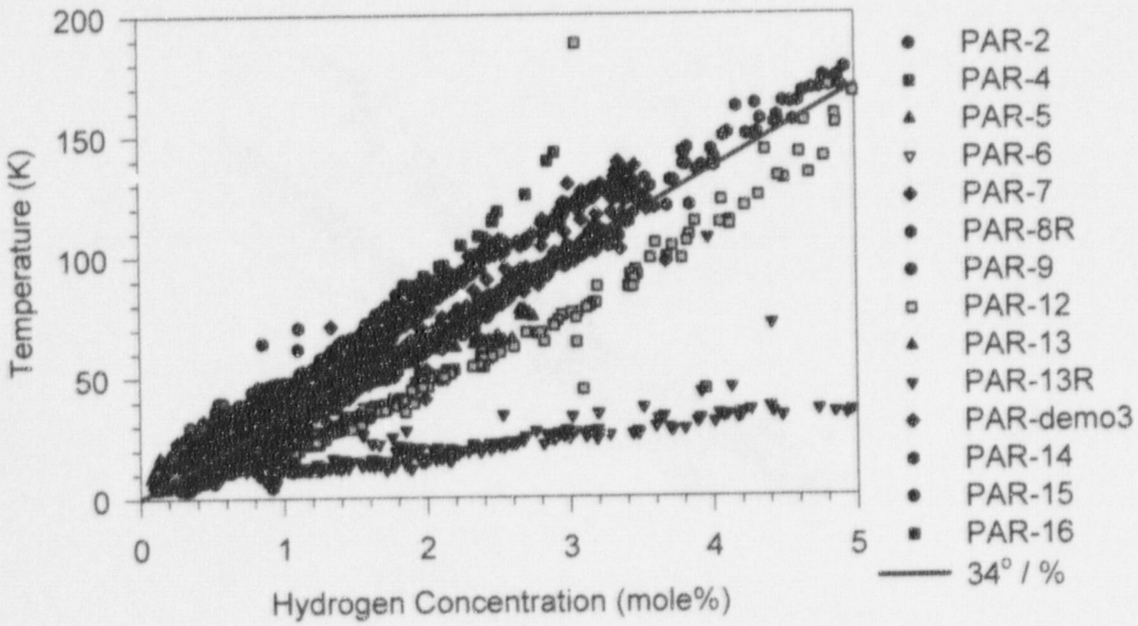

Figure 263. PAR ΔT versus hydrogen concentration.

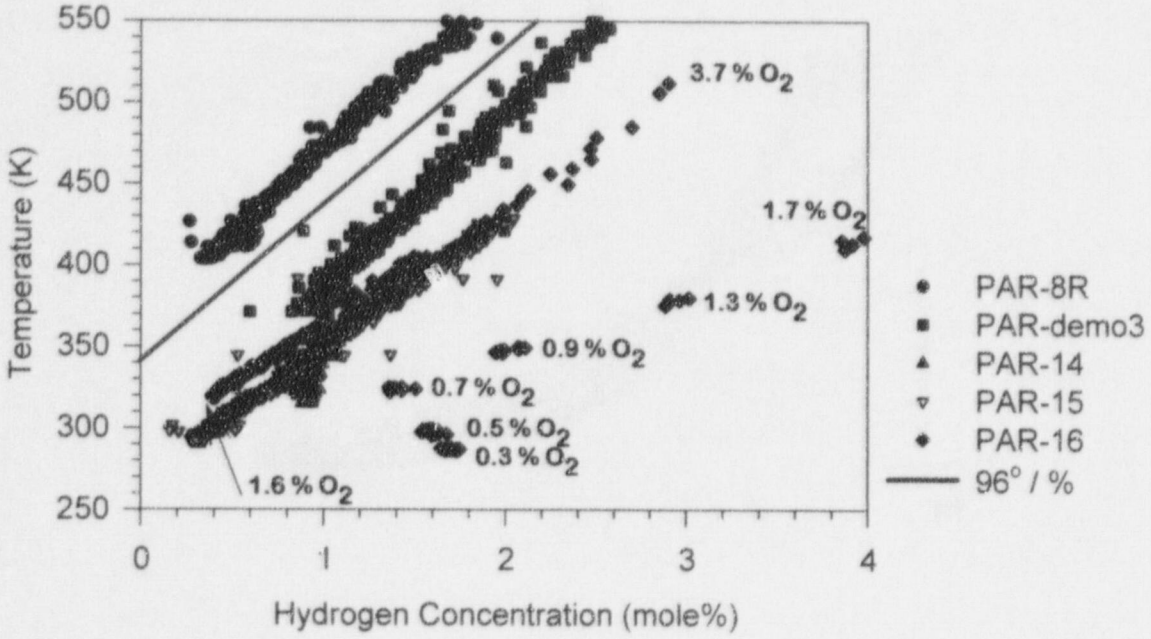

Figure 264. Cartridge temperature versus hydrogen concentration in PAR-16.

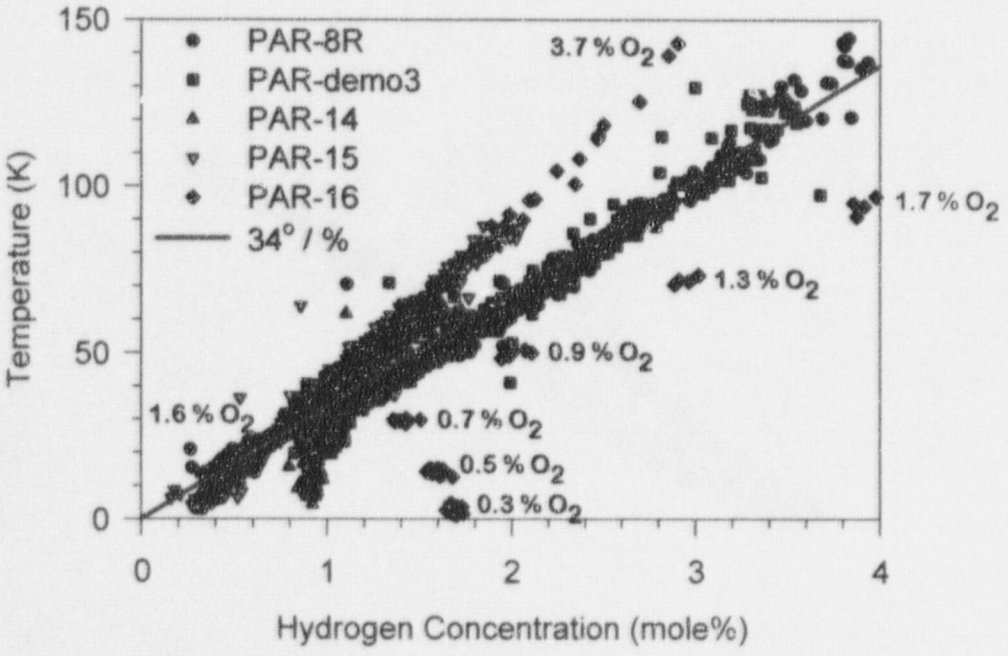

Figure 265. PAR ΔT versus hydrogen concentration in PAR-16.

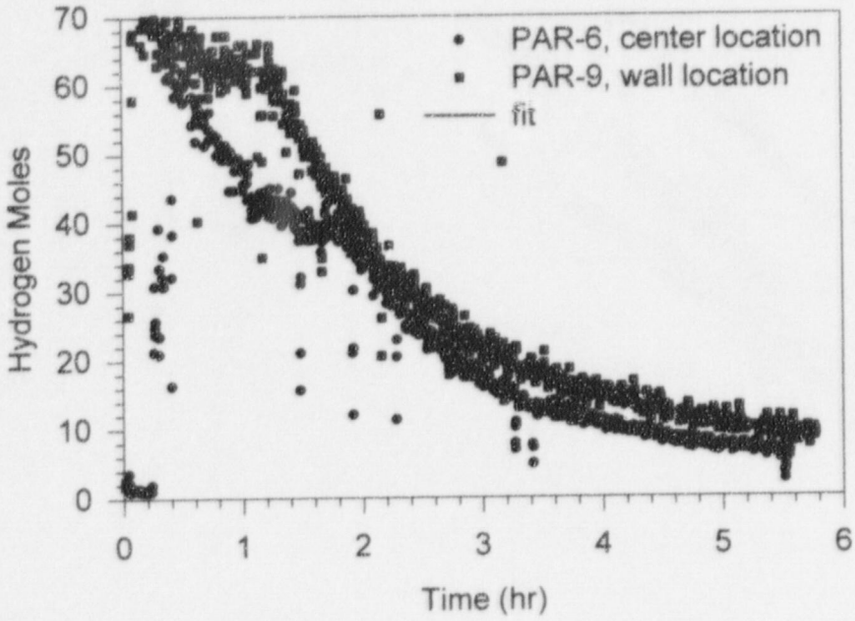

Figure 266. Hydrogen moles in Surtsey during tests for the wall effect.

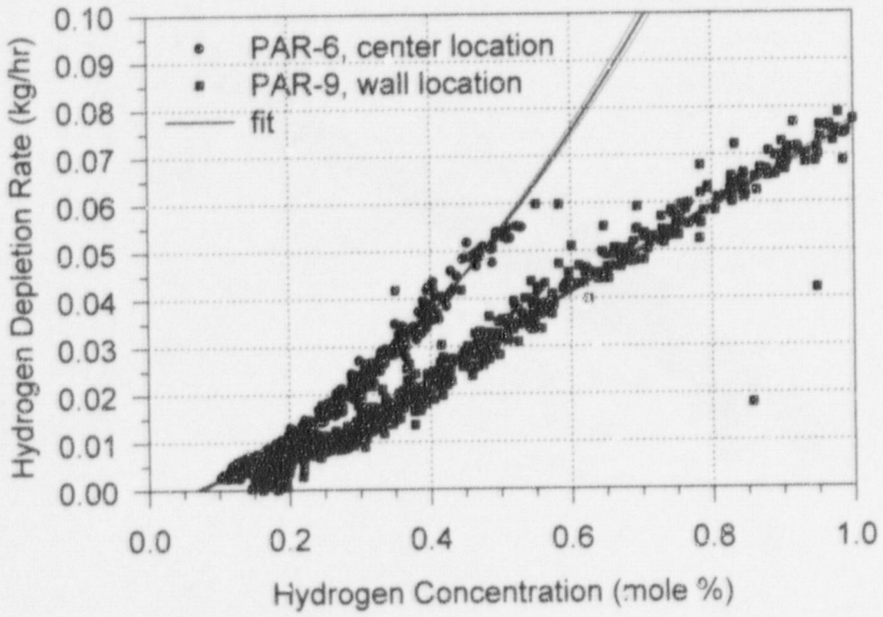

Figure 267. Hydrogen depletion rate comparison for the wall effect.

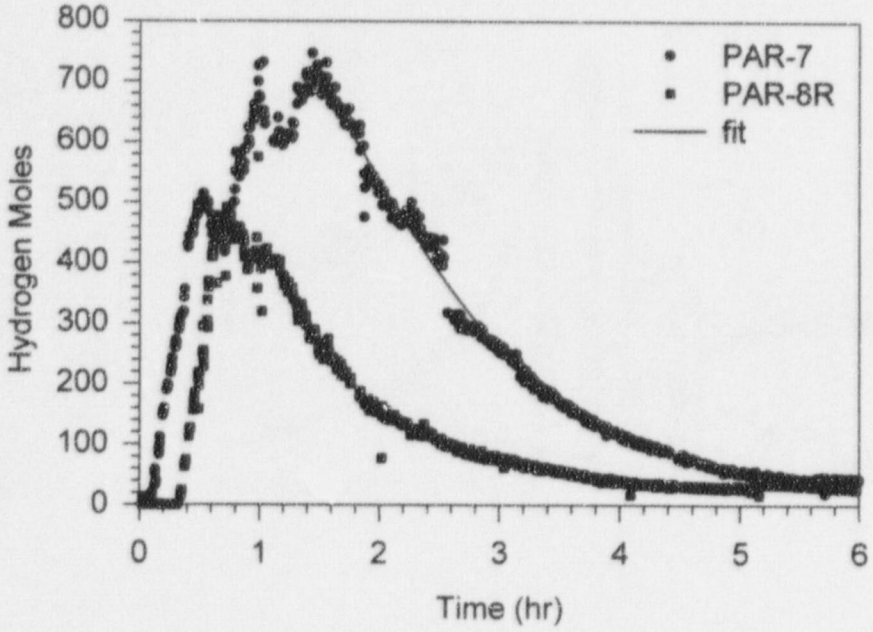

Figure 268. Hydrogen moles in Surtsey during tests for the oxygen limit effect.

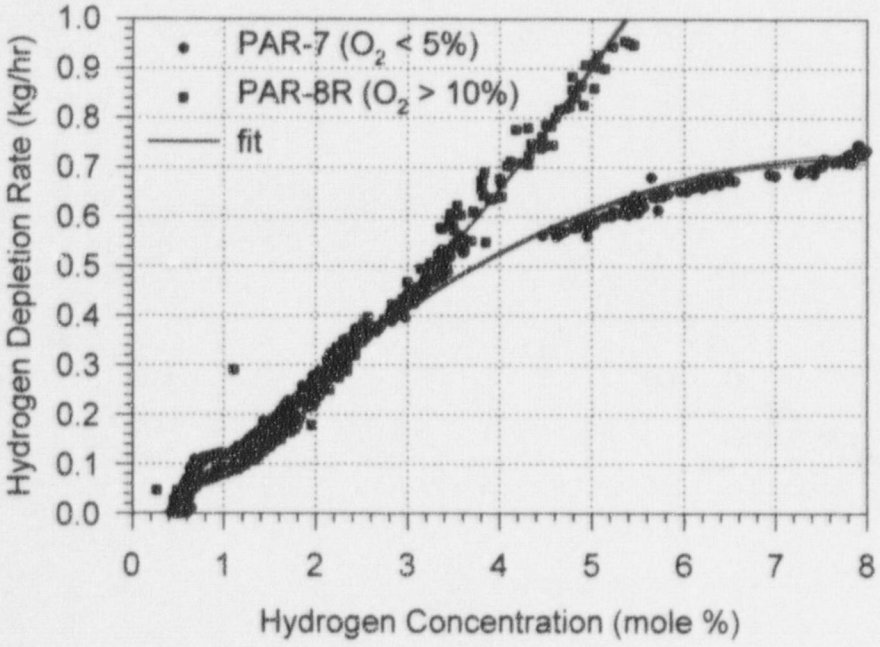

Figure 269. Hydrogen depletion rate comparison for oxygen limit effect.

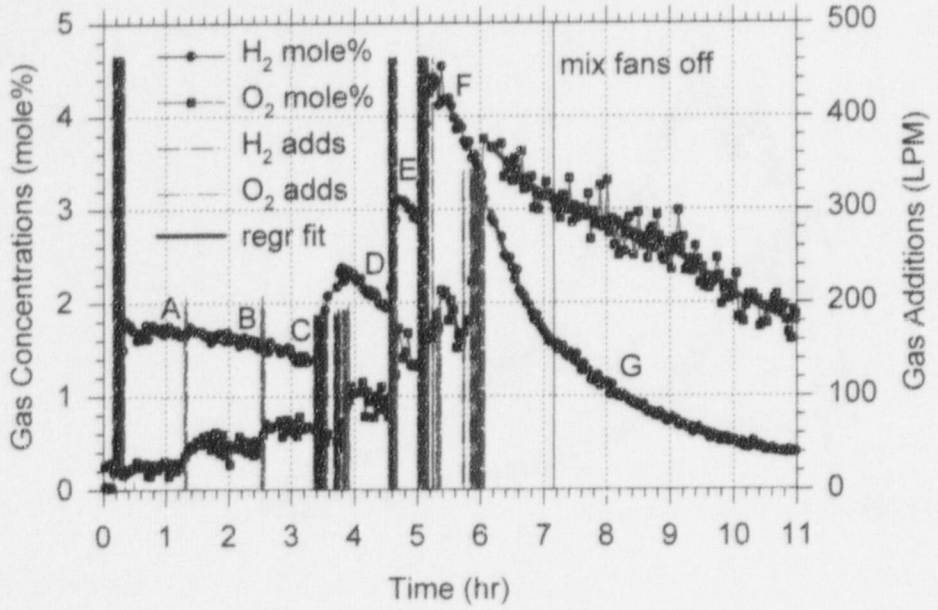

Figure 270. Hydrogen and oxygen concentration during PAR-16.

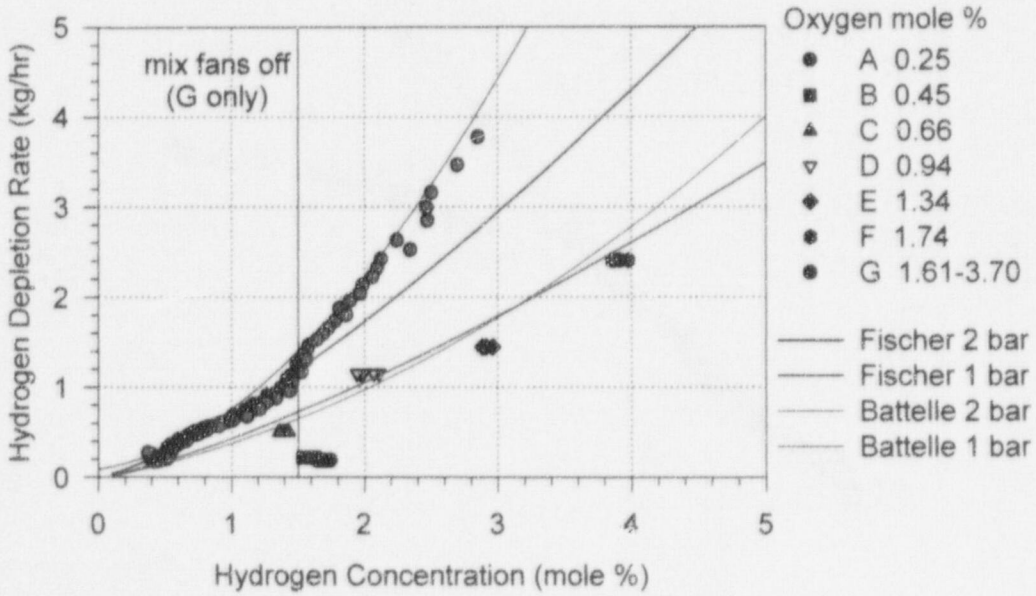

Figure 271. Normalized hydrogen depletion rates as a function of hydrogen and oxygen concentration in PAR-16.

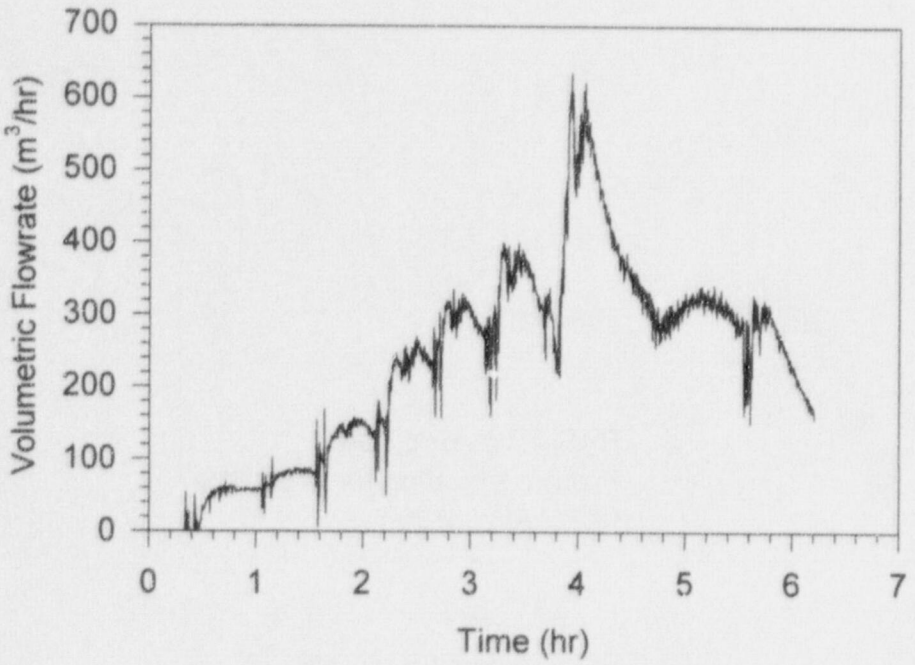

Figure 272. PAR-2 volumetric flowrate versus time.

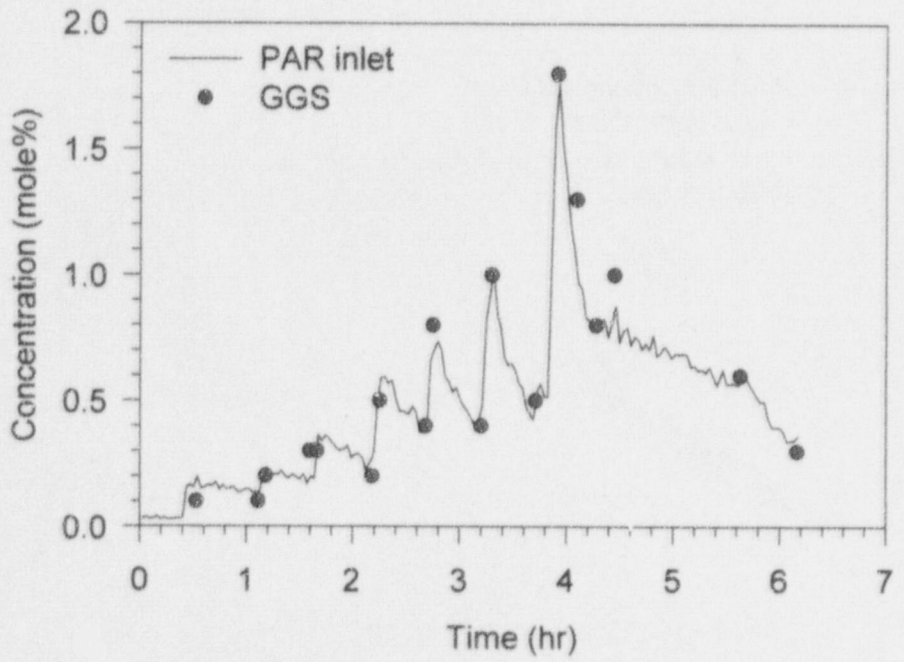

Figure 273. PAR-2 hydrogen concentration (dry-basis).

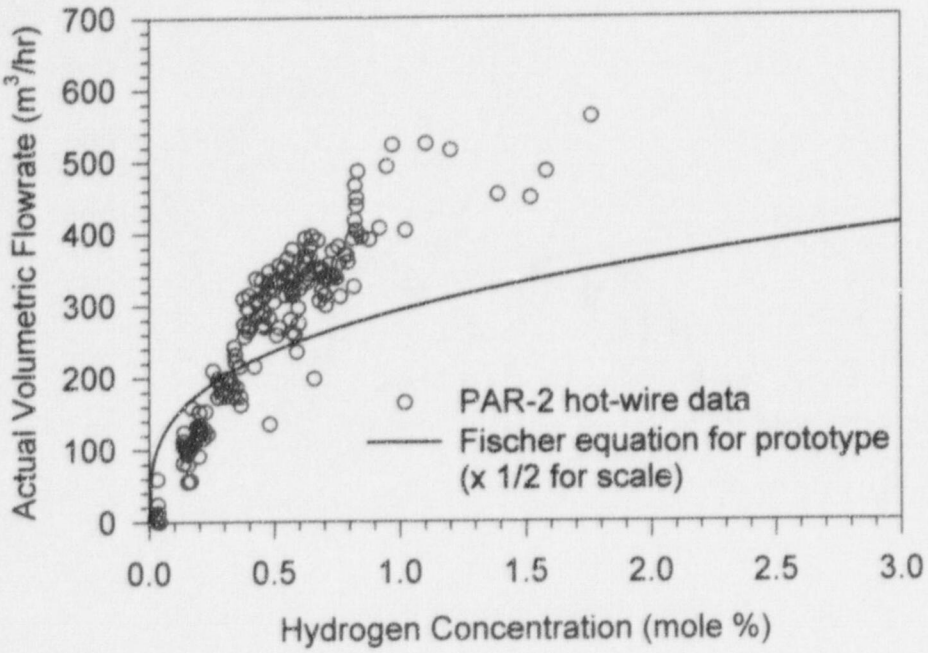

Figure 274. PAR-2 flowrate versus concentration.

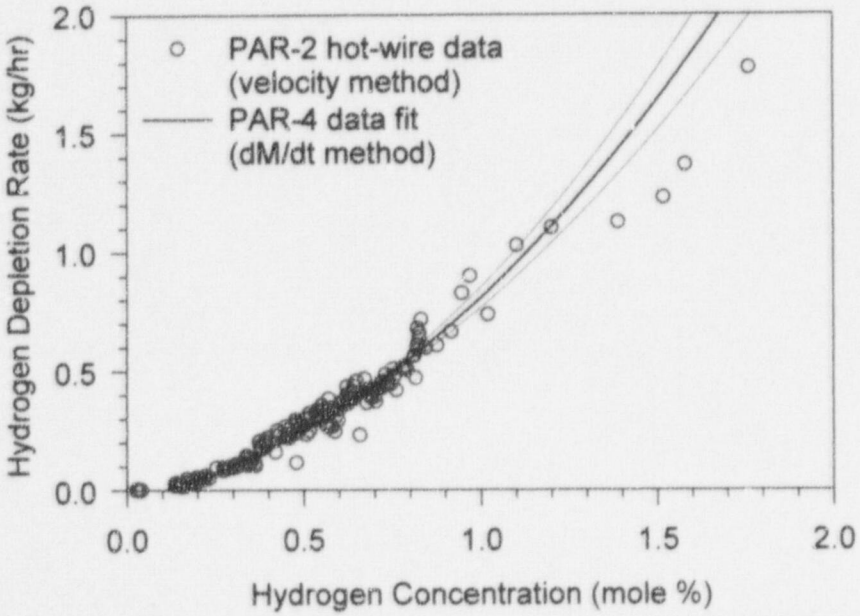

Figure 275. Hydrogen depletion rate by two methods.

NRC FORM 335 (2-89) NRCM 1102, 3201, 3202

U.S. NUCLEAR REGULATORY COMMISSION

BIBLIOGRAPHIC DATA SHEET

(See instructions on the reverse)

1. REPORT NUMBER (Assigned by NRC. Add Vol., Supp., Rev., and Addendum Numbers, if any.)

NUREG/CR-6580
SAND97-2632

2. TITLE AND SUBTITLE

Performance Testing of Passive Autocatalytic Recombiners

3. DATE REPORT PUBLISHED

MONTH	YEAR
June	1998

4. FIN OR GRANT NUMBER

L2443

5. AUTHOR(S)

T. K. Blanchat/SNL
A. Malliakos/NRC

6. TYPE OF REPORT

Technical

7. PERIOD COVERED *(Inclusive Dates)*

8. PERFORMING ORGANIZATION – NAME AND ADDRESS *(If NRC, provide Division, Office or Region, U.S. Nuclear Regulatory Commission, and mailing address; if contractor, provide name and mailing address.)*

Sandia National Laboratories
Albuquerque, NM 87185

9. SPONSORING ORGANIZATION – NAME AND ADDRESS *(If NRC, type "Same as above"; if contractor, provide NRC Division, Office or Region, U.S. Nuclear Regulatory Commission, and mailing address.)*

Division of Systems Technology
Office of Nuclear Regulatory Research
U.S. Nuclear Regulatory Commission
Washington, DC 20555-0001

10. SUPPLEMENTARY NOTES

A. Malliakos, NRC Project Manager

11. ABSTRACT *(200 words or less)*

Performance tests of a scaled passive autocatalytic recombiner (PAR) were performed in the Surtsey test vessel at Sandia National Laboratories. The test program included experiments to: 1) define the startup characteristics of PARs, 2) confirm a hydrogen depletion rate curve of PARs, 3) define the PAR performance in the presence of steam, 4) evaluate the effect of scale (number of cartridges) on the PAR performance at both low and high hydrogen concentrations, 5) define the PAR performance with and without the hydrophobic coat, 6) determine if the PAR could ignite hydrogen mixtures, 7) define the PAR performance in well-mixed conditions, and 8) define the PAR performance in a low oxygen environment. The tests determined that the PAR startup delay times decrease with increasing hydrogen concentrations in steamy environments. Measured depletion rate data were obtained and compared with previous work. Depletion rate appears to be proportional to scale. PAR performance in steamy environments and the lack of hydrophobic coating was investigated. Placement of the PAR near a wall (as opposed to a center location) appeared to have an effect on depletion rates. The PAR ignited hydrogen at relatively high concentrations (5-10 mole %). Low oxygen concentrations appeared to have an effect on the hydrogen/oxygen recombination rate. The effect of well-mixed conditions during depletion rate measurements were inconclusive.

12. KEY WORDS/DESCRIPTORS *(List words or phrases that will assist researchers in locating the report.)*

Passive autocatalytic recombiner, PAR, hydrogen combustion, combustible gas control, hydrogen depletion, palladium, passive catalytic filter

13. AVAILABILITY STATEMENT

Unlimited

14. SECURITY CLASSIFICATION

(This Page)
Unclassified

(This Report)
Unclassified

15. NUMBER OF PAGES

16. PRICE

Federal Recycling Program

ISBN 0-16-049654-3

90000

9 780160 496547